BioMed Research International

Novel Developments in Acute Kidney Injury

Guest Editors: Jeremiah R. Brown, Peter A. McCullough, and Michael E. Matheny

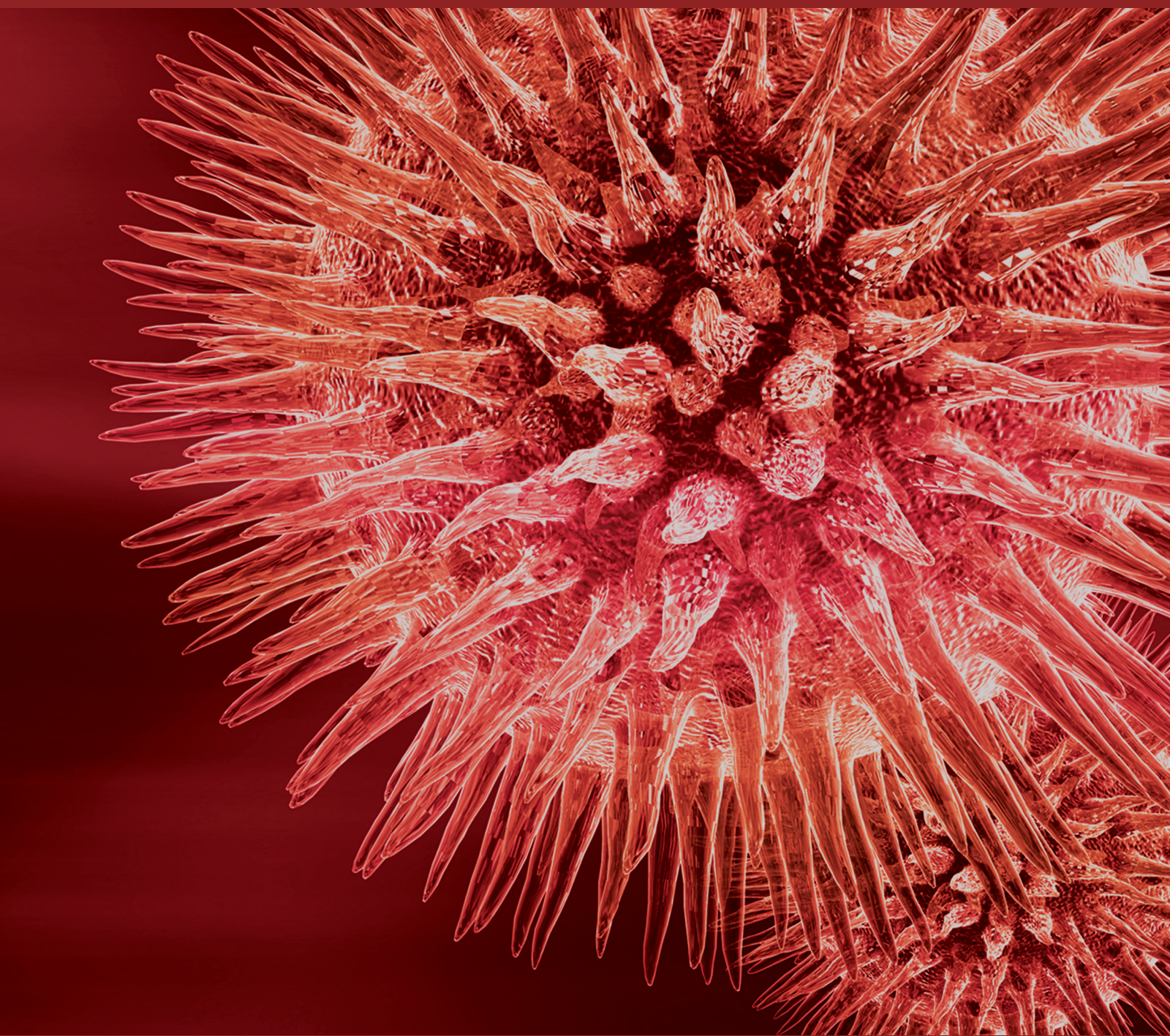

Novel Developments in Acute Kidney Injury

BioMed Research International

Novel Developments in Acute Kidney Injury

Guest Editors: Jeremiah R. Brown, Peter A. McCullough, and Michael E. Matheny

Contents

Hindawi Publishing Corporation
BioMed Research International
Volume 2016, Article ID 2756204, 2 pages
http://dx.doi.org/10.1155/2016/2756204

Editorial
Novel Developments in Acute Kidney Injury

Jeremiah R. Brown,[1,2,3] Peter A. McCullough,[4] and Michael E. Matheny[5,6,7,8]

[1]*The Dartmouth Institute for Health Policy and Clinical Practice, Geisel School of Medicine, HB 7505, 1 Medical Center Drive, Lebanon, NH 03756, USA*
[2]*Department of Medicine, Dartmouth-Hitchcock Medical Center, (DHMC), HB 7505, 1 Medical Center Drive, Lebanon, NH 03756, USA*
[3]*Department of Community and Family Medicine, Dartmouth-Hitchcock Medical Center (DHMC), HB 7505, 1 Medical Center Drive, Lebanon, NH 03756, USA*
[4]*Baylor Heart and Vascular Institute, 621 North Hall Street, H030, Dallas, TX 75226, USA*
[5]*Geriatrics Research Education & Clinical Center (GRECC), Tennessee Valley Healthcare System (TVHS), Veteran's Health Administration, USA*
[6]*Division of General Internal Medicine, Department of Medicine, Vanderbilt University School of Medicine, Nashville, TN 37232, USA*
[7]*Department of Biomedical Informatics, Vanderbilt University School of Medicine, Nashville, TN 37232, USA*
[8]*Department of Biostatistics, Vanderbilt University School of Medicine, Nashville, TN 37232, USA*

Correspondence should be addressed to Jeremiah R. Brown; jbrown@dartmouth.edu

Received 30 June 2016; Accepted 30 June 2016

Over the past decade, acute kidney injury (AKI) has emerged rapidly in the scientific literature and clinical awareness. There have been great strides in understanding the pathophysiology and adverse outcomes associated with AKI. In this special issue on acute kidney injury (AKI), contributing authors discuss novel clinical and experimental research emerging in the field of AKI.

Clinical. Several contributions provide evaluations of AKI in clinical practice. J. Brown et al. start off the special issue on AKI by reviewing the trends in AKI related hospitalization in the United States of America over the past decade. O. E. Ibrahim et al. evaluated the association of elevated serum creatine kinase (>2500 U/mL) as a marker for rhabdomyolysis and AKI after high risk adult cardiac surgery. A. Kwizera et al. explore the association of intermittent hemodialysis for treating AKI in an African Intensive Care Unit.

Basic Science. Likewise, novel experiments and investigations to better our understanding of AKI in animal models provide important insights into future AKI exploration. C. Jiang et al. report on a novel active ingredient of a Chinese herb known to be kidney protective called Tanshinone IIA showing a reduction in folic-acid induced kidney dysfunction through attenuating renal fibrosis after acute kidney injury in a mouse model through inhibition of fibrocytes recruitment. S. M. Fernandes et al. investigate the association between iodinated contrast and renal function in rats with chronic kidney disease and chronic hyperglycemia.

Several experiments focused on the issue of renal ischemia-reperfusion injury in animal models. E. C. Costalonga et al. examined whether valproic acid could prevent renal ischemia-reperfusion injury and subsequent AKI in male Wistar rats. S. Ozbilgin et al. explored whether ischemic preconditioning could prevent reperfusion injury in diabetic rats. Lastly, D. Wen et al. in an in vivo model discuss the role of a DNA binding 1 inhibitor during renal ischemia-reperfusion injury.

Review of the Literature. Two reviews provide a critical appraisal of the literature on the role of cisplatin nephrotoxicity and a technology evaluation on the role of renal magnetic resonance imaging in patients with AKI. G. Oh et al. provide a review on cisplatin nephrotoxicity operating through oxidative stress and inflammation and by the reduction of the intracellular NAD^+/NADH ratio. H. Y. Zhou et al. discuss the

role of functional renal magnetic resonance imaging as an assessment tool to evaluate renal morphology and function in the management of AKI.

Jeremiah R. Brown
Peter A. McCullough
Michael E. Matheny

Hindawi Publishing Corporation
BioMed Research International
Volume 2016, Article ID 4278579, 6 pages
http://dx.doi.org/10.1155/2016/4278579

Review Article

Hospital Mortality in the United States following Acute Kidney Injury

Jeremiah R. Brown,[1,2,3] Michael E. Rezaee,[1,4] Emily J. Marshall,[1] and Michael E. Matheny[5,6,7,8]

[1] *The Dartmouth Institute for Health Policy and Clinical Practice, Geisel School of Medicine, Lebanon, NH 03756, USA*
[2] *Department of Medicine, Dartmouth-Hitchcock Medical Center, Lebanon, NH 03756, USA*
[3] *Department of Community and Family Medicine, Lebanon, NH 03756, USA*
[4] *Oakland University William Beaumont School of Medicine, Rochester, MI 48309, USA*
[5] *Geriatrics Research Education & Clinical Center (GRECC), Tennessee Valley Healthcare System (TVHS), Veterans Health Administration, Nashville, TN 37232, USA*
[6] *Division of General Internal Medicine, Department of Medicine, Vanderbilt University School of Medicine, Nashville, TN 37232, USA*
[7] *Department of Biomedical Informatics, Vanderbilt University School of Medicine, Nashville, TN 37232, USA*
[8] *Department of Biostatistics, Vanderbilt University School of Medicine, Nashville, TN 37232, USA*

Correspondence should be addressed to Jeremiah R. Brown; jbrown@dartmouth.edu

Received 15 March 2016; Accepted 8 May 2016

Academic Editor: George Seki

Acute kidney injury (AKI) is a common reason for hospital admission and complication of many inpatient procedures. The temporal incidence of AKI and the association of AKI admissions with in-hospital mortality are a growing problem in the world today. In this review, we discuss the epidemiology of AKI and its association with in-hospital mortality in the United States. AKI has been growing at a rate of 14% per year since 2001. However, the in-hospital mortality associated with AKI has been on the decline starting with 21.9% in 2001 to 9.1 in 2011, even though the number of AKI-related in-hospital deaths increased almost twofold from 147,943 to 285,768 deaths. We discuss the importance of the 71% reduction in AKI-related mortality among hospitalized patients in the United States and draw on the discussion of whether or not this is a phenomenon of hospital billing (coding) or improvements to the management of AKI.

1. Introduction

Acute kidney injury (AKI) is a serious condition characterized by a sudden decline in kidney function, leading to inept excretion of nitrogenous waste from the body and deficient serum volume and electrolyte regulation. Common life-threatening complications of AKI include volume overload, hyperkalemia, acidosis, and uremia [1]. Acute tubular necrosis (ATN) caused by ischemia, exposure to nephrotoxic agents (e.g., medications and contrast media), or sepsis is the leading cause of AKI among hospitalized patients in the US [2]. Patients at risk for AKI include those with advanced age, diabetes mellitus, heart failure, liver failure, chronic kidney disease, hypotension, and sepsis. Patients who undergo cardiac/vascular surgery, organ transplantation, and mechanical ventilation or who are exposed to contrast media, nonsteroidal-inflammatory drugs (NSAIDs), antimicrobial drugs, or chemotherapeutic agents commonly experience AKI as a complicating condition [3].

According to various reports, AKI occurs in anywhere from five to twenty percent of hospitalizations in the US [4, 5]. Patients that experience AKI are at increased risk for adverse health outcomes such as end stage renal disease (ESRD), pulmonary complications, and cardiovascular events [6–9]. In addition, prior research has found that AKI patients have greater odds of all-cause mortality, increased length of

stay, and an additional hospital cost of approximately $7,500 [7, 10]. AKI severity is positively associated with patient morbidity and mortality [11, 12].

The patient characteristics, procedures, and nephrotoxic agents associated with increased risk of AKI are on the rise in the United States. For example, the US population is aging and has experienced stark increases in the incidences of diabetes, heart failure, and sepsis over the last few decades [13–16]. Additionally, the utilization of procedures requiring nephrotoxic contrast media, such as cardiac catheterization, computerized tomography scans, and peripheral angiograms, as well as the use of antimicrobial drugs and NSAIDs, has grown tremendously over the same time period [2, 17–22]. Since patients developing AKI without requiring dialysis have an increased risk of in-hospital and long-term mortality, we have sought to evaluate the national trends in AKI admissions and hospital mortality [23–25].

Due to the large increase in the prevalence of risk factors for AKI, we hypothesized that the incidence of AKI has correspondingly increased among hospitalized patients. Using a nationally representative sample, we determined the incidence and associated in-hospital mortality of AKI among hospitalized patients in the US from 2001 to 2011.

2. Methods

2.1. Study Population. We extracted discharge data from 2001 to 2011 from the Healthcare Cost and Utilization Project's (HCUP) National Inpatient Sample (NIS). The NIS is a nationally representative, stratified sample of approximately 20 percent of community hospitals in the US each year. It is the largest deidentified US all-payer inpatient database publically available for research purposes. In 2001, 986 hospitals in 33 states contributed over 7.4 million discharge records to the NIS. By 2011, the NIS grew to 1,049 hospitals in 46 states and over 8 million discharge records. The committee for the Protection of Human Subjects at Dartmouth College waived required approval for this study as a publically available limited dataset.

We identified cases of AKI using the following ICD-9-CM codes for acute renal failure: 584.5 (with tubular necrosis), 584.6 (with lesion of renal cortical necrosis), 584.7 (with lesion of renal medullary necrosis), 584.8 (other specified pathologic lesions in kidney), or 584.9 (unspecified). The final cohort included 18,870,662 admissions.

We used adjusted analyses to account for comorbid conditions, age, sex, and hospital utilization practices, such as annual median length of stay and the proportion of patients discharged to skilled nursing facilities (SNF). Congestive heart failure, pulmonary circulation disorders, peripheral vascular disease, hypertension, neurological disorders, chronic pulmonary disease, diabetes without chronic complications, diabetes with chronic complications, obesity, fluid and electrolyte disorders, blood loss anemia, and deficiency anemias were identified using NIS comorbidity indicators. We also identified comorbid sepsis (038.x, 112.5, 112.81, 020.2, 790.7, 785.59). Specific ICD-9-CM codes used to identify comorbid conditions are available for review elsewhere [26].

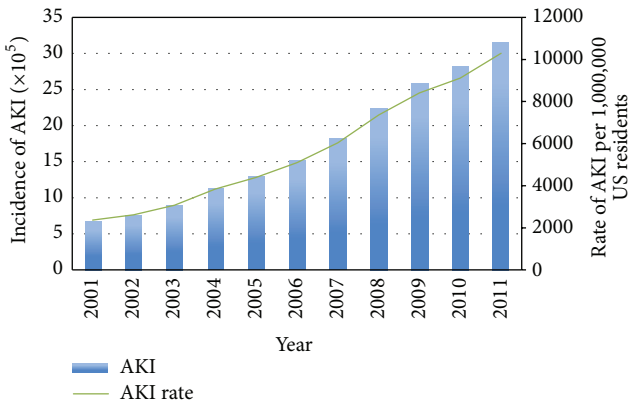

Figure 1: Population incidence of acute kidney injury in the United States, 2001 to 2011.

2.2. Statistical Analysis. We calculated population incidence rates for AKI in the US from 2001 to 2011 by dividing the number of discharges with AKI by the US population in each year, using estimates from the US Census Bureau [27, 28]. Incidence estimates were stratified by sex and age for subgroup investigation. With data from 2001 as a reference, we used multiple logistic regression models to determine the odds of AKI and corresponding in-hospital mortality for each year included in the study. Models were adjusted for age, sex, race, congestive heart failure, pulmonary circulation disorders, peripheral vascular disease, hypertension, other neurological disorders, chronic pulmonary disease, diabetes without chronic complications, diabetes with chronic complications, obesity, fluid and electrolyte disorders, blood loss anemia, deficiency anemias, sepsis, and cardiac catheterization. Population attributable risk of in-hospital death associated AKI was calculated to approximate the proportion of patient deaths that could have been prevented if AKI was avoided. All data was analyzed using Stata 11.2 (StataCorp, College Station, TX) and weighted at the discharge level to account for the NIS sampling scheme.

3. Results

We identified 18,870,662 hospitalizations associated with AKI from 2001 to 2011. Over this period, significant differences were observed in all AKI patient characteristics except for sex, age, chronic pulmonary disease, and diabetes with chronic complications. Comorbid hypertension (22.9% to 61.2%), obesity (2.9% to 14.1%), and deficiency anemias (20.2% to 35.9%) increased the most for AKI patients from 2001 to 2011. Complete annual characteristics for patients with AKI are displayed in Table 1.

3.1. Acute Kidney Injury. We identified 18,870,662 hospitalizations associated with an AKI diagnosis over the study period. The number of cases of AKI grew from 674,845 in 2001 to 3,151,937 in 2011, an almost fivefold increase in the incidence of AKI in the US (Figure 1). Compared to 2001, the odds of AKI increasing per year in 2002 to 2011 were 1.18 (95% CI: 1.17–1.18) in unadjusted analyses (Table 2). After adjustment for patient and hospital characteristics the odds

Table 1: Characteristics of patients with acute kidney injury in the United States, 2001 to 2011.

	All years	2001	2002	2003	2004	2005	2006	2007	2008	2009	2010	2011	*P* value
N	18,870,662	674,845	752,472	891,353	1,125,378	1,299,289	1,522,004	1,818,011	2,236,412	2,581,314	2,817,647	3,151,937	
Female (%)	47.6	47.42	47.37	48.02	47.99	47.69	47.35	47.45	47.85	47.56	47.44	47.65	0.46
Age (median)	72	72	72	72	72	72	72	72	72	71	71	71	0.72
Age (IQR)	58–81	59–81	59–81	59–81	59–81	58–81	58–81	58–81	59–82	58–81	58–81	58–82	0.72
Length of stay (median)	6	7	7	7	7	6	6	6	6	5	5	5	<0.001
Length of stay (IQR)	3–11	4–13	4–13	4–13	3–12	3–12	3–11	3–11	3–10	3–10	3–10	3–9	<0.001
Heart failure (%)	22.78	23.68	23.99	24.42	25.22	25.37	24.75	23.65	21.43	21.18	21.06	22.04	<0.001
Pulmonary disease (%)	3.53	1.33	1.51	1.54	1.56	1.61	2.1	3.25	3.94	4.19	4.59	5.03	<0.001
Peripheral vascular disease (%)	8.94	6.34	7.2	6.88	6.85	6.73	7.42	8.37	9.43	9.59	9.36	10.89	<0.001
Hypertension (%)	52.86	22.91	26.78	44.15	45.44	46.4	49.19	48.69	53.42	56.73	58.14	61.21	<0.001
Neurological disease (%)	9.61	3.62	9.2	7.55	7.81	7.79	8.3	9.3	9.79	10.05	10.3	11.12	<0.001
Chronic pulmonary disease (%)	23.4	20.9	22.23	22.62	22.91	23.8	24.31	24.36	22.36	22.9	22.84	24.11	0.29
Diabetes (%)	23.72	17.12	18.6	19.18	19.56	19.36	21.17	22.71	24.15	25.65	25.97	27.26	<0.001
Diabetes with sequelae (%)	10.94	9.55	10.86	10.61	10.17	10.32	10.83	11.23	10.75	10.53	10.41	11.57	0.28
Obesity (%)	9.26	2.94	3.9	4.17	4.37	4.89	5.96	7.35	9.8	11.09	11.26	14.08	<0.001
Anemia (%)	30.47	20.19	22.85	23.86	23.6	23.58	26.27	28.9	32.11	32.84	32.48	35.87	<0.001
Sepsis (%)	20.8	19.31	19.87	19.65	19.88	20.35	20.58	20.55	20.87	20.52	20.58	21.12	<0.001
In-hospital mortality (%)	12.32	21.92	20.38	18.76	16.76	15.38	14.09	12.36	11.8	10.49	9.74	9.07	<0.001

Table 2: Crude and adjusted odds ratios for acute kidney injury in the United States, 2011 compared to 2001.

	AKI			
Population at risk	Crude OR/yr	95% CI	Adjusted OR/yr	95% CI
Overall	1.18	(1.17–1.18)	1.14	(1.13–1.15)
Age groups				
0–19	1.10	(1.07–1.14)	1.07	(1.05–1.09)
20–44	1.17	(1.16–1.19)	1.12	(1.11–1.13)
45–64	1.18	(1.17–1.19)	1.13	(1.13–1.15)
65–74	1.17	(1.16–1.18)	1.14	(1.13–1.15)
75+	1.19	(1.18–1.19)	1.15	(1.15–1.16)
Sex				
Male	1.18	(1.17–1.18)	1.14	(1.13–1.15)
Female	1.18	(1.17–1.18)	1.14	(1.13–1.15)

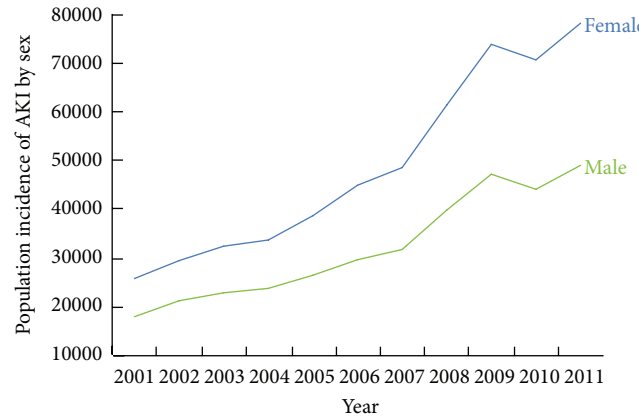

Figure 2: Population incidence of acute kidney injury by sex in the United States, 2001 to 2011.

of AKI increasing per year in 2002 to 2011 compared to 2001 were 1.14 (95% CI: 1.13–1.15). Subgroup analyses revealed that men and women experienced a similar increasing pattern of AKI incidence over the study period (Figure 2). Similar patterns of AKI incidence were also found among age groups, although the highest increase in AKI incidence was observed among patients greater than 75 years of age (Figure 3).

Table 3: Crude and adjusted odds ratios for mortality amongst acute kidney injury and dialysis-requiring acute kidney injury in the United States, 2011 compared to 2001.

	Odds of mortality following AKI			
Year	Crude OR	95% CI	Adjusted OR	95% CI
2001	Referent			
2002	0.90	(0.87–0.94)	0.92	(0.88–0.97)
2003	0.82	(0.79–0.85)	0.87	(0.83–0.91)
2004	0.72	(0.69–0.75)	0.74	(0.70–0.77)
2005	0.65	(0.62–0.68)	0.65	(0.62–0.69)
2006	0.58	(0.56–0.61)	0.60	(0.58–0.63)
2007	0.50	(0.48–0.53)	0.52	(0.49–0.55)
2008	0.48	(0.46–0.50)	0.51	(0.48–0.53)
2009	0.42	(0.40–0.44)	0.45	(0.43–0.48)
2010	0.38	(0.37–0.40)	0.42	(0.40–0.44)
2011	0.36	(0.34–0.37)	0.29	(0.28–0.30)

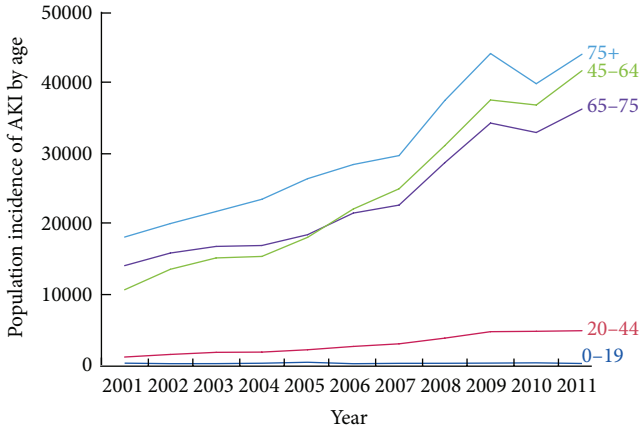

Figure 3: Population incidence of acute kidney injury by age group in the United States, 2001 to 2011.

In-hospital mortality for AKI patients decreased from 21.9% in 2001 to 9.1% in 2011. Likewise, the odds of in-hospital mortality for AKI patients in 2011 compared to 2001 were significantly reduced (unadjusted OR 0.36, 95% CI: 0.34 to 0.37; adjusted OR 0.29, 95% CI: 0.28 to 0.30; Table 3). Despite declining mortality estimates, the number of AKI patients experiencing in-hospital mortality increased twofold over the study period, from 147,943 to 285,744. In addition, the population attributable risk of death associated with AKI increased from 19.2% to 35.5% from 2001 to 2011 (Table 4).

4. Discussion

With this nationally representative study of hospitalizations in the US, we are the first to show that while AKI has increased, hospital mortality rates for AKI have decreased significantly from 2001 to 2011. The incidence of AKI increased fivefold over the study period. While we found a downward trend in the proportion of AKI patients with hospital mortality, the raw number of deaths and attributable population risk of death for AKI increased significantly from

Table 4: Population attributable risk of mortality associated with acute kidney injury and dialysis-requiring acute kidney injury in the United States, 2001 through 2011.

Year	Population attributable risk of mortality following AKI
2001	19.2
2002	21.0
2003	22.4
2004	23.7
2005	24.8
2006	26.5
2007	28.6
2008	31.1
2009	33.7
2010	34.4
2011	35.5

2001 to 2011. By 2011, AKI was present in over 35% of all in-hospital death cases, a 16.3% increase since the beginning of the study period. Our findings demonstrate both the clinical and public health significance of AKI in the US, and the immense opportunity that exists to prevent and manage these life-threatening complications.

Our foremost contribution is to report on the growing incidence of AKI in the United States from 2001 to 2011 and to demonstrate that while AKI admissions are on the rise, hospital mortality for AKI has declined significantly. Hsu and colleagues did not study the epidemiology of nondialysis-requiring AKI due to concerns about the validity of ICD-9-CM codes without the use of companion dialysis codes to correctly identify cases [27, 29]. However, as discussed in our limitations section, it is becoming increasingly more common for studies to leverage AKI ICD-9-CM codes in claims data without dialysis as a companion code [30–32]. As a result, we were able to observe a significant increase in AKI incidence and associated in-hospital mortality among patients in our study.

The early 2000s saw the first investigations into the incidence of acute renal failure and associated in-hospital mortality. These studies expressed their findings in terms of either cases per hospitalization or intensive care unit days, making the results difficult to interpret and generalize across providers, as the number of admissions and length of stay vary between hospitals [2, 11, 33]. More recent studies have taken a more population-based approach, estimating the population incidence of AKI to be 2,000–3,000 per million people per year [27, 34, 35]. To date, only Hsu and colleagues have investigated the temporal incidence of any kind of AKI in the US (in their case, dialysis-requiring AKI (AKI-D) specifically) [27, 36]. Our analysis now provides the most up-to-date and comprehensive description of AKI and related hospital mortality epidemiology in the US. The observed increase in the incidence of AKI in our study was likely driven by the increasing commonality of patient risk factors for AKI in the US population, as well as the more frequent use of procedures and medications known to cause renal damage. However, it is important to note that the observed

increase in the incidence of AKI may be due to improved recognition of AKI and coding for smaller degrees of AKI. The availability of diagnostic criteria for AKI (e.g., RIFLE) and growing provider awareness, regarding the relationship between serum creatinine and renal impairment, may have led to increased rates of AKI diagnosis over the study period [37–39]. Though unlikely, inappropriate ICD-9-CM coding practice could also have led to increased incidence estimates. In order to determine if the increase of AKI incidence is true and not a consequence of increased AKI identification through ICD-9-CM codes, we have measured AKI-D trends over the same time period in a different study [40]. AKI-D is more likely to be defined consistently over the years, and it still experiences an upward trend from 2001 to 2011, suggesting that increasing AKI incidence is not solely a result of inappropriate ICD-9-CM coding [40].

The strengths of our study include the use of a large nationally representative sample of hospitalizations in the US reporting on the incidence of AKI and hospital mortality. In addition, our use of population attributable risk of mortality estimates allows readers to understand both the clinical and public health significance of AKI in the US.

However, our study has several important limitations. First, as stated previously, we utilized ICD-9-CM codes to identify cases of AKI. Prior analyses have not utilized ICD-9-CM codes alone to identify cases of AKI due to concerns of validity [27, 29]. We leveraged prior research demonstrating the high specificity (97.7%) and low sensitivity (35.4%) of ICD-9-CM codes in identifying cases of AKI for this analysis [29, 41]. Second, administrative billing codes are less useful than clinical data for identifying AKI. Clinical or laboratory data, such as serum creatinine levels, would have provided the most accurate marker of renal impairment had they been available [29]. Third, the NIS is a completely deidentified dataset, making it impossible to track specific patients over time.

Although our study establishes the significance of the problem, additional research is needed on the drivers of drastic increase of AKI incidence in the US. More research is also needed to understand geographic and subgroup variation, as well as which prevention and management strategies result in the greatest decline and control of AKI among hospitalized patients.

In summary, our study demonstrates that the incidence of AKI increased significantly in the US between 2001 and 2011. The percentage of all in-hospital deaths occurring in combination with AKI rose by 16.3% over the study period. AKI represents a growing clinical and public health problem for Americans.

Competing Interests

All authors have no competing interests or financial information to disclose in relation to this research.

Acknowledgments

This project was supported in part by HS018443 (Jeremiah R. Brown) from the Agency for Healthcare Research and Quality, the Veterans Health Administration Health Services Research and Development (HSR&D) CDA-08-020 (Michael E. Matheny), and HSR&D IIR-11-292 (Michael E. Matheny, Jeremiah R. Brown).

References

[1] M. D. Okusa and M. H. Rosner, *Overview of the Management of Acute Kidney Injury (Acute Renal Failure)*, UpToDate, 2014, http://www.uptodate.com.huaryu.kl.oakland.edu/contents/overview-of-the-management-of-acute-kidney-injury-acute-renal-failure?source=preview&search=acute+kidney+injury+adult&selectedTitle=1~150&language=en-US&anchor=H24600525-H6570002.

[2] K. Nash, A. Hafeez, and S. Hou, "Hospital-acquired renal insufficiency," *American Journal of Kidney Diseases*, vol. 39, no. 5, pp. 930–936, 2002.

[3] M. Leblanc, J. A. Kellum, R. T. N. Gibney, W. Lieberthal, J. Tumlin, and R. Mehta, "Risk factors for acute renal failure: inherent and modifiable risks," *Current Opinion in Critical Care*, vol. 11, no. 6, pp. 533–536, 2005.

[4] H. E. Wang, P. Muntner, G. M. Chertow, and D. G. Warnock, "Acute kidney injury and mortality in hospitalized patients," *American Journal of Nephrology*, vol. 35, no. 4, pp. 349–355, 2012.

[5] S. H. Hou, D. A. Bushinsky, J. B. Wish, J. J. Cohen, and J. T. Harrington, "Hospital-acquired renal insufficiency: a prospective study," *The American Journal of Medicine*, vol. 74, no. 2, pp. 243–248, 1983.

[6] S. Faubel, "Pulmonary complications after acute kidney injury," *Advances in Chronic Kidney Disease*, vol. 15, no. 3, pp. 284–296, 2008.

[7] S. G. Coca, B. Yusuf, M. G. Shlipak, A. X. Garg, and C. R. Parikh, "Long-term risk of mortality and other adverse outcomes after acute kidney injury: a systematic review and meta-analysis," *American Journal of Kidney Diseases*, vol. 53, no. 6, pp. 961–973, 2009.

[8] A. Ishani, J. L. Xue, J. Himmelfarb et al., "Acute kidney injury increases risk of ESRD among elderly," *Journal of the American Society of Nephrology*, vol. 20, no. 1, pp. 223–228, 2009.

[9] R. Bellomo, J. A. Kellum, and C. Ronco, "Acute kidney injury," *The Lancet*, vol. 380, no. 9843, pp. 756–766, 2012.

[10] G. M. Chertow, E. Burdick, M. Honour, J. V. Bonventre, and D. W. Bates, "Acute kidney injury, mortality, length of stay, and costs in hospitalized patients," *Journal of the American Society of Nephrology*, vol. 16, no. 11, pp. 3365–3370, 2005.

[11] O. Liangos, R. Wald, J. W. O'Bell, L. Price, B. J. Pereira, and B. L. Jaber, "Epidemiology and outcomes of acute renal failure in hospitalized patients: a national survey," *Clinical Journal of the American Society of Nephrology*, vol. 1, no. 1, pp. 43–51, 2006.

[12] C.-Y. Hsu, G. M. Chertow, C. E. McCulloch, D. Fan, J. D. Ordoñez, and A. S. Go, "Nonrecovery of kidney function and death after acute on chronic renal failure," *Clinical Journal of the American Society of Nephrology*, vol. 4, no. 5, pp. 891–898, 2009.

[13] E. Selvin, C. M. Parrinello, D. B. Sacks, and J. Coresh, "Trends in prevalence and control of diabetes in the United States, 1988–1994 and 1999–2010," *Annals of Internal Medicine*, vol. 160, no. 8, pp. 517–525, 2014.

[14] A. Elixhauser, B. Friedman, and E. Stranges, "Septicemia in U.S., 2009," HCUP Statistical Brief #122. 2011, http://www.hcup-us.ahrq.gov/reports/statbriefs/sb122.pdf.

[15] G. F. Anderson and P. S. Hussey, "Population aging: a comparison among industrialized countries," *Health Affairs*, vol. 19, no. 3, pp. 191–203, 2000.

[16] V. L. Roger, "Epidemiology of heart failure," *Circulation Research*, vol. 113, no. 6, pp. 646–659, 2013.

[17] R. Mehran and E. Nikolsky, "Contrast-induced nephropathy: definition, epidemiology, and patients at risk," *Kidney International. Supplement*, no. 100, pp. S11–S15, 2006.

[18] K. Lang, H. Huang, D. W. Lee, V. Federico, and J. Menzin, "National trends in advanced outpatient diagnostic imaging utilization: an analysis of the medical expenditure panel survey, 2000–2009," *BMC Medical Imaging*, vol. 13, article 40, 2013.

[19] A. Hassan, A. Newman, D. T. Ko et al., "Increasing rates of angioplasty versus bypass surgery in Canada, 1994–2005," *American Heart Journal*, vol. 160, no. 5, pp. 958–965, 2010.

[20] A. J. Epstein, D. Polsky, F. Yang, L. Yang, and P. W. Groeneveld, "Coronary revascularization trends in the United States, 2001–2008," *The Journal of the American Medical Association*, vol. 305, no. 17, pp. 1769–1776, 2011.

[21] Y. Zhou, D. M. Boudreau, and A. N. Freedman, "Trends in the use of aspirin and nonsteroidal anti-inflammatory drugs in the general U.S. population," *Pharmacoepidemiology and Drug Safety*, vol. 23, no. 1, pp. 43–50, 2014.

[22] A. L. Pakyz, C. MacDougall, M. Oinonen, and R. E. Polk, "Trends in antibacterial use in US academic health centers: 2002 to 2006," *Archives of Internal Medicine*, vol. 168, no. 20, pp. 2254–2260, 2008.

[23] J. R. Brown, R. P. Cochran, L. J. Dacey et al., "Perioperative increases in serum creatinine are predictive of increased 90-day mortality after coronary artery bypass graft surgery," *Circulation*, vol. 114, no. 1, supplement, pp. I409–I413, 2006.

[24] J. R. Brown, D. J. Malenka, J. T. DeVries et al., "Transient and persistent renal dysfunction are predictors of survival after percutaneous coronary intervention: insights from the Dartmouth Dynamic Registry," *Catheterization and Cardiovascular Interventions*, vol. 72, no. 3, pp. 347–354, 2008.

[25] J. R. Brown, R. S. Kramer, S. G. Coca, and C. R. Parikh, "Duration of acute kidney injury impacts long-term survival after cardiac surgery," *The Annals of Thoracic Surgery*, vol. 90, no. 4, pp. 1142–1148, 2010.

[26] Healthcare Cost and Utilization Project, *HCUP Comorbidity Software*, 2013, http://www.hcup-us.ahrq.gov/toolssoftware/comorbidity/comorbidity.jsp.

[27] R. K. Hsu, C. E. McCulloch, R. A. Dudley, L. J. Lo, and C.-Y. Hsu, "Temporal changes in incidence of dialysis-requiring AKI," *Journal of the American Society of Nephrology*, vol. 24, no. 1, pp. 37–42, 2013.

[28] U.S. Census Bureau, "Population Estimates 2013," 2014, https://www.census.gov/popest/data/index.html.

[29] S. S. Waikar, R. Wald, G. M. Chertow et al., "Validity of international classification of diseases, ninth revision? Clinical modification codes for acute renal failure," *Journal of the American Society of Nephrology*, vol. 17, no. 6, pp. 1688–1694, 2006.

[30] J. R. Brown, R. Katz, J. H. Ix et al., "Fibroblast growth factor-23 and the long-term risk of hospital-associated AKI among community-dwelling older individuals," *Clinical Journal of the American Society of Nephrology*, vol. 9, no. 2, pp. 239–246, 2014.

[31] C. R. Lenihan, M. E. Montez-Rath, C. T. Mora Mangano, G. M. Chertow, and W. C. Winkelmayer, "Trends in acute kidney injury, associated use of dialysis, and mortality after cardiac surgery, 1999 to 2008," *Annals of Thoracic Surgery*, vol. 95, no. 1, pp. 20–28, 2013.

[32] L. S. Chawla, R. L. Amdur, A. D. Shaw, C. Faselis, C. E. Palant, and P. L. Kimmel, "Association between AKI and long-term renal and cardiovascular outcomes in United States veterans," *Clinical Journal of the American Society of Nephrology*, vol. 9, no. 3, pp. 448–456, 2014.

[33] J. L. Xue, F. Daniels, R. A. Star et al., "Incidence and mortality of acute renal failure in Medicare beneficiaries, 1992 to 2001," *Journal of the American Society of Nephrology*, vol. 17, no. 4, pp. 1135–1142, 2006.

[34] E. A. J. Hoste and M. Schurgers, "Epidemiology of acute kidney injury: how big is the problem?" *Critical Care Medicine*, vol. 36, supplement 4, pp. S146–S151, 2008.

[35] T. Z. Ali, I. Khan, W. Simpson et al., "Incidence and outcomes in acute kidney injury: a comprehensive population-based study," *Journal of the American Society of Nephrology*, vol. 18, no. 4, pp. 1292–1298, 2007.

[36] R. K. Hsu, C. E. McCulloch, E. Ku, R. A. Dudley, and C.-Y. Hsu, "Regional variation in the incidence of dialysis-requiring AKI in the United States," *Clinical Journal of the American Society of Nephrology*, vol. 8, no. 9, pp. 1476–1481, 2013.

[37] J. M. Boyle, S. Moualla, S. Arrigain et al., "Risks and outcomes of acute kidney injury requiring dialysis after cardiac transplantation," *American Journal of Kidney Diseases*, vol. 48, no. 5, pp. 787–796, 2006.

[38] C. M. Mangano, L. S. Diamondstone, J. G. Ramsay, A. Aggarwal, A. Herskowitz, and D. T. Mangano, "Renal dysfunction after myocardial revascularization: risk factors, adverse outcomes, and hospital resource utilization. The Multicenter Study of Perioperative Ischemia Research Group," *Annals of Internal Medicine*, vol. 128, no. 3, pp. 194–203, 1998.

[39] E. A. J. Hoste, G. Clermont, A. Kersten et al., "RIFLE criteria for acute kidney injury are associated with hospital mortality in critically ill patients: a cohort analysis," *Critical Care*, vol. 10, no. 3, article R73, 2006.

[40] J. R. Brown, M. E. Rezaee, E. L. Nichols, E. J. Marshall, E. D. Siew, and M. E. Matheny, "Incidence and in–hospital mortality of Acute Kidney Injury (AKI) and dialysis–requiring AKI (AKI–D) after cardiac catheterization in the national inpatient sample," *Journal of the American Heart Association*, vol. 5, no. 3, Article ID e002739, 2016.

[41] A. Mittalhenkle, C. O. Stehman-Breen, M. G. Shlipak et al., "Cardiovascular risk factors and incident acute renal failure in older adults: the cardiovascular health study," *Clinical Journal of the American Society of Nephrology*, vol. 3, no. 2, pp. 450–456, 2008.

Hindawi Publishing Corporation
BioMed Research International
Volume 2016, Article ID 5985903, 10 pages
http://dx.doi.org/10.1155/2016/5985903

Research Article

Valproic Acid Prevents Renal Dysfunction and Inflammation in the Ischemia-Reperfusion Injury Model

Elerson C. Costalonga,[1] Filipe M. O. Silva,[1] and Irene L. Noronha[1,2]

[1] *Laboratory of Cellular, Genetic, and Molecular Nephrology, Renal Division, University of São Paulo, 01246-903 São Paulo, SP, Brazil*
[2] *Center for Cellular and Molecular Studies and Therapy (NETCEM), University of São Paulo, 01246-903 São Paulo, SP, Brazil*

Correspondence should be addressed to Irene L. Noronha; irenenor@usp.br

Received 27 December 2015; Revised 29 February 2016; Accepted 27 March 2016

Academic Editor: Peter A. McCullough

Ischemia-reperfusion injury (IRI) is a major contributor to acute kidney injury (AKI). At present, there are no effective therapies to prevent AKI. The aim of this study was to analyse whether valproic acid (VPA), a histone deacetylase inhibitor with anti-inflammatory properties, prevents renal IRI. Male Wistar rats were divided into three groups: SHAM rats were subjected to a SHAM surgery, IRI rats underwent bilateral renal ischemia for 45 min, and IRI + VPA rats were treated with VPA at 300 mg/kg twice daily 2 days before bilateral IRI. Animals were euthanized at 48 hours after IRI. VPA attenuated renal dysfunction after ischemia, which was characterized by a decrease in BUN (mg/dL), serum creatinine (mg/dL), and FENa (%) in the IRI + VPA group (39 ± 11, 0.5 ± 0.05, and 0.5 ± 0.06, resp.) compared with the IRI group (145 ± 35, 2.7 ± 0.05, and 4.9 ± 1, resp.; $p < 0.001$). Additionally, significantly lower acute tubular necrosis grade and number of apoptotic cells were found in the IRI + VPA group compared to the IRI group ($p < 0.001$). Furthermore, VPA treatment reduced inflammatory cellular infiltration and expression of proinflammatory cytokines. These data suggest that VPA prevents the renal dysfunction and inflammation that is associated with renal IRI.

1. Introduction

The incidence of acute kidney injury (AKI) is increasing and it is associated with high mortality and healthcare costs [1, 2]. Despite an increase in the knowledge of AKI pathogenesis and epidemiology, AKI remains without any effective treatment. Renal ischemia-reperfusion injury (IRI) is a major contributor to AKI in different clinical conditions. In some of these conditions, such as transplantation, aortic surgeries, and other major surgeries, there is a favourable period of time to implement preventive measures. It seems reasonable to assume that preventing AKI can avoid a significant number of deaths.

IRI induces tubular epithelial cell dysfunction and death through apoptosis and necrosis. Local hemodynamic changes, endothelial injury, and inflammation represent hallmarks of ischemic injury of the kidney [3]. In this setting, damaged and necrotic tubular epithelial cells (TECs) play a central role by actively inducing the production of cytokines and other inflammatory mediators (TNF-α, MCP-1, and IL-6), leading to the accumulation of inflammatory cells, which in turn worsen cell necrosis in an autoamplification loop process [4]. In AKI, the blockade of the initial inflammatory renal response is associated with decreased cytokine production and inflammatory cell infiltration that hampers kidney injury following IRI [5–8]. Thus, interventions that ameliorate tubular necrosis, apoptosis, and inflammation are promising for the prevention of AKI secondary to IRI.

Acetylation of histone and nonhistone proteins is well known to regulate gene transcription and cell signalling pathways involved in inflammation and apoptosis. Two enzymes, histone acetyl transferase (HAT) and histone deacetylase (HDAC), mediate this process [9]. HDAC inhibitors (HDACi) are promising therapeutic options for inflammatory diseases [10, 11]. The anticonvulsivant valproic acid (VPA) has been recognized as an HDAC inhibitor [12]. VPA

inhibits nuclear factor κ-B (NFκ-B), TNF-α, and interleukin-6 (IL-6) production in human monocytic leukaemia cells stimulated with lipopolysaccharide [13]. VPA also reduced the inflammatory response and oxidative stress in septic mice in a model of caecum ligation and puncture, thereby protecting against renal injury [14]. In rats undergoing AKI due to haemorrhagic shock, the administration of VPA improved animal survival and inhibited the apoptosis of kidney cells [15]. VPA is an attractive HDACi because it has been clinically used for decades to treat epilepsy and mood disorders; it is cheap and available on the market.

Given that VPA modulates important pathways involved in AKI, we hypothesized that VPA might prevent the kidney dysfunction and inflammation that is induced in ischemia-reperfusion injury. Thus, the aim of this study was to evaluate the efficacy of VPA administration as a preventive intervention in an experimental renal IRI model. Specifically, we evaluated the ability of VPA to modulate inflammatory mediators and apoptosis in the injured kidney.

2. Materials and Methods

2.1. Animals. The experiments described were conducted using male Wistar rats weighing from 250 g to 300 g that were obtained from an established colony at the University of São Paulo, Brazil. The animals were housed in rodent cages in a 22°C room on a 12-hour light-dark cycle with free access to standard rat chow and water. All of the procedures received the approval of the Ethical Research Board of the University of São Paulo, Brazil (approval number: 381/13).

2.2. IRI Model and Study Design. All of the surgery procedures were performed under anaesthesia via the intraperitoneal administration of xylazine (36 mg/kg) and ketamine (5.7 mg/kg). During all of the procedures, animals were kept on a heat controlled thermal pad to maintain body temperature. Briefly, after a midline abdominal incision and careful dissection of the renal hilum, occlusion of the renal arteries of both kidneys with atraumatic vascular clamps for 45 minutes was performed to induce the experimental IRI. Clamps were removed and a remarkable change in the renal colour (pale to bright red) was observed ensuring good reperfusion. Animals were placed in heated cages until complete recovery from anaesthesia. Animals ($n = 26$) were divided into 3 groups, where SHAM ($n = 6$) rats were subjected to a SHAM surgery, IRI ($n = 10$) rats underwent IRI surgery and received vehicle administration, and IRI + VPA ($n = 10$) rats were treated with VPA (Abbot, Chicago, USA) at 300 mg/kg by gavage, twice daily, 2 days before the induction of IRI.

Animals were euthanized (pentobarbital sodium 100 mg/kg) at 48 hours after IRI, and then blood and kidney tissue samples were collected. The kidneys were perfused *in situ* and excised, and a midcoronal section was fixed in 10% phosphate buffered formalin. The other kidney sample was snap frozen and stored at −80°C for molecular analyses. One day before euthanasia, rats were placed in metabolic cages to collect 24-hour urine samples.

2.3. Biochemical Analysis. Serum and urinary creatinine (Cr), blood urea nitrogen (BUN), sodium, and potassium levels were measured using a Cobas C111 analyzer (Roche, Indianapolis, IN, United States). Fractional excretion of sodium (FeNa) and fractional excretion of potassium (FeK) were calculated. Urinary protein excretion was measured using a colorimetric assay (Labtest, Lagoa Santa, Brazil).

2.4. Acute Tubular Necrosis Grade. Kidneys sections (3 μm) were stained with Periodic-Acid Schiff (PAS). Markers of tubular damage (tubular dilation, necrosis, and cast formation) were graded by calculation of the percentage of tubules in the cortex and corticomedullary junction presenting these features [16]. The scores were as follows: 0, none; 1, 1%–10%; 2, 11%–25%; 3, 26%–45%; 4, 46%–75%; and 5, >75%. Twenty microscopic fields (×200) of the kidney cortex and corticomedullary junction from each animal were analysed blind to the groups.

2.5. TUNEL Apoptosis Assay. The apoptosis of tubular cells was evaluated using nonradioactive TdT-mediated fluorescein-dUTP nick end labelling technique (TUNEL; ApopTag Peroxidase *in situ* Apoptosis Detection Kit Millipore Corporation, Billerica, MA, USA) on paraffin-embedded tissue. Briefly, paraffin sections were deparaffinised, digested with proteinase K (20 g/mL), and incubated with hydrogen peroxidase to block endogenous peroxidase activity. After washing, slides were incubated with the TdT enzyme, then incubated with antidigoxigenin peroxidase, and developed using a substrate containing diaminobenzidine. Negative controls included the omission of TdT. Positive apoptotic cells presented a strong brown nuclear reactivity [17]. The number of apoptotic cells per high power field (×200) from 20 sections of corticomedullary junction was obtained from each animal, and the results were expressed as mean number of positive cells/mm^2.

2.6. Immunohistochemistry. Immunohistochemistry for inflammatory cells was carried out as previously described [18]. Paraffin-embedded renal biopsy specimens were processed for immunohistochemistry, and heating in citrate buffer, pH 6.0, was performed for antigenic recovery. After rinsing with pH 7.6 Tris-buffered saline (TBS), endogenous peroxidase activity was blocked and slides were incubated at 4°C overnight with the following monoclonal antibodies diluted in the primary antibody solution: anti-rat ED1 (Serotec, Oxford, UK) and anti-rat CD43 (Serolab, Oxford, UK). Both antibodies were diluted at 1 : 200. After primary antibodies incubation, the slides were submitted to another reaction with rat-biotinylated anti-mouse IgG (Vector Labs, Burlingame, USA) or with biotinylated anti-rabbit IgG (Vector Labs, Burlingame, USA). The streptavidin-biotin-alkaline phosphatase complex reaction was performed (Dako Co., Denmark). Finally, sections were incubated with a freshly prepared substrate consisting of naphthol-AS-MX-Phosphate (Sigma Chemical Co., St. Louis, USA) and fast red dye (Sigma Chemical Co., St. Louis, USA). Cellular proliferation was analysed using immunohistochemistry for proliferating cell

nuclear antigen (PCNA) as previously described [19]. Quantitative analysis of macrophages (ED1), T-cells (CD43), and cellular proliferative activity was performed in a blind fashion under magnification (×200) and was expressed as cells/mm^2. For each section, 20 microscopic fields were examined, and the results were expressed as the mean number of positive cells/mm^2.

2.7. Analyses of Inflammatory Mediators in Kidney Tissue. The mRNA expression of TNF-α, IL-6, and MCP-1 in kidney samples was analysed using quantitative PCR as previously described [18]. In brief, total RNA was extracted from kidney samples using the TRIZOL Reagent (Ambion, Austin, TX). After total RNA reverse-transcription into cDNA, quantitative PCR was carried out. Reactions were performed using the StepOne Plus Real-Time PCR system, and quantitative comparisons were obtained using the ΔΔCT method (Applied Biosystems, Singapore). The RT-PCR cycle profile was 10 min at 95°C, followed by 40 cycles of 15 s at 95°C for denaturation, 20 s at 60°C for combined annealing, and 10 s at 72°C for extension. The primer sequences for amplifying the target genes were (forward) 5′-TGGCCCAGACCCTCACACTCA-3′ and (reverse) 5′-GGCTCAGCCACTCCAGCTGC-3′ for TNF-α, (forward) 5′-CCGGAGAGGAGACTTCACAGA-GGA-3′ and (reverse) 5′-AGCCTCCGACTTGTGAAG-TGGTATA-3′ for IL-6, and (forward) 5′-GCCCCACTC-ACCTGCTGCT-3′ and (reverse) 5′-TCTTTGGGACAC-CTGCTGCTGG-3′ for Monocyte Chemoattractant Protein (MCP-1). The 18S rRNA was used as a housekeeping control (forward 5′-AGTCCCTGCCCTTTGTACACA-3′ and reverse 5′-GCCTCACTAAACCATCCAATCG-3′). The levels of TNF-α were measured in protein extracts of kidney tissue samples using a commercial MILLIPLEX® MAP Kit (Millipore Corporation, Billerica, MA, USA).

2.8. Serum Thiobarbituric Acid Reactive Substances. To evaluate systemic oxidative stress, serum levels of thiobarbituric acid reactive substances (TBARS) were measured using the thiobarbituric acid assay [20]. Briefly, a 0.2 mL serum sample was diluted in 0.8 mL of distilled water. Next, 1 mL of 17.5% trichloroacetic acid was added. Following the addition of 1 mL of 0.6% thiobarbituric acid, the sample was placed in a boiling water bath at 100°C for 15 min. After cooling, 1 mL of 70% trichloroacetic acid was added, and the mixture was incubated for 20 min. The sample was then centrifuged for 15 min at 2,000 rpm. The optical density of the supernatant was read at 534 nm using a spectrophotometer. The concentration of malondialdehyde (MDA) was calculated using a molar extinction coefficient of $1.56 \times 10^5\ M^{-1}\ cm^{-1}$ and was expressed as nmol/L.

2.9. Statistical Analysis. Data are presented as mean ± standard error of mean, and statistical analyses were performed with the Prism statistical program (GraphPad, San Diego, CA, USA). A one-way ANOVA with *post hoc* (Tukey) correction was used to compare all of the groups. To study the correlation between NTA grade, macrophages, and PCNA positive cells, a Pearson correlation coefficient was calculated. A p value < 0.05 was considered statistically significant.

Table 1: Effects of VPA on renal function and urinary biochemistry.

	SHAM ($n = 6$)	IRI ($n = 10$)	IRI + VPA ($n = 10$)
BUN (mg/dL)	13 ± 1	145 ± 35*	39 ± 11
Creatinine (mg/dL)	0.2 ± 0.0	2.7 ± 0.4*	0.5 ± 0.1
FENa (%)	0.2 ± 0.1	4.9 ± 1*	0.5 ± 0.1
FEK (%)	22 ± 3	129 ± 17*	17 ± 1.4
Urinary protein/creatinine	1.85 ± 0.2	3.9 ± 0.8	2.18 ± 0.2

BUN: blood urea nitrogen; FENa: fractional excretion of sodium; FEK: fraction excretion of potassium; IRI: ischemia-reperfusion injury; VPA: valproic acid.
Results are expressed as mean ± SEM. * $p < 0.001$ versus SHAM and IRI + VPA.

3. Results

3.1. Valproic Acid Prevented the Kidney Dysfunction Induced by IRI. In the IRI group, BUN and serum creatinine levels were significantly higher than the SHAM group. VPA therapy attenuated the renal dysfunction induced by IRI, as shown by the significantly lower BUN and creatinine levels in the IRI + VPA group (Table 1). As expected, FeNa and FeK were increased in the IRI compared with the SHAM group. Notably, tubular function was protected by VPA administration (Table 1).

3.2. Valproic Acid Protected Acute Tubular Necrosis and Apoptosis. The IRI model induced necrosis and detachment of tubular epithelial cells, hyaline casts, and tubular dilatation, resulting in a significant grade of acute tubular necrosis (ATN, Figure 1). When compared with the IRI group, the ATN associated with IRI injury was significantly attenuated in animals treated with VPA, in both cortico (4.4 ± 0.1 versus 2.9 ± 0.4; $p < 0.001$) and corticomedullary junctions (2.3 ± 0.3 versus 1.1 ± 0.1; $p < 0.001$, Figure 1). Apoptosis, an important process of tubular cell death in renal IRI, was evaluated using a TUNEL assay. The number of apoptotic cells was significantly increased in the IRI group, although treatment with VPA prevented the apoptosis of tubular cells (57 ± 6 versus 15 ± 1 cells/high power field; $p < 0.001$; Figure 1).

3.3. Valproic Acid Prevented Leukocyte Infiltration and Cellular Proliferation. Inflammatory infiltration in the renal interstitial compartment constitutes one important feature of IRI. In the SHAM group, few inflammatory cells were detected. However, there was a striking number of macrophages (ED1$^+$ cells) and T-cells (CD43$^+$ cells) infiltrating the interstitium of the kidney in the IRI group (resp., ED1$^+$ cells 13 ± 1 versus 141 ± 26 cells/mm^2, $p < 0.001$; T-cells 23 ± 5 versus 94 ± 15 cells/mm^2, $p < 0.001$). Treatment with VPA significantly reduced cellular inflammatory infiltration (ED1$^+$ cells 40 ± 7 cells/mm^2; T-cells 35 ± 4 cells/mm^2, $p < 0.001$) (Figure 2). A positive correlation was found between the

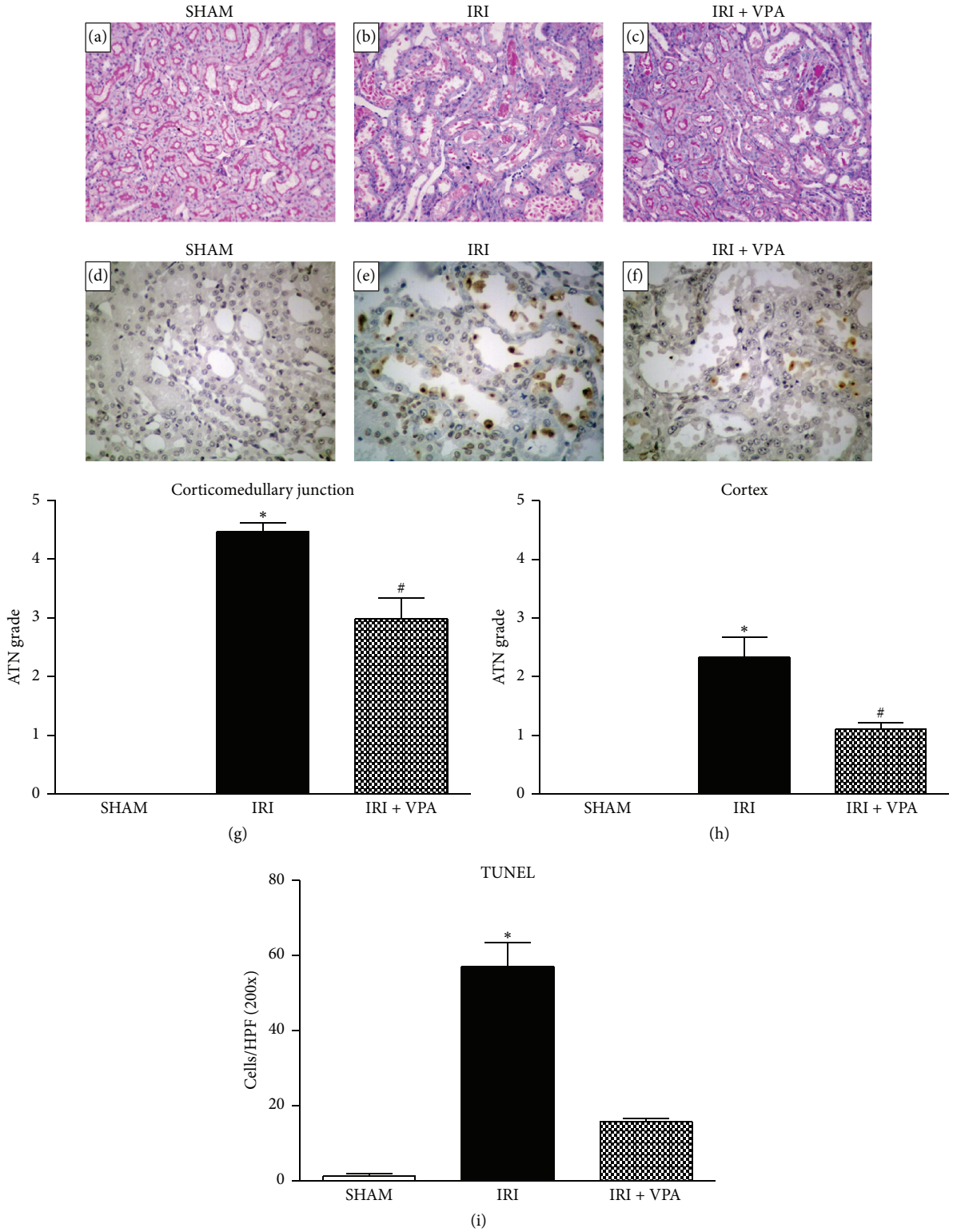

Figure 1: Effects of VPA in kidney acute tubular necrosis and apoptosis. (a)–(c) Representative photomicrographs of kidney sections stained with PAS (×200). (a) SHAM group. (b) IRI group showing an intense acute tubular necrosis (ATN). (c) In the IRI + VPA group, ATN was attenuated. (d)–(f) Representative photomicrographs of kidney sections (×400) stained with the TUNEL technique. (d) SHAM group. (e) IRI group showing a high number of apoptotic cells characterized by the presence of apoptotic bodies identified by brown staining. (f) VPA treatment attenuated apoptosis. (g, h) Graphs presenting the ATN grades in all of the groups. (i) Graph presenting the quantification of apoptotic cells in all of the groups. Results are expressed as mean ± standard error of mean. $^{*}p < 0.001$ versus SHAM and IRI + VPA. $^{\#}p < 0.001$ versus SHAM.

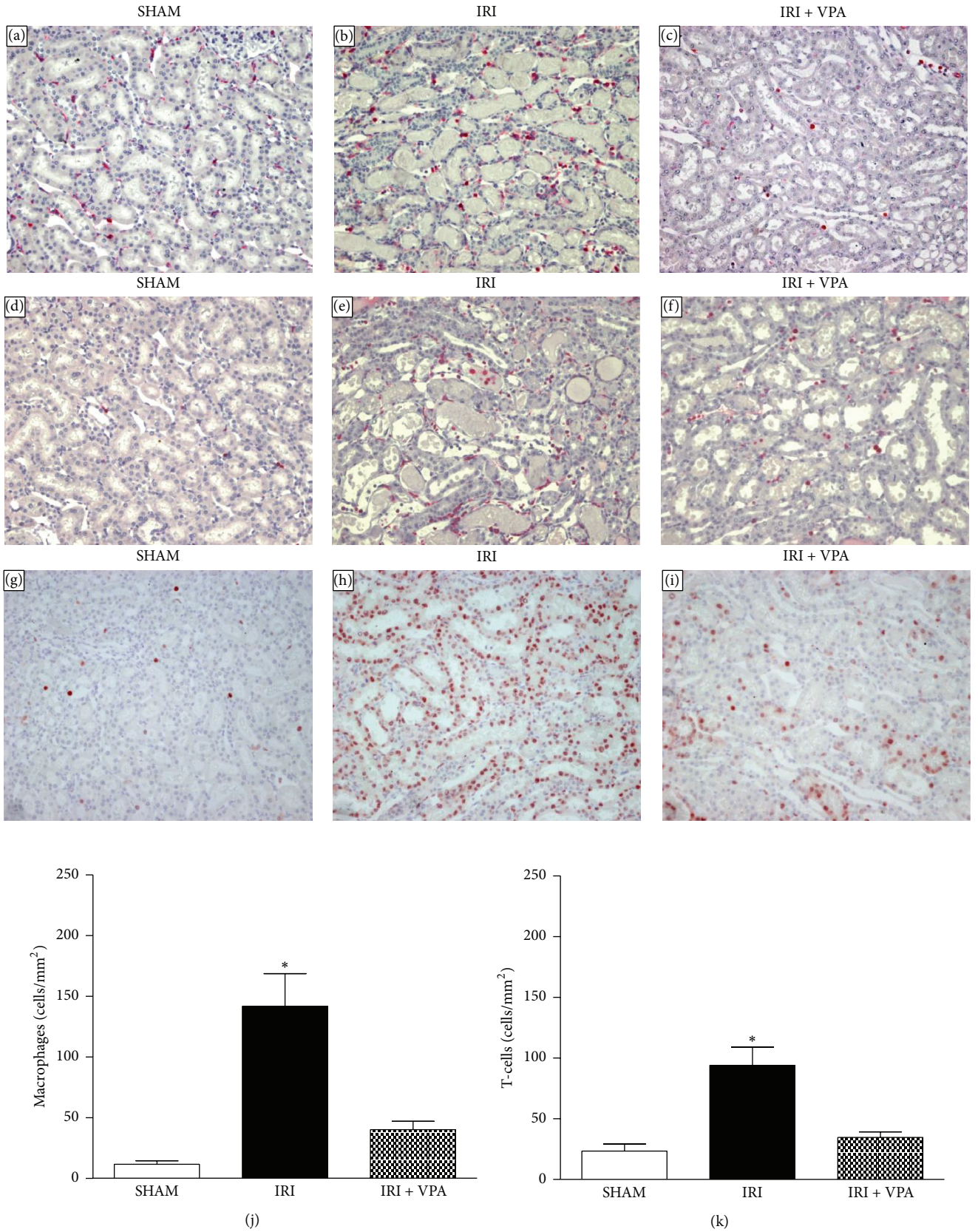

Figure 2: Continued.

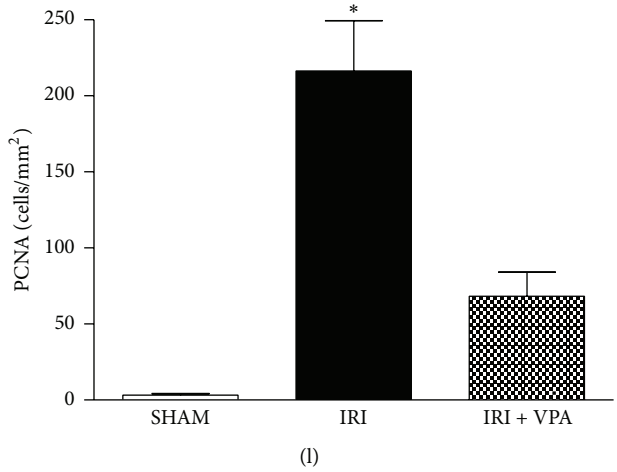

Figure 2: Immunohistochemistry for macrophages, T-cells, and proliferating cell nuclear antigen (PCNA). Representative photomicrographs (×100) of immunohistochemistry for macrophages (a)–(c), T-cells (d)–(f), and cellular proliferation (g)–(i). (a, d, g) SHAM groups. In the IRI group, an increased number of macrophages (b) and T-cells (e) were observed infiltrating the renal interstitium. Cellular proliferation activity was also markedly enhanced in the IRI group (h). VPA treatment significantly attenuated the number of mononuclear inflammatory cells and proliferative activity in the IRI model (c, f, i). Graph presenting the quantification of macrophages (j), T-cells (k), and PCNA (l). $^*p < 0.001$ versus SHAM and IRI + VPA.

number of interstitial macrophages and the ATN grade ($r^2 = 0.65$; $p = 0.02$). Furthermore, compared with the SHAM group, the IRI group showed a higher cellular proliferation, as measured by PCNA immunohistochemistry (3 ± 1 versus 216 ± 33 cells/mm^2, resp.; $p < 0.001$). Moreover, IRI + VPA animals showed a lower number of PCNA positive cells (68 ± 15 cells/mm^2, Figure 2). In addition, we found a positive significant correlation between the ATN grade and the number of PCNA positive cells ($r^2 = 0.67$; $p = 0.003$).

3.4. Valproic Acid Diminished the Upregulated Expression of Inflammatory Cytokines in the Kidney. To further explore whether VPA could reduce inflammation, real-time quantitative PCR (qPCR) for inflammatory cytokines, such as TNF-α, IL-6, and MCP-1, was performed (Figure 3). In the IRI group, mRNA levels of TNF-α, IL-6, and MCP-1 were significantly upregulated compared with the SHAM group. VPA treatment significantly reduced the gene expression of these cytokines in the renal tissue compared with the IRI group ($p < 0.01$, Figure 3). Moreover, in the IRI + VPA group, the increase of the TNF-α protein level induced by IRI was suppressed compared to the IRI group (SHAM group = 6.6 ± 0.4 versus IRI group = 10.0 ± 1.0 versus IRI + VPA group = 6.2 ± 0.7 pg/protein mg; $p < 0.01$).

3.5. Antioxidant Effect of Valproic Acid. Serum malondialdehyde (MDA), a marker of lipid peroxidation, was measured to evaluate systemic oxidative stress due to IRI. The IRI group showed a significant increase in the serum concentration of MDA. In contrast, VPA treatment resulted in an antioxidant effect (resp., 7.9 ± 0.4 versus 5.3 ± 0.3 nmol/L; $p < 0.01$). Notably, in the IRI + VPA group, the MDA concentration was maintained at a level similar to the control (Figure 4).

4. Discussion

The results of the present study demonstrated that administration of VPA was effective for preventing kidney dysfunction in the rat IRI experimental model. The rise in serum creatinine and BUN following IRI was reduced by VPA treatment. The tubular function was also protected, as confirmed by the lower FENa and FEK in VPA-treated animals compared to the IRI group. A marked decrease in acute tubular injury, apoptosis, and inflammation was also observed in IRI rats treated with VPA. The attenuation of all of these pathways may have contributed to the preservation of kidney function in the IRI + VPA group. Reduced levels of BUN and serum creatinine observed in VPA-treated animals in the present study are consistent with previous reports that investigated the effect of VPA in AKI, secondary to experimental haemorrhagic shock [15] and IRI [21]. Notably, no side effects such as cardiac arrest and sudden death, as described by Speir et al. [21], were observed in the present study in animals receiving VPA doses of 300 mg/kg twice daily. The absence of adverse effects was also reported in other experimental models using VPA at a similar dosage [15, 22–24].

Reduced acute tubular necrosis at 48 h after ischemia reperfusion confirmed the protective effect of VPA treatment. The actions of VPA in protection against IRI injury may be due to its ability to suppress inflammatory mediators [15, 21] and the oxidative stress [22, 25] that occurs following IRI. In addition, apoptosis of TECs is an important mechanism of cell death in renal IRI. VPA treatment in animals subjected to IRI inhibited the apoptosis of kidney cells, confirming previous findings [15, 21]. This effect is possibly related to the upregulation of the antiapoptotic BCL-2 expression [21]. These findings provide evidence of VPA preventing acute tubular necrosis and apoptosis in renal IRI.

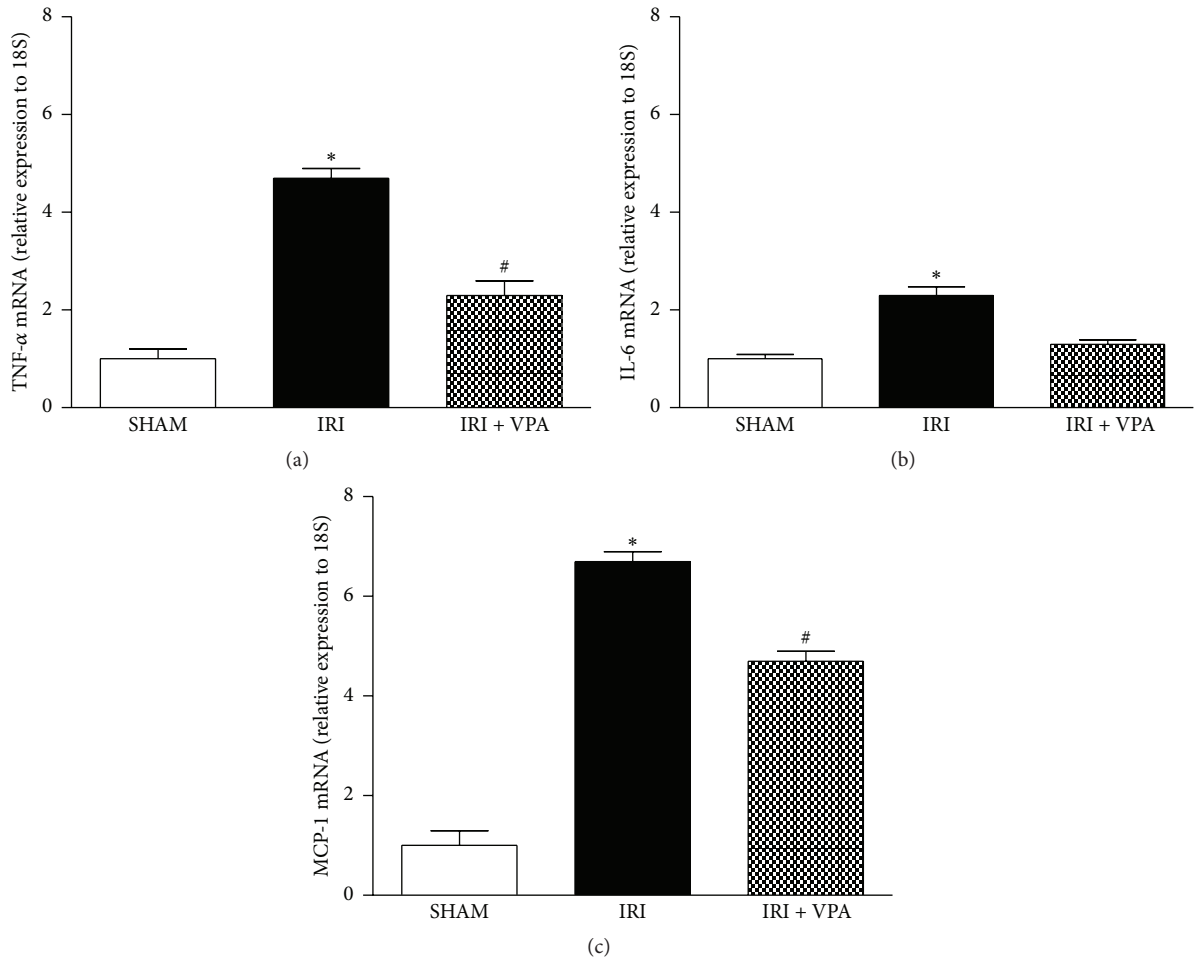

Figure 3: Renal expression of TNF-α, IL-6, and MCP-1 by qPCR in the IRI model. VPA prevented the increased expression of TNF-α, IL-6, and MCP-1 that is induced by IRI. $^{*}p < 0.001$ versus SHAM and IRI + VPA. $^{\#}p < 0.001$ versus SHAM.

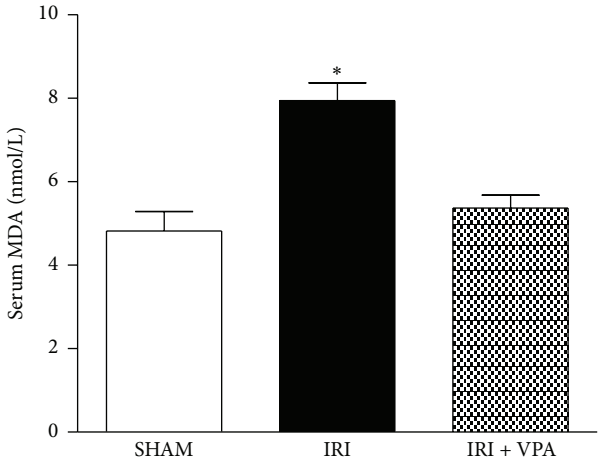

Figure 4: Antioxidant effect of VPA on the IRI model. Serum malondialdehyde (MDA), a marker of lipid peroxidation, was measured to evaluate the systemic oxidative stress in the IRI model. The IRI group showed a significant increase in the serum concentration of MDA. In contrast, the VPA treatment demonstrated an antioxidant effect. $^{*}p < 0.001$ versus SHAM and IRI + VPA.

In the present study, macrophages were the main interstitial inflammatory cells found 48 h after IRI. VPA treatment promoted a marked reduction of macrophages in the tubulointerstitial compartment. Likewise, VPA also reduced the macrophage infiltration in an adriamycin nephropathy model [26]. These results can be attributed to the inhibitory effect of VPA in the expression of inflammatory cytokines involved in leukocyte trafficking, such as TNF-α and MCP-1 [26, 27]. Another interesting finding was the positive correlation between the ATN grade and the number of macrophages, highlighting the interplay between inflammation and TEC necrosis. Necrotic TECs are considered to be important sources of inflammation that activate reminiscent tubular cells to produce cytokines that promote inflammatory cell infiltration [3]. Subsequently, the attenuation of macrophage infiltration may be the result of a lower tubular necrosis grade in the VPA-treated group.

The number of T-cells detected in the kidney at 48 h after IRI was also lower in animals treated with VPA. In the early period after IRI, $CD4^{+}$ T-cells are the primary pathogenic T-cells. In nu/nu mice (CD4 and CD8 T-cell-deficient mice),

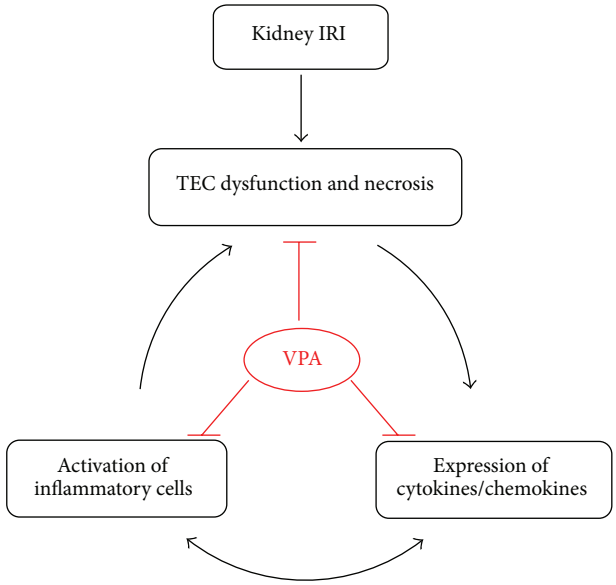

Figure 5: Possible effects of VPA on the kidney inflammation that is induced by ischemia-reperfusion injury. Acute kidney injury (AKI) following ischemia-reperfusion injury (IRI) leads to tubular epithelial cell (TEC) dysfunction, necrosis, and endothelial activation, which in turn induces the production of proinflammatory cytokines and infiltration of inflammatory cells into the kidney, in addition to an increase in the expression of cytokines and chemokines. This autoamplification loop of inflammation and tubular damage leads to an extension of kidney damage, despite the interruption of ischemia. In the IRI model, valproic acid (VPA) attenuated kidney dysfunction and acute tubular necrosis. These findings were associated with a marked decrease of macrophage and T-cell infiltration and proliferative activity and an inhibition of proinflammatory cytokines and chemokines (TNF-α and MCP-1).

renal IRI was significantly reduced compared to wild-type controls and reconstitution with $CD4^+$ T-cells alone restored kidney injury [28]. Thus, the reduction of lymphocytes in the kidney of VPA-treated animals contributed to the protection of kidney function and structure.

The analysis of cellular proliferation by PCNA immunostaining showed that VPA-treated animals presented lower renal tubular cellular proliferation than the IRI + VPA group. There was also a significant positive correlation between ATN and cellular proliferation. After IRI there is an intense increase in TEC turnover to replace necrotic and apoptotic cells [3]. The results observed in the present study suggest that the reduction of cellular proliferation is secondary to a lower grade of ATN presented by rats receiving VPA. However, VPA may directly inhibit cellular proliferation. MS-275, a class I HDAC inhibitor similar to VPA, reduced the expression of PCNA in AKI that is induced by rhabdomyolysis [29]. Although VPA protected kidney function in the present study, the inhibition of cellular proliferation may have a detrimental effect on tubular regeneration.

There is increasing evidence of the anti-inflammatory effects of VPA [30]. In our experiments, we observed significantly lower expression of proinflammatory genes TNF-α, IL-6, and MCP-1 in the kidneys of VPA-treated animals compared to the IRI group, which confirmed previous reports [31, 32]. This effect may be due to the inhibition of NF-κB signalling, a key transcription factor involved in inflammatory gene activation [31, 32]. Moreover, in early kidney IRI, macrophages synthesize TNF-α, which in turn stimulates inflammation and apoptosis [8], thereby promoting extension of the injury. The exposure to VPA significantly repressed the production of TNF-α in the mouse macrophage cell line RAW264.7 that was stimulated with LPS [33]. Thus, the inhibition of TNF-α production by VPA may account for its beneficial effect in kidney IRI.

In the present study, the increased MCP-1 mRNA expression induced by IRI in the kidney was attenuated by VPA pretreatment. In a previous report, the magnitude of renal IRI was diminished in mice lacking the receptor for MCP-1 [34]. Through unknown mechanisms, VPA was shown to reduce the expression of MCP-1 in different experimental models [26, 27]. Thus, the inhibition of MCP-1 expression by VPA may have hampered the macrophage infiltration preventing inflammation and extension of kidney damage.

VPA reduced lipid peroxidation, as evidenced by the lower levels of MDA found in the IRI + VPA group in comparison to the IRI group. Oxidative stress has an important role in the pathogenesis of ATN [3]. In previous studies, VPA administration prevented kidney dysfunction, reduced superoxide anion generation, and increased the activity of antioxidant enzymes after ischemic and septic kidney injuries [14, 25]. Hence, in this study, VPA may have prevented kidney dysfunction through antioxidant mechanisms.

It should be pointed out that the present study has some limitations. So far, the exact mechanism of VPA effects could not be entirely understood. As reported in previous studies, VPA might offer kidney protection by increasing histone acetylation and enhancing the expression of genes involved in apoptosis inhibition [21]. Considering that acetylation modulates the activity of nonhistone proteins, it can be hypothesized that VPA could modulate molecular activity of some transcription factors, such as NF-κB. It has been shown that acetylation of p65 NF-κB subunit reduces the binding of NF-κB to promoter regions and facilitates its IκBα-dependent nuclear export [35]. Furthermore, we studied the effect of VPA in the first 48 hours following kidney IRI. Whether the beneficial effect of VPA on kidney function will be maintained in the long term remains an open question and deserves further investigation. The present study confirmed previous findings about the beneficial effects of HDACi and VPA in the treatment of IRI.

5. Conclusion

In summary, AKI following IRI is associated with the production of proinflammatory cytokines and the infiltration of inflammatory cells into the kidney. This process leads to an extension of kidney damage despite a cessation of the ischemic stimuli. We have demonstrated that VPA prevented kidney dysfunction and structural injury after kidney IRI. VPA affected kidney inflammatory cell infiltration and the expression of important proinflammatory cytokines (TNF-α and MCP-1), demonstrating the anti-inflammatory effect

of VPA on kidney IRI (Figure 5). VPA may represent a new treatment option for the prevention of kidney ischemia-reperfusion injury, but future studies are needed to investigate its efficacy and safety.

Competing Interests

The authors declare that there is no conflict of interests regarding the publication of this study.

References

[1] E. Macedo and R. L. Mehta, "Preventing acute kidney injury," *Critical Care Clinics*, vol. 31, no. 4, pp. 773–784, 2015.

[2] P. Susantitaphong, D. N. Cruz, J. Cerda et al., "World incidence of AKI: a meta-analysis," *Clinical Journal of the American Society of Nephrology*, vol. 8, no. 9, pp. 1482–1493, 2013.

[3] J. V. Bonventre and L. Yang, "Cellular pathophysiology of ischemic acute kidney injury," *Journal of Clinical Investigation*, vol. 121, no. 11, pp. 4210–4221, 2011.

[4] S. R. Mulay, A. Linkermann, and H. Anders, "Necroinflammation in kidney disease," *Journal of the American Society of Nephrology*, vol. 27, no. 1, pp. 27–39, 2015.

[5] K. J. Kelly, W. W. Williams Jr., R. B. Colvin et al., "Intercellular adhesion molecule-1-deficient mice are protected against ischemic renal injury," *The Journal of Clinical Investigation*, vol. 97, no. 4, pp. 1056–1063, 1996.

[6] L. Li and M. D. Okusa, "Blocking the immune response in ischemic acute kidney injury: the role of adenosine 2A agonists," *Nature Clinical Practice Nephrology*, vol. 2, no. 8, pp. 432–444, 2006.

[7] S. Lee, S. Huen, H. Nishio et al., "Distinct macrophage phenotypes contribute to kidney injury and repair," *Journal of the American Society of Nephrology*, vol. 22, no. 2, pp. 317–326, 2011.

[8] R. Di Paola, T. Genovese, D. Impellizzeri, A. Ahmad, S. Cuzzocrea, and E. Esposito, "The renal injury and inflammation caused by ischemia-reperfusion are reduced by genetic inhibition of TNF-αR1: a comparison with infliximab treatment," *European Journal of Pharmacology*, vol. 700, no. 1–3, pp. 134–146, 2013.

[9] M. A. Glozak, N. Sengupta, X. Zhang, and E. Seto, "Acetylation and deacetylation of non-histone proteins," *Gene*, vol. 363, no. 1-2, pp. 15–23, 2005.

[10] F. J. Dekker, T. van den Bosch, and N. I. Martin, "Small molecule inhibitors of histone acetyltransferases and deacetylases are potential drugs for inflammatory diseases," *Drug Discovery Today*, vol. 19, no. 5, pp. 654–660, 2014.

[11] N. Liu and S. Zhuang, "Treatment of chronic kidney diseases with histone deacetylase inhibitors," *Frontiers in Physiology*, vol. 6, article 121, 2015.

[12] B. Monti, E. Polazzi, and A. Contestabile, "Biochemical, molecular and epigenetic mechanisms of valproic acid neuroprotection," *Current Molecular Pharmacology*, vol. 2, no. 1, pp. 95–109, 2009.

[13] T. Ichiyama, K. Okada, J. M. Lipton, T. Matsubara, T. Hayashi, and S. Furukawa, "Sodium valproate inhibits production of TNF-α and IL-6 and activation of NF-κB," *Brain Research*, vol. 857, no. 1-2, pp. 246–251, 2000.

[14] Q. Zheng, W. Liu, Z. Liu, H. Zhao, X. Han, and M. Zhao, "Valproic acid protects septic mice from renal injury by reducing the inflammatory response," *Journal of Surgical Research*, vol. 192, no. 1, pp. 163–169, 2014.

[15] N. Zacharias, E. A. Sailhamer, Y. Li et al., "Histone deacetylase inhibitors prevent apoptosis following lethal hemorrhagic shock in rodent kidney cells," *Resuscitation*, vol. 82, no. 1, pp. 105–109, 2011.

[16] N. M. Rogers, A. W. Thomson, and J. S. Isenberg, "Activation of parenchymal CD47 promotes renal ischemia-reperfusion injury," *Journal of the American Society of Nephrology*, vol. 23, no. 9, pp. 1538–1550, 2012.

[17] I. L. Noronha, S. G. Oliveira, T. S. Tavares et al., "Apoptosis in kidney and pancreas allograft biopsies," *Transplantation*, vol. 79, no. 9, pp. 1231–1235, 2005.

[18] H. Dellê, J. R. C. Rocha, R. C. Cavaglieri, J. M. Vieira Jr., D. M. A. C. Malheiros, and I. L. Noronha, "Antifibrotic effect of tamoxifen in a model of progressive renal disease," *Journal of the American Society of Nephrology*, vol. 23, no. 1, pp. 37–48, 2012.

[19] R. J. Ramalho, P. S. de Oliveira, R. C. Cavaglieri et al., "Hyperbaric oxygen therapy induces kidney protection in an ischemia/reperfusion model in rats," *Transplantation Proceedings*, vol. 44, no. 8, pp. 2333–2336, 2012.

[20] L. V. B. Pereira, M. H. M. Shimizu, L. P. M. R. Rodrigues, C. C. Leite, L. Andrade, and A. C. Seguro, "N-Acetylcysteine protects rats with chronic renal failure from gadolinium-chelate nephrotoxicity," *PLoS ONE*, vol. 7, no. 7, Article ID e39528, 2012.

[21] R. W. Speir, J. D. Stallings, J. M. Andrews, M. S. Gelnett, T. C. Brand, and S. K. Salgar, "Effects of Valproic acid and dexamethasone administration on early bio-markers and gene expression profile in acute kidney ischemia-reperfusion injury in the rat," *PLoS ONE*, vol. 10, no. 5, Article ID e0126622, 2015.

[22] Z. Zhang, X. Qin, X. Zhao et al., "Valproic acid regulates antioxidant enzymes and prevents ischemia/reperfusion injury in the rat retina," *Current Eye Research*, vol. 37, no. 5, pp. 429–437, 2012.

[23] M. K. Tso, E. Lass, J. Ai, and R. Loch Macdonald, "Valproic acid treatment after experimental subarachnoid hemorrhage," in *Neurovascular Events after Subarachnoid Hemorrhage*, J. Fandino, S. Marbacher, A.-R. Fathi, C. Muroi, and E. Keller, Eds., vol. 120 of *Acta Neurochirurgica Supplement*, pp. 81–85, 2015.

[24] Z. Wang, L.-K. Tsai, J. Munasinghe et al., "Chronic valproate treatment enhances postischemic angiogenesis and promotes functional recovery in a rat model of ischemic stroke," *Stroke*, vol. 43, no. 9, pp. 2430–2436, 2012.

[25] R. Brar, J. P. Singh, T. Kaur, S. Arora, and A. P. Singh, "Role of GABAergic activity of sodium valproate against ischemia-reperfusion-induced acute kidney injury in rats," *Naunyn-Schmiedeberg's Archives of Pharmacology*, vol. 387, no. 2, pp. 143–151, 2014.

[26] K. Van Beneden, C. Geers, M. Pauwels et al., "Valproic acid attenuates proteinuria and kidney injury," *Journal of the American Society of Nephrology*, vol. 22, no. 10, pp. 1863–1875, 2011.

[27] D.-I. Sinn, S.-J. Kim, K. Chu et al., "Valproic acid-mediated neuroprotection in intracerebral hemorrhage via histone deacetylase inhibition and transcriptional activation," *Neurobiology of Disease*, vol. 26, no. 2, pp. 464–472, 2007.

[28] M. J. Burne, F. Daniels, A. El Ghandour et al., "Identification of the $CD4^+$ T cell as a major pathogenic factor in ischemic acute renal failure," *The Journal of Clinical Investigation*, vol. 108, no. 9, pp. 1283–1290, 2001.

[29] J. Tang, Y. Yan, T. C. Zhao et al., "Class I HDAC activity is required for renal protection and regeneration after acute kidney injury," *American Journal of Physiology-Renal Physiology*, vol. 307, no. 3, pp. F303–F316, 2014.

[30] S. Chateauvieux, F. Morceau, M. Dicato, and M. Diederich, "Molecular and therapeutic potential and toxicity of valproic acid," *Journal of Biomedicine and Biotechnology*, vol. 2010, Article ID 479364, 18 pages, 2010.

[31] Z. Zhang, N. Tong, Y. Gong et al., "Valproate protects the retina from endoplasmic reticulum stress-induced apoptosis after ischemia-reperfusion injury," *Neuroscience Letters*, vol. 504, no. 2, pp. 88–92, 2011.

[32] S.-Y. Wu, S.-E. Tang, F.-C. Ko, G.-C. Wu, K.-L. Huang, and S.-J. Chu, "Valproic acid attenuates acute lung injury induced by ischemia-reperfusion in rats," *Anesthesiology*, vol. 122, no. 6, pp. 1327–1337, 2015.

[33] C. Wu, A. Li, Y. Leng, Y. Li, and J. Kang, "Histone deacetylase inhibition by sodium valproate regulates polarization of macrophage subsets," *DNA and Cell Biology*, vol. 31, no. 4, pp. 592–599, 2012.

[34] K. Furuichi, T. Wada, Y. Iwata et al., "CCR2 signaling contributes to ischemia-reperfusion injury in kidney," *Journal of the American Society of Nephrology*, vol. 14, no. 10, pp. 2503–2515, 2003.

[35] R. Kiernan, V. Brès, R. W. M. Ng et al., "Post-activation turn-off of NF-κB-dependent transcription is regulated by acetylation of p65," *The Journal of Biological Chemistry*, vol. 278, no. 4, pp. 2758–2766, 2003.

Hindawi Publishing Corporation
BioMed Research International
Volume 2016, Article ID 4634386, 10 pages
http://dx.doi.org/10.1155/2016/4634386

Research Article

Inhibitor of DNA Binding 1 Is Induced during Kidney Ischemia-Reperfusion and Is Critical for the Induction of Hypoxia-Inducible Factor-1α

Dan Wen,[1] Yan-Fang Zou,[1] Yao-Hui Gao,[2] Qian Zhao,[3] Yin-Yin Xie,[4] Ping-Yan Shen,[1] Yao-Wen Xu,[1] Jing Xu,[1] Yong-Xi Chen,[1] Xiao-Bei Feng,[1] Hao Shi,[1] and Wen Zhang[1]

[1]*Department of Nephrology, Ruijin Hospital, School of Medicine, Shanghai Jiaotong University, Shanghai 200025, China*
[2]*Department of Science and Education, MinHang Central Hospital, Shanghai, China*
[3]*Shanghai Universities E-Institute for Chemical Biology, Key Laboratory of Cell Differentiation and Apoptosis of National Ministry of Education, School of Medicine, Shanghai Jiaotong University, Shanghai 200025, China*
[4]*Shanghai Institute of Hematology, Shanghai, China*

Correspondence should be addressed to Hao Shi; shihaohp@163.com and Wen Zhang; zhangwen255@163.com

Received 21 November 2015; Revised 25 February 2016; Accepted 28 February 2016

Academic Editor: Jeremiah R. Brown

In this study, rat models of acute kidney injury (AKI) induced by renal ischemia-reperfusion (I/R) and HK-2 cell models of hypoxia-reoxygenation (H/R) were established to investigate the expression of inhibitor of DNA binding 1 (ID1) in AKI, and the regulation relationship between ID1 and hypoxia-inducible factor 1 alpha (HIF-1α). Through western blot, quantitative real-time PCR, immunohistochemistry, and other experiment methods, the induction of ID1 after renal I/R in vivo was observed, which was expressed mainly in renal tubular epithelial cells (TECs). ID1 expression was upregulated in in vitro H/R models at both the protein and mRNA levels. Via RNAi, it was found that ID1 induction was inhibited with silencing of HIF-1α. Moreover, the suppression of ID1 mRNA expression could lead to decreased expression and transcription of HIF-1α during hypoxia and reoxygenation. In addition, it was demonstrated that both ID1 and HIF-1α can regulate the transcription of twist. This study demonstrated that ID1 is induced in renal TECs during I/R and can regulate the transcription and expression of HIF-1α.

1. Introduction

Ischemia-reperfusion- (I/R-) induced acute kidney injury (AKI) is a common clinical event and frequently results in the development of chronic kidney disease (CKD) or end-stage renal disease, leading to high mortality [1]. Tubular epithelial cells (TECs) are vulnerable to renal I/R injury, contributing significantly to the loss of kidney function [2]. Following I/R injury to the kidneys, the TECs, which have a relatively high oxygen requirement, are easily injured, because hypoxia can trigger a series of reactions and lead to cell apoptosis and/or necrosis and tissue damage. However, renal TECs have the potential to regenerate after ischemia. The normal repair process after TECs injury is critical for the recovery of kidney function and structure.

Hypoxia-inducible factor-1 alpha (HIF-1α) is a master gene switch for major adaptive responses to hypoxia. It is a basic helix-loop-helix (bHLH) transcription factor that is degraded during normoxia. During hypoxia, HIF-1α accumulates and dimerizes with constitutively expressed HIF-1β and mediates the expression of target genes, including erythropoietin and vascular endothelial growth factor [3]. Many studies have demonstrated that HIF-1α is activated in AKI with or without ischemia and serves to ameliorate AKI by improving hypoxia [4]. Thus, HIF-1α is critical for the survival of TECs [5]. As the normal expression of HIF-1α plays an important role in the survival of TECs, regulators of HIF-1α at the transcriptional or protein level might have potential applications. Kim et al. found that inhibitor of DNA binding 1 (ID1) can enhance the stability and activity of

HIF-1α in human endothelial and breast cancer cells [6]. Whether ID1 can regulate HIF-1α in TECs has not been reported, and the relationship between ID1 and HIF-1α remains to be completely understood.

ID1 is also a bHLH transcription factor and is referred to as an inhibitor of DNA binding because it does not possess a basic DNA-binding domain. The ID family functions as dominant-negative regulators of other bHLH proteins through the formation of inactive heterodimers with intact bHLH transcription factors [7]. Overexpression of ID1 is associated with cell dedifferentiation and proliferation in several cell lineages [8]. It has been shown that the expression of ID1 is increased in CKD models [9]. However, the role of ID1 in kidney I/R injury is not clear, and whether hypoxia can upregulate ID1 in TECs remains to be explored.

Based on the possibility of ID1 induction in AKI and the potential relationship between ID1 and HIF-1α, the authors hypothesized that ID1 is an important factor in AKI that may be induced under hypoxia and may regulate the expression of HIF-1α in TECs. In the present study, the expression of ID1 in both in vitro and in vivo kidney I/R models was evaluated and its effects on HIF-1α expression in HK-2 cells were analyzed. It was observed that ID1 expression was upregulated during I/R and hypoxia-reoxygenation (H/R) and that ID1 can regulate HIF-1α expression at the transcriptional level.

2. Materials and Methods

2.1. Rat Kidney I/R Injury Model. Male Sprague-Dawley rats weighing 250–280 g were obtained from the Animal Center of Ruijin Hospital. The experimental protocol was approved by the Ethics Committee for Animal Care and Use of the Research Center for Experimental Medicine of Ruijin Hospital. These rats were divided into groups of 5-6 animals for each condition. Renal I/R injury was applied under inhalational anesthetics by clamping bilateral renal pedicles for 45 min, and the animals were kept on a warming table at 37°C during the surgery. Rats in the sham group were operated using the same procedure without clamping. Rats were sacrificed at different time points before ischemia and during reperfusion, and their blood and kidney cortex specimens were obtained for analysis.

2.2. Renal Function Test. Serum creatinine and blood urea nitrogen, recognized as renal function indexes, were measured in serum samples collected from rats. The detection methods for the 2 parameters were described previously [10].

2.3. Cell Culture and H/R Model. Human proximal tubular cells (HK-2, CRL-2190) were purchased from ATCC. HK-2 cells were cultured in Dulbecco's Modified Eagle's Medium (DMEM/F12 medium; GIBCO) containing 10% fetal bovine serum (FBS; GIBCO) in a humidified atmosphere with 5% CO_2 at 37°C. The medium was changed every 2 days, and all experiments were performed using cells in a 70%–90% confluent monolayer. For exposure to hypoxia, new complete medium was added to cell monolayers after 24 hours of serum starvation. Culture plates were placed in a humidified hypoxic chamber (Thermo Electron) with an atmosphere of 1% O_2, 94% N_2, and 5% CO_2 for 24 hours. After exposure to hypoxia, the medium was refreshed again and the plates were moved to a normoxic cell incubator (21% O_2 and 5% CO_2).

2.4. Immunohistochemistry. Parts of kidney cortex specimens were fixed in 10% neutral buffered formalin, and 4 μm paraffin-embedded kidney sections were treated with peroxidase blocking solution and goat serum (Fuzhou Maixin, China) at room temperature. The sections were incubated with primary antibodies (ID1; Santa Cruz Biotechnology, HIF-1α; Santa Cruz Biotechnology) overnight at 4°C and then with biotinylated anti-IgG secondary antibody (Fuzhou Maixin, China). Streptavidin conjugated with horseradish peroxidase (HRP) was used to identify biotin, which was visualized by staining with DAB solution (Fuzhou Maixin, China). Sections were imaged with a spot-cam digital camera (Carl Zeiss).

2.5. Western Blot Analysis. Kidney cortex tissue that had been stored at −80°C was homogenized in radioimmunoprecipitation (RIPA) buffer (Sigma-Aldrich) containing phenylmethylsulfonyl fluoride for 30 min on ice followed by centrifugation (12,000 rpm, 20 min) at 4°C and collection of supernatants. HK-2 cells were washed with phosphate-buffered saline (PBS) and lysed in cell lysis buffer containing 4% sodium dodecyl sulfate, 20% glycerol, 100 mM dithiothreitol, and Tris-HCl, pH 6.8. The cell lysates were also centrifuged (12,000 rpm, 10 min) at 4°C. Then, 40 μg of supernatant proteins was loaded and separated by 8%–15% sodium dodecyl sulfate-polyacrylamide gel electrophoresis. Proteins were transferred to a polyvinylidene difluoride membrane (Millipore) after electrophoresis. The blot was blocked with 5% dried skim milk in Tris-buffered saline containing 0.1% Tween-20 (TBST) at room temperature for 2 hours, followed by incubation with primary antibodies overnight at 4°C. Dilutions of 1 : 2000 for β-actin (Santa Cruz Biotechnology), 1 : 1000 for HIF-1α (BD Transduction Laboratories, Abclonal), 1 : 200 for ID1 (Santa Cruz Biotechnology), 1 : 1000 for vimentin (Santa Cruz Biotechnology), and 1 : 200 for twist (Santa Cruz Biotechnology) were used. The membranes were washed and then incubated with HRP-conjugated secondary antibodies (Cell Signaling Technology) at room temperature for 2 hours. After several washes, the proteins were visualized with enhanced chemiluminescence (ECL) kits (Amersham) and quantified by gray scale analysis by using ImageJ software (National Institutes of Health). For all western blots, β-actin was used as an internal control.

2.6. Quantitative Real-Time PCR. Total RNA was extracted from HK-2 cells using TRIzol reagent (Invitrogen). Reverse transcription for cDNA synthesis was performed with a High Capacity cDNA Reverse Transcription Kit (Invitrogen). Expression levels of ID1, HIF-1α, vimentin, twist, and β-actin were quantified by real-time PCR using SYBR Premix Ex Taq (TaKaRa, Dalian, China) according to the manufacturer's cycling protocol, and amplification was performed on triplicate samples. The PCR primers used were as follows: ID1 sense (5′-CTACGACATGAACGGCTGTTACTC-3′) and ID1 antisense (5′-CTTGCTCACCTTGCGGTTCT-3′),

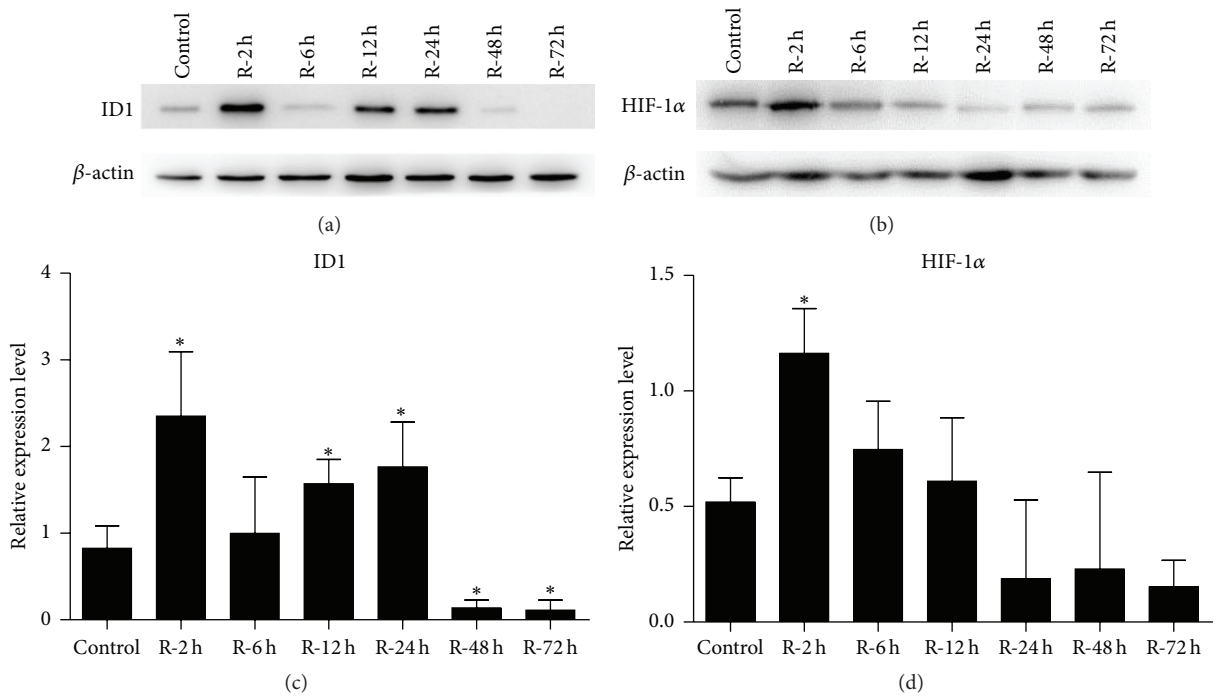

Figure 1: ID1 and HIF-1α protein induction in the rat I/R injury model. (a, b) Western blot analysis of ID1 and HIF-1α expression in the kidney cortex after I/R. The expression of β-actin was examined as the loading control. A representative blot from 3 independent experiments is shown. (c, d) The histogram shows the average volume densities corrected for β-actin ($n = 3$). $^*P < .05$ compared with the preischemia controls. ID1, inhibitor of DNA binding 1; HIF-1α, hypoxia-inducible factor-1 alpha; I/R, ischemia-reperfusion.

HIF-1α sense (5′-GTTTACTAAAGGACAAGTCACC-3′) and HIF-1α antisense (5′-TTCTGTTTGTTGAAGGGAG-3′), vimentin sense (5′-CCAGAGGGAGTGAATCCAGA-3′) and vimentin antisense (5′-AGATGGCCCTTGACA-TTGAG-3′), twist sense (5′-GCAAGATTCAGACCCTCA-AG-3′) and twist antisense (5′-CATCCTCCAGACCGA-GAAG-3′), and β-actin sense (5′-GATCTTCGGCACCCA-GCACAATGAAGATC-3′) and β-actin antisense (5′-AAG-TCATAGTCCGCCTAGAAGCAT-3′). Gene expression was expressed as $2^{-\Delta\Delta(Ct)}$, and the control samples were unstimulated cells.

2.7. Small Interfering RNA Transfection in HK-2 Cells. The small interfering RNA (siRNA) technique was used for gene silencing. SiRNA for ID1 and HIF-1α and a negative control were designed and purchased from Invitrogen (ID1-siRNA-427, ID1-siRNA-269, ID1-siRNA-529; HIF-1α-siRNA-1511, HIF-1α-siRNA-964, and HIF-1α-siRNA-2107). HK-2 cells were cultured in 6-well plates, and complete medium was removed at 50%–60% confluence when Opti-MEM (Invitrogen) was added. ID1 or HIF-1α siRNA and negative siRNA were diluted in Opti-MEM and incubated with diluted Lipofectamine RNAiMAX Reagent (Invitrogen) for 5 min according to the manufacturer's protocol. SiRNA-lipid complexes were added to cells and 25 pmol siRNA was used per well. After 24 hours, the medium was replaced by DMEM/F12 medium containing 10% FBS, and the plates were moved to the hypoxic chamber for application of the H/R procedure as described above. Western blot and real-time PCR analyses were used to confirm the transfection efficiency.

2.8. Statistical Analysis. All data were expressed as mean ± standard deviation (SD), and the results for 2 groups were compared by t tests. Multigroup comparisons were made using one-way analysis of variance (ANOVA). Probability values of <.05 were considered to be statistically significant. All statistical analyses were performed with SPSS software (Version 11.0; SPSS, Inc.).

3. Results

3.1. ID1 and HIF-1α Expressions Are Induced after Renal I/R In Vivo. To investigate ID1 and HIF-1α expression in vivo, the I/R model in Sprague-Dawley rats was established as described previously [10]. Western blot analysis of kidney cortex showed the induction of ID1 and HIF-1α expression during reperfusion in vivo. ID1 expression was elevated immediately and transiently after reperfusion for 2 hours, and a reinduction was observed after reperfusion for 12 hours (Figure 1(a)). After statistical analysis of the grey level, ID1 was determined to be induced significantly after reperfusion for 2, 12, and 24 hours, and it was markedly reduced after 48 and 72 hours of reperfusion (Figure 1(c)). HIF-1α protein was elevated after reperfusion for 2 hours (Figure 1(b)), and the analysis of the grey level showed significant upregulation of it (Figure 1(d)).

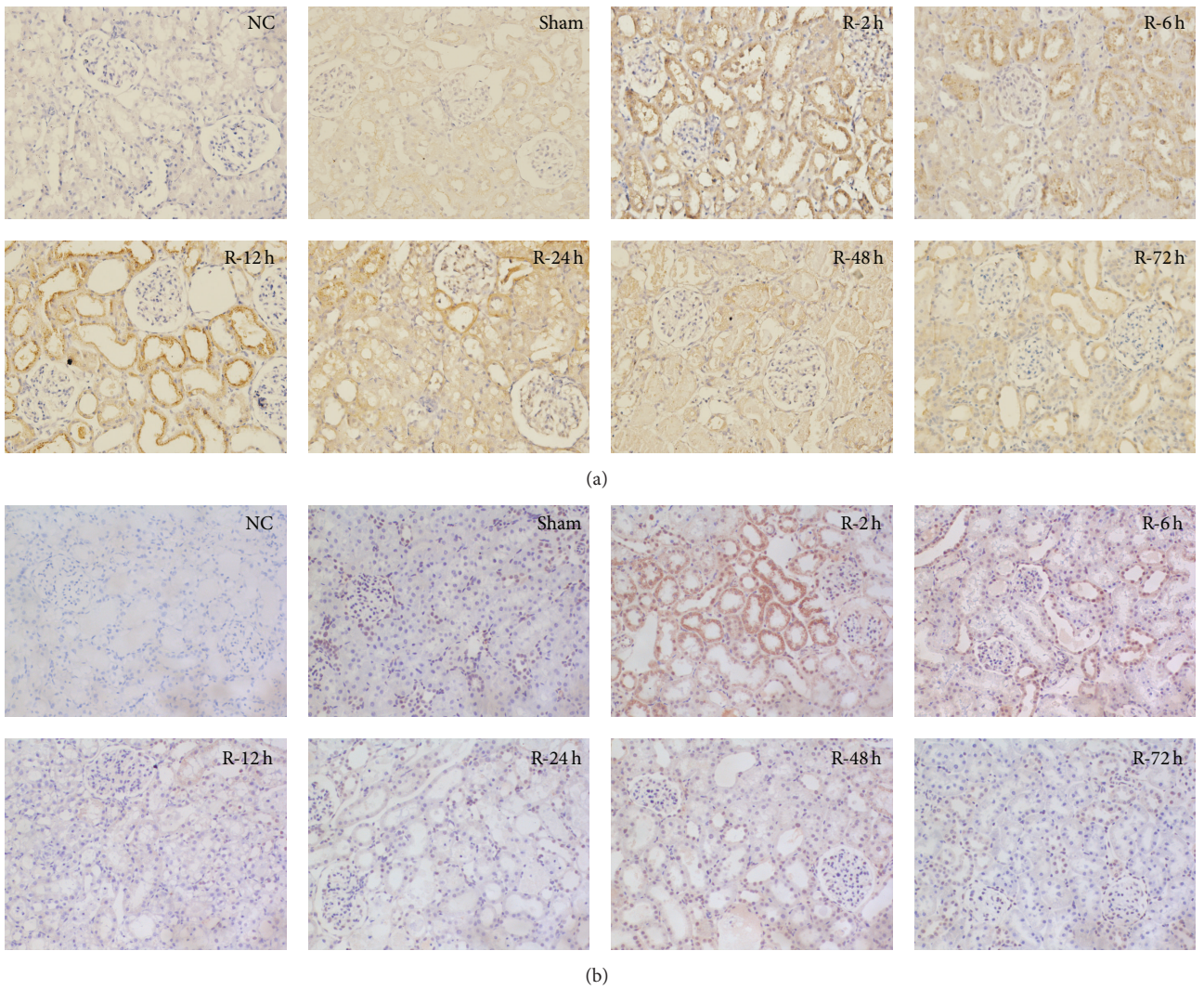

FIGURE 2: Location of ID1 and HIF-1α expression in I/R-injured rat kidney tissue. Immunohistochemical staining for ID1 and HIF-1α in the kidney tissue of I/R and sham-operated rats. (a) Increased staining for ID1 in renal TECs after 2, 6, 12, and 24 hours of reperfusion. (b) Increased staining for HIF-1α in renal TECs after 2 hours of reperfusion. Original magnification, ×200. ID1, inhibitor of DNA binding 1; HIF-1α, hypoxia-inducible factor-1 alpha; I/R, ischemia-reperfusion; TECs, tubular epithelial cells.

Immunohistochemical staining was applied to determine the location of ID1 and HIF-1α expression. As expected, ID1 was mainly expressed in the cytoplasm of renal TECs and was strongly expressed after reperfusion for 2 and 12 hours (Figure 2(a)). HIF-1α was mainly expressed in TECs, in both the cytoplasm and the nucleus. The elevated expression of HIF-1α was observed after reperfusion for 2 hours (Figure 2(b)).

3.2. Establishment of H/R Model in HK-2 Cells. To study ID1 expression in vitro, an H/R model in HK-2 cells was established, which reproduces the renal I/R injury process to a great extent. Because there is no standard or classical H/R model, a preliminary study was conducted, and the authors found that oxygen deprivation for 24 hours may mimic in vivo I/R. The expression of HIF-1α and dedifferentiation-related markers were the main indicators for determining the establishment of the H/R model in this study.

The detailed dynamic expression of HIF-1α and vimentin by western blot (Figures 3(a) and 3(b)) was observed. HIF-1α expression was induced obviously during hypoxia and reduced immediately at the beginning of reoxygenation, followed by a transient induction during reoxygenation. Vimentin expression was increased gradually and significantly upregulated during the reoxygenation phase. qRT-PCR was performed to estimate the mRNA levels of HIF-1α and vimentin (Figures 3(c) and 3(d)). The HIF-1α mRNA levels were significantly changed during the latter half of hypoxia and reoxygenation. In addition, there was an upregulation of vimentin at the transcription level.

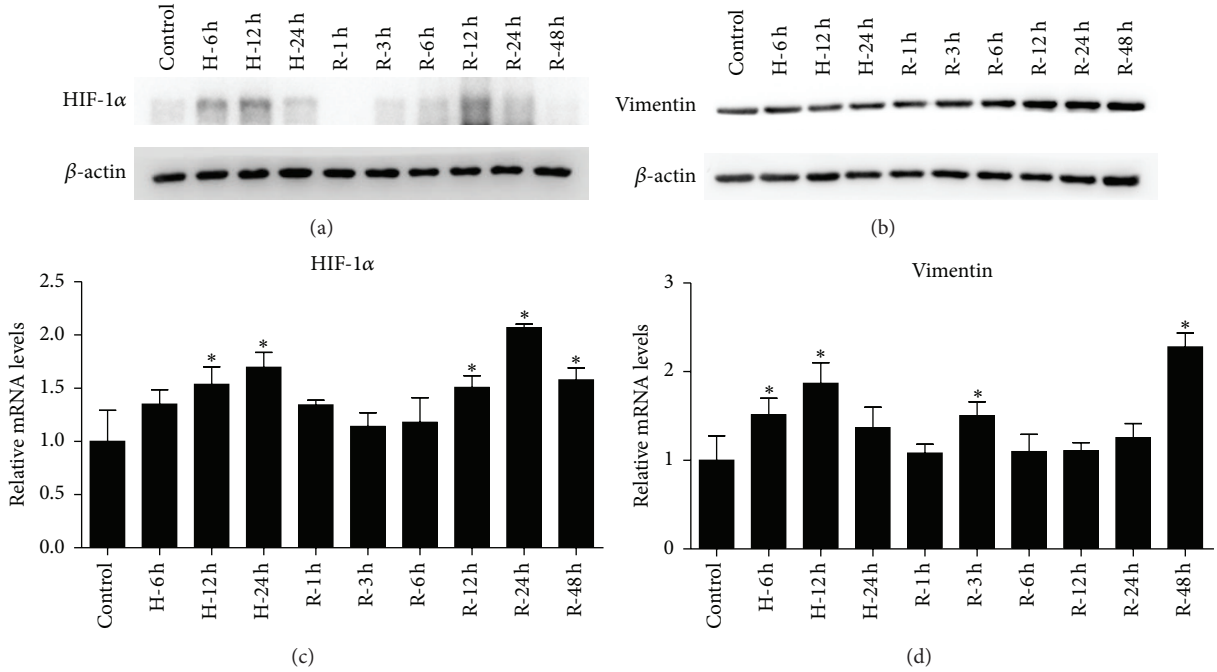

Figure 3: HIF-1α and vimentin induction in the HK-2 cell H/R model. (a, b) Western blot analysis of HIF-1α and vimentin in HK-2 cells under hypoxia (H) and reoxygenation (R). Cells for reoxygenation experienced 24 hours of hypoxia. β-actin was examined as the loading control. A representative blot from 3 independent experiments is shown. (c, d) Quantitative RT-PCR was used for the analysis of HIF-1α and vimentin mRNA levels in HK-2 cells under H/R. Data are expressed as mean ± SD for HIF-1α and vimentin levels using β-actin mRNA as an internal control ($n = 3$). $^*P < .05$ compared with the prehypoxia controls. HIF-1α, hypoxia-inducible factor-1 alpha; H/R, hypoxia-reoxygenation.

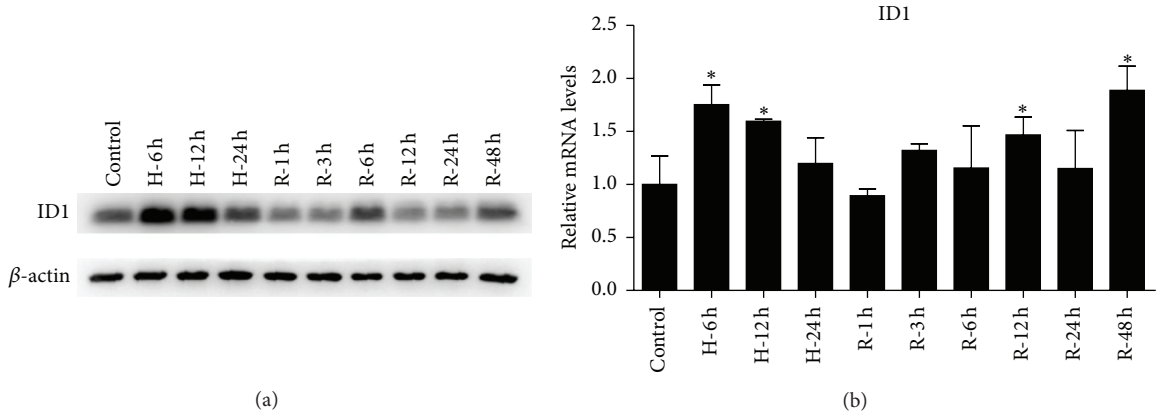

Figure 4: ID1 induction in HK-2 cells H/R model. (a) Western blot analysis of ID1 in HK-2 cells under hypoxia (H) and reoxygenation (R). Cells for reoxygenation experienced 24 hours of hypoxia. β-actin served as the loading control. A representative blot from 3 independent experiments is shown. (b) Quantitative RT-PCR was used for analysis of ID1 mRNA levels in HK-2 cells under H/R. Data are expressed as mean ± SD for ID1 levels. β-actin mRNA served as the internal control ($n = 3$). $^*P < .05$ compared with the prehypoxia controls. ID1, inhibitor of DNA binding 1; H/R, hypoxia-reoxygenation.

These results suggest that HIF-1α is induced during both hypoxia and reoxygenation and that HIF-1α is regulated more sensitively and earlier at the protein level than at the transcriptional level. The upregulation of vimentin indicates a dedifferentiation process in this model.

3.3. ID1 Expression Is Induced during H/R and Is Regulated by HIF-1α. After establishment of the H/R model in HK-2 cells, ID1 expression was assessed through western blot and qRT-PCR. The expression of ID1 was significantly increased during hypoxia and reduced following reoxygenation (Figure 4(a)). After 6 and 48 hours of reoxygenation, ID1 was upregulated again, although not remarkably. Moreover, the mRNA levels of ID1 were markedly elevated during hypoxia and reinduced after reoxygenation (Figure 4(b)).

Subsequently, siRNAs for HIF-1α were used to investigate whether ID1 was mediated by HIF-1α. The expression of

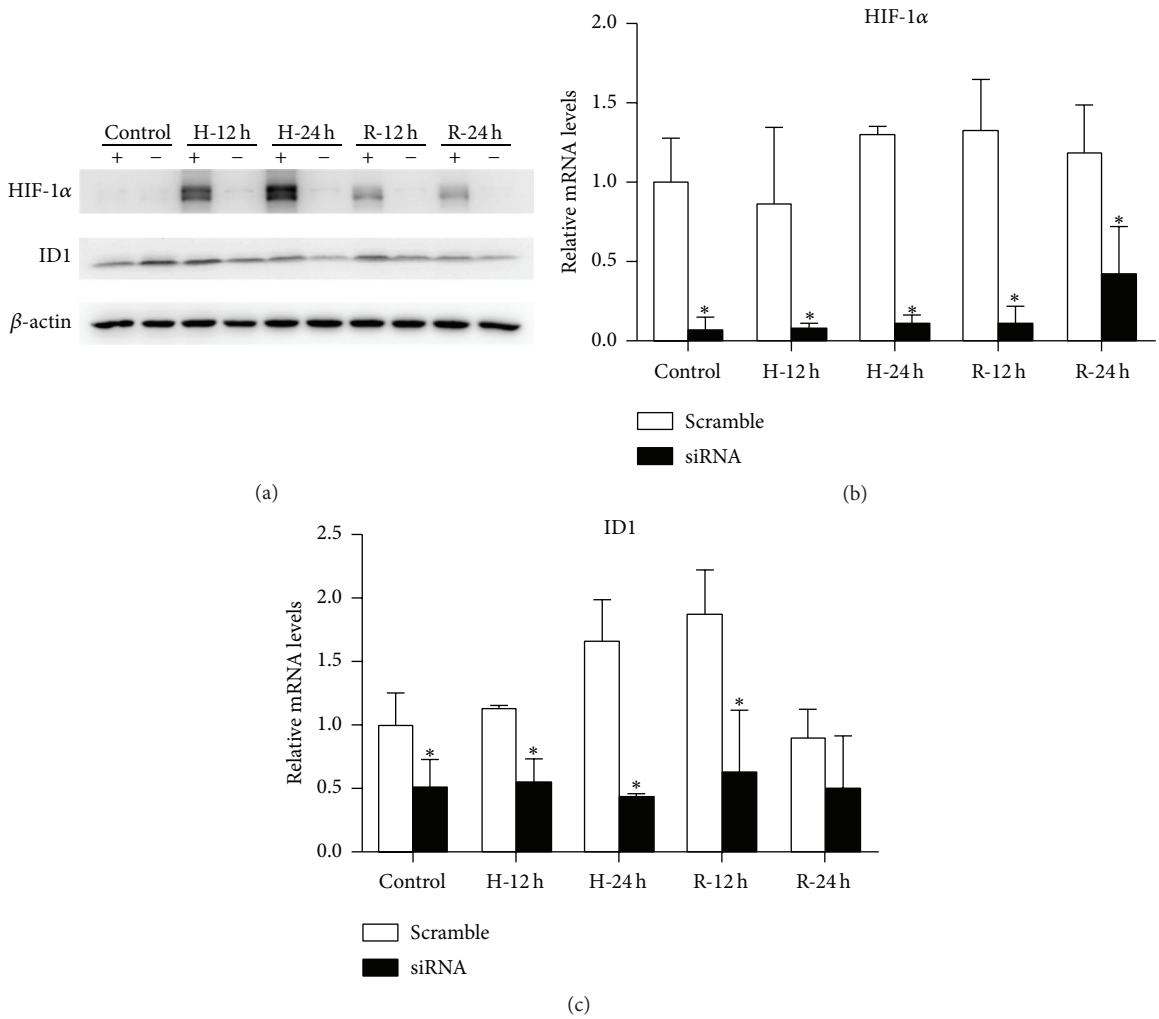

Figure 5: HIF-1α is required for ID1 induction in the H/R model. HK-2 cells were transiently transfected with specific siRNA for HIF-1α or siRNA for negative control and then subjected to H/R. (a) In cells transfected with HIF-1α siRNA, the expression of HIF-1α was markedly inhibited and ID1 was suppressed, although not remarkable. β-actin served as the loading control. A representative blot from 3 independent experiments is shown. (b, c) In cells transfected with HIF-1α siRNA, relative mRNA levels of HIF-1α were efficiently reduced. Relative mRNA levels of ID1 were decreased significantly at the prehypoxia, 12-hour and 24-hour time points for hypoxia, and after 12 hours of reoxygenation. β-actin mRNA was used as the internal control ($n = 3$). $^*P < .05$ compared with the negative control (scramble). ID1, inhibitor of DNA binding 1; HIF-1α, hypoxia-inducible factor-1 alpha; H/R, hypoxia-reoxygenation.

HIF-1α was inhibited and this outcome was confirmed by western blot and qRT-PCR (Figures 5(a) and 5(b)). Cells in which HIF-1α expression was suppressed showed reduced expression of ID1 through H/R, and mRNA levels were significantly downregulated (Figures 5(a) and 5(c)). The results indicate that ID1 is induced in the H/R model and is regulated by HIF-1α.

3.4. ID1 Regulates the Induction of HIF-1α Expression in Response to H/R In Vitro. To study the function of ID1, siRNA was used to inhibit ID1 expression. The mRNA levels of ID1 were lowered significantly through the whole H/R process, and the protein levels were also reduced markedly (Figures 6(a) and 6(b)).

As ID1 was inhibited, the protein expression of HIF-1α was reduced after exposure to hypoxia for 24 hours (Figure 6(a)). The mRNA levels of HIF-1α were suppressed significantly at the end of the hypoxic treatment and the early stage of reoxygenation (Figure 6(c)). These results demonstrate that ID1 is critical for the induction of HIF-1α expression during H/R in HK-2 cells, and ID1 can regulate HIF-1α expression at the transcription level.

3.5. Twist Is Induced in the H/R Model and Is Regulated by HIF-1α and ID1. Twist is a bHLH transcription factor that can be induced by HIF-1α in TECs subjected to hypoxia [11]. In the present study, the expression of twist in the H/R model was observed. Twist was induced during hypoxia and reoxygenation at the protein level (Figure 7(a)).

To explore whether twist could be mediated by HIF-1α, the changes in twist when HIF-1α was silenced by siRNA transfection were measured (Figure 7(b)). Silencing HIF-1α

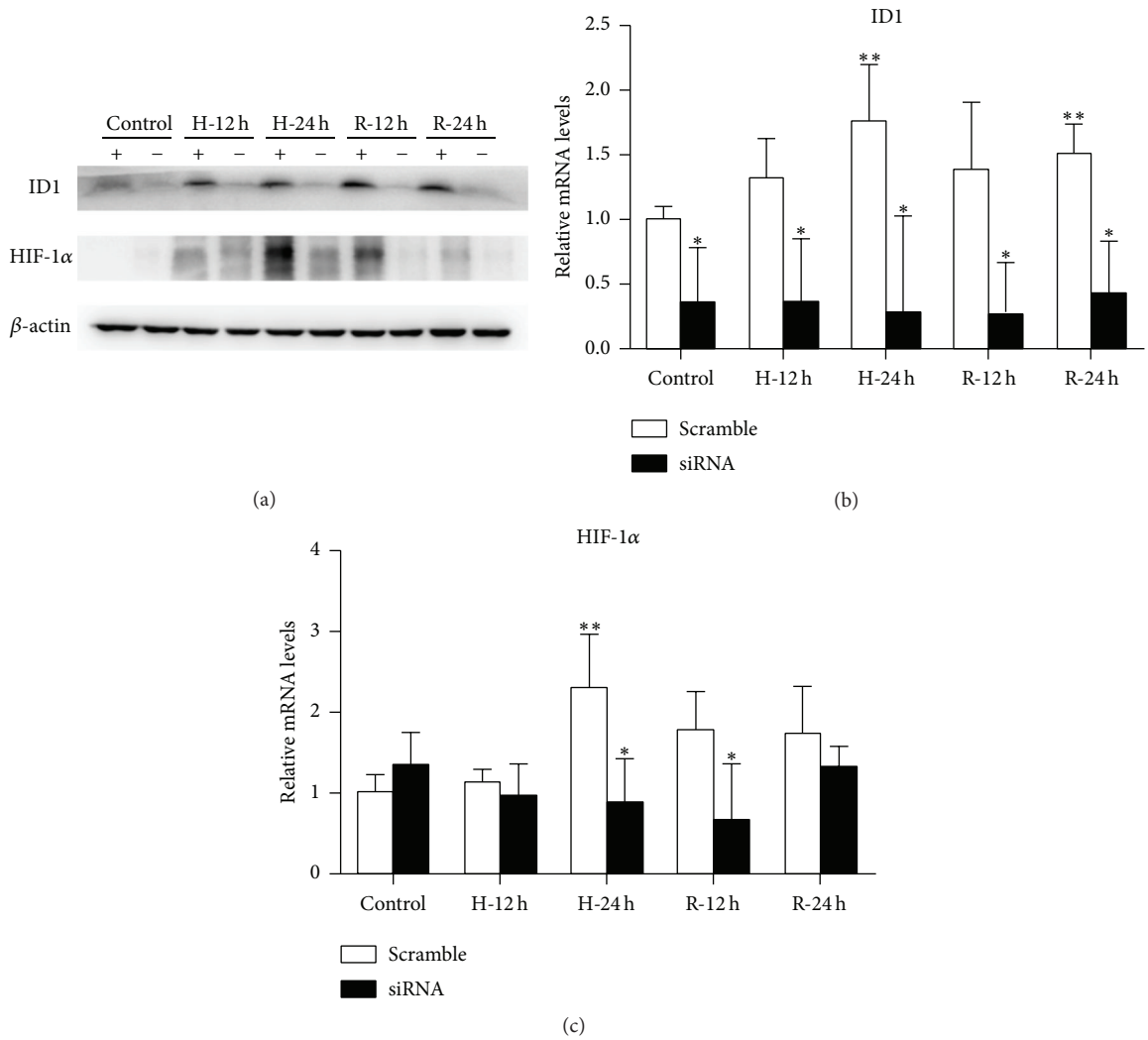

Figure 6: ID1 is required for HIF-1α induction in the H/R model. HK-2 cells were transiently transfected with specific siRNA for ID1 or siRNA for negative control and then subjected to H/R. (a) In cells transfected with ID1 siRNA, the expression of ID1 was markedly inhibited. HIF-1α protein expression was remarkably suppressed after exposure to hypoxia for 24 hours or to reoxygenation for 12 or 24 hours. β-actin expression was examined as the loading control. A representative blot from 3 independent experiments is shown. (b, c) In cells transfected with ID1 siRNA, relative mRNA levels of ID1 were efficiently reduced. Relative mRNA levels of HIF-1α were decreased significantly after 24 hours of hypoxia and 12 hours of reoxygenation. β-actin mRNA served as an internal control ($n = 3$). $^{*}P < .05$ compared with the negative control (scramble). $^{**}P < .05$ compared with the prehypoxia controls. ID1, inhibitor of DNA binding 1; HIF-1α, hypoxia-inducible factor-1 alpha; H/R, hypoxia-reoxygenation.

could reduce the mRNA levels of twist in HK-2 cells during H/R, showing that HIF-1α may regulate the expression of twist at the transcriptional level. In addition, the mRNA levels of twist were decreased as ID1 was repressed endogenously (Figure 7(c)). Thus, twist seems to be regulated by both ID1 and HIF-1α.

4. Discussion

In this study, the authors observed the induction of ID1 in rat renal I/R injury and demonstrated that its expression was mainly localized in TECs. In the in vitro H/R model, ID1 was upregulated during both hypoxia and reoxygenation. The expression of HIF-1α was observed to be suppressed by siRNA and ID1 was found to be inhibited at the transcriptional level, which suggests that HIF-1α may regulate the induction of ID1 in the H/R model. In addition, according to previous findings, ID1 may have the ability to regulate HIF-1α [6]. Hence, the authors inhibited the expression of ID1 and demonstrated that ID1 could regulate HIF-1α at the transcriptional level and was critical for the induction of HIF-1α during H/R.

The renal I/R injury model is already a mature animal model that mimics clinical situations. In a previous study [10], the authors successfully established the renal I/R model that was applied in the present study. However, there is no in vitro I/R model that is generally accepted worldwide. Sauvant et al. set up an in vitro model of I/R, in which NRK-52E

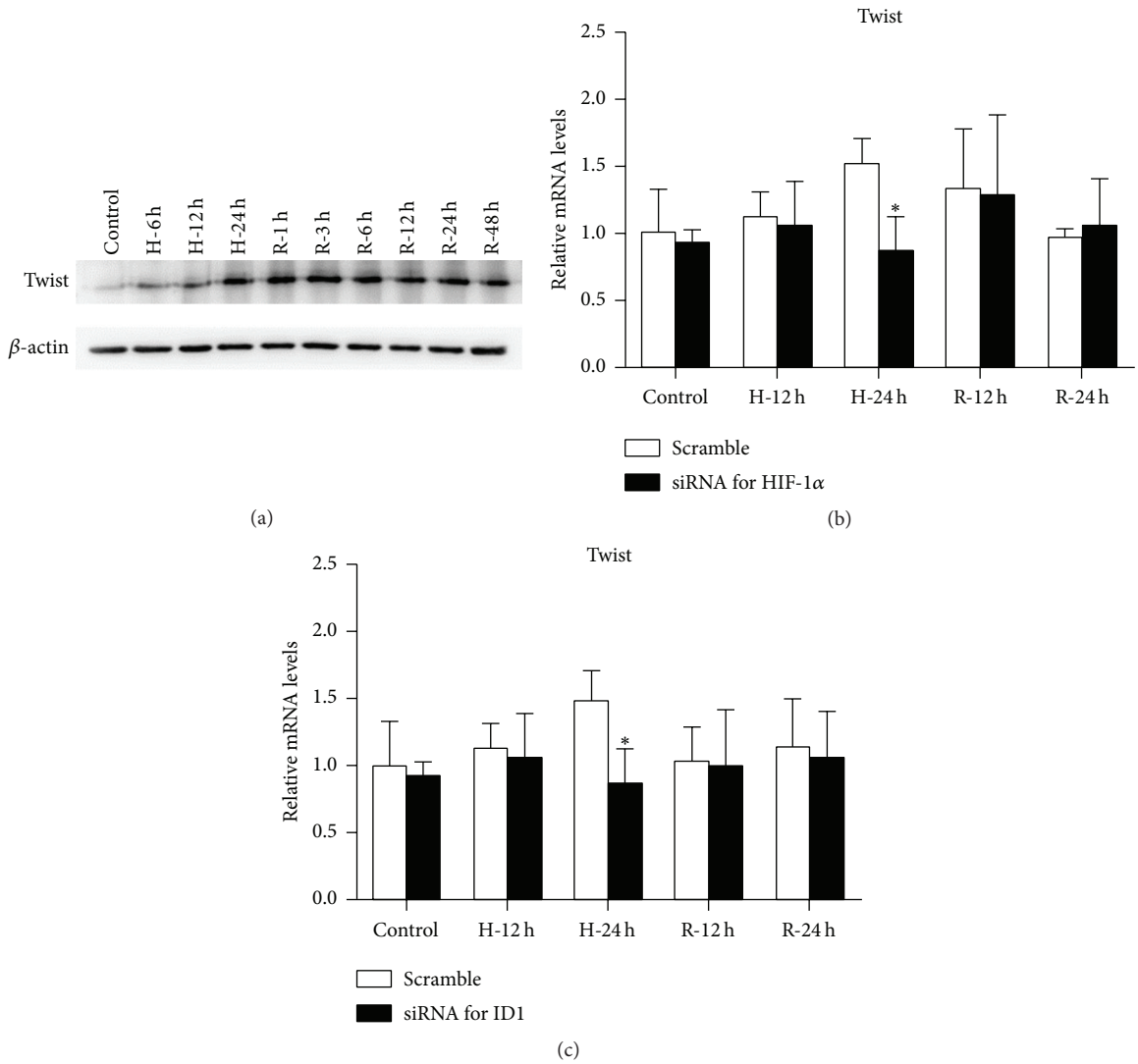

Figure 7: Twist is induced in the H/R model and is regulated by HIF-1α and ID1. (a) Western blot analysis of twist expression in HK-2 cells during H/R. β-actin was examined as the loading control. A representative blot from 3 independent experiments is shown. (b) In cells transfected with HIF-1α siRNA, and relative mRNA levels of twist were significantly reduced after 24 hours of hypoxia. β-actin mRNA served as the internal control ($n = 3$). $^*P < .05$ compared with the negative control (scramble). (c) In cells transfected with ID1 siRNA, relative mRNA levels of twist were significantly reduced after 24 hours of hypoxia. β-actin mRNA served as the internal control ($n = 3$). $^*P < .05$ compared with the negative control (scramble). ID1, inhibitor of DNA binding 1; HIF-1α, hypoxia-inducible factor-1 alpha; H/R, hypoxia-reoxygenation.

cells were exposed to hypoxia in a chamber with acid (pH 6.6) and glucose-deprived buffer for 2 hours and recultured under standard conditions for 48 hours [12]. Although most markers of apoptosis, dedifferentiation, and inflammation were expressed as anticipated, this model has not been widely applied, likely because of its poor standardization and repeatability. Different durations of hypoxia between 2 and 24 hours have been applied in different studies of AKI [13–15]. In their preliminary experiments, the authors observed the expression of HIF-1α after hypoxia for 6, 12, and 24 hours. With several repetitions, they found that only hypoxia exposure for 24 hours could induce stable upregulation of HIF-1α and vimentin.

In the H/R model, it was demonstrated that HIF-1α is induced during both hypoxia and reoxygenation and the dynamic expression of HIF-1α was shown following intensive observation. The preliminary study found that HIF-1α protein accumulates instantly after hypoxia for 1 hour. Conde et al. also identified the biphasic expression of HIF-1α in a HK-2 H/R model, but the duration of hypoxia was different from this study and they did not describe the expression process in detail [5]. In addition, this study confirmed that HIF-1α mRNA expression was significantly elevated during hypoxia and reoxygenation in HK-2 cells. Evidence has shown that hypoxia and oxidative stress can activate transcription of HIF-1α mRNA in other cell lines [16]. In contrast, no significant changes in HIF-1α mRNA expression were observed in the study by Conde et al., and this may mainly be attributed to a short hypoxia time and insufficient stimulation [5]. According to the results of this study, the

authors consider that HIF-1α protein instantly accumulated at the start of exposure to hypoxia and its expression was induced following responses that relieve hypoxic injury and promote cellular repair. If exposure to hypoxia continues, transcription of HIF-1α may be elevated to ensure or increase its expression.

It has been reported that ID1 expression is induced exclusively in the degenerated, dilated renal tubular epithelium after unilateral ureteral obstruction [9]. The findings from the present study indicated that ID1 was significantly induced and mainly expressed in renal TECs during in vivo reperfusion after acute ischemia, which means ID1 may have important functions in AKI. Through an in vitro H/R model, the authors found that ID1 expression is markedly elevated during hypoxia at both the protein and mRNA levels. To determine whether HIF-1α is necessary for the induction of ID1 during hypoxia and reoxygenation, HIF-1α was silenced and a reduction of ID1 mRNA was observed. Therefore, HIF-1α could regulate ID1 transcriptionally as seen in HK-2 cells. In neuroblastoma cells [17], ID1 is downregulated in a hypoxic situation, but it is upregulated by HIF-1α in the absence of hypoxia-induced ATF-3. Therefore, it is obvious that the expression of ID1 under hypoxia differs in different cell lines, and the mechanism by which HIF-1α regulates ID1 may also be different and requires further research.

ID1 has been a hot topic in cancer research for years, and numerous cancer cells are reported to overexpress ID1, which is in relation to tumor angiogenesis. In renal TECs, ID1 was shown to drive dedifferentiation by suppressing E-cadherin expression [9]. Moreover, ID1 is involved in cell cycle progression and development and probably cross talks with HIF-1α. ID1 can stabilize HIF-1α protein in hepatocellular carcinoma cells [18]. In the study by Kim et al., ID1 was shown to enhance nuclear translocation and the transcriptional activity of HIF-1α by recruiting CBP into endothelial cells [6]. As there is potential for regulation of HIF-1α by ID1, this study explored the relationship between HIF-1α and ID1. The results demonstrated that ID1 is a regulator of HIF-1α. The induction of HIF-1α transcription was inhibited when ID1 was silenced. Thus, the authors hypothesized that HIF-1α could induce the increased expression of ID1 during H/R, and the augmented ID1 expression could elevate HIF-1α expression in return, which acts as a positive feedback loop.

Twist is an important member of the bHLH family and a master regulator of gastrulation and mesoderm specification that is also essential in mediating metastasis [19, 20]. Several studies have shown that twist may be regulated by HIF-1α and ID1. The transcriptional activity of twist is inhibited by ID1 in a kidney fibroblast cell line [21]. HIF-1α can induce twist expression in TECs subjected to hypoxia, leading to epithelial-to-mesenchymal transition [11]. The present study indicates that HIF-1α can regulate twist during H/R in HK-2 cells, and the transcription of twist could also be regulated by ID1. Thus, the mechanism of the regulation of twist expression by ID1 will be a focus of future research.

In summary, the results presented here demonstrate the induction of ID1 expression in renal TECs during in vivo and in vitro I/R injury, which could regulate the expression of HIF-1α transcriptionally. As a critical and protective factor for the repair of TECs, HIF-1α has been considered to be an important therapeutic target. Interventions based on its regulator, ID1, may offer new insight into strategies for ameliorating I/R injury.

Competing Interests

The authors declare no conflict of interests.

Authors' Contributions

Dan Wen and Yan-Fang Zou contributed equally to this work.

Acknowledgments

This study was supported by grants from National Science Foundation (nos. 81470967 and 81470041) and Science and Technology Commission of Shanghai Municipality (12DJ1400303, 11JC1407901, and 15411963800), China.

References

[1] N. H. Lameire, A. Bagga, D. Cruz et al., "Acute kidney injury: an increasing global concern," *The Lancet*, vol. 382, no. 9887, pp. 170–179, 2013.

[2] A. A. Sharfuddin and B. A. Molitoris, "Pathophysiology of ischemic acute kidney injury," *Nature Reviews Nephrology*, vol. 7, no. 4, pp. 189–200, 2011.

[3] G. L. Wang, B.-H. Jiang, E. A. Rue, and G. L. Semenza, "Hypoxia-inducible factor 1 is a basic-helix-loop-helix-PAS heterodimer regulated by cellular O2 tension," *Proceedings of the National Academy of Sciences of the United States of America*, vol. 92, no. 12, pp. 5510–5514, 1995.

[4] M. Nangaku, C. Rosenberger, S. N. Heyman, and K.-U. Eckardt, "Regulation of hypoxia-inducible factor in kidney disease," *Clinical and Experimental Pharmacology and Physiology*, vol. 40, no. 2, pp. 148–157, 2013.

[5] E. Conde, L. Alegre, I. Blanco-Sánchez et al., "Hypoxia inducible factor 1-alpha (Hif-1 alpha) is induced during reperfusion after renal ischemia and is critical for proximal tubule cell survival," *PLoS ONE*, vol. 7, no. 3, Article ID e33258, 2012.

[6] H.-J. Kim, H. Chung, Y.-G. Yoo et al., "Inhibitor of DNA binding 1 activates vascular endothelial growth factor through enhancing the stability and activity of hypoxia-inducible factor-1α," *Molecular Cancer Research*, vol. 5, no. 4, pp. 321–329, 2007.

[7] H. A. Sikder, M. K. Devlin, S. Dunlap, B. Ryu, and R. M. Alani, "Id proteins in cell growth and tumorigenesis," *Cancer Cell*, vol. 3, no. 6, pp. 525–530, 2003.

[8] M. B. Ruzinova and R. Benezra, "Id proteins in development, cell cycle and cancer," *Trends in Cell Biology*, vol. 13, no. 8, pp. 410–418, 2003.

[9] Y. Li, J. Yang, J.-H. Luo, S. Dedhar, and Y. Liu, "Tubular epithelial cell dedifferentiation is driven by the helix-loop-helix transcriptional inhibitor Id1," *Journal of the American Society of Nephrology*, vol. 18, no. 2, pp. 449–460, 2007.

[10] W. Zhang, L. Zhang, Y.-X. Chen et al., "Identification of nestin as a urinary biomarker for acute kidney injury," *American Journal of Nephrology*, vol. 39, no. 2, pp. 110–121, 2014.

[11] S. Sun, X. Ning, Y. Zhang et al., "Hypoxia-inducible factor-1α induces Twist expression in tubular epithelial cells subjected

to hypoxia, leading to epithelial-to-mesenchymal transition," *Kidney International*, vol. 75, no. 12, pp. 1278–1287, 2009.

[12] C. Sauvant, R. Schneider, H. Holzinger, S. Renker, C. Wanner, and M. Gekle, "Implementation of an in vitro model system for investigation of reperfusion damage after renal ischemia," *Cellular Physiology and Biochemistry*, vol. 24, no. 5-6, pp. 567–576, 2009.

[13] Q. Peng, K. Li, L. A. Smyth et al., "C3a and C5a promote renal ischemia-reperfusion injury," *Journal of the American Society of Nephrology*, vol. 23, no. 9, pp. 1474–1485, 2012.

[14] J. Chen, W. Wang, Q. Zhang et al., "Low molecular weight fucoidan against renal ischemia-reperfusion injury via inhibition of the MAPK signaling pathway," *PLoS ONE*, vol. 8, no. 2, Article ID e56224, 2013.

[15] W.-H. Liu, H.-B. Liu, D.-K. Gao et al., "ABCG2 protects kidney side population cells from hypoxia/reoxygenation injury through activation of the MEK/ERK pathway," *Cell Transplantation*, vol. 22, no. 10, pp. 1859–1868, 2013.

[16] S. Galbán and M. Gorospe, "Factors interacting with HIF-1α mRNA: novel therapeutic targets," *Current Pharmaceutical Design*, vol. 15, no. 33, pp. 3853–3860, 2009.

[17] S. M. Nemetski and L. B. Gardner, "Hypoxic regulation of Id-1 and activation of the unfolded protein response are aberrant in neuroblastoma," *Journal of Biological Chemistry*, vol. 282, no. 1, pp. 240–248, 2007.

[18] T. K. Lee, R. T. P. Poon, A. P. Yuen et al., "Regulation of angiogenesis by Id-1 through hypoxia-inducible factor-1α-mediated vascular endothelial growth factor up-regulation in hepatocellular carcinoma," *Clinical Cancer Research*, vol. 12, no. 23, pp. 6910–6919, 2006.

[19] J. Yang, S. A. Mani, J. L. Donaher et al., "Twist, a master regulator of morphogenesis, plays an essential role in tumor metastasis," *Cell*, vol. 117, no. 7, pp. 927–939, 2004.

[20] I. Castanon and M. K. Baylies, "A twist in fate: evolutionary comparison of twist structure and function," *Gene*, vol. 287, no. 1-2, pp. 11–22, 2002.

[21] M. Hayashi, K. Nimura, K. Kashiwagi et al., "Comparative roles of Twist-1 and Id1 in transcriptional regulation by BMP signaling," *Journal of Cell Science*, vol. 120, no. 8, pp. 1350–1357, 2007.

Hindawi Publishing Corporation
BioMed Research International
Volume 2016, Article ID 2015251, 6 pages
http://dx.doi.org/10.1155/2016/2015251

Research Article

Clinical Characteristics and 30-Day Outcomes of Intermittent Hemodialysis for Acute Kidney Injury in an African Intensive Care Unit

Arthur Kwizera,[1,2] Janat Tumukunde,[1] Lameck Ssemogerere,[1] Emmanuel Ayebale,[1] Peter Agaba,[1] Jamali Yakubu,[2] Aggrey Lubikire,[1] Mary Nabukenya,[1] and Robert Kalyesubula[3]

[1]*Department of Anaesthesia, Makerere University, P.O. Box 7072, Kampala, Uganda*
[2]*Dialysis and Intensive Care Unit, International Hospital Kampala, P.O. Box 8177, Kampala, Uganda*
[3]*Departments of Physiology and Internal Medicine Nephrology Unit, Makerere University, P.O. Box 7072, Kampala, Uganda*

Correspondence should be addressed to Arthur Kwizera; akwizera@chs.mak.ac.ug

Received 19 November 2015; Revised 4 February 2016; Accepted 8 February 2016

Academic Editor: Jeremiah R. Brown

Introduction. Acute kidney injury (AKI) is a common occurrence in the intensive care unit (ICU). Studies have looked at outcomes of renal replacement therapy using intermittent haemodialysis (IHD) in ICUs with varying results. Little is known about the outcomes of using IHD in resource-limited settings where continuous renal replacement therapy (CRRT) is limited. We sought to determine outcomes of IHD among critically ill patients admitted to a low-income country ICU. *Methods*. A retrospective review of patient records was conducted. Patients admitted to the ICU who underwent IHD for AKI were included in the study. Patients' demographic and clinical characteristics, cause of AKI, laboratory parameters, haemodialysis characteristics, and survival were interpreted and analyzed. Primary outcome was mortality. *Results*. Of 62 patients, 40 had complete records. Median age of patients was 38.5 years. Etiologic diagnoses associated with AKI included sepsis, malaria, and ARDS. Mortality was 52.5%. APACHE II (OR 4.550; 95% CI 1.2–17.5, $p = 0.028$), mechanical ventilation (OR 13.063; 95% CI 2.3–72, $p = 0.003$), and need for vasopressors (OR 16.8; 95% CI 3.4–82.6, $p = 0.001$) had statistically significant association with mortality. *Conclusion*. IHD may be a feasible alternative for RRT in critically ill haemodynamically stable patients in low resource settings where CRRT may not be available.

1. Introduction

Acute kidney injury (AKI) occurs in 5.7–24% of intensive care unit (ICU) patients [1]. It is commonly associated with multiorgan failure, preexisting renal disease, sepsis, and renal hypoperfusion. In addition to morbidity, AKI is also a common cause of increased length of stay and increased costs of healthcare. Mortality of patients with AKI in ICU ranges from 46.8% to 60% and use of vasopressors, mechanical ventilation, and shock (septic and cardiogenic) are some common independent predictors of mortality [1–3]. The management of AKI ranges from conservative (including etiologic management, hemodynamic support, maintaining fluid and electrolyte balance, avoiding nephrotoxic drugs, and appropriate drug dosing for level of glomerular filtration rate) to renal replacement therapy (RRT) [4]. RRT includes peritoneal hemodialysis (PD), IHD, or CRRT. The preferred choice for RRT among peritoneal dialysis (PD), intermittent hemodialysis (IHD), and continuous renal replacement therapy (CRRT) remains unresolved despite several randomized controlled trials [5].

In low-income countries, studies from India have previously reported the profile and outcome of AKI in ICUs and one study described treatment characteristics of RRT, therapy modification, and sickness profile [6]. Patients from low-income countries with AKI are quite different from those of developed countries in that they are often younger, have less comorbidities, and are likely to have higher rates of HIV infection [7]. It is therefore important to appreciate the notion that studies of patients with AKI from developed

countries may not represent the true picture of what happens in low resource settings. Unfortunately, few to no studies have looked at renal replacement therapies in the ICU.

We aimed to study the patient characteristics, RRT practice of a modified IHD, and the outcome of patients with AKI in an ICU in a low-income country university teaching hospital.

2. Materials and Methods

A retrospective study of all consecutive patients over the age of 18 who underwent modified IHD in the ICU between January 2012 and May to December 2014 was performed. International Hospital Kampala is a 100-bed private tertiary teaching hospital in Kampala, Uganda, served by 18 outpatient clinics and serving an accessible population of one million people in Kampala. It has a 10-bed multidisciplinary ICU. Patient demographics, clinical characteristics, APACHE II score, reasons for renal replacement, vasopressor use, mechanical ventilation, and biochemical and hematological parameters at the onset of hemodialysis were noted.

Hemodialysis (HD) was performed using the Gambro AK95 machine. Standard water treatment was used. Dialysate concentrates were commercially purchased. F5 polysulfone dialyzers were used (surface area of the dialyzer was 0.9 m^2). All the patients were anticoagulated with unfractionated heparin based on clinical risk assessment. The intensive care team (intensivist and nephrologist) decided on ultrafiltration based on clinical risk assessment and hemodynamics. IHD characteristics that included blood flow rate (BFR), dialysate flow rate (DFR), anticoagulation, and ultrafiltration (UF) were reviewed. Major complications were documented. Patient survival was defined as dialysis-free discharge from the ICU. Patient characteristics were shown as percentages, mean ± SD, and/or median where necessary. Microsoft Excel and SPSS version 22 (IMB Corporation, Armonk, New York, USA) were used for data analysis. Analysis of variance was used to compare the mean of various parameters with the outcome variable (survival and nonsurvival) and conclusions on associations were made using statistical tests of $p < 0.05$ as being significant. Multivariate analysis was also done using logistics regressions for selected characteristics against the outcome variable (survival and nonsurvival) and results concluded using unadjusted odds ratios above 1 with $p < 0.05$ signifying existence of associations. Other variables were continuous in nature and were categorized into two groups using median to distinguish the groups.

3. Results

Out of 62 patients who underwent dialysis, 40 patients had complete records according to the study protocol. They underwent 192 IHD treatments. Among these, 32 (80%) were male. The median age was 38.5 ± 12 years. Distribution by etiology was as follows: sepsis in 33 patients (82%) and malaria in 14 patients (33%). Twenty-three (57.5%) patients required vasopressor treatment for septic shock (see Table 1).

Table 1: Clinical features of patients with acute kidney failure.

$N = 40$	n (%)
Gender	
Male	32 (80.0)
Female	8 (20.0)
AKI etiological diagnoses	
Sepsis	33 (82.0)
Cardiac	9 (22.5)
Malaria	14 (33.0)
ARDS	17 (42.5)
TBI	2 (5.0)
Poisoning	1 (2.5)
Organ support	
Mechanical ventilation	27 (67.5)
APACHE II (mean)	24.5 ± 3.7
Vasopressors	23 (57.5)
Enteral feeds	25 (62.0)
Laboratory characteristics	
Creatinine (mmol/L)	6.25 ± 1.8
Sodium (mEq/mL)	134.9 ± 4.7
Potassium (mEq/mL)	5.0 ± 0.3
pH	7.1 ± 0.7
Haemoglobin (g/dL)	10.4 ± 3.7
White blood count (10^3)	14.3 ± 4.2
Platelets	143.2 ± 14.5

AKI: acute kidney injury; APACHE II: Acute Physiological and Chronic Health Evaluation; ARDS: acute respiratory distress syndrome; TBI: traumatic brain injury.

APACHE II mean score was 24.5 ± 3.7. The median BUN was 44.5 + 7.2 mg/dL, and the mean creatinine level was 6.25 ± 1.8 mg/dL.

Mean serum sodium was 134.9 ± 4.7 mEq/L, pH was 7.1, serum potassium was 5.0 ± 0.3 mEq/L, hemoglobin was 10.4 ± 3.7 g/dL, mean total white cell count was 14.3 ± 4.2 cells/mm^3, and mean platelet count was 143.2 ± 14.5 cells/mm^3 (see Table 1).

Dialysis sessions were 192 and majority (61.2%) were for <4 h (Table 2). Mean blood flow rate (BFR) was 264.5 ± 42.5 mL/min and dialysate flow rate (DFR) was 474.9 ± 109.8 mL/min. Heparin used was 281 ± 339 U/h, while mean UF was 242.1 ± 27.3 mL/h.

The major complications during dialysis included hypotension in 9 patients (22.5%) and anemia in 7 (17.5%), but majority of the patients did not have any complication.

Analysis of outcome was done at 30 days from the start of IHD and out of the 40 patients, 19 (47.5%) were alive (survivors) and 21 (57.5%) died (nonsurvivors).

In Tables 3 and 4, comparisons of trends and predictors of survival were done among survivors and nonsurvivors. Two patterns were observed after performing analysis of variance: the mean APACHE II score (27.6) for nonsurvivors was higher than for survivors and mean platelet count for nonsurvivors (104.9) was lower than for the survivors (216). These were statistically significant.

Table 2: Hemodialysis prescription characteristics and outcomes.

$N = 40$	n (%)
Total number of dialysis sessions	192
Duration of dialysis (hours)	
<4	118 (61.2)
4–6	30 (17.3)
>6	44 (22.5)
Blood flow rate (mL/min)	264.5 ± 42.5
Heparin (U/hr)	281 ± 39
Ultrafiltration rate	242.1 ± 27
BUN	44.5 ± 7.2
Creatinine (mmol/L)	6.5 ± 1.85
Complications during dialysis	
Anemia	7 (17.5)
Hypotension	9 (22.5)
Hypotension/anemia	2 (5.0)
No complication	22 (55.0)
Outcome	
Alive/discharged (survivors)	19 (47.5)
Dead (nonsurvivors)	21 (52.5)

AKI: acute kidney injury; APACHE II: Acute Physiological and Chronic Health Evaluation.

Other predictors for nonsurvival identified were vasopressors and mechanical ventilation (Table 4). The majority n (90.5%) of nonsurvivors received mechanical ventilation for ARDS and 85.7% of nonsurvivors had also been treated with vasopressors for septic shock ($p = 0.01$). There was no significant association between age, number of dialysis sessions, serum sodium, and serum potassium, hemoglobin, creatinine, urine output, WBC, pH, UF, PT/INR, and blood flow rate between the two groups. Illnesses such as malaria and other complications like anemia, hypotension, and cardiac problems did not have any significant association with ICU admission outcomes.

At multivariate analysis, APACHE II score, vasopressor use for septic shock, and mechanical ventilation were significantly associated with mortality (see Table 5).

4. Discussion

This retrospective study was conducted to characterize and determine outcomes and factors associated with critically ill AKI patients undergoing IHD in a low-income tertiary hospital. Our study found that IHD methods were similar to those reported in the literature [8]. However, our mortality differed somewhat from studies in similar settings and was higher than that reported in higher income countries [9]. Our study population was generally younger than that in HICs and similar to previously described populations in similar settings. This may have contributed to the lower mortality than that observed in the Indian setting [6]. The causes of AKI were in keeping with known etiology; however, malaria sepsis emerged as an unusual cause of AKI in our population, considered to be endemic and therefore conferring active immunity. ARDS/need for mechanical ventilation was also of significant association. This could be because high PEEP levels have been associated with AKI even though the mechanism is not fully understood [10].

IHD in this study was complicated by hypotension. This is not an uncommon complication of IHD among patients with CKD. However, septic shock being treated by vasopressors may have worsened outcomes due to the dialyzable nature of vasopressors used. No cardiac arrests occurred during the study period.

Significant predictors of mortality included ARDs/need for mechanical ventilation and septic shock. Sepsis-induced AKI is prevalent in our population and is a documented cause of mortality [7].

The study population illustrated that appropriate modified practice of IHD could be customized to the clinical needs of patients with AKI in ICU. It helped achieve reasonable clinical outcome in environments with resource constraints. Centers similar to our setting have adopted modifications in their practice to minimize complications [11]. The spectrum of ICU patients developing AKI and the age profile in our patient population were similar to ICU in the developing world. They are younger and more likely to be male. The large proportion of sepsis in our series accounted for the high prevalence of multiorgan failure.

While the choice of modality for RRT varies across centers globally [12], the preferred choice in our setting is IHD. It is commonly used for CKD patients [13]. Peritoneal dialysis (PD) is infrequently used and when so is used to treat AKI in paediatric patients [14]. The choice of RRT is due to CRRT being labor-intensive and expensive [15]. This is compounded by a dearth of ICU beds and dialysis equipment in this setting [16]. The above factors are major limitations to utilizing CRRT in Uganda and other low resource settings. Modifications of conventional IHD such as sustained low efficiency dialysis, short daily dialysis, and isolated ultrafiltration have been shown to achieve satisfactory patient outcomes in developing world ICUs. The retrospective nature of the study limited reviewing other important adverse effects including new onset of infections from access, major bleeding, and transient cardiac arrhythmias. Poor hemodynamic tolerance of IHD was a common problem for patients in the ICU. Hypotension occurred in 22.5% of the IHD sessions in this study. This is more than what was reported in other studies [6, 17]. The salient feature was that the patient survival in our study was similar to that published in developed countries. This fact may indirectly indicate that major adverse effects may not have been missed in our data review.

There is yet no consensus on the timing of initiation of RRT [18–20]. The mean BUN and creatinine of patients in our study reflect the timing of initiation to be reasonably consistent with contemporary practice. Additionally, serum urea at initiation of dialysis has no predictive value on in-hospital mortality in ICU patients with AKI [21].

A recent meta-analysis, which attempted to analyze modified IHD versus CRRT, noted no difference in survival with either modality; however, there was significant heterogeneity in these studies [22, 23].

Table 3: Comparison of characteristics of survivors and nonsurvivors with acute renal failure in ICU.

Variable	Survivors	Nonsurvivors	p value
APACHE II score	20.9	27.6	0.004
Age (years)	38.9	49.7	0.082
Number of dialysis sessions	5.2	4.5	0.603
Sodium (mEq/mL)	130.0	138.0	0.078
Potassium (mEq/mL)	5.0	5.0	0.989
Hemoglobin (g/dL)	10.3	10.6	0.783
WBC count (10^3 cells/mm^3)	15.4	13.3	0.613
PT/INR	1.7	2.3	0.156
Platelet count (cells/mm^3)	216.0	104.9	0.002
pH	7.16	7.21	0.279
Blood flow rate (mL/min)	270.0	251.0	0.517
UF (liters)	2.01	1.84	0.558
Average duration (hours)	3.63	3.514	0.730
Creatinine (mg/dL)	41.2	65.6	0.781

Table 4: Comparison of characteristics of survivors and nonsurvivors with acute renal failure in ICU.

	Survivors n (%)	Nonsurvivors n (%)	$N = 40$	X^2	p value
Mechanical ventilation					
Ventilated	8 (42.1)	19 (90.5)	27		
Not ventilated	11 (57.9)	2 (9.5)	13	10.639	0.01
Vasopressors					
Applied	5 (26.3)	18 (85.7)	23		
Not applied	14 (73.7)	3 (14.3)	17	14.401	0.01
ARDS	5 (26.3)	12 (57.1)	17		
Non-ARDS	14 (73.7)	9 (42.9)	23	3.879	0.05
Complications					
Anemia	3 (15.8)	4 (19.0)	7		
Hypotension	2 (10.5)	7 (33.3)	9		
Anemia/hypotension	0 (0.0)	2 (9.5)	2	6.473	0.09
No complication	14 (73.3)	8 (38.2)	22		
Malaria cases	7 (36.8)	7 (33.3)	14		
Nonmalaria cases	12 (63.2)	14 (66.7)	26	1.054	0.86
Cardiac cases	15.5 (3)	6 (6)	9		
Noncardiac cases	84.2 (16)	15 (71.4)	31	0.933	0.34

AKI: acute kidney injury; APACHE II: Acute Physiological and Chronic Health Evaluation.

Table 5: Multivariate (risk factors) analysis of the predictors of survival and nonsurvival.

	Nonsurvivors n (%)	Survivors n (%)	Odds (95% CI)	p value
APACHE II > median (24)	13 (61.9)	5 (26.3)	4.550 (1.181–17.524)	0.028
Mechanical ventilation	19 (90.5)	8 (42.1)	13.063 (2.343–7.818)	0.003
Use of vasopressors	18 (85.7)	5 (26.3)	16.854 (3.416–82.602)	0.001
ARDS			3.733 (0.979–14.222)	0.054

Mortality among patients treated with RRT was associated with organ dysfunction and comorbidity, and it was approximately 58%. This was also reflected in the Indian study (58% at 30 days) [6]. This is however higher than what has been reported in the Ugandan ICU setting (40.1%) [16].

Our study is the first to report on characteristics of RRT in an African setting; however, it was limited by its retrospective nature, missed patient records, inadequate details of dosage, unclear duration of vasopressor use, and possible underreporting of adverse effects.

5. Conclusion

These study findings suggest that IHD may be a technically feasible option for RRT in low resource settings that have limited or no access to CRRT. More work needs to be done to determine the viability of IHD for RRT among patients with AKI in low resource settings.

Conflict of Interests

The authors declare that there is no conflict of interests regarding the publication of this paper.

Authors' Contribution

Arthur Kwizera and Jamali Yakubu conceived the study and performed the study design. Arthur Kwizera, Lameck Ssemogerere, Janat Tumukunde, Emmanuel Ayebale, Peter Agaba, Mary Nabukenya, Aggrey Lubikire, and Robert Kalyesubula performed data collection and paper drafting. Arthur Kwizera and Jamali Yakubu performed statistical analysis. Robert Kalyesubula provided senior authorship and content expertise. All authors read and approved the final paper.

Acknowledgments

The authors would like to acknowledge Mr. Francis Opolot for his help with statistical analysis and Mr. Kato William for help in accessing patient records. Appreciation goes to the study nurses at International Hospital Kampala for participating in the research.

References

[1] S. Uchino, J. A. Kellum, R. Bellomo et al., "Acute renal failure in critically ill patients: a multinational, multicenter study," *The Journal of the American Medical Association*, vol. 294, no. 7, pp. 813–818, 2005.

[2] R. M. Fagugli, F. Patera, S. Battistoni, F. Mattozzi, and G. Tripepi, "Six-year single-center survey on AKI requiring renal replacement therapy: epidemiology and health care organization aspects," *Journal of Nephrology*, vol. 28, no. 3, pp. 339–349, 2015.

[3] C. Deepa and K. Muralidhar, "Renal replacement therapy in ICU," *Journal of Anaesthesiology Clinical Pharmacology*, vol. 28, no. 3, pp. 386–396, 2012.

[4] S. John and K.-U. Eckardt, "Renal replacement strategies in the ICU," *Chest*, vol. 132, no. 4, pp. 1379–1388, 2007.

[5] M. Legrand, M. Darmon, M. Joannidis, and D. Payen, "Management of renal replacement therapy in ICU patients: an international survey," *Intensive Care Medicine*, vol. 39, no. 1, pp. 101–108, 2013.

[6] S. Sankarasubbaiyan, J. D. Janardan, and P. Kaur, "Outcomes and characteristics of intermittent hemodialysis for acute kidney injury in an intensive care unit," *Indian Journal of Nephrology*, vol. 23, no. 1, pp. 30–33, 2013.

[7] P. Bagasha, F. Nakwagala, A. Kwizera, E. Ssekasanvu, and R. Kalyesubula, "Acute kidney injury among adult patients with sepsis in a low-income country: clinical patterns and short-term outcomes," *BMC Nephrology*, vol. 16, article 4, 2015.

[8] R. Vanholder, W. Van Biesen, and N. Lameire, "What is the renal replacement method of first choice for intensive care patients?" *Journal of the American Society of Nephrology*, vol. 12, supplement 17, pp. S40–S43, 2001.

[9] B. Delannoy, B. Floccard, F. Thiolliere et al., "Six-month outcome in acute kidney injury requiring renal replacement therapy in the ICU: a multicentre prospective study," *Intensive Care Medicine*, vol. 35, no. 11, pp. 1907–1915, 2009.

[10] T. Akbaş, S. Karakurt, and S. Tuğlular, "Renal replacement therapy in the ICU: comparison of clinical features and outcomes of patients with acute kidney injury and dialysis-dependent end-stage renal disease," *Clinical and Experimental Nephrology*, vol. 19, no. 4, pp. 701–709, 2015.

[11] T. Naka, I. Baldwin, R. Bellomo, N. Fealy, and L. Wan, "Prolonged daily intermittent renal replacement therapy in ICU patients by ICU nurses and ICU physicians," *International Journal of Artificial Organs*, vol. 27, no. 5, pp. 380–387, 2004.

[12] Z. Ricci, C. Ronco, G. D'Amico et al., "Practice patterns in the management of acute renal failure in the critically ill patient: an international survey," *Nephrology, Dialysis, Transplantation*, vol. 21, no. 3, pp. 690–696, 2006.

[13] R. Kalyesubula, J. Lunyera, G. Makanga, B. Kirenga, and T. K. Amukele, "A 4-year survey of the spectrum of renal disease at a National Referral Hospital Outpatient Clinic in Uganda," *Kidney International*, vol. 87, no. 3, p. 663, 2015.

[14] M. Carter, K. Kilonzo, A. Odiit et al., "Acute peritoneal dialysis treatment programs for countries of the East African community," *Blood Purification*, vol. 33, no. 1–3, pp. 149–152, 2012.

[15] W. De Becker, "Starting up a continuous renal replacement therapy program on ICU," *Contributions to Nephrology*, vol. 156, pp. 185–190, 2007.

[16] A. Kwizera, M. Dunser, and J. Nakibuuka, "National intensive care unit bed capacity and ICU patient characteristics in a low income country," *BMC Research Notes*, vol. 5, article 475, 2012.

[17] P. M. Palevsky, J. H. Zhang, T. Z. O'Connor et al., "Intensity of renal support in critically ill patients with acute kidney injury," *The New England Journal of Medicine*, vol. 359, no. 1, pp. 7–20, 2008.

[18] Y.-H. Chou, T.-M. Huang, V.-C. Wu et al., "Impact of timing of renal replacement therapy initiation on outcome of septic acute kidney injury," *Critical Care*, vol. 15, no. 3, article R134, 2011.

[19] S. M. Bagshaw, S. Uchino, R. Bellomo et al., "Timing of renal replacement therapy and clinical outcomes in critically ill patients with severe acute kidney injury," *Journal of Critical Care*, vol. 24, no. 1, pp. 129–140, 2009.

[20] C. J. Karvellas, M. R. Farhat, I. Sajjad et al., "A comparison of early versus late initiation of renal replacement therapy in critically ill patients with acute kidney injury: a systematic review and meta-analysis," *Critical Care*, vol. 15, no. 1, article R72, 2011.

[21] W. De Corte, R. Vanholder, A. W. Dhondt et al., "Serum urea concentration is probably not related to outcome in ICU patients with AKI and renal replacement therapy," *Nephrology, Dialysis, Transplantation*, vol. 26, no. 10, pp. 3211–3218, 2011.

[22] L. Zhang, J. Yang, G. M. Eastwood, G. Zhu, A. Tanaka, and R. Bellomo, "Extended daily dialysis versus continuous renal replacement therapy for acute kidney injury: a meta-analysis," *American Journal of Kidney Diseases*, vol. 66, no. 2, pp. 322–330, 2015.

[23] S. Uchino, R. Bellomo, and C. Ronco, "Intermittent versus continuous renal replacement therapy in the ICU: impact on electrolyte and acid-base balance," *Intensive Care Medicine*, vol. 27, no. 6, pp. 1037–1043, 2001.

Hindawi Publishing Corporation
BioMed Research International
Volume 2016, Article ID 3019410, 5 pages
http://dx.doi.org/10.1155/2016/3019410

Research Article

Impact of Iodinated Contrast on Renal Function and Hemodynamics in Rats with Chronic Hyperglycemia and Chronic Kidney Disease

Sheila Marques Fernandes,[1] Daniel Malisani Martins,[1] Cassiane Dezoti da Fonseca,[1] Mirian Watanabe,[1] and Maria de Fátima Fernandes Vattimo[1,2]

[1]*Experimentation Laboratory in Animal Model, School of Nursing, University of São Paulo, São Paulo, Brazil*
[2]*Department Medical-Surgical Nursing, School of Nursing, University of São Paulo, São Paulo, Brazil*

Correspondence should be addressed to Cassiane Dezoti da Fonseca; cassianedezoti@usp.br

Received 1 December 2015; Revised 26 January 2016; Accepted 4 February 2016

Academic Editor: Jeremiah R. Brown

Iodinated contrast (IC) is clinically used in diagnostic and interventional procedures, but its use can result in contrast-induced acute kidney injury (CI-AKI). Chronic kidney disease (CKD) and chronic hyperglycemia (CH) are important predisposing factors to CI-AKI. The aim of this study was to investigate the impact of iodinated contrast on the renal function and hemodynamics in rats with chronic hyperglycemia and chronic kidney disease. A total of 30 rats were divided into six groups; Sham: control of chronic renal disease; Citrate: control of chronic hyperglycemia (CH); Nx5/6: rats with 5/6 nephrectomy; Chronic Hyperglycemia: rats receiving Streptozotocin 65 mg/kg; Nx5/6 + IC: rats Nx5/6 received 6 mL/kg of IC; CH + IC: Chronic hyperglycemia rats receiving 6 mL/kg of IC. Renal function (inulin *clearance*; urinary neutrophil gelatinase-associated lipocalin, NGAL) and hemodynamics (arterial blood pressure; renal blood flow; renal vascular resistance) were evaluated. Iodinated contrast significantly increased urinary NGAL and reduced inulin *clearance*, while the hemodynamics parameters showed changes in arterial blood pressure, renal blood flow, and renal vascular resistance in both CKD and CH groups. The results suggest that the iodinated contrast in risk factors models has important impact on renal function and hemodynamics. NGAL was confirmed to play a role of highlight in diagnosis of CI-AKI.

1. Introduction

Contrast-induced acute kidney injury (CI-AKI) is an iatrogenic complication secondary to iodinated contrast (IC) exposure in diagnostic and interventional procedures [1, 2]. It is the third leading cause of hospital-acquired acute kidney injury (AKI) and accounts for about 11% of cases, with adverse effects on prognosis and health care costs [2, 3]. Chronic kidney disease (CKD), chronic hyperglycemia (CH), hypertension, and cardiovascular diseases are important predisposing factors for CI-AKI. The incidence in these individuals may reach 20–50% [4–6].

It has been shown that the administration of IC can result in significant increases in serum creatinine levels and urinary and serum NGAL levels and decrease on glomerular filtration rate (GFR) by reduction of creatinine or inulin *clearance* [7, 8]. The renal vulnerability at CKD is featured by loss of nephron units with reduction on renal function. The renal damage caused by chronic hyperglycemia results in changes in GFR and renal hemodynamics, enhanced tubular transport activity which increases the oxygen consumption, and the generation of reactive oxygen species (ROS) [9]. Therefore, IC exposure in these situations has been associated with important changes in renal function and hemodynamics [10].

The pathogenesis of CI-AKI is unclear; however experimental studies suggest that CI-AKI is due to endothelial dysfunction, inflammation, cellular toxicity, and tubular apoptosis resulting in hemodynamic alterations, hypoxia, and oxidative damage [1, 8]. The use of IC has demonstrated the vasoconstriction effect induced by adenosine and endothelin through a direct receptor-mediated event. Initially, it increases the renal blood flow followed by constriction of

renal vasculature [8]. Additionally, the new kidney function markers of CI-AKI have been shown to improve the early detection of renal injury. NGAL has been extensively studied in the field of AKI. In the late phase of AKI, NGAL is believed to play a role as a growth and differentiation factor for restoring tubular epithelial function with the assistance of siderophore-iron complexes [11].

The aim of this study was to investigate the impact of IC on renal function and hemodynamics in rats with chronic hyperglycemia and chronic kidney disease.

2. Materials and Methods

2.1. Animals. Thirty adult male Wistar rats weighing 280–390 g were used. They were housed in a controlled temperature (25°C/77°F) room with alternating light/dark cycles and were allowed free access to water and rat chow before experimentation.

All procedures in this study are consistent with the ethical principles of animal experimentation adopted by the Brazilian College of Animal Experimentation (COBEA) and were approved by the Ethics Commission on the use of animals, University of Sao Paulo (CEUA-ICBUSP), record of protocol 60, leaves 128 of the book 02.

On the 29th day of the protocol the animals were placed in metabolic cages for the measurement of 24 h urinary volume and collection of a urine sample. After this period, the animals were anesthetized for hemodynamics and renal function studies and blood sample collection through puncture of the abdominal aorta. At the end of the experiment, the animals were sacrificed according to guidelines for animal experimentation.

2.2. Streptozotocin-Induced Chronic Hyperglycemia Model. In the first day of the protocol, Streptozotocin (STZ; 65 mg/kg) was dissolved in 0.5 mL citrate buffer (0.1 mol/L; pH 4.5) just before the injection and administrated in the caudal vein. The control animals received only 0.5 mL citrate buffer. Blood glucose levels were measured 48 h after the injection to confirm hyperglycemia (Accu-Chek, Roche; measurement range: 10–600 mg/dL). The animals which consistently showed blood glucose level more than 250 mg/dL were considered hyperglycemic and included in the study.

2.3. 5/6-Nephrectomy. In the first day of the protocol, the five-sixths nephrectomy (5/6Nx) was performed under anesthesia with 4% sodium thiopental (30 mg/kg), intraperitoneal (i.p.). After laparotomy, the removal of the right kidney and ligation of 2 branches of the left renal artery were performed, and infarction of two-thirds of the left kidney was achieved.

2.4. Iodinated Contrast Administration. The animals received 6 mL/kg of IC (meglumine ioxithalamate and sodium) i.p., single dose on the 28th day of both experimental protocols.

2.5. Groups. The groups are as follows:

(i) Sham: control of chronic kidney disease, rats subject only to laparotomy.

(ii) Citrate: control of chronic hyperglycemia model, rats that received 0.5 mL of citrate buffer, intravenous (i.v.).

(iii) Nx5/6: rats subject to nephrectomy of the right kidney and ligation of 2 branches of the left renal artery and received 6 mL/kg/body weight of single saline i.p., injection on 28th day.

(iv) Chronic Hyperglycemia (CH): rats receiving 65 mg/kg of Streptozotocin dissolved in 0.5 mL citrate buffer i.v. and received 6 mL/kg of single saline injection i.p. on 28th day.

(v) Nx5/6 + IC: rats subject to Nx5/6 and received 6 mL/kg of IC, single injection i.p. on 28th day.

(vi) CH + IC: rats receiving 65 mg/kg Streptozotocin dissolved in 0.5 mL citrate buffer i.v. and received 6 mL/kg of IC i.p. on 28th day.

2.6. Experimental Protocol. The rats were anesthetized with sodium thiopental (50 mg/kg i.p.). Tracheostomy was performed and the rats maintained breathing spontaneously. To measure BP and allow blood sampling a PE-60 catheter was inserted into the left carotid artery. BP was assessed using Biopac Systems MP150 (Santa Barbara, CA). Right jugular vein was cannulated with PE-60 for the administration of inulin and fluids. A small abdominal incision was made and the urinary bladder was cannulated with PE-240 catheter, to collect urine samples.

After the surgical procedure, inulin was injected as a loading dose (100 mg/kg), followed by a continuous infusion of 0.04 mL/min. After a 30 min equilibration period, three urine collections and two blood samples were then obtained at the beginning and at the end. The plasm and urine inulin were measured using the anthrone method [12].

At the end of the experiment, a midline incision was performed; the left renal pedicle was carefully dissected, and the renal artery was isolated. Total RBF was monitored by a perivascular ultrasonic flowmeter (T402; Transonic Systems, Bethesda, MD). RVR was calculated by dividing the BP by total RBF. Finally, the distal abdominal aorta was punctured for terminal blood collection.

2.7. Renal Function and Hemodynamics. Forty-eight hours after contrast infusion, the renal function was evaluated based on inulin *clearance* (GFR, $\text{mL} \cdot \text{min}^{-1} \cdot 100\,\text{g body wt}^{-1}$) and urinary NGAL (Rat-NGAL ELISA kit, BioVendor, research and diagnostic products). Also, arterial blood pressure (BP, mmHg) and total renal blood flow (RBF, mL/min) were assessed and renal vascular resistance (RVR, $\text{mmHg} \cdot \text{mL}^{-1} \cdot \text{min}^{-1}$) was calculated.

2.8. Statistical Analysis. One-factor analysis of variance (ANOVA) with confidence intervals for the mean and pairwise comparisons was used. Overlapping intervals indicated no difference between treatments, which was subsequently confirmed by the Tukey test. The results are reported as the mean ± SD. Statistical analysis was made with GraphPad

Table 1: Body weight and kidney weight ratio (BW/KW).

Group	n	Weight (grams)	BW/KW
Sham	5	404.40 ± 20.90	0.32 ± 0.04
Citrate	5	378.86 ± 49.30	0.34 ± 0.05
Nx5/6	5	340.80 ± 18.30	0.52 ± 0.03[a]
CH	5	277.43 ± 35.72	0.58 ± 0.11[b]
Nx5/6 + IC	5	322.40 ± 14.40[a]	0.43 ± 0.06
CH + IC	5	274.38 ± 36.25	0.58 ± 0.13[b]

[a] $p < 0.05$ versus Sham.
[b] $p < 0.05$ versus Citrate.

Prism (version 3.0). Statistical significance was also attained with values $p < 0.05$.

3. Results

3.1. Effects of Iodinated Contrast on Kidney Weight/Body Weight Ratio. Sham and Citrate groups were considered control groups for kidney weight/body weight ratio. As shown in Table 1, CH and CKD rats had significantly increased this ratio (Nx5/6: 0.52 ± 0.03 versus Sham: 0.32 ± 0.04; CH + IC: 0.58 ± 0.13, CH: 0.58 ± 0.11 versus Citrate: 0.34 ± 0.05).

3.2. Effects of Iodinated Contrast on Renal Function. Chronic hyperglycemic groups had urinary flow significantly increased compared with the citrate group (CH + IC: 0.042 ± 0.01, CH: 0.032 ± 0.01 versus Citrate: 0.016 ± 0.03) (Table 2). CH and Nx5/6 groups had impairment of GFR as demonstrated for decreased inulin *clearance* (Nx5/6: 0.25 ± 0.08 versus Sham: 0.68 ± 0.05; CH: 0.43 ± 0.03 versus Citrate: 0.74 ± 0.30). After IC use, a significant decrease was observed in GFR in CH + IC and Nx5/6 + IC groups (Nx5/6: 0.25 ± 0.08 versus Nx5/6 + IC: 0.09 ± 0.03; CH: 0.43 ± 0.03 versus CH + IC: 0.17 ± 0.03).

The values of renal function parameters obtained for urinary NGAL were significantly higher in IC groups than in control groups (Nx5/6 + IC: 153.49 ± 70.06 versus Sham: 47.97 ± 19.19; CH + IC: 138.14 ± 74.80 versus Citrate: 45.62 ± 0.95).

3.3. Effects of Iodinated Contrast on Renal Hemodynamic. Hemodynamic analysis (Table 3) exhibited that Nx5/6 and Nx5/6 + IC had a higher BP than Sham (Nx5/6: 141.40 ± 11.30, Nx5/6 + IC: 120.20 ± 1.79 versus Sham: 88.75 ± 5.20). Significant reduction of RBF in CH and Nx5/6 groups was observed when compared with citrate and Sham groups ($p < 0.05$). After IC exposure, the groups showed significant increase of RVR (CH + IC: 44.78 ± 7.52 versus CH: 20.85 ± 0.32, Citrate: 18.02 ± 2.29; Nx5/6 + IC: 37.82 ± 10.16 versus Nx + 5/6 : 19.73 ± 4.62, Sham: 11.15 ± 1.62).

4. Discussion

In our study, IC exposure in CKD and CH models demonstrated significant changes on renal function and hemodynamics. These effects confirm the pathogenic mechanisms of CI-AKI in risk factors models and can lead to preventive strategies that reduce the chances of kidney damages. NGAL was showed to be an important biomarker at the detection of CI-AKI.

Evidence has shown that the use of IC is associated with a nephrotoxic risk [13]. The presence of CKD and CH increases the risks of IC; also, the morphological alterations on nephrons contributed to direct IC toxicity [5, 6, 9]. Previous reports have shown that renal hypertrophy is a classical feature of Nx5/6 nephrectomy and diabetes models [14, 15]. In the present study, the elevation on KW/BW ratio in the both chronic models could be associated with the hypertrophy, which is due to glomerular basement membrane (GBM) thickening and expansion of the mesangial matrix. Chronic hyperglycemia and Nx5/6 nephrectomy models are characterized by an inflammatory response and accumulation of extracellular matrix (ECM) proteins such as fibronectin, collagen, and laminin [15].

Renal function was evaluated by urinary NGAL and the GFR by inulin *clearance*. Several studies have shown that NGAL presents greater sensitivity for the early detection of AKI [7, 11]. A short period of ischemia (30 min) is sufficient to produce important renal damage in either morphology or function with significant elevations in urinary and serum NGAL [16]. Our results highlighted important increase in urinary NGAL in the CKD and CH groups that were exposed to IC. First, the reduction of inulin *clearance* was almost 50% in CKD and CH animals confirming the renal dysfunction on chronic models. Second, the use of IC on chronic models reduced more than 30% of renal function, resulting in severe CI-AKI. Fonseca et al. [17] also reported a significant reduction in creatinine *clearance* in diabetic rats that were exposed to IC. Third, CI-AKI is associated with a renal insufficiency and hypertension secondary to renin-dependent hypertension in the CKD model and in the chronic hyperglycemia model it results in increased renal plasmatic flow, glomerular hyperfiltration, and hyperosmolar urine [18–20].

Our results demonstrated that use of IC decreased RBF and, consequently, increased RVR in both 5/6 nephrectomy and chronic hyperglycemia rats. The use of IC resulted in severe impairment in renal hemodynamics by constriction of renal vasculature that reduces RBF and induces the development of CI-AKI. The CI-AKI has been associated with the changes in renal hemodynamics through increase of renal vasoconstrictors activity, as vasopressin, angiotensin II, dopamine-1, endothelin, and adenosine, and decreased activity of renal vasodilators, such as nitric oxide and prostaglandins [1, 21–23]. The decreased RBF may also be attributed to increased viscosity or high osmolality of contrast media and increased erythrocyte aggregation, which results in diminished oxygen delivery. The high oxygen consumption results in generation of ROS and cellular apoptosis [1, 8, 24, 25].

CI-AKI is not common in patients with normal renal function; rather, it occurs frequently in patients with CKD and CH. Thus, rats with 5/6 nephrectomy develop hypertension, proteinuria, while the chronic hyperglycemia is associated with intrarenal vasoconstriction that compromises the RBF, resulting in some mechanisms that may be responsible for decrease of GFR [19, 23].

Table 2: Renal function.

Group	n	Urinary flow (mL/mim)	Inulin *clearance*/100 g (mL/min/100 g)	Urinary NGAL (pg/mL)
Sham	5	0.013 ± 0.003	0.68 ± 0.05	47.97 ± 19.19
Citrate	5	0.011 ± 0.002	0.74 ± 0.30	45.62 ± 0.95
Nx5/6	5	0.014 ± 0.004	0.25 ± 0.08[b]	76.75 ± 31.33
CH	5	0.032 ± 0.014[a]	0.43 ± 0.03[a]	53.72 ± 21.02
Nx5/6 + IC	5	0.021 ± 0.005	0.09 ± 0.03[bc]	153.49 ± 70.06[b]
CH + IC	5	0.042 ± 0.009[a]	0.17 ± 0.03[ad]	138.14 ± 74.80[a]

[a] $p < 0.05$ versus Citrate.
[b] $p < 0.001$ versus Sham.
[c] $p < 0.001$ versus Nx5/6.
[d] $p < 0.001$ versus CH.

Table 3: Renal hemodynamics.

Groups	n	Cardiac frequency (bpm)	Blood pressure (mmHg)	Renal blood flow (mL/min)	Renal vascular resistance, (mmHg·mL^{-1}·min^{-1})
Sham	5	464.00 ± 57.40	88.75 ± 5.20	9.28 ± 1.73	11.15 ± 1.62
Citrate	5	417.83 ± 44.59	100.71 ± 6.57	8.38 ± 0.84	18.02 ± 2.29
Nx + 5/6	5	503.80 ± 57.00	141.40 ± 11.30[a]	6.74 ± 1.73[a]	19.73 ± 4.62
CH	5	399.25 ± 63.60	98.93 ± 8.63	4.60 ± 0.28[b]	20.85 ± 0.32
Nx + 5/6 + IC	5	539.20 ± 60.20	120.20 ± 1.79[a]	3.64 ± 1.38[ac]	37.82 ± 10.16[ac]
CH + IC	5	385.37 ± 115.32	97.65 ± 7.22	2.16 ± 0.60[bd]	44.78 ± 7.52[bd]

[a] $p < 0.05$ versus Sham.
[b] $p < 0.05$ versus Citrate.
[c] $p < 0.05$ versus Nx + 5/6.
[d] $p < 0.05$ versus CH.

In conclusion, our data confirms that the presence of risk factors for renal dysfunction, as CKD and CH, contributes to enhancing the vulnerability to IC nephrotoxicity, once the renal impairment was significantly higher in animals twice insulted: CKD and CH treated with IC. Additionally, NGAL played an important role in signaling CI-AKI in these models. However, as in this study we could not account for interaction between risk factors, future investigations involving clinical practice data to experimental models, in a translational view, are needed to confirm the mechanisms involved in the CI-AKI.

Conflict of Interests

The authors declare that there is no conflict of interests regarding the publication of this paper.

Acknowledgment

This study was supported by a research grant from Sao Paulo Research Foundation (FAPESP) (2013/26560-2).

References

[1] P. A. McCullough and S. S. Soman, "Contrast-induced nephropathy," *Critical Care Clinics*, vol. 21, no. 2, pp. 261–280, 2005.

[2] P. A. McCullough, A. Adam, C. R. Becker et al., "Epidemiology and prognostic implications of contrast-induced nephropathy," *The American Journal of Cardiology*, vol. 98, no. 6, supplement 1, pp. 5k–13k, 2006.

[3] C. S. Rihal, S. C. Textor, D. E. Grill et al., "Incidence and prognostic importance of acute renal failure after percutaneous coronary intervention," *Circulation*, vol. 105, no. 19, pp. 2259–2264, 2002.

[4] P. Roy, V. Raya, T. Okabe et al., "Incidence, predictors, and outcomes of post-percutaneous coronary intervention nephropathy in patients with diabetes mellitus and normal baseline serum creatinine levels," *The American Journal of Cardiology*, vol. 101, no. 11, pp. 1544–1549, 2008.

[5] O. Toprak, M. Cirit, M. Yesil et al., "Impact of diabetic and prediabetic state on development of contrast-induced nephropathy in patients with chronic kidney disease," *Nephrology Dialysis Transplantation*, vol. 22, no. 3, pp. 819–826, 2007.

[6] S. N. Heyman, C. Rosenberger, S. Rosen, and M. Khamaisi, "Why is diabetes mellitus a risk factor for contrast-induced nephropathy?" *BioMed Research International*, vol. 2013, Article ID 123589, 8 pages, 2013.

[7] C. Briguori, C. Quintavalle, E. Donnarumma, and G. Condorelli, "Novel biomarkers for contrast-induced acute kidney injury," *BioMed Research International*, vol. 2014, Article ID 568738, 5 pages, 2014.

[8] P. C. Y. Wong, Z. Li, J. Guo, and A. Zhang, "Pathophysiology of contrast-induced nephropathy," *International Journal of Cardiology*, vol. 158, no. 2, pp. 186–192, 2012.

[9] S. A. Silver, P. M. Shah, G. M. Chertow, S. Harel, R. Wald, and Z. Harel, "Risk prediction models for contrast induced nephropathy: systematic review," *The British Medical Journal*, vol. 351, Article ID h4395, 2015.

[10] A. Caiazza, L. Russo, M. Sabbatini, and D. Russo, "Hemodynamic and tubular changes induced by contrast media," *BioMed Research International*, vol. 2014, Article ID 578974, 7 pages, 2014.

[11] K. M. Schmidt-Ott, K. Mori, Y. L. Jau et al., "Dual action of neutrophil gelatinase-associated lipocalin," *Journal of the American Society of Nephrology*, vol. 18, no. 2, pp. 407–413, 2007.

[12] P. Whiter and F. E. Samson, "Determination of inulin in plasm and urine by use of antrone," *Journal of Laboratory and Clinical Medicine*, vol. 43, no. 3, pp. 45–48, 1954.

[13] K. J. Berg, "Nephroltoxicity related to contrast media," *Scandinavian Journal of Urology*, vol. 34, no. 5, pp. 317–322, 2000.

[14] J. Ahmad, "Management of diabetic nephropathy: recent progress and future perspective," *Diabetes & Metabolic Syndrome: Clinical Research & Reviews*, vol. 9, no. 4, pp. 343–358, 2015.

[15] M. Kurdián, I. Herrero-Fresneda, N. Lloberas et al., "Delayed mTOR inhibition with low dose of everolimus reduces TGFβ expression, attenuates proteinuria and renal damage in the renal mass reduction model," *PLoS ONE*, vol. 7, no. 3, Article ID e32516, 2012.

[16] M. A. C. de Resende, A. V. Pantoja, B. M. Barcellos et al., "Ischemic postconditioning and subanesthetic S(+)-ketamine infusion: effects on renal function and histology in rats," *BioMed Research International*, vol. 2015, Article ID 864902, 8 pages, 2015.

[17] C. D. Fonseca, M. Watanabe, M. H. Mendonca, S. M. Fernandes, and M. F. F. Vattimo, "Heme oxigenasse-1 as a potetial antioxidante agente for contrast induced nephropathy in diabetic rats," *Nephrology Dialysis Transplantation*, vol. 29, supplement 3, pp. i63–i64, 2014.

[18] T.-Q. Liu, W.-L. Luo, X. Tan et al., "A novel contrast-induced acute kidney injury model based on the 5/6-nephrectomy rat and nephrotoxicological evaluation of iohexol and iodixanol in vivo," *Oxidative Medicine and Cellular Longevity*, vol. 2014, Article ID 427560, 14 pages, 2014.

[19] J. Šochman, J. H. Peregrin, M. Bürgelová, L. Kopkan, H. J. Kramer, and L. Červenka, "N-acetylcysteine attenuates iodine contrast agent-induced nephropathy in 5/6-nephrectomized rats," *Kidney and Blood Pressure Research*, vol. 33, no. 2, pp. 149–156, 2010.

[20] P. Deedwania, M. Kosiborod, E. Barrett et al., "Hyperglycemia and acute coronary syndrome: a scientific statement from the American Heart association Diabetes Committee of the Council of Nutrition," *Circulation*, vol. 117, no. 12, pp. 1610–1619, 2008.

[21] D. Russo, R. Minutolo, B. Cianciaruso, B. Memoli, G. Conte, and L. De Nicola, "Early effects of contrast media on renal hemodynamics and tubular function in chronic renal failure," *Journal of the American Society of Nephrology*, vol. 6, no. 5, pp. 1451–1458, 1995.

[22] P. Persson, P. Hansell, and F. Palm, "Adenosine A2 receptor-mediated regulation of renal hemodynamics and glomerular filtration rate is abolished in diabetes," *Advances in Experimental Medicine and Biology*, vol. 765, pp. 225–230, 2013.

[23] T. H. Hostetter, J. L. Troy, and B. M. Brenner, "Glomerular hemodynamics in experimental diabetes mellitus," *Kidney International*, vol. 19, no. 3, pp. 410–415, 1981.

[24] S. N. Heyman, S. Rosen, and C. Rosenberger, "Renal parenchymal hypoxia, hypoxia adaptation, and the pathogenesis of radiocontrast nephropathy," *Clinical Journal of the American Society of Nephrology*, vol. 3, no. 1, pp. 288–296, 2008.

[25] S. N. Heyman, J. Reichman, and M. Brezis, "Pathophysiology of radiocontrast nephropathy: a role for medullary hypoxia," *Investigative Radiology*, vol. 34, no. 11, pp. 685–691, 1999.

Hindawi Publishing Corporation
BioMed Research International
Volume 2016, Article ID 7497936, 7 pages
http://dx.doi.org/10.1155/2016/7497936

Research Article

Rhabdomyolysis following Cardiac Surgery: A Prospective, Descriptive, Single-Center Study

Amr S. Omar,[1,2] Hesham Ewila,[1,3] Sameh Aboulnaga,[1,4] Alejandro Kohn Tuli,[1] and Rajvir Singh[5]

[1]*Department of Cardiothoracic Surgery/Cardiac Anaesthesia & ICU Section, Heart Hospital, Hamad Medical Corporation, P.O. Box 3050, Doha, Qatar*
[2]*Department of Critical Care Medicine, Beni-Suef University, P.O. Box 62511, Beni-Suef, Egypt*
[3]*Department of Anesthesia, Suez Canal University, P.O. Box 351-41511, Ismailia, Egypt*
[4]*Department of Anesthesia, Ain Shams University, Kasr-El-Zaafaran, P.O. Box 11566, Cairo, Egypt*
[5]*Department of Cardiology Research Centre, Hamad Medical Corporation, P.O. Box 3050, Doha, Qatar*

Correspondence should be addressed to Amr S. Omar; a_s_omar@yahoo.com

Received 14 October 2015; Accepted 8 February 2016

Academic Editor: Jeremiah R. Brown

Purpose. Rhabdomyolysis (RML) following cardiac surgery and its relationship with acute kidney injury (AKI) require investigation. *Patients and Methods*. All patients undergoing cardiac surgery in our hospital were enrolled in this prospective study during a 1-year period. To investigate the occurrence of RML and its association with AKI, all patients in the study underwent serial assessment of serum creatine kinase (CK) and myoglobin levels. Serial renal function, prior statin treatment, and outcome variables were recorded. *Results*. In total, 201 patients were included in the study: 185 men and 16 women with a mean age of 52.0 ± 12.4 years. According to the presence of RML (CK of ≥2,500 U/L), the patients were divided into Group I (RML present in 17 patients) and Group II (RML absent in 184 patients). Seven patients in Group I had AKI (41%) where 34 patients in group II had AKI (18.4%), $P = 0.025$. We observed a significantly longer duration of ventilation, length of stay in the ICU, and hospitalization in Group I ($P < 0.001$ for all observations). *Conclusions*. An early elevation of serum CK above 2500 U/L postoperatively in high-risk cardiac surgery could be used to diagnose RML that may predict the concomitance of early AKI.

1. Introduction

Muscle necrosis and subsequent release of intracellular muscular constituents in the circulation are characteristic of rhabdomyolysis (RML). Asymptomatic elevation of muscle enzymes may be the only manifestation of RML. However, extreme cases may be associated with marked elevation of these enzymes, electrolyte disturbances, and development of acute kidney injury (AKI). Bywaters and Beall were the first to report RML in 1941, when four victims of crush injuries died after 1 week of developing AKI. An autopsy study revealed pigmented casts in the renal tubules, but the association of muscle injury and renal failure was unexplained [1].

Immediate circumstances may precede RML, such as surgical trauma, postictal state, or extraordinary physical exertion. However, in some cases no precipitating factors of RML are found. Inherited enzymatic deficiencies, electrolyte disturbances, infections, toxins, drugs, and endocrinopathies could be possible causes of RML [2]. RML can be a complication of bariatric surgeries [3]. The incidence of RML after cardiac surgery is still unclear, although cases of RML after cardiac surgery have been reported [4]. Some individual case reports have mentioned a severe form of RML after coronary artery bypass grafting (CABG) with renal failure that required hemodialysis for 40 days [5].

Clinical and biochemical consequences following RML could lead to compartment syndrome, or even death. Excessive weight in obese patients may act as compressive pressure and is recognized as a risk factor of RML [6]. Increased serum myoglobin levels after cardiac surgery are linked to increased mortality and the need for renal replacement therapy [7]. Myoglobin is a low-molecular-weight heme protein, which is

plentiful in cardiac and skeletal muscles. Myoglobin is rapidly released from necrotic muscle, while subsequent rapid renal clearance and high concentrations are associated with RML-induced renal failure [8].

Lagandré et al. [9] described precipitating factors that may lead to RML after bariatric surgery. These factors included obesity, prolonged supine postures, duration of the procedure when it is extended longer than 7 h in nonobese patients, and diabetes with concomitant microangiopathy and its possible metabolic complications, such as hypernatremia with hyperosmolarity, hypokalemia, hypocalcemia, and hypophosphatemia. Patients with American Society of Anesthesiologists (ASA) III and IV physical status are at higher risk of developing RML. Obese patients with ASA classification III and IV especially those with a body mass index > 55 kg/m^{-2} are at the highest ASA risk for RML [9].

The first signs and symptoms of RML are usually reported during the first 24 h after injury, although these may appear earlier. Suspicion of RML is usually based on clinical manifestations (reddish-brown urine, gluteal and back pain, and oliguria) and must be confirmed by laboratory studies. A five-fold elevation of serum creatine kinase (CK) levels (1050 U/L) is considered diagnostic for RML (males: CK > 1160 U/L; females: CK > 1075 U/L) [3, 10]. In cardiac surgery a higher set value to diagnose RML is described due to release of CK from related myocardial injury (2500 U/L) [11]. Severe RML is diagnosed when CK levels are higher than 10,000 U/L [12].

This study aimed to investigate the development of RML following cardiac surgery and its association with AKI. We also examined perioperative risk factors that may facilitate the occurrence of RML in cardiac surgery and the consequences of RML in this setting.

2. Methods

We performed a prospective, descriptive, single-center study with purposive sampling that examined the occurrence of RML and its association with AKI. All of the patients in the study underwent serial assessment of serum CK and myoglobin levels from baseline in the postoperative period. The study was conducted from February 2013 to February 2014 over 12 months in the cardiothoracic intensive care unit, Hamad Medical Corporation (12 beds). Approval for the study was obtained from the ethical committee (reference number 13001/13). Informed consent was waived for all patients by the Hamad Medical Corporation ethics committee because no specific intervention was carried out and sampling was part of routine care to make an early diagnosis of RML. In our patients, baseline muscular injury markers (CK, myoglobin, CK-MB isoform, and high-sensitivity troponin T) were measured, while two of these parameters (CK-MB isoform and high-sensitivity troponin T) were measured to quantify myocardial injury. Serum myoglobin levels were assessed by immunoassay from Beckman Coulter (Analis, Suarlée, Belgium). These laboratory markers were measured at the same time points by accredited hospital laboratory.

The following data were obtained: laboratory data that are routinely obtained in our intensive care unit (ICU) on admission; and demographic and clinical information, including age, sex, race, medical comorbidities, drugs, type of surgery, anesthesia time, cardiopulmonary bypass (CPB) time, aortic cross-clamp time, use of inotropes and vasopressors, Euro-SCORE, statin therapy, length of mechanical ventilation, and stay in the ICU and hospital. We systematically searched for risk factors for RML, as reported in previous studies. Complications and outcomes (AKI, arrhythmia, infection, stroke, need for dialysis, and mortality) were recorded for each patient. Patients with preexisting renal failure on dialysis or hepatic failure were excluded from the study. Once the diagnosis of RML was made, we used fluid loading and diuresis to treat our patients.

2.1. Study Definitions. Postcardiac surgery RML was suspected when serum CK levels were 2500 U/L or higher [11]. According to the consensus definition proposed by the Acute Kidney Injury Network, AKI was defined as an abrupt (within 48 h) reduction in kidney function, defined as an absolute increase in serum creatinine concentration of 0.3 mg/dL or greater (26.4 μmol/L) or a percentage increase of 50% or greater (1.5-fold from baseline) [13]. Myoglobin was used to confirm diagnosis of RML [14]. Measuring the change in high sensitive troponin T is useful to quantify the extent of perioperative myocardial injury [15]. The European system for cardiac operative risk evaluation (Euro-SCORE) [16] was used to assess differences in patients' risk profiles, and the ASA classification was used to categorize the surgical risk [17].

2.2. Statistical Analysis. Results are presented as mean ± standard deviation for quantitative data and frequency and proportion for qualitative data. The data were analyzed to test for statistically significant differences between variants. For quantitative data, Student's t-test was used to compare two groups. For qualitative data, the chi-squared test was used and odds ratio was calculated. Multivariate regression analysis was performed for statistically significant data in the univariate analysis. Variables influencing RML in our and previous analyses were assessed by multivariate regression analysis. The primary data parameter for the study was defined as the peak CK level. Clinical and laboratory data were entered into a database (Microsoft Excel 2010; Microsoft Corporation, Redmond, WA, USA), and statistical analyses were performed using statistical software (SPSS, version 16; SPSS, Inc., Chicago, IL, USA).

3. Results

3.1. Clinical Variables in the Groups. Two hundred and one patients were enrolled in our study, with a mean age of 52.0 ± 12.4 years. Patients were divided into two groups according to the peak level of CK. Group I had a CK level equal to or higher than 2500 U/L; Group II had CK levels less than 2500 U/L. The dynamic changes in CK over time were noted in Figure 1. Seventeen out of the 201 patients (8.4%) developed RML according to our cutoff point. Both groups were matched regarding age and sex (Table 1). No significant difference in hypertension or diabetes, whether insulin-dependent or non-insulin-dependent, was found between both groups.

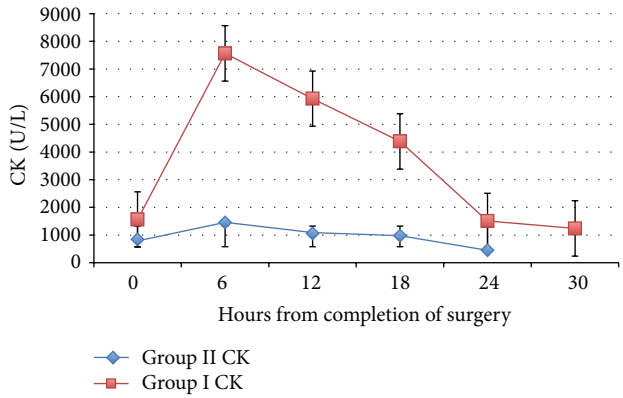

Figure 1: Dynamic changes in creatine kinase over time. The patients were divided into two groups: Group I (CK ≥ 2500 U/L) and Group II (CK < 2500 U/L). Postoperative changes in the CK level in both groups are shown above (0-hour sampling immediately after surgery). Error bars: ±SD.

Preexisting chronic renal disease or liver disease was not different between the groups. Ethnic predisposition was not associated with prevalence of RML. Among stating users RML was lower in Group I than Group II (47.1 versus 73.5%). There was no significant difference between the groups who underwent CABG. For patients who had valvular surgery, fewer patients had RML in Group I (11.7%) than in Group II (21.7%). All of the patients who entered the ICU after surgery for aortic dissection developed RML (three patients). The urgency of the procedure was not associated with RML. Dopamine was used more in Group I (62%) than in Group II (25%, $P = 0.03$). Preexisting heart failure or use of intra-aortic balloon pump (IABP) was not associated with a higher incidence of RML. Infectious complications were significantly higher in Group I (11.8%) compared with Group II (2.2%, $P = 0.05$), while other complications (arrhythmia and myocardial infarction) were not different between the groups.

3.2. Laboratory and Prognostic Variables in the Groups. Baseline creatinine levels were not significantly different between the groups (Table 2, 95.6 ± 35.3 μmol/L in Group I versus 92.7 ± 61 μmol/L in Group II, $P = 0.8$). Patients with RML showed a significant association with AKI (41% in Group I versus 18% in Group II, $P = 0.02$), and two patients required regular hemodialysis. High-sensitivity troponin T and CK-MB levels were significantly higher in Group I than in Group II (3606 ± 110 ng/L versus 1064 ± 81 ng/L and 83.4 ± 26 U/L versus 40.3 ± 3.1 U/L, resp., both $P = 0.001$). Myoglobin levels were significantly higher in Group I than in Group II (1120 ± 250 ng/mL versus 450 ± 195 ng/mL, $P = 0.0001$). The length of stay in the ICU and in hospital, and the length of mechanical ventilation, were significantly higher in Group I than in Group II (all $P = 0.001$).

Patients were divided again according to the myoglobin cutoff point of 1000 ng/mL. Dynamic changes in myoglobin in both groups in relation to time were noted in Figure 2. Three out of the 8 patients who had high myoglobin levels above 1000 ng/mL had higher incidence of AKI, and 38 out of 193 patients who had low myoglobin levels had AKI (37.5 versus 19.6%, $P = 0.05$). Myoglobin and CK levels tended to show an early rise, but CK longer than myoglobin (Figure 3). Hyperkalemia was encountered as an early warning sign because six out of 17 patients who developed RML had unexplained high potassium levels at an early stage in the first 4 hours after surgery (35.2%). Multivariate analysis (Table 3) showed that high CK is likely to associate CABG surgery and dopamine usage ($P = 0.03$ and 0.037, resp.). Finally,

Table 1: Clinical variables in both groups.

Variable	Group I (RML) $N = 17$	Group II (no RML) $N = 184$	P value
Age	47 ± 11	52 ± 11	0.08
Sex male	16 (94.1%)	169 (91.8%)	0.74
Hypertension	14 (82.5%)	123 (66.8%)	0.15
IDDM	0	16	0.28
NIDDM	4	79	0.07
BMI	28.7 ± 5.9	27.4 ± 4.8	0.4
Ethnicity (Arab)	4 (23.5%)	56 (30.4%)	0.43
ASA III	7 (41.1)	88 (47.8)	0.7
ASA IV	10 (58.8)	96 (52.1)	0.6
Euro score	3 ± 2.5	2.5 ± 2.3	0.47
Liver diseases	1 (5.8%)	2 (1%)	0.23
CRD	3 (17.6%)	18 (9.6%)	0.25
Statin usage	8 (47.1)	136 (73.5)	0.02
Inotrops			
Dopamine	10 (58.8%)	47 (25.5%)	0.03
Adrenaline	3 (17.6%)	24 (13%)	0.4
Noradrenline	6 (35.3)	52 (28.4%)	0.3
Surgery			
CABG	12 (70.6%)	140 (76%)	0.6
Valvular	2 (11.7%)	40 (21.7%)	0.01
Aortic dissec.	3 (17.7%)	0	0.001
Procedure type (urgent)	5 (29.4%)	41 (22.2%)	0.59
CPB time (minutes)	181.7 ± 75	110.7 ± 47	0.004
ACC time (minutes)	110.2 ± 12	68.6 ± 2.4	0.0001
Anesthesia time (min)	478.5 ± 168	362.7 ± 25	0.017
IABP	1 (5.8%)	9 (4.8%)	0.7
CHF	6 (35.3%)	66 (35%)	0.6
Complication			
Arrhythmia	3 (17%)	17 (7.5%)	0.2
MI	0	9 (4.9%)	0.4
Infection	2 (11.8%)	4 (2.2%)	0.05
Early stroke	1	0	

IDDM: insulin-dependant diabetes mellitus; NIDDM: non-insulin-dependent diabetes mellitus; BMI: body mass index; CBG: coronary artery bypass graft; CPB: cardiopulmonary bypass; ACC: aortic cross-clamp; IABP: intra-aortic balloon pump; CHF: congestive heart failure; MI: myocardial infarction.

Table 2: Laboratory and prognostic variables in both groups.

Variable	Group I (RML) $N = 17$	Group II (no RML) $N = 184$	P value
Basal creatinine (micromole/L)	95.6 ± 35.3	92.7 ± 61	0.8
AKI	7 (41%)	34 (18%)	0.025
HsTnT (ng/L)	3606 ± 110	1064 ± 81	0.001
CK MB (U/L)	83.4 ± 26	40.3 ± 3.1	0.001
Myoglobin (ng/mL)	1120 ± 250	450 ± 195	0.0001
LOS_{ICU} (hours)	203 ± 142	50 ± 11	0.001
LOS_{hosp} (days)	13.06 ± 11	7.5 ± 3.7	0.001
Ventilation time (minutes)	856 ± 199	486 ± 24	0.001

AKI: acute kidney injury; HsTnT: high sensitive troponin T; CK MB: creatine kinase MB; LOS_{ICU}: length of stay in intensive care; LOS_{hosp}: hospital length of stay.

Table 3: Multivariate logistic regression analysis for CK above 2500.

Variable	Adjusted OR	95% CI	Significance
Age	0.934	.852–1.023	0.934
Anesthesia time	2.02	.994–1.004	0.7
CPB time		.976–1.023	0.85
ACC time		.999–1.071	0.06
Surgery			
CABG	0.72	0.002–0.73	0.03
Valvular	1.34	0.019–20.6	0.7
Dopamine usage	0.8	.034–.898	0.037
LOV (minutes)	1	.998–1.002	0.8
LOS_{ICU} (hours)	.99	0.998–1.003	0.8
LOS_{hosp} (days)	.99	0.954–1.174	0.2
AKI	0.37	0.073–2.962	0.08

CPB: cardiopulmonary bypass; ACC: aortic cross clamp; CABG: coronary artery bypass graft; LOV: length of mechanical ventilation; LOS_{ICU}: ICU length of stay; LOS_{hosp}: hospital length of stay; AKI: acute kidney injury.

Table 4: CK and myoglobin relation.

Variable	r	P
CK & myoglobin	0.63	0.001

CK: creatine kinase.

within the AKI group (44 patients) we studied the value of cut point of myoglobin (1000 ng/mL); there was high association of AKI in the high myoglobin group but without statistical difference 37.5% versus 19.5% ($P = 0.2$). We found a relationship between CK and myoglobin levels in the form of a significant increase in the myoglobin level with the rise in the CK level r value = 0.63 ($P = 0.001$) (Figure 3 and Table 4).

4. Discussion

The incidence of RML after cardiac surgery remains unclear, and some authors have mentioned an incidence of 19% for RML after CABG, with a direct relation between AKI and RML [6]. Myocardial injury that is experienced after cardiac surgeries cannot completely explain the observed myoglobinemia [6]. Our study was designed to investigate the incidence of RML after cardiac surgery and its relation to AKI. In our study, 17 patients developed RML, with an incidence of 8.41%. Black et al. described racial variation in serum CK levels where they found that Afro-Caribbean persons have higher levels of CK than the Caucasian population [18]. Based on this finding, we compared Arabs and Asians regarding the association of RML but did not find any significant correlation ($P = 0.4$).

Numerous factors may raise the propensity of RML after cardiac surgery but it is relatively uncommon after CPB [19]. Direct femoral artery cannulation [20], arterial diseases, a long extracorporeal circulation, low cardiac output syndrome, and continuous epinephrine infusion have been described as participatory factors of RML. Moreover, diabetes mellitus, extremes of age, and preexisting renal diseases are also thought to be participatory factors of RML [21, 22]. Incorrect positioning during surgery with pressure necrosis has also been reported [23, 24] and patients with an IABP

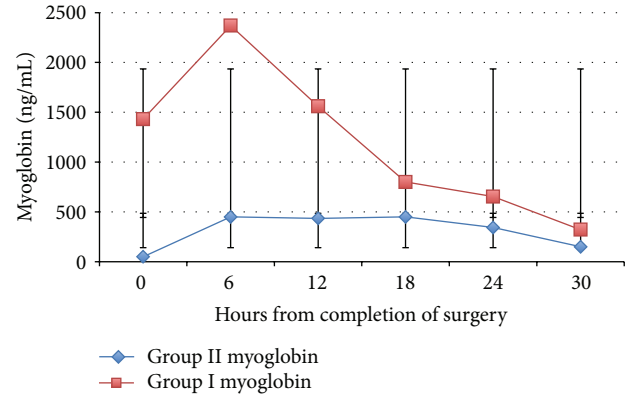

Figure 2: Dynamic changes in myoglobin in both groups in relation to time. The patients were divided into 2 groups: Group I (myoglobin ≥ 1000 ng/mL), and Group II (myoglobin < 1000 ng/mL). Postoperative changes in myoglobin both groups are shown above (0-hour sampling immediately after surgery). Error bars: ±SD.

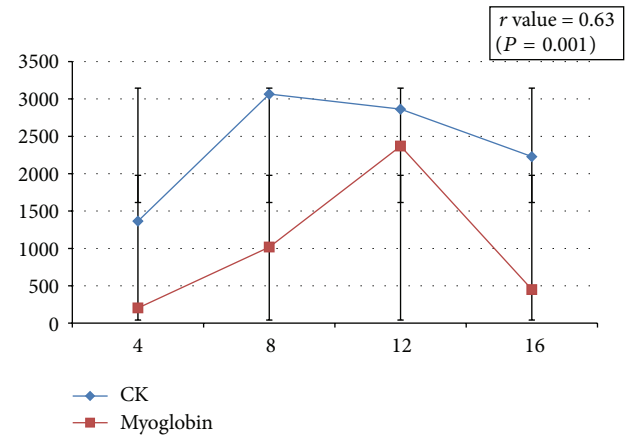

Figure 3: Relationship between CK and myoglobin.

are associated with RML [20]. In our study, both groups were matched regarding age and sex. However, our study did not include extremes of age, and patients who had diabetes or hypertension were not associated with a high incidence of RML in our study. In addition, both groups were matched regarding the Euro-SCORE and BMI. Our patients generally had a low body mass index (27.8 ± 5.1). The use of an IABP was not associated with a higher incidence of RML, and only 10 (4.9%) patients in our study required this intervention. It might induce RML when it causes limb ischemia, which was encountered in two patients in Group II, but they did not have compartment syndrome.

Unusual positions and increased pressure in certain areas during anesthesia allow sustained high pressure on the muscles. This results in muscle ischemia, sarcolemma injury, sodium-potassium pump disruption, electrolyte imbalance, and failure of energy supply to muscle fibers [25].

Statin users were not associated with the development of RML in our study. In fact, we found a significantly lower incidence of RML among patients taking statins ($P = 0.02$). Some studies have shown that statins have a high association with perioperative mortality [26]. The advantages of statins on surgical mortality might outweigh the postoperative risks. Eventually, all CABG patients should receive lifelong statin therapy in the absence of contraindications [27]. Kulik and Ruel [28] emphasized that statin-associated RML is more pronounced in patients with certain metabolic abnormalities, whereas our study population exhibited a relatively lower mean age and number of metabolic complications. The mean length of ventilation in our study was 503 ± 405 min. During this time, propofol was used at a dose of less than 1 mg/kg/h. Propofol infusion syndrome with concomitant development of RML has been encountered with use of doses as a high as 5 mg/kg/h for more than 48 h [29]. We did not find a significant association with use of epinephrine or norepinephrine in the patients who developed RML. However, dopamine users were associated with more RML events (Tables 2 and 3). We found that patients who developed an early infection had a higher incidence of RML, but this did not reach statistical significance. Viral as well as bacterial infections have been claimed to cause RML [30].

The urgency of the procedure did not appear to be associated with RML. Patients who underwent CABG had a higher incidence of RML than those who underwent valvular surgeries in multivariate analysis. All of the patients who had aortic dissection surgeries developed RML. Benedetto et al. [6] reported a 40% incidence of RML after CABG, but the incidence of CABG in our study was lower. No previous studies have addressed the association of RML after valvular surgery. In our study, two patients developed RML after valvular surgery. RML could be a common complication after surgeries for aortic dissection where preexisting peripheral vascular disease and femoral cannulation may be sources of skeletal muscle ischemia. Aortic dissection surgery had a longer CPB and anesthesia time [26, 31]. In our study, patients with RML had significantly longer anesthesia and CPB and aortic cross-clamp times. According to Benedetto et al., longer CPB is associated with a higher incidence of AKI in which RML could be the precipitating factor [6]. Similarly, Conlon et al. reported that longer CPB could be a predictor of AKI [32].

We consider that multiple factors could explain this association in our patients, including prolonged CPB and surgery time. Severe RML triggers a cascade with many consequences, including hypovolemia, hypoalbuminemia, anemia, disseminated intravascular coagulation, hyperkalemia, hypocalcemia, hypercalcemia, hyperphosphatemia, and acute tubular necrosis. Higher pressure on the back muscles related to increased weight and other potential mechanisms related to metabolic derangement are probably present [33] in prolonged surgeries, which are associated with a higher propensity of development of RML in many studies on cardiac and noncardiac surgery [6, 23, 25].

Basal creatinine levels were matched in both groups. While Group I was associated with a significantly high incidence of AKI, it seems that patients with higher levels of CK and myoglobin exhibited a higher association with AKI (Table 2). The incidence of AKI after cardiac surgery is variable. Benedetto et al. found a 2.6-fold increase in the incidence of AKI when myoglobin concentrations reached higher than 465 mg/mL [6]. AKI associated with RML may occur with CK levels as low as 5000 U/L when there is an association of hypovolemia, sepsis, and acidosis. AKI associated with RML usually carries a higher mortality than when RML develops alone (59% versus 22%) [34].

Surgical procedures are currently receiving attention after RML has been linked to trauma that is more pronounced in hypotensive patients. Muscles in the back, as well as the gluteal regions, are compressed against the operating table, leading to RML. This is aggravated by patients' weight, a longer duration of surgery, and CPB-induced hypotension. Peripheral hypoperfusion induced by peripheral vascular disease in CABG patients is hypothesized to exacerbate the condition [6].

Dynamic changes in serum CK and myoglobin levels were studied (Figures 1 and 2), and we observed early diagnostic accuracy for myoglobin with rapid clearance. However, CK levels increased later and were more persistent than myoglobin, which appears to be suitable for follow-up. This finding is consistent with Laurence, who suggested that, as long as the peak of CK had been obtained, estimation of serum CK levels could be helpful for estimating the extent of muscle damage when myocardial infarction is ruled out [35]. Our finding is also consistent with the previous finding that serum myoglobin has faster elimination kinetics in patients treated with forced alkaline diuresis for RML [36].

Our patients were usually placed under sedation after surgery for at least 4 h and received postoperative analgesia. Moreover, pain encountered from a sternotomy incision could mask possible pain from the back. Therefore, early clinical signs for RML were difficult for diagnosis. A high index of suspicion was needed for RML because early prevention is sensible before renal dysfunction is imminent. Six patients in the RML group (35.2%) developed early, unexplained hyperkalemia. Rosenberry et al. mentioned the concomitance of RML and severe hyperkalemia [37]. Receiving sedation and analgesia as well as vasoactive drugs after cardiac surgery could be associated with loss of early clinical signs of RML

including fever, malaise, tachycardia, nausea, and vomiting [8].

Patients with RML had a prolonged length of stay in hospital and in the ICU, as well as a prolonged length of mechanical ventilation. We believe that early diagnosis is important for preventing the sequelae of RML. Omar and Abouelnagah suggested that a preventive bundle for RML in bariatric surgery should include adequate padding of pressure points in the preoperative and postoperative periods, proper positioning, with close exposure of the pressure points, reducing the operative time, adequate hydration, and close postoperative monitoring [38]. We think that prevention of RML after cardiac surgery could start with early monitoring.

5. Conclusions

An early elevation of serum CK above 2500 U/L postoperatively in high-risk cardiac surgery could be used to diagnose RML that may predict the concomitance of early AKI. Hyperkalemia may be an early warning sign for RML development. Proper intervention may prevent the sequelae of organ dysfunction.

Abbreviations

ASA: American Society of Anesthesiologists
AKI: Acute kidney injury
CABG: Coronary artery bypass grafting
CAD: Coronary artery disease
CK: Creatine kinase
CPB: Cardiopulmonary bypass
IABP: Intra-aortic balloon pump
RML: Rhabdomyolysis.

Ethical Approval

Approval for the study was obtained from the ethical committee (Reference no. 13001/13).

Disclosure

The authors feel that this case adds to the already existing published medical literature regarding rhabdomyolysis and acute kidney injury after cardiac surgery. The authors think that this particular area needs investigation, no previous studies in the Middle East addressed rhabdomyolysis after cardiac surgery, and few studies went through the later subject. The poster was presented in the 34th ISICEM (International Symposium of Intensive Care and Emergency Medicine). The study was conducted from February 2013 to February 2014 over 12 months in the cardiothoracic intensive care unit, Hamad Medical Corporation (12 beds).

Conflict of Interests

We did not receive in the past 5 years reimbursements, fees, funding, or salary from an organization that may in any way gain or lose financially from the publication of this paper now; however Hamad Medical Corporation is going to fund for paper processing charges. We did not hold any stocks or shares in an organization that may in any way gain or lose financially from the publication of this paper, either now or in the future. We did not hold or are you currently applying for any patents relating to the content of the paper. We did not receive reimbursements, fees, funding, or salary from an organization that holds or has applied for patents relating to the content of the paper. We do not have any other financial competing interests. There are no other nonfinancial competing interests (political, personal, religious, ideological, academic, intellectual, commercial, or any other) to declare in relation to this paper.

Authors' Contribution

Amr S. Omar wrote the main paper and designed the study plan and submission. Hesham Ewila and Sameh Aboulnaga contributed to data collection, Rajvir Singh contributed to statistical analysis, and Alejandro Kohn Tuli, as chair of intensive care, provided general support. All authors read and approved the final paper.

Acknowledgments

The authors thank all members of cardiothoracic surgery, Heart Hospital, and the research department, Hamad Medical Corporation, for supporting this paper. The statistical part was done by senior consultant biostatistics (5th author), and the English, grammar, and punctuation were reviewed through Edanz group (certificate available).

References

[1] R. Lane and M. Phillips, "Rhabdomyolysis," *The British Medical Journal*, vol. 327, no. 7407, pp. 115–116, 2003.

[2] E. G. Bywaters and D. Beall, "Crush injuries with impairment of renal function," *British Medical Journal*, vol. 1, article 427, 1941.

[3] J. D. Warren, P. C. Blumbergs, and P. D. Thompson, "Rhabdomyolysis: a review," *Muscle and Nerve*, vol. 25, no. 3, pp. 332–347, 2002.

[4] M. Maccario, C. Fumagalli, V. Dottori et al., "Rhabdomyolytic acute renal failure in cardiac surgery. A clinical case," *Minerva Anestesiologica*, vol. 61, no. 9, pp. 397–400, 1995.

[5] S. Sudarsanan, A. S. Omar, R. A. Pattath, and A. Al Mulla, "Acute kidney injury associated with rhabdomyolysis after coronary artery bypass graft: a case report and review of the literatures," *BMC Research Notes*, vol. 7, no. 1, article 152, 2014.

[6] U. Benedetto, E. Angeloni, R. Luciani et al., "Acute kidney injury after coronary artery bypass grafting: does rhabdomyolysis play a role?" *Journal of Thoracic and Cardiovascular Surgery*, vol. 140, no. 2, pp. 464–470, 2010.

[7] D. Hofmann, M. Buettner, F. Rissner, M. Wahl, and S. G. Sakka, "Prognostic value of serum myoglobin in patients after cardiac surgery," *Journal of Anesthesia*, vol. 21, no. 3, pp. 304–310, 2007.

[8] A. L. Huerta-Alardín, J. Varon, and P. E. Marik, "Bench-to-bedside review: rhabdomyolysis—an overview for clinicians," *Critical Care*, vol. 9, no. 2, pp. 158–169, 2005.

[9] S. Lagandré, L. Arnalsteen, B. Vallet et al., "Predictive factors for rhabdomyolysis after bariatric surgery," *Obesity Surgery*, vol. 16, no. 10, pp. 1365–1370, 2006.

[10] B. J. Minnema, P. C. Neligan, N. A. Quraishi, M. G. Fehlings, and S. Prakash, "A case of occult compartment syndrome and nonresolving rhabdomyolysis," *Journal of General Internal Medicine*, vol. 23, no. 6, pp. 871–874, 2008.

[11] L. Hajjar, S. Grande, F. Galas, A. Roquim, L. Sampaio, and J. Auler, "Risk factors and outcome of rhabdomyolysis after cardiac surgery," *Critical Care*, vol. 12, supplement 2, p. P470, 2008.

[12] P. Mognol, S. Vignes, D. Chosidow, and J.-P. Marmuse, "Rhabdomyolysis after laparoscopic bariatric surgery," *Obesity Surgery*, vol. 14, no. 1, pp. 91–94, 2004.

[13] R. L. Mehta, J. A. Kellum, S. V. Shah et al., "Acute Kidney Injury Network: report of an initiative to improve outcomes in acute kidney injury," *Critical Care*, vol. 11, no. 2, article R31, 2007.

[14] K. Rodríguez-Capote, C. M. Balion, S. A. Hill, R. Cleve, L. Yang, and A. E. Sharif, "Utility of urine myoglobin for the prediction of acute renal failure in patients with suspected rhabdomyolysis: a systematic review," *Clinical Chemistry*, vol. 55, no. 12, pp. 2190–2197, 2009.

[15] P. Nagele, F. Brown, B. F. Gage et al., "High-sensitivity cardiac troponin T in prediction and diagnosis of myocardial infarction and long-term mortality after noncardiac surgery," *American Heart Journal*, vol. 166, no. 2, pp. 325.e1–332.e1, 2013.

[16] S. A. M. Nashef, F. Roques, P. Michel, E. Gauducheau, S. Lemeshow, and R. Salamon, "European system for cardiac operative risk evaluation (EuroSCORE)," *European Journal of Cardio-thoracic Surgery*, vol. 16, no. 1, pp. 9–13, 1999.

[17] L. Tiret, F. Hatton, J. M. Desmonts, and G. Vourc'h, "Prediction of outcome of anaesthesia in patients over 40 years: a multifactorial risk index," *Statistics in Medicine*, vol. 7, no. 9, pp. 947–954, 1988.

[18] H. R. Black, H. Quallich, and C. B. Gareleck, "Racial differences in serum creatine kinase levels," *The American Journal of Medicine*, vol. 81, no. 3, pp. 479–487, 1986.

[19] I. Alterman, A. Sidi, L. Azamfirei, S. Copotoiu, and T. Ezri, "Rhabdomyolysis: another complication after prolonged surgery," *Journal of Clinical Anesthesia*, vol. 19, no. 1, pp. 64–66, 2007.

[20] M. Maccario, C. Fumagalli, V. Dottori et al., "The association between rhabdomyolysis and acute renal failure in patients undergoing cardiopulmonary bypass," *Journal of Cardiovascular Surgery*, vol. 37, no. 2, pp. 153–159, 1996.

[21] G. Zanardo, P. Michielon, A. Paccagnella et al., "Acute renal failure in the patient undergoing cardiac operation: prevalence, mortality rate, and main risk factors," *Journal of Thoracic and Cardiovascular Surgery*, vol. 107, no. 6, pp. 1489–1495, 1994.

[22] G. J. Mangos, D. Horton, M. A. Brown, P. Trew, W. Y. L. Chan, and J. A. Whitworth, "Acute renal failure following cardiac surgery: incidence, outcomes and risk factors," *Australian and New Zealand Journal of Medicine*, vol. 25, no. 4, pp. 284–289, 1995.

[23] M. Goldberg, J. F. Stecker Jr., J. E. Scarff Jr., and D. G. Wombolt, "Rhabdomyolysis associated with urethral stricture repair: report of a case," *Journal of Urology*, vol. 124, no. 5, pp. 730–731, 1980.

[24] G. R. Nimmo, S. M. Stewart, and P. J. English, "Myoglobinuric acute renal failure associated with major urological surgery—an avoidable problem?" *Intensive Care Medicine*, vol. 14, no. 3, pp. 244–245, 1988.

[25] J. E. M. T. de Menezes Ettinger, P. V. Dos Santos Filho, E. Azaro, C. A. Bastos Melo, E. Fahel, and P. B. Pena Batista, "Prevention of rhabdomyolysis in bariatric surgery," *Obesity Surgery*, vol. 15, no. 6, pp. 874–879, 2005.

[26] M. Wilhelmi, M. Winterhalter, S. Fischer et al., "Massive postoperative rhabdomyolysis following combined CABG/abdominal aortic replacement: a possible association with HMG-CoA reductase inhibitors," *Cardiovascular Drugs and Therapy*, vol. 16, no. 5, pp. 471–475, 2002.

[27] K. A. Antons, C. D. Williams, S. K. Baker, and P. S. Phillips, "Clinical perspectives of statin-induced rhabdomyolysis," *The American Journal of Medicine*, vol. 119, no. 5, pp. 400–409, 2006.

[28] A. Kulik and M. Ruel, "Statins and coronary artery bypass graft surgery: preoperative and postoperative efficacy and safety," *Expert Opinion on Drug Safety*, vol. 8, no. 5, pp. 559–571, 2009.

[29] R. J. Bray, "Propofol infusion syndrome in children," *Paediatric Anaesthesia*, vol. 8, no. 6, pp. 491–499, 1998.

[30] U. Singh and W. M. Scheld, "Infectious etiologies of rhabdomyolysis: three case reports and review," *Clinical Infectious Diseases*, vol. 22, no. 4, pp. 642–649, 1996.

[31] R.-B. Hsu, Y.-L. Ho, R. J. Chen, S.-S. Wang, F.-Y. Lin, and S.-H. Chu, "Outcome of medical and surgical treatment in patients with acute type B aortic dissection," *Annals of Thoracic Surgery*, vol. 79, no. 3, pp. 790–794, 2005.

[32] P. J. Conlon, M. Stafford-Smith, W. D. White et al., "Acute renal failure following cardiac surgery," *Nephrology Dialysis Transplantation*, vol. 14, no. 5, pp. 1158–1162, 1999.

[33] L. S. Sharp, G. S. Rozycki, and D. V. Feliciano, "Rhabdomyolysis and secondary renal failure in critically ill surgical patients," *American Journal of Surgery*, vol. 188, no. 6, pp. 801–806, 2004.

[34] E. El-Abdellati, M. Eyselbergs, H. Sirimsi et al., "An observational study on rhabdomyolysis in the intensive care unit. Exploring its risk factors and main complication: acute kidney injury," *Annals of Intensive Care*, vol. 3, no. 1, pp. 1–8, 2013.

[35] A. S. Laurence, "Serum myoglobin and creatine kinase following surgery," *British Journal of Anaesthesia*, vol. 84, no. 6, pp. 763–766, 2000.

[36] H. Lappalainen, E. Tiula, L. Uotila, and M. Mänttäri, "Elimination kinetics of myoglobin and creatine kinase in rhabdomyolysis: implications for follow-up," *Critical Care Medicine*, vol. 30, no. 10, pp. 2212–2215, 2002.

[37] C. Rosenberry, F. Stone, and K. Kalbfleisch, "Rhabdomyolysis-induced severe hyperkalemia," *The Western Journal of Emergency Medicine*, vol. 10, no. 4, article 302, 2009.

[38] A. S. Omar and G. Abouelnagah, "Successful prevention of rhabdomyolysis (RML) after bariatric surgery (BS) in intensive care settings," *Critical Care & Shock*, vol. 16, no. 1, pp. 12–18, 2013.

Hindawi Publishing Corporation
BioMed Research International
Volume 2016, Article ID 8580475, 9 pages
http://dx.doi.org/10.1155/2016/8580475

Research Article

Renal Ischemia/Reperfusion Injury in Diabetic Rats: The Role of Local Ischemic Preconditioning

Sule Ozbilgin,[1] Sevda Ozkardesler,[1] Mert Akan,[1] Nilay Boztas,[1] Mucahit Ozbilgin,[2] Bekir Ugur Ergur,[3] Serhan Derici,[2] Mehmet Ensari Guneli,[4] and Reci Meseri[5]

[1]*Department of Anesthesiology and Reanimation, School of Medicine, Dokuz Eylul University, Izmir, Turkey*
[2]*Department of General Surgery, School of Medicine, Dokuz Eylul University, Izmir, Turkey*
[3]*Department of Histology and Embryology, School of Medicine, Dokuz Eylul University, Izmir, Turkey*
[4]*Department of Experienced Laboratory Animal Science, School of Medicine, Dokuz Eylul University, Izmir, Turkey*
[5]*Department of Nutrition and Dietetics, Izmir Ataturk School of Health, Ege University, Izmir, Turkey*

Correspondence should be addressed to Sule Ozbilgin; sozbilginmd@gmail.com

Received 3 November 2015; Revised 22 December 2015; Accepted 4 January 2016

Academic Editor: Jeremiah R. Brown

Background. The aim of this study was to evaluate the effects of local ischemic preconditioning using biochemical markers and histopathologically in the diabetic rat renal IR injury model. *Methods*. DM was induced using streptozotocin. Rats were divided into four groups: Group I, nondiabetic sham group ($n = 7$), Group II, diabetic sham group ($n = 6$), Group III, diabetic IR group (diabetic IR group, $n = 6$), and Group IV, diabetic IR + local ischemic preconditioning group (diabetic IR + LIPC group, $n = 6$). Ischemic renal injury was induced by clamping the bilateral renal artery for 45 min. 4 h following ischemia, clearance protocols were applied to assess biochemical markers and histopathologically in rat kidneys. *Results*. The histomorphologic total cell injury scores of the nondiabetic sham group were significantly lower than diabetic sham, diabetic IR, and diabetic IR + LIPC groups. Diabetic IR group scores were not significantly different than the diabetic sham group. But diabetic IR + LIPC group scores were significantly higher than the diabetic sham and diabetic IR groups. *Conclusion*. Local ischemic preconditioning does not reduce the risk of renal injury induced by ischemia/reperfusion in diabetic rat model.

1. Introduction

Diabetes mellitus (DM) is a common and increasing chronic metabolic disease progressing with hyperglycemia, dyslipidemia, glycosuria, and metabolic disorders [1, 2]. Diabetic nephropathy is a cause of end-stage renal failure [3]. Diabetes mellitus is defined as a risk factor for the development of acute renal damage in a variety of clinical situations such as radiocontrast nephropathy or after cardiopulmonary bypass [4, 5].

Clinical studies of diabetes mellitus patients have previously reported increased susceptibility of the kidney to acute kidney injury (AKI). Studies of experimental models of this disease have shown that diabetic rats have increased susceptibility to renal ischemia/reperfusion injury (IRI) [6–8]. Various methods have been developed to prevent ischemia-reperfusion (IR) injury. One of these methods is local ischemic preconditioning (LIPC) which was described for the heart by Murry et al. in 1986. In local ischemia preconditioning the aim is to expose the organ to short IR periods before the ischemia duration to protect from IR damage. However this method has disadvantages such as causing trauma to large veins and stress to organs [7]. Another method is remote ischemic preconditioning (RIPC). Increasing the resistance of an organ to ischemia with the application of short ischemia-reperfusion episodes to another organ is called RIPC [8]. Thus the target organ is not exposed to direct stress [8]. For the treatment of renal IRI, supportive therapy remains, and therefore improved treatment strategies to prevent renal IR injury are drawing attention from scholars [7].

Renal IRI may be shown histomorphologically and biochemically. Both inflammation and apoptosis coexist in renal

IR injury. During hypoxia, caspase activity increases as a result of intracellular Ca^{2+} accumulation. Caspase becomes activated in ischemic tissues and is an indicator of cell death [7, 9]. These changes, which can be observed in tubular cells, may cause the loss of brush borders of proximal tubular cells and spill out from the basement membrane of the cells into the tubular lumen, with eventual tubule obstruction. Biochemically, in addition to BUN, creatinine, and GFR, the new marker of NGAL has entered the agenda recently. Neutrophil gelatinase-associated lipocalin is shown to be the most expressed protein in the kidney a short time before creatinine after acute ischemic and nephrotoxic injury. Renal function can be monitored using the neutrophil gelatinase-associated lipocalin (NGAL) biomarker. After acute kidney injury NGAL protein is easily identified in blood and urine. In fact, NGAL is one of the earliest markers of renal injury after ischemia or nephrotoxic injury in animal models [10]. Most of the studies pertaining to the use of NGAL have come from cardiothoracic surgery, transplant, and critical care literature. Based on some of these findings, it has been noted that increased levels of serum NGAL may be seen as soon as two hours after a renal insult [10]. It seems that urine and plasma levels of NGAL are both equally acceptable as markers of acute kidney injury (AKI) [11], although there are some reports that urinary NGAL may have a slightly higher predictive value, at least in the critical care environment.

The aim of this study was to evaluate the effects of local ischemic preconditioning using biochemical markers (BUN, Cr, and NGAL) and histopathologically in the diabetic rat renal IR injury model.

2. Methods

After obtaining permission from the Dokuz Eylul University School of Medicine (DEUSM) Local Animal Experiments Ethical Committee (Date: 03.09.2014, protocol number: 27/2014, Yılmaz O), the research was carried out at the DEUSM Animal Experiment Laboratories. Twenty-eight adult Wistar albino rats weighing 230–300 g were used in this study. The animals were housed in a light controlled room with a 12 h light/dark cycle and allowed access to food and water. Experimental protocols and animal care methods in the experiment were approved by the Experimental Animal Research Committee of our institution.

2.1. Induction of Diabetes. STZ was used to induce diabetes as described previously [12]. To induce the diabetes model, 45 mg/kg streptozotocin (STZ) (STZ, Sigma Chemical Co., St. Louis, MO, USA) was administered intraperitoneally in a single dose. STZ was prepared in a 0.1 M phosphate-citrate buffer (pH: 4.5) and an equal volume of buffer was injected ip into the control sham group without induced diabetes. STZ was prepared freshly and used immediately. Three days after this application a blood sample was taken from the tail. Rats with blood sugar > 250 mg/dL on glycometry of the sample were accepted as diabetic. The rats were monitored for one month in the experimental animals laboratory and then the study began. Within this time, weight changes and blood glucose measurements were recorded.

2.2. Study Design. Rats were divided into four groups: *Group I*, nondiabetic sham group ($n = 7$), *Group II*, diabetic sham group ($n = 7$), *Group III*, diabetic IR group (diabetic IR group, $n = 7$), and *Group IV*, diabetic IR + local ischemic preconditioning group (diabetic IR + LIPC group, $n = 7$).

The rats were anesthetized with ketamine (50 mg/kg ip) and xylazine hydrochloride (10 mg/kg ip) and bilateral renal pedicles were exposed after laparotomy. After anesthesia, the rats were heated with a heating lamp to maintain a rectal body temperature of 37°C. At the beginning of the study, 1 mL of blood sample was drawn from the lateral tail vein for the measurement of basal blood glucose before abdominal incision. For IRI induction, bilateral renal pedicle occlusion was performed with hemostasis atraumatic microvascular clamp for 45 min. At the end of the ischemic period, the clips were removed to allow blood reperfusion. In nondiabetic sham and also diabetic sham group, bilateral renal pedicles were exposed without any intervention after laparotomy. In diabetic IR group, after 45 min of ischemia, the bilateral atraumatic microvascular clamp was removed and reperfusion of the kidneys was allowed to continue for 4 hours. In diabetic IR + LIPC group, bilateral renal pedicles were exposed. Left renal pedicles were maintained with atraumatic microvascular clamp compression. Four cycles of 4 min of ischemia were performed followed by 11 min of reperfusion for the left kidney (65 minutes total). For total renal ischemia, after 5 min the bilateral renal pedicles were clamped for 45 min and then these clamps were removed and reperfusion of the kidneys was allowed for 4 hours.

To protect the rats from hypothermia, the operating table was heated with a lamp heater throughout the study and rectal body temperature was measured with a probe and maintained at 37–37.5°C. To avoid dehydration and hypothermia 3 mL/kg/h subcutaneous isotonic fluid solution was administered during the operation. During the waiting time, the abdomen was closed with a moist sterile pad and surgical forceps. At the end of reperfusion, the animals were anesthetized, blood samples were drawn from the right atrium for the measurement of renal function parameters, and left kidneys were excised. The kidneys were fixed in 10% buffered formalin and embedded in paraffin wax, cut to 4-5 μm, and stained with hematoxylin and eosin for histological studies using a light microscope.

2.3. Exclusion Criteria. Rats in need of resuscitation were excluded from the study.

2.4. Renal Ischemia-Reperfusion Model. The right and left renal pedicles were exposed after laparotomy. Total renal ischemia was maintained by compressing the bilateral renal pedicles with microvascular clips. Adequate occlusion was confirmed by a lack of pulsation in the renal pedicles and presence of pallor in the kidneys. After the ischemic period, the microvascular clips were removed and reperfusion occurred. The cessation of blood flow was confirmed using a laser current meter (Laser Flo BPM2, Vasamedic, USA).

2.5. Local Ischemic Preconditioning Model. For local ischemic preconditioning, a method that has been shown to be effective by perfusion scintigraphy and a laser meter was used [13, 14]. For this purpose, bilateral renal pedicles were exposed. Left renal pedicles were maintained with atraumatic microvascular clip compression. Four cycles of 4 min of ischemia were performed followed by 11 min of reperfusion for the left kidney (65 minutes total). For total renal ischemia purposes, after 5 min, the bilateral renal pedicles were clamped for 45 min and then these clips were removed and reperfusion of the kidneys was allowed for 4 hours.

2.6. Histomorphological Evaluation of Renal Tissue. Renal tissue sections were evaluated after ischemia-reperfusion using light microscopy by two histologists blinded to the animal groups for structural changes in proximal tubules (tubular atrophy, loss of tubular brush border, vacuolization, tubular dilatation, and cast formation), mononuclear cells (MNCs) infiltration, interstitial structural changes, and renal corpuscle morphology. The cross-sectional images were scored semiquantitatively in terms of tubulointerstitial damage. Scoring was conducted as follows: 0 = not at all, 1 = 0–25%, 2 = 26–45%, 3 = 46–75%, and 4 = 76–100% [15].

2.7. Biochemical Evaluation. The blood urea nitrogen, blood creatinine level, and serum NGAL levels were measured 4 hours after reperfusion in Dokuz Eylul University Medical Faculty Hospital Biochemistry Laboratory. Blood urea nitrogen and blood creatinine levels were analyzed photometrically with a *Beckman AU 5800* autoanalyzer. Serum NGAL levels were analyzed with the ELISA method using a Boster trade kit (Boster Biological Technology Co., CA; cat number: EK0855, USA). According to the manufacturer's prospectus, the NGAL detection limit is 10 pg/mL with measurement interval of 78 to 5000.

2.8. Statistical Analysis. SPSS 15.0 (Statistical Package for the Social Sciences ver. 15, Chicago, IL, USA) was used. Continuous variables are presented as mean ± SD and median (minimum-maximum). For univariate analysis, Mann-Whitney U test was used for comparison of two groups. In order to determine weight and blood glucose level fluctuations over time Friedman repeated measurement was conducted. The level of statistical significance was accepted as $p < 0.05$.

3. Results

A total of 28 rats were included in the study. In 21 rats monitored for one month for the diabetes protocol, 2 rats were exitus. One rat in the diabetic IR group died during the ischemia period and was excluded from the study; thus, 25 subjects completed the study.

There was no significant difference between diabetic and nondiabetic rats in terms of basal weight ($p = 0.060$) and glucose values ($p = 0.611$). During the month of monitoring, the weight measurements of diabetic rats significantly decreased over time, while the weight of nondiabetic rats was found to increase during the same period (Figure 1). Body weights were not significantly different between the groups. However, blood glucose values were significantly different among the nondiabetic and diabetic rat groups. Blood glucose levels in nondiabetics rats were significantly lower than those in diabetic rats (all $p < 0.001$) (Table 1). Blood glucose levels were not significantly different between Groups II, III, and IV ($p > 0.05$).

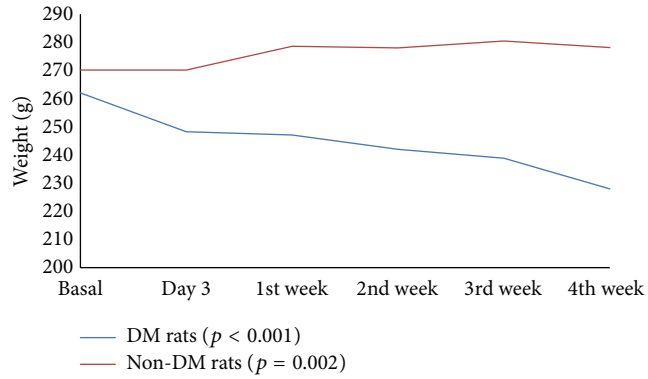

Figure 1: Weight comparison of diabetic and nondiabetic rats. p value: Friedman repeated measures.

The histopathological scores and biochemical evaluation of the rats in all groups are presented in Tables 2 and 3. The histomorphologic total cell injury scores (presented in Table 1) of the nondiabetic sham group were significantly lower than diabetic sham, diabetic IR, and diabetic IR + LIPC groups (resp., $p = 0.004$, $p = 0.002$, and $p = 0.002$). Diabetic IR group scores were not significantly different to the diabetic sham group ($p = 0.082$). But diabetic IR + LIPC group scores were significantly higher than in the diabetic sham and diabetic IR groups (resp., $p = 0.003$ and $p = 0.020$).

3.1. Mononuclear Cell Infiltration. The mononuclear cell infiltration scores of the nondiabetic sham group were significantly lower than those of the diabetic sham, diabetic IR, and diabetic IR + LIPC groups (resp., $p = 0.008$, $p = 0.004$, and $p = 0.003$). The difference between the scores of the diabetic sham and diabetic IR ($p = 0.269$) groups was not statistically significant. Also the difference between the scores of the diabetic IR and diabetic IR + LIPC groups was not statistically significant ($p = 0.206$) (Table 2, Figure 2).

The capillary vasodilation of the nondiabetic sham group was statistically significantly lower than that of diabetic sham, diabetic IR, and diabetic IR + LIPC groups (resp., $p = 0.010$, $p = 0.006$, and $p = 0.001$). The scores of the diabetic IR + LIPC group were significantly higher than the diabetic sham and diabetic IR groups (resp., $p = 0.006$ and $p = 0.043$) (Table 2, Figure 2).

3.2. Structural Changes in the Proximal Tubules. Structural changes in the proximal tubules of the nondiabetic sham group were significantly lower than those of the diabetic sham, diabetic IR, and diabetic IR + LIPC groups ($p = 0.003$, $p = 0.001$, and $p = 0.001$, resp.). The diabetic IR + LIPC

Table 1: Glucose values in rats.

Blood glucose	Basal	Day 3	1st week	2nd week	4th week	p value
Nondiabetic rats	109,1	109,3	107,5	111,6	110,9	<0.005
Diabetic rats	105,3	373,8	309,4	325,8	392,6	

p value: Friedman repeated measures.

Table 2: Histopathologic scores in groups.

Groups	Proximal tubulus	Mononuclear cell infiltration	Capillary vasodilation	Total cell injury score
Group I (nondiabetic sham) ($n = 7$)	0.14 ± 0.38 0.0 0-1	0.29 ± 0.49 0.0 0-1	0.29 ± 0.49 0.0 0-1	0.71 ± 1.11 0.0 0–3
Group II (diabetic sham) ($n = 6$)	1.33 ± 0.52 1.0 1-2	1.33 ± 0.52 1.0 1-2	1.17 ± 0.41 1.0 1-2	3.83 ± 0.98 3.5 3–5
Group III (diabetic IR) ($n = 6$)	1.83 ± 0.41 2.0 1-2	1.66 ± 0.52 2.0 1-2	1.5 ± 0.55 1.5 1-2	5.0 ± 1.09 5.0 4–6
Group IV (diabetic IR + LIPC) ($n = 6$)	2.33 ± 0.52 2.0 2-3	2.17 ± 0.75 2.0 1–3	2.17 ± 0.41 2.0 2-3	6.67 ± 0.82 6.5 6–8
p values				
p_{12}	0.003	0.008	0.010	0.004
p_{13}	0.001	0.004	0.006	0.002
p_{14}	0.001	0.003	0.001	0.002
p_{23}	0.093	0.269	0.241	0.082
p_{24}	0.014	0.057	0.006	0.003
p_{34}	0.092	0.206	0.043	0.020

Group I: nondiabetic sham, Group II: diabetic sham, Group III (diabetic IR): renal ischemia/reperfusion injury in diabetic rats group, and Group IV (diabetic IR + LIPC): renal ischemia/reperfusion injury in diabetic rats group and local ischemia preconditioning; Mann-Whitney U test was conducted to compare two independent groups. Values are mean ± 1 SD, median (minimum-maximum).
p_{12}: comparison of nondiabetic sham and diabetic sham.
p_{13}: comparison of nondiabetic sham and diabetic IR.
p_{14}: comparison of nondiabetic sham and diabetic IR + LIPC.
p_{23}: comparison of diabetic sham and diabetic IR.
p_{24}: comparison of diabetic sham and diabetic IR + LIPC.
p_{34}: comparison of diabetic IR and diabetic IR + LIPC.

group displayed significantly higher scores than the diabetic sham group ($p = 0.014$) (Table 2, Figure 2).

3.3. Biochemical Parameters. There were no significant differences between nondiabetic sham group and the diabetic sham group in the mean values for BUN ($p = 0.086$), creatinine ($p = 0.567$), and NGAL ($p = 0.153$). In the diabetic IR group, the BUN, Cr, and NGAL levels were higher than in the diabetic sham group, though this was not statistically significant (resp., $p = 0.423$, $p = 0.128$, and $p = 0.423$). In the diabetic sham group, the BUN, Cr, and NGAL values were found to be significantly low compared to the diabetic IR + LIPC group (resp., $p = 0.037$, $p = 0.016$, and $p = 0.006$). In the diabetic IR + LIPC group, though all 3 values were higher than the diabetic IR group, this difference was not statistically significant (resp., $p = 0.423$, $p = 0.065$, and $p = 0.201$). Biochemical data of the groups are presented in Table 3.

4. Discussion

This study found that histomorphological assessment results in diabetic rats showed that LIPC did not reduce or have a protective effect against IR injury. In fact, in addition to not having a protective effect, in the LIPC group, the histological score values for renal mononuclear cell infiltration, capillary vasodilatation, and structural changes in proximal tubules were higher than the values in the other groups, leading to the consideration that it had negative effects on renal IR injury. Biochemically the 3 biomarkers of BUN, Cr, and NGAL in diabetic rats showed that LIPC had no protective effect on renal IR injury.

Diabetes mellitus (DM) is a common and increasing chronic metabolic disease characterized by hyperglycemia, dyslipidemia, glycosuria, and metabolic disorders [6]. In diabetic kidneys initially diffuse and later exudative lesions

Table 3: Biochemical data of the groups.

Groups	BUN	Cr	NGAL
Group I (nondiabetic sham) ($n = 7$)	49.83 ± 21.80 44.20 31.90–95.60	0.46 ± 0.18 0.44 0.27–0.80	446.43 ± 179.17 386.00 314.00–839.00
Group II (diabetic sham) ($n = 6$)	68.52 ± 15.07 72.20 39.30–83.50	0.43 ± 0.21 0.39 0.24–0.82	350.17 ± 35.62 352.5 295.00–395.00
Group III (diabetic IR) ($n = 6$)	79.62 ± 14.93 78.20 62.10–101.70	0.62 ± 0.20 0.66 0.29–0.83	891.17 ± 1308.03 363.50 296.00–3560.00
Group IV (diabetic IR + LIPC) ($n = 6$)	84.68 ± 16.79 89.75 52.00–96.80	0.81 ± 0.80 0.81 0.69–0.91	1107.40 ± 1294.21 412 397.00–3385.00
p values			
p_{12}	0.086	0.567	0.153
p_{13}	0.022	0.153	0.568
p_{14}	0.032	0.010	0.167
p_{23}	0.423	0.128	0.423
p_{24}	0.037	0.016	0.006
p_{34}	0.423	0.065	0.201

Group I: nondiabetic sham, Group II: diabetic sham, Group III (diabetic IR): renal ischemia/reperfusion injury in diabetic rats group, Group IV (diabetic IR + DIPC): renal ischemia/reperfusion injury in diabetic rats group and local ischemia preconditioning, BUN: blood urea nitrogen, and serum NGAL: Cr: blood creatinine level, Mann-Whitney U test was conducted to compare two independent groups. Values are mean ± 1 SD, median, minimum, and maximum.
p_{12}: comparison of nondiabetic sham and diabetic sham.
p_{13}: comparison of nondiabetic sham and diabetic IR.
p_{14}: comparison of nondiabetic sham and diabetic IR + LIPC.
p_{23}: comparison of diabetic sham and diabetic IR.
p_{24}: comparison of diabetic sham and diabetic IR + LIPC.
p_{34}: comparison of diabetic IR and diabetic IR + LIPC.

develop. Hyalinization occurs in arterioles. Hyalinization in efferent arterioles forms histopathological lesions unique to diabetes. In the diabetic process, apart from diffuse and nodular intercapillary glomerulosclerosis (Kimmelstiel-Wilson syndrome), renal involvement may be observed linked to renal papilla necrosis, chronic pyelonephritis, atherosclerotic renal artery stenosis, and toxic nephropathy. Diabetic nephropathy is reported to increase linked to the increase in incidence of type II diabetes mellitus (DM). Though glomerular lesions are the best defined change in diabetic nephropathy, tubular atrophy, interstitial fibrosis, and inflammatory cell infiltration are the most significant characteristics of this disease. Diabetic nephropathy is a significant cause of mortality in diabetic patients. In Europe and America, 30–50% of type I diabetic patients and 5–15% of type II diabetic patients develop diabetic nephropathy. Patients with diabetic nephropathy present with glomerular hypertension and hyperperfusion and are more susceptible to I/R-induced renal injury. With the occurrence of DM-induced vessel lesions, renal tolerance to I/R is significantly compromised and the kidney is more likely to develop acute renal failure [16]. Many studies have previously reported an increased sensitivity to renal ischemia/reperfusion injury in DM rats. In these studies of the diabetic rat model induced with streptozotocin, 30 minutes of IR injury was shown to induce irreversible progressive renal damage. In diabetic rats this is characterized by interstitial fibrosis, inflammation, and tubular atrophy [17–19]. The mechanisms underlying enhanced vulnerability of the kidney to I/R injury in diabetes are not fully elucidated [17]. Thus, preventing renal I/R injury in DM by investigating possible protective strategies is clinically important.

Abu-Saleh et al. [20] in a diabetic rat model induced with streptozotocin identified histological changes in both diabetic and nondiabetic rats after 30 minutes of renal ischemia. They reported a broader pattern of injury in the diabetic ischemic kidney noted in the inner stripe of the outer medulla, including also congestion and inflammation, with all pathological parameters higher than 2.5 in morphological score. In our study in both the diabetic control group and the IR diabetic group the histomorphological scores for proximal tubules, mononuclear cell infiltration, and capillary vasodilation were higher than in the nondiabetic group. These different results compared to the study by Mejía-Vilet et al. [6] may be related to the diabetic monitoring duration of rats. In the study by Mejía-Vilet et al. rats were diabetically monitored for 5 days, while in our study this duration was 4 weeks. In our study all histomorphological scores in the diabetic control group were not statistically significant and were lower than in the diabetic IR group. This shows the negative effects expected in ischemia-reperfusion injury. Fouad et al. [17], with the same diabetic monitoring duration as our study, evaluated IR injury in nondiabetic and diabetic rats and showed dilatation

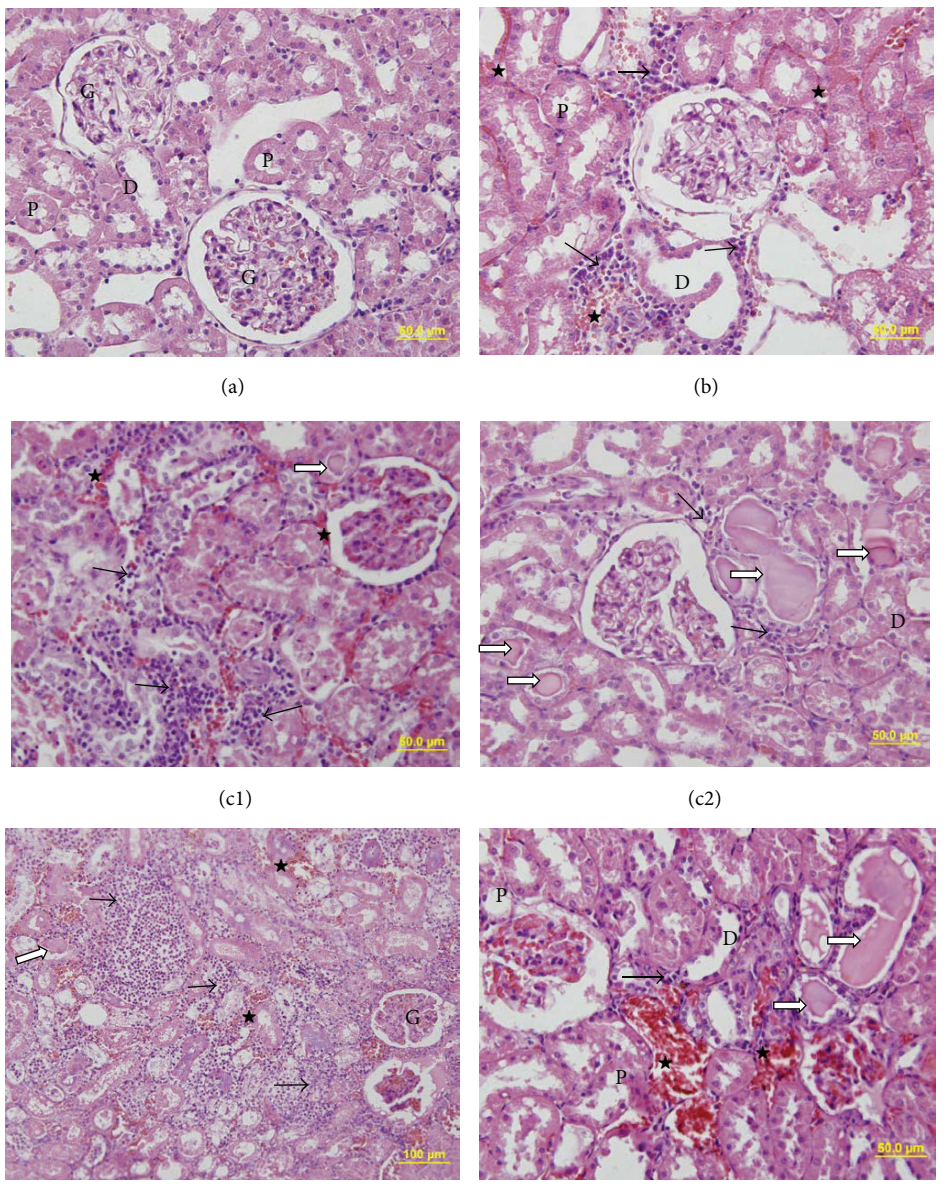

Figure 2: Representative kidney sections belong to (a) nondiabetic sham group, (b) diabetic sham group, (c1 and c2) diabetic ischemia-reperfusion (diabetic IR) group, and (d1 and d2) diabetic IR + LIPC group, respectively. Mononuclear infiltrations marked with black arrow (→), hyalin substance deposition marked with white arrow with black edges (⇒), and erythrocyte extravasations marked with (★). In micrographs proximal tubules, distal tubules and renal glomerulus are shown with (P), (D), and (G), respectively.

especially of proximal tubules, vacuolar degeneration, and widespread necrosis in the diabetic IR group especially. The results of another study with two-week diabetic rats reported that the diabetic IR group had higher histomorphological scores compared to the diabetic control group [16]. Some of these studies aimed to better understand the mechanisms of renal ischemia injury while some researched the reducing and protective effect of a variety of agents on diabetes and IR injury. However, no study investigated the effects of mechanical ischemic preconditioning like LIPC, as in our study.

Mıcılı et al. [21] evaluated the therapeutic effects of LA administration histomorphometrically, ultrastructurally, and biochemically on renal damage formed as a result of hypertension and diabetes models together and separately in rats. They showed interstitial fibrosis, glomerulosclerosis index, mesangial matrix proliferation, and renal fibrosis increased significantly in diabetic and hypertensive rats, whereas in lipoic acid treatment groups these parameters were found to decrease significantly. There was a significant increase in the biochemical values and histomorphometric findings of this study in diabetic, 5/6 nephrectomy versus

5/6 nephrectomy + diabetic groups. In this study findings from all histological investigations, like proximal tubules, mononuclear cell infiltration, capillary vasodilation, and total cell injury score, in the diabetic rat groups were found to be significantly high compared to nondiabetic rats.

IR, where blood flow begins again after ischemia due to medication or mechanical intervention in ischemic tissues, paradoxically increases the injury caused by ischemia and causes greater injury to ischemic tissue than the injury caused by ischemia [22, 23]. Clinically IR injury is frequently observed after transplantation, stroke, myocardial infarction, shock/resuscitation, tourniquet applications, and extracorporeal shock-wave lithotomy [24]. Ischemic preconditioning is a method applied mechanically or pharmacologically prior to target organ ischemia to reduce the level of subsequent IR injury. Ischemic tolerance is induced by regulation of endothelial function, blood flow, and decreased macrophage as well as neutrophilic activity. This results in decreased endothelial injury and eventually decreased parenchymal injury. The aim in ischemic preconditioning is to apply ischemia and reperfusion to target organs in short intervals, to ensure that the target organs can tolerate ischemia well. High energy demands and the intense microvascular network of the kidneys make them vulnerable to IR injury, which is considered a major cause of kidney damage in renal artery stenosis and renal microvascular surgery. Wever et al. [25] in a meta-analysis of IPC studies in animal kidneys found many animal studies evaluating the protective effects of LIPC and RIPC on renal IRI using different stimuli and methods. The results of this meta-analysis stated there was no consensus on how long the ischemia stimulus should be applied and what the ischemia duration and reperfusion intervals should be. They emphasized that there was still no full explanation of the role played by age, sex, genetics, and comorbidities. Our results are one of the first studies evaluating the efficacy of LIPC on diabetic renal IRI. We propose that future clinical studies should be designed to optimize IPC efficacy for certain patient groups and that animal studies in this area can inform the design of such clinical trials. Furthermore, a better mechanistic insight is needed for the cause of the observed interspecies difference. Limiting factors are that oxidative stress and inflammatory mediators which are also responsible for IR injury and the neurogenic pathway were not examined in the study.

Renal IR injury can be induced using two different methods in experimental animal models. One of these is contralateral renal artery or renal pedicle clamping and unilateral nephrectomy while the other is bilateral renal pedicle or renal artery clamping [17, 26, 27]. In addition the duration of renal ischemia is very important and generally is limited to 30–60 minutes. Renal ischemia duration of more than sixty minutes may cause acute tubular necrosis and renal failure. With renal ischemia durations of less than 30 minutes, rapid proliferation of tubular epithelial cells may repair damaged renal tubules and this may be accompanied by improved renal functions [17, 26, 27]. Forty-five minutes of renal ischemia duration may cause findings of IR injury. Additionally, this injury may include renal failure linked to tubular epithelial cell proliferation with irreversible acute tubular necrosis. In previous studies, renal vessels were noninvasively clamped to induce ischemia for 45 min followed by reperfusion for 4, 6, 12, and 24 h [28]. Thus, in the present study, bilateral renal pedicles were clamped to induce ischemia for 45 min followed by reperfusion for 4 h.

Local ischemic preconditioning has been investigated as a surgical tool for many years [29]. Although LIPC does reduce reperfusion injury [28] as well as its systemic consequences [30], in a literature search, we found no study that evaluated the effects of LIPC for renal IR injury in a diabetic rat model. This study showed that LIPC treatment could not provide significant nephroprotective effects in streptozotocin-induced diabetic rats exposed to renal I/R.

In a review, McCafferty et al. [31] debated the relationship and possible mechanisms between ischemic conditioning in animal models and accompanying comorbidities. The results of this review found that comorbidities such as diabetes, hypertension, hypercholesterolemia, kidney disease, multiple medication use, and cerebrovascular disease reduced the clinical efficacy of ischemic preconditioning strategies. In the DM IR group, all histopathological scores were found to increase, though not significantly, compared to the DM sham group. The total cell injury score value especially was close to significance. These findings suggest that renal I/R injury may have severely impaired renal function; thus, renal I/R injury was successfully induced in these rats. Our findings are similar to the study findings of Zhou et al. [16] evaluating the protective effects of sevoflurane pretreatment of diabetic rats. Additionally when our biochemical results are compared with the diabetic sham, IR diabetic, and nondiabetic rats in the Zhou study, the clearly high serum Cr and BUN levels are similar. However, according to our results when the diabetic sham group and diabetic IR group are compared, the increase in serum BUN, Cr, and NGAL levels was not statistically significant. There was a clear significant increase histopathologically and biochemically between the diabetic sham and diabetic IR + LIPC groups. This leads to the consideration that LIPC application additionally increased ischemic damage in diabetic kidneys.

Many studies in recent times, especially on acute kidney injury, have proven the importance of the early diagnostic biomarker of NGAL, a protein with monomeric structure [32, 33] first determined as a protein linked to neutrophil gelatinase [25]. Neutrophil gelatinase-associated lipocalin was initially characterized as found in neutrophil lysosomes but later was observed to be expressed in a variety of tissues such as renal tubular epithelium, colon, prostate, and breast tissue [34]. NGAL production rapidly increases in response to renal epithelium damage or inflammation. After acute kidney injury, NGAL protein is easily identified in blood and urine. Experimentally after acute tubular injury mRNA of NGAL in the kidney increases 1000 times, with 10-fold increase in plasma and 100-fold increase in urine shown with acute kidney injury using the Western-blotting technique [34].

In our study we identified that serum NGAL levels were higher in diabetic rats compared to nondiabetic rats. However there was no significant difference found between the serum NGAL levels in the diabetic sham group and diabetic IR group. In diabetic kidneys after IR injury, higher

serum NGAL levels were identified; however this difference was not statistically significant. One potential drawback to NGAL is the considerable extrarenal production that can be seen in states of systemic stress, even in the absence of renal damage; it has also been noted to increase in states of chronic, not just acute, kidney dysfunction. Nevertheless, in a large meta-analysis, NGAL did have prognostic significance for clinical outcomes, notably the need for dialysis and also mortality [11].

In conclusion, LPIC application did not reduce renal IR injury in the histomorphological and biochemical parameters of diabetic rats. As a result to better understand the physiopathological changes caused by diabetes and develop multidisciplinary approaches for preventive strategies, more advanced studies to determine underlying mechanisms are required. This data will provide clues about whether translation to humans is feasible. As LIPC has no effect in preventing diabetic IRI, in fact causing more harm, we believe research is required into other methods such as remote ischemic preconditioning and pharmacological agents.

Conflict of Interests

The authors declare that there is no conflict of interests regarding the publication of this paper.

References

[1] C. R. Nolan and R. W. Schrier, "Kidney in hypertension," in *Renal and Electrolyte Disorders*, R. W. Schrier, Ed., pp. 272–324, Williams & Wilkins Lippincott, Philadelphia, Pa, USA, 6th edition, 2005.

[2] M. D. Oldfield and M. E. Cooper, "The biochemistry and pathophysiology of renal lesions in type 2 diabetes," in *Diabetic Nephropathy in Type 2 Diyabetes*, C. E. Mogensen, Ed., pp. 41–56, Science Press, London, UK, 1st edition, 2002.

[3] P. Maisonneuve, L. Agodoa, R. Gellert et al., "Distribution of primary renal diseases leading to end-stage renal failure in the United States, Europe, and Australia/New Zealand: results from an international comparative study," *American Journal of Kidney Diseases*, vol. 35, no. 1, pp. 157–165, 2000.

[4] H. Shi, D. Patschan, T. Epstein, M. S. Goligorsky, and J. Winaver, "Delayed recovery of renal regional blood flow in diabetic mice subjected to acute ischemic kidney injury," *American Journal of Physiology—Renal Physiology*, vol. 293, no. 5, pp. F1512–F1517, 2007.

[5] G. Woodrow, A. M. Brownjohn, and J. H. Turney, "Acute renal failure in patients with type 1 diabetes mellitus," *Postgraduate Medical Journal*, vol. 70, no. 821, pp. 192–194, 1994.

[6] J. M. Mejía-Vilet, V. Ramírez, C. Cruz, N. Uribe, G. Gamba, and N. A. Bobadilla, "Renal ischemia-reperfusion injury is prevented by the mineralocorticoid receptor blocker spironolactone," *The American Journal of Physiology—Renal Physiology*, vol. 293, no. 1, pp. F78–F86, 2007.

[7] P. S. T. Yuen, S.-K. Jo, M. K. Holly, X. Hu, and R. A. Star, "Ischemic and nephrotoxic acute renal failure are distinguished by their broad transcriptomic responses," *Physiological Genomics*, vol. 25, no. 3, pp. 375–386, 2006.

[8] J. M. Mejía-Vilet, V. Ramírez, C. Cruz, N. Uribe, G. Gamba, and N. A. Bobadilla, "Renal ischemia-reperfusion injury is prevented by the mineralocorticoid receptor blocker spironolactone," *American Journal of Physiology: Renal Physiology*, vol. 293, no. 1, pp. F78–F86, 2007.

[9] E. Bagcik, S. Ozkardesler, N. Boztas et al., "Effects of dexmedetomidine in conjunction with remote ischemic preconditioning on renal ischemia-reperfusion injury in rats," *Revista Brasileira de Anestesiologia*, vol. 64, no. 6, pp. 382–390, 2014.

[10] J. Mishra, C. Dent, R. Tarabishi et al., "Neutrophil gelatinase-associated lipocalin (NGAL) as a biomarker for acute renal injury after cardiac surgery," *The Lancet*, vol. 365, no. 9466, pp. 1231–1238, 2005.

[11] M. Haase, R. Bellomo, P. Devarajan et al., "Accuracy of Neutrophil Gelatinase-Associated Lipocalin (NGAL) in diagnosis and prognosis in acute kidney injury: a systematic review and meta-analysis," *American Journal of Kidney Diseases*, vol. 54, no. 6, pp. 1012–1024, 2009.

[12] E. Guneli, K. Tugyan, H. Ozturk, M. Gumustekin, S. Cilaker, and N. Uysal, "Effect of melatonin on testicular damage in streptozotocin-induced diabetes rats," *European Surgical Research*, vol. 40, no. 4, pp. 354–360, 2008.

[13] W. Yang, J. Lu, J. Weng et al., "Prevalence of diabetes among men and women in China," *The New England Journal of Medicine*, vol. 362, no. 12, pp. 1090–1101, 2010.

[14] I. Satman, T. Yilmaz, A. Sengul et al., "Population-based study of diabetes and risk characteristics in Turkey: results of the turkish diabetes epidemiology study (TURDEP)," *Diabetes Care*, vol. 25, no. 9, pp. 1551–1556, 2002.

[15] W. H. Herman, "Eye disease and nephropathy in NIDDM," *Diabetes Care*, vol. 13, no. 2, pp. 24–29, 1990.

[16] S.-P. Zhou, W.-T. Liao, L.-K. Yang, and L. Sun, "Effects of sevoflurane pretreatment on renal Src and FAK expression in diabetic rats after renal ischemia/reperfusion injury," *Molecular and Cellular Biochemistry*, vol. 384, no. 1-2, pp. 203–211, 2013.

[17] A. A. Fouad, A. S. Al-Mulhim, I. Jresat, and M. A. Morsy, "Protective effects of captopril in diabetic rats exposed to ischemia/reperfusion renal injury," *Journal of Pharmacy and Pharmacology*, vol. 65, no. 2, pp. 243–252, 2013.

[18] G. Kuramochi and S. Homma, "Effects of furosemide on renal oxygen consumption after ischemia in normal and streptozotocin diabetic rats," *Nephron*, vol. 64, no. 3, pp. 436–442, 1993.

[19] H. Wald, H. Markowitz, S. Zevin, and M. M. Popovtzer, "Opposite effects of diabetes on nephrotoxic and ischemic acute tubular necrosis," *Proceedings of the Society for Experimental Biology and Medicine*, vol. 195, no. 1, pp. 51–56, 1990.

[20] N. Abu-Saleh, E. Ovcharenko, H. Awad et al., "Involvement of the endothelin and nitric oxide systems in the pathogenesis of renal ischemic damage in an experimental diabetic model," *Life Sciences*, vol. 91, no. 13-14, pp. 669–675, 2012.

[21] S. C. Mıcılı, B. U. Ergur, C. Ozoğul et al., "Effects of lipoic acid in an experimentally induced hypertensive and diabetic rat model," *Clinical and Experimental Hypertension*, vol. 35, no. 5, pp. 373–381, 2012.

[22] J. Zhu, X. Chen, H. Wang, and Q. Yan, "Catalpol protects mice against renal ischemia/reperfusion injury via suppressing PI3K/Akt-eNOS signaling and inflammation," *International Journal of Clinical and Experimental Medicine*, vol. 8, no. 2, pp. 2038–2044, 2015.

[23] S.-S. Huang, F.-C. Wei, and L.-M. Hung, "Ischemic preconditioning attenuates postischemic leukocyte-endothelial cell interactions—role of nitric oxide and protein kinase C," *Circulation Journal*, vol. 70, no. 8, pp. 1070–1075, 2006.

[24] N. Gill, J. V. Nally Jr., and R. A. Fatica, "Renal failure secondary to acute tubular necrosis: epidemiology, diagnosis, and management," *Chest*, vol. 128, no. 4, pp. 2847–2863, 2005.

[25] K. E. Wever, T. P. Menting, M. Rovers et al., "Ischemic preconditioning in the animal kidney, a systematic review and meta-analysis," *PLoS ONE*, vol. 7, no. 2, Article ID e32296, 2012.

[26] H. Kocoglu, H. Ozturk, H. Ozturk, F. Yilmaz, and N. Gulcu, "Effect of dexmedetomidine on ischemia-reperfusion injury in rat kidney: a Histopathologic study," *Renal Failure*, vol. 31, no. 1, pp. 70–74, 2009.

[27] P. D. Williams, H. Lopez, D. Britt, C. Chan, A. Ezrin, and R. Hottendorf, "Characterization of renal ischemia-reperfusion injury in rats," *Journal of Pharmacological and Toxicological Methods*, vol. 37, no. 1, pp. 1–7, 1997.

[28] M. Kou, R. Li, Y. Zhou et al., "The intermediate and the differential receptor expression on renal ischemia/reperfusion rats," *The Journal of Medical Research*, vol. 38, pp. 25–28, 2009.

[29] C. E. Murry, R. B. Jennings, and K. A. Reimer, "Preconditioning with ischemia: a delay of lethal cell injury in ischemic myocardium," *Circulation*, vol. 74, no. 5, pp. 1124–1136, 1986.

[30] S. Wolfrum, J. Nienstedt, M. Heidbreder, K. Schneider, P. Dominiak, and A. Dendorfer, "Calcitonin gene related peptide mediates cardioprotection by remote preconditioning," *Regulatory Peptides*, vol. 127, no. 1–3, pp. 217–224, 2005.

[31] K. McCafferty, S. Forbes, C. Thiemermann, and M. M. Yaqoob, "The challenge of translating ischemic conditioning from animal models to humans: the role of comorbidities," *Disease Models and Mechanisms*, vol. 7, no. 12, pp. 1321–1333, 2014.

[32] J. Mishra, M. A. Qing, A. Prada et al., "Identification of neutrophil gelatinase-associated lipocalin as a novel early urinary biomarker for ischemic renal injury," *Journal of the American Society of Nephrology*, vol. 14, no. 10, pp. 2534–2543, 2003.

[33] T. L. Nickolas, J. Barasch, and P. Devarajan, "Biomarkers in acute and chronic kidney disease," *Current Opinion in Nephrology and Hypertension*, vol. 17, no. 2, pp. 127–132, 2008.

[34] L. Kjeldsen, A. H. Johnsen, H. Sengelov, and N. Borregaard, "Isolation and primary structure of NGAL, a novel protein associated with human neutrophil gelatinase," *Journal of Biological Chemistry*, vol. 268, no. 14, pp. 10425–10432, 1993.

Hindawi Publishing Corporation
BioMed Research International
Volume 2016, Article ID 2027370, 7 pages
http://dx.doi.org/10.1155/2016/2027370

Review Article

Functional Magnetic Resonance Imaging in Acute Kidney Injury: Present Status

Hai Ying Zhou, Tian Wu Chen, and Xiao Ming Zhang

Sichuan Key Laboratory of Medical Imaging, Department of Radiology, Affiliated Hospital of North Sichuan Medical College, 63 Wenhua Road, Shunqing District, Nanchong, Sichuan 637000, China

Correspondence should be addressed to Xiao Ming Zhang; zhangxm@nsmc.edu.cn

Received 1 December 2015; Revised 5 January 2016; Accepted 6 January 2016

Academic Editor: Jeremiah R. Brown

Acute kidney injury (AKI) is a common complication of hospitalization that is characterized by a sudden loss of renal excretory function and associated with the subsequent development of chronic kidney disease, poor prognosis, and increased mortality. Although the pathophysiology of renal functional impairment in the setting of AKI remains poorly understood, previous studies have identified changes in renal hemodynamics, perfusion, and oxygenation as key factors in the development and progression of AKI. The early assessment of these changes remains a challenge. Many established approaches are not applicable to humans because of their invasiveness. Functional renal magnetic resonance (MR) imaging offers an alternative assessment tool that could be used to evaluate renal morphology and function noninvasively and simultaneously. Thus, the purpose of this review is to illustrate the principle, application, and role of the techniques of functional renal MR imaging, including blood oxygen level-dependent imaging, arterial spin labeling, and diffusion-weighted MR imaging, in the management of AKI. The use of gadolinium in MR imaging may exacerbate renal impairment and cause nephrogenic systemic fibrosis. Therefore, dynamic contrast-enhanced MR imaging will not be discussed in this paper.

1. Introduction

Acute kidney injury (AKI) is a common complication of hospitalization that occurs in various clinical settings, particularly in the setting of critical illness. It is characterized by a sudden loss of renal excretory function and associated with the subsequent development of chronic kidney disease, poor prognosis, and increased mortality. A variety of causes, such as renal ischemic events, exposure to nephrotoxic substances, acute tubular necrosis (ATN), and acute upper urinary tract obstruction, can trigger AKI [1, 2]. Although previous studies have identified changes in renal hemodynamics, perfusion, and oxygenation as key factors in the development and progression of AKI, the pathophysiology of renal functional impairment in the setting of AKI remains poorly understood [3–5]. In clinical practice, the serum creatinine (sCr) levels are attractive for the routine diagnosis and staging of AKI due to the relative simplicity and convenience of the test. However, the sCr level has major limitations as a biomarker for AKI [6]. First, it does not change until approximately 50% of kidney function is lost. Therefore, it is not sensitive to the rapid changes in renal function induced by AKI. Moreover, the lag time between renal injury and the increase in the sCr level results in missed therapeutic opportunities, which may be responsible for the high mortality associated with AKI. Second, the sCr level depends on many other factors, such as muscle mass, age, sex, medications, and hydration status. Thus, a better understanding and early detection of AKI are important for its treatment.

With the development of magnetic resonance (MR) imaging, functional renal MR imaging has rapidly grown and could be used to evaluate renal morphology and function noninvasively and simultaneously [7, 8]. The main MR imaging techniques include blood oxygen level-dependent (BOLD) imaging, arterial spin labeling (ASL), dynamic contrast-enhanced MR imaging (DCE-MRI), diffusion-weighted imaging (DWI), intravoxel incoherent motion (IVIM), diffusion tensor imaging (DTI), and diffusion kurtosis imaging (DKI). These approaches can provide information on intrarenal oxygenation, perfusion, and diffusion

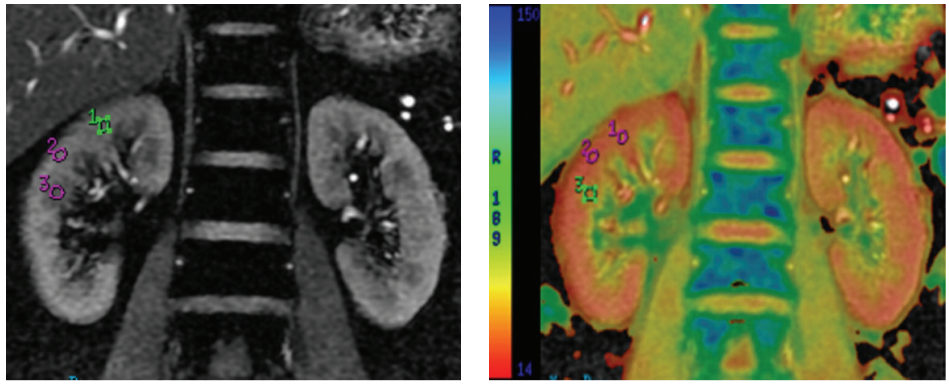

(a) (b)

Figure 1: Representative mGRE images obtained from a healthy volunteer. (a) An mGRE image with long TE is used to place regions of interest (ROIs) on the medulla and cortex. Regions of cortex appear bright with high signal intensity, whereas medullary pyramids appear darker with a low signal intensity on the mGRE image. (b) The $R2^*$ map is from the same slice position, which was scaled from 14 (red) to 150 (blue), representing a range of $R2^*$ levels. Larger $R2^*$ values correspond to higher levels of hypoxia. In this map, the medulla can be clearly distinguished from the cortex because the medulla has a higher $R2^*$ value or a colder color in the $R2^*$ map.

on a microstructural level, which may not only allow the noninvasive detection of the presence and severity of renal abnormalities associated with AKI in preclinical setting, but also demonstrate the pathophysiology and progress of AKI. Because the use of gadolinium in MR imaging may exacerbate renal impairment and cause nephrogenic systemic fibrosis [9], DCE-MRI will not be discussed in this paper. Thus, the objective of this paper is to provide a brief overview of the principle, application, and role of the remaining techniques in the management of AKI.

2. BOLD MR Imaging

The pathophysiology of AKI is not yet fully understood, but renal tissue hypoperfusion and hypoxia are well accepted to be closely related to the pathophysiology of all forms of AKI [5]. The direct measurement of oxygen partial pressure (pO_2) by oxygen-sensing electrodes that penetrate the renal parenchyma remains the gold standard for assessing renal tissue oxygenation. However, this measurement technique is invasive and highly complex, which makes it not applicable for widespread use [10, 11]. Therefore, a noninvasive approach to assess renal oxygenation status in vivo is needed.

In the mid 1990s, BOLD MR imaging was demonstrated as an important noninvasive technique to assess intrarenal oxygenation under physiologic and pathophysiologic conditions in experimental animals and humans [8, 12–14]. The paramagnetic properties of deoxyhemoglobin are utilized as an endogenous marker to acquire images to measure tissue oxygenation. Specifically, increased deoxyhemoglobin concentrations change the magnetic spin properties of neighboring water molecules, which accelerates magnetic spin dephasing and decreases the signal intensity on apparent spin-spin relaxation time-weighted ($T2^*$) MR images. The rate of magnetic spin dephasing, $R2^*(= 1/T2^*)$, has been used as a quantitative parameter to reflect renal oxygenation (Figure 1). An increase in $R2^*$ implies an increased deoxyhemoglobin concentration and decreased tissue pO_2, which may result from impaired renal perfusion, decreased blood O_2 content, or increased O_2 consumption [12]. A strong correlation has been proved between renal BOLD MRI to tissue oxygen partial pressure (pO_2) [15].

Recently, BOLD has been widely used to study intrarenal oxygenation in human and animal studies of AKI [8, 13, 14]. BOLD MR imaging was demonstrated to effectively detect changes in intrarenal oxygenation by measuring the $R2^*$ levels of the renal cortex and medulla. In pig models of AKI induced by acute renal ischemia, the $R2^*$ values of the cortex and medulla both increased, which demonstrated a reduction in intrarenal oxygenation in parallel with decreased intrarenal blood flow during acute ischemia. After reperfusion, the intrarenal oxygenation levels immediately returned to baseline oxygenation, which demonstrated that some of the early changes in renal oxygenation due to AKI may reverse [16, 17]. Furthermore, the degree of ischemic reperfusion injury commonly influences the recovery of renal function [18].

BOLD MRI has also been utilized to study the mechanisms of contrast-induced AKI (CIAKI). It is indicated that the administration of contrast agent caused an early and transient decrease in the medullary $R2^*$ followed by a sustained increase above the baseline in animal models of contrast-induced AKI (CIAKI), whereas minimal changes were observed in the renal cortex [19, 20]. The differences in the variations in $R2^*$ between the renal medullary and cortex agree with the basis of renal pathophysiology. Specifically, most of the oxygen consumed by the kidney is due to the reabsorption of filtered sodium by the medullary thick ascending limb of the loop of Henle, but only approximately 5% of renal blood flow is supplied to the medulla, which makes it more susceptible to hypoperfusion and hypoxia. However, conflicting mechanisms of the initial decrease in the medullary $R2^*$ after contrast agent injection have been reported, and a consensus has not been reached. Arakelyan et al. [21] attributed this change to an increase in renal tubular volume due to dye-induced osmotic diuresis, which

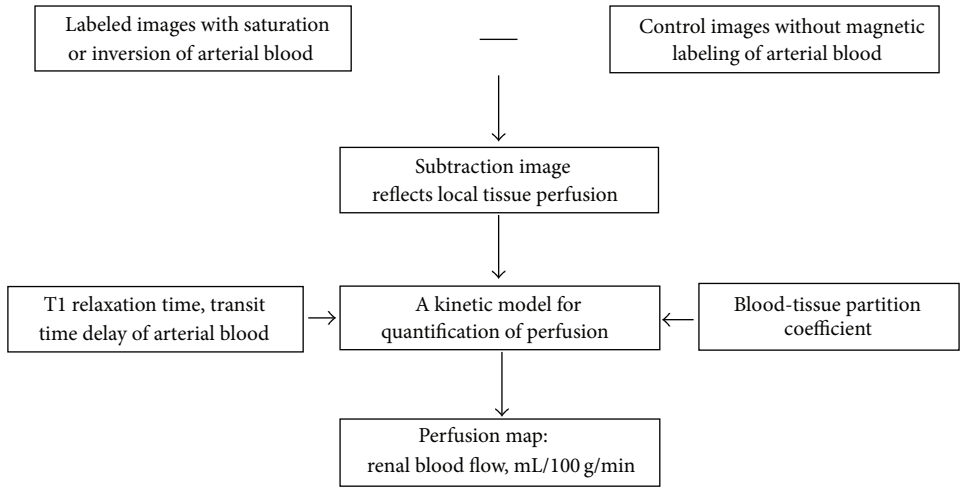

Figure 2: Schematic diagram of ASL imaging. Knowledge of parameters, such as the tissue T1 relaxation time, blood-tissue partition coefficient, and transit time of the blood water to tissue water, is generally required to quantify the perfusion.

decreased the blood volume fraction. Conversely, other investigators demonstrated that this change may be due to an initial increase in medullary blood flow. Li et al. [20] used 4 contrast media with different physicochemical properties to assess the differences in intrarenal oxygenation in CIAKI-susceptible rats by BOLD MR imaging. They also demonstrated that the immediate increase in $R2^*$ in the renal inner stripe of the outer medulla (ISOM) after the injection of contrast agent may be the earliest biomarker of AKI. Furthermore, the different viscosities of the contrast agents may lead to a difference in the $R2^*$ level in the renal cortex and medulla after injection. In addition, the effects of some interventions to mitigate the adverse effects of contrast media have been evaluated using BOLD MRI, and the results showed that the rate of increase in $R2^*$ in the renal ISOM can be reduced by treatment with furosemide (diuretic) or N-acetylcysteine (NAC; antioxidant) before contrast media injection, but the optimum dose of furosemide and NAC for mitigating the negative effects of contrast media has not yet been determined [22].

Renal oxygenation in renal allografts with ATN has also been studied using BOLD MR imaging, but the current data are controversial and difficult to interpret [23–25]. The $R2^*$ values of the cortex and medulla reportedly increased in allografts with ATN compared with normally functioning allografts, which suggested decreased oxygen bioavailability both in the cortex and medulla in allografts with ATN [23]. Conversely, Djamali et al. [24] found that the medulla $R2^*$ levels of ATN allografts decreased compared with normally functioning allografts, which reflected a significant increase in the medullary oxygen bioavailability in ATN allografts. In addition, Sadowski et al. [25] reported that the $R2^*$ levels of the cortex and medulla did not significantly differ between the ATN group and the normal functioning allografts.

Renal oxygenation in AKI due to other causes, such as sepsis-associated AKI and other nephrotoxin-induced AKI, has also been studied in several experimental animal models and humans using BOLD MRI [26, 27]. However, the number of studies is small, and unifying conclusions or significant insights are lacking. Therefore, this aspect will not be discussed in this review.

In conclusion, BOLD MR imaging not only can noninvasively assess changes in renal oxygenation due to AKI by measuring the $R2^*$ levels of the renal cortex and medulla, but also can investigate the role of hypoxia in the pathogenesis and progress of AKI. In recent years, this strategy has been widely used to assess AKI. However, further studies are necessary to establish the cut-off $R2^*$ values for the diagnosis of AKI and evaluate the specificity of $R2^*$ for the renal oxygenation status.

3. ASL

ASL is a novel, noninvasive MRI technique to measure tissue perfusion, that is, tissue blood flow [28], by magnetically labeling water protons in the blood as an endogenous contrast agent. First, the water in the blood is labeled before it enters the tissue of interest. The labeled water then flows into tissue and is exchanged with tissue water, thereby altering its magnetization. The perfusion-weighted image is obtained by subtracting the labeled image from a control image with unlabeled blood water to obtain the difference, and the signal intensity is proportional to perfusion. Finally, a kinetic model is used to directly quantify perfusion if other parameters, such as the tissue T1 relaxation time, blood-tissue partition coefficient, and transit time of the blood water to tissue water, are known (Figure 2). Recently, this technique has been widely used to evaluate cerebral perfusion [29]. With respect to the kidney, published studies demonstrated that this approach is another ideal candidate for ASL imaging due to its high physiologic perfusion (both kidneys, which results in approximately 0.5% of the total body mass receiving approximately 25% of the cardiac output) and the perfusion difference between the cortex and medulla (the cortex receives approximately 92~94% of the renal blood flow, whereas only approximately 5% of this flow is supplied

to the medulla). The feasibility of flow-sensitive alternating inversion recovery (FAIR) perfusion preparation with a steady-state free precession (True-FISP) ASL quantification of renal perfusion has also been demonstrated in both healthy and disease states [30].

Dong et al. [31] performed a pilot study to demonstrate the feasibility of ASL perfusion MRI in the detection of AKI and found that the cortical, medullary, and global kidney blood flows were significantly lower in AKI patients than in healthy volunteers. This finding suggested that the decrease in renal perfusion is critical to the pathophysiology of AKI which is in agreement with previous reports on the basis of the evaluation of renal blood flow of AKI [3–5]. Furthermore, ASL was also shown to be able to noninvasively detect the severity of AKI and monitor renal perfusion impairment over time in a mouse model of ischemia-induced AKI. The degree of perfusion impairment measured using ASL is related to kidney volume loss, the severity of histopathologic alterations of renal tissue, and the impairment of renal function. In addition, renal perfusion measured by means of ASL may also serve as a noninvasive biomarker to predict the extent of subsequent histologic alterations of the kidney early after the organ is damaged. Thus, ASL may be very valuable for the clinical follow-up of patients who are at risk for AKI and for drug development in experimental renal disease models [32].

Zimmer et al. [33] reported that ASL is a valid alternative to DCE-MRI, and ASL might be preferred for patients with impaired kidney function because the injection of Gd-based contrast agents may exacerbate renal impairment and cause nephrogenic systemic fibrosis. In addition, Chen et al. [34] used ASL and BOLD MRI to evaluate the damage to renal function in CIAKI rats at 3T and found that ASL combined with BOLD can further identify the primary cause of the decrease in renal oxygenation in CIAKI. Compared with BOLD, ASL perfusion MRI can absolutely quantify a well characterized physiological parameter, whereas the quantified parameter obtained by BOLD imaging is a result of complex interactions among renal blood flow, renal blood volume, and oxygen consumption.

However, the relatively low signal-to-noise ratio (SNR) and short signal decay rate of the ASL technique will delay its clinical application. A high-field MR scanner is necessary to enhance the image quality and provide a more accurate analysis of renal perfusion using the ASL technique [35].

4. Diffusion-Weighted Imaging

DWI is a powerful technique that provides information on the renal microstructure and function by characterizing water motion on a molecular level [7, 36]. The apparent diffusion coefficient (ADC) is utilized as a quantitative parameter of diffusion, which is calculated from DW images with a monoexponential decay model. Structural changes, such as interstitial fibrosis or tubular atrophy, could result in a decrease in the ADC value, which has been demonstrated to correlate with renal function. Renal diffusion in both healthy and disease states has been evaluated using this technique [7]. In a mouse model of ischemia-induced AKI, the ability of the DWI value to characterize acute and chronic pathology after unilateral AKI was investigated. The ADC value of the renal medulla was shown to be significantly decreased at every time point after AKI, and the renal ADC values changed with the severity of AKI and the degree of interstitial renal fibrosis 4 weeks after AKI. This finding suggested that the decrease in renal diffusion is critical to the pathophysiology of AKI which is associated with renal tissue edema, inflammatory cell infiltration, and subsequent development of interstitial renal fibrosis and tubular atrophy [37].

Nevertheless, the ADC values, which derive from the conventional monoexponential model, provide a mix of information on capillary perfusion and water diffusion in the extravascular space [38]. The accurate diffusion of water molecules, which is considered as a result of altered tissue structures, is difficult to calculate.

Thus, the intravoxel incoherent motion (IVIM) biexponential model of postprocessing was developed. This model allows the pure diffusion and perfusion-dependent diffusion to be differentiated by calculating quantitative parameters using multi-b-value DWI [38, 39]. At low b-values ($b < 200\ \mathrm{s/mm^2}$), the intravoxel spin dephasing caused by the pseudorandom blood flow in the presence of a diffusion gradient will contribute more to signal attenuation, leading to the dependence of the ADC values on perfusion effects. Conversely, at high b-values ($b > 400\ \mathrm{s/mm^2}$), diffusion attenuation will primarily be due to molecular water diffusion because the blood signal will be mostly suppressed by the large diffusion gradients. Thus, the effects of pseudodiffusion can be excluded to yield the true diffusion measurement. Quantitative parameters, including pure molecular diffusion (D), which is closely related to the abnormal biophysical processes, the volume fraction (f) of diffusion, which is sensitive to renal fluid loading, and perfusion-related diffusion (D^*), which is linked to arteriolar vasoconstriction or vasodilation, are simultaneously measured by IVIM MR imaging to obtain information about microvascular dynamics and renal fluid loading.

The potential clinical applications of IVIM in renal lesions have been demonstrated in several pilot studies [40, 41], but AKI has rarely been assessed using IVIM. Liang et al. [42] evaluated pathophysiological alterations in a CIAKI animal model using IVIM. The study demonstrated that IVIM can provide useful information to noninvasively evaluate renal pathophysiological processes in a CIAKI model in vivo. Large-scale animal and human clinical studies should be performed in the future to assess the use of IVIM in AKI due to other causes.

The studies mentioned above all assume that diffusion in the kidney is isotropic. In fact, due to the radial distribution characteristics of the important anatomic structures of the kidney, like vessels and tubules, diffusion is anisotropic and should be assessed by another DWI technique, diffusion tensor imaging (DTI) [43]. This technique not only evaluates the intensity of water diffusion in the kidney but also the locally preferred direction of this diffusion by analyzing multiple measurements with six diffusion gradient directions. This information is used to calculate the pixel-per-pixel fractional anisotropy (FA) map and FA value, which is a dimensional parameter quantifying the amount of diffusion anisotropy

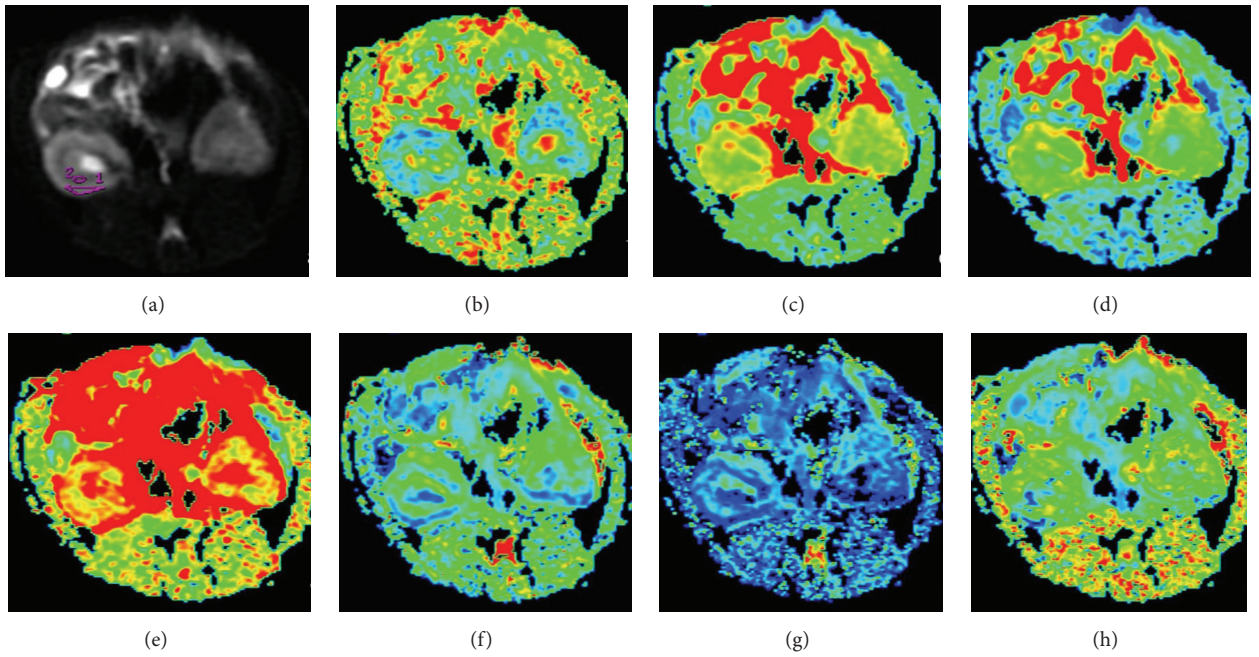

FIGURE 3: Representative diffusivity and kurtosis maps obtained from diffusional kurtosis imaging for one healthy Sprague Dawley rat. (a) Representative locations of regions of interest (ROIs) for the cortex and medulla at the mid-zone of the right kidney on the $b = 0\,\text{mm}^2/\text{s}$ image. The same ROIs were then copied to maps of all metrics. (b–h) Maps of the fractional anisotropy (FA), mean diffusivity (MD), radial diffusivity ($D_\perp$), axial diffusivity ($D_{||}$), mean kurtosis (MK), radial kurtosis ($K_\perp$), and axial kurtosis ($K_{||}$) are given, respectively.

within a region of interest. Respiratory motion has been identified as a key factor that limits the application of DTI in abdominal organs, but the use of breath-hold sequences and respiratory triggering has yielded higher quality images with acceptable acquisition times. Thus, DTI has become popular in renal studies [44].

Obvious diffusion anisotropy in the renal medulla has been demonstrated by DTI [45], and decreases in the FA of the medulla are observed in animal models of ischemia-induced AKI [46]. Although the biophysics underlying this anisotropy remains poorly understood, particularly the roles of the structural restrictions of tubules and collecting ducts, it was suggested that the decrease of FA may result from the necrosis of tubular epithelial cells in medulla, which likely led to water diffusion along the oriented tubular structure impaired [46].

Due to the presence of structural hindrances in the renal medulla, like membranes or directional structures, the diffusion of water molecules in the kidney is restricted and does not follow a Gaussian distribution. Thus, mathematical models considering the non-Gaussian behavior are needed to more accurately describe the diffusion process. Diffusional kurtosis imaging (DKI), which is a technique based on non-Gaussian water diffusion analysis, has been regarded as an extension of the DTI model that features minor changes in data acquisition and processing [47]. It provides different diffusion parameters, such as the mean kurtosis (MK), radial kurtosis ($K_\perp$), and axial kurtosis ($K_{||}$), which can provide more useful information about the microstructural complexity of tissue. It has been widely applied to brain studies [48, 49]. Pentang et al. [50] and Huang et al. [51] evaluated the feasibility of DKI in normal human kidneys and demonstrated that the kidney is well suited for the application of DKI due to the presence of anisotropy in renal tissue. In our preliminary study (the findings of which have not been published), DKI has also been utilized to study the renal diffusion of healthy Sprague Dawley rat (Figure 3). However, DKI has not been shown to detect changes in non-Gaussian water diffusion in the kidneys due to AKI.

5. Conclusion

In summary, functional renal imaging is a growing field of interest with tremendous potential, particularly the BOLD, ASL, and DWI techniques, which assess the oxygenation, perfusion, and diffusion of the kidney. Moreover, because these techniques do not require the administration of exogenous contrast agents, they can also be applied in patients with impaired renal function. Although the lack of standardized sequences, postprocessing software, and models hinders the widespread use of these techniques in clinical settings, numerous published papers have demonstrated the feasibility of the techniques for assessing the renal pathophysiology of AKI triggered by different causes. Further explorations that feature improvements in the hardware and postprocessing software are essential to improve our understanding of the renal pathophysiology and progress of AKI.

Conflict of Interests

The authors declare that there is no conflict of interests regarding the publication of this paper.

Acknowledgment

This study was supported by the National Natural Science Foundation of China (Grant no. 81541127).

References

[1] N. Srisawat and J. A. Kellum, "Acute kidney injury: definition, epidemiology, and outcome," *Current Opinion in Critical Care*, vol. 17, no. 6, pp. 548–555, 2011.

[2] S. Dirkes, "Acute kidney injury: not just acute renal failure anymore?" *Critical Care Nurse*, vol. 31, no. 1, pp. 37–50, 2011.

[3] X. Wen, R. Murugan, Z. Peng, and J. A. Kellum, "Pathophysiology of acute kidney injury: a new perspective," *Contributions to Nephrology*, vol. 165, pp. 39–45, 2010.

[4] D. P. Basile, M. D. Anderson, and T. A. Sutton, "Pathophysiology of acute kidney injury," *Comprehensive Physiology*, vol. 2, no. 2, pp. 1303–1353, 2012.

[5] P. Singh, S.-E. Ricksten, G. Bragadottir, B. Redfors, and L. Nordquist, "Renal oxygenation and haemodynamics in acute kidney injury and chronic kidney disease," *Clinical and Experimental Pharmacology and Physiology*, vol. 40, no. 2, pp. 138–147, 2013.

[6] S. G. Coca, R. Yalavarthy, J. Concato, and C. R. Parikh, "Biomarkers for the diagnosis and risk stratification of acute kidney injury: a systematic review," *Kidney International*, vol. 73, no. 9, pp. 1008–1016, 2008.

[7] M. Notohamiprodjo, M. F. Reiser, and S. P. Sourbron, "Diffusion and perfusion of the kidney," *European Journal of Radiology*, vol. 76, no. 3, pp. 337–347, 2010.

[8] J. Neugarten, "Renal BOLD-MRI and assessment for renal hypoxia," *Kidney International*, vol. 81, no. 7, pp. 613–614, 2012.

[9] S. Sanyal, P. Marckmann, S. Scherer, and J. L. Abraham, "Multiorgan gadolinium (Gd) deposition and fibrosis in a patient with nephrogenic systemic fibrosis—an autopsy-based review," *Nephrology Dialysis Transplantation*, vol. 26, no. 11, pp. 3616–3626, 2011.

[10] R. G. Evans, B. S. Gardiner, D. W. Smith, and P. M. O'Connor, "Methods for studying the physiology of kidney oxygenation," *Clinical and Experimental Pharmacology and Physiology*, vol. 35, no. 12, pp. 1405–1412, 2008.

[11] A. Pohlmann, K. Cantow, J. Hentschel et al., "Linking non-invasive parametric MRI with invasive physiological measurements (MR-PHYSIOL): towards a hybrid and integrated approach for investigation of acute kidney injury in rats," *Acta Physiologica*, vol. 207, no. 4, pp. 673–689, 2013.

[12] P. V. Prasad, R. R. Edelman, and F. H. Epstein, "Noninvasive evaluation of intrarenal oxygenation with BOLD MRI," *Circulation*, vol. 94, no. 12, pp. 3271–3275, 1996.

[13] L.-P. Li, S. Halter, and P. V. Prasad, "Blood oxygen level-dependent MR imaging of the kidneys," *Magnetic Resonance Imaging Clinics of North America*, vol. 16, no. 4, pp. 613–625, 2008.

[14] P. V. Prasad, "Evaluation of intra-renal oxygenation by BOLD MRI," *Nephron—Clinical Practice*, vol. 103, no. 2, pp. c58–c65, 2006.

[15] A. Pohlmann, K. Arakelyan, J. Hentschel et al., "Detailing the relation between renal T2* and renal tissue pO2 using an integrated approach of parametric magnetic resonance imaging and invasive physiological measurements," *Investigative Radiology*, vol. 49, no. 8, pp. 547–560, 2014.

[16] S. K. Alford, E. A. Sadowski, O. Unal et al., "Detection of acute renal ischemia in swine using blood oxygen level-dependent magnetic resonance imaging," *Journal of Magnetic Resonance Imaging*, vol. 22, no. 3, pp. 347–353, 2005.

[17] L. Juillard, L. O. Lerman, D. G. Kruger et al., "Blood oxygen level-dependent measurement of acute intra-renal ischemia," *Kidney International*, vol. 65, no. 3, pp. 944–950, 2004.

[18] M. Pedersen, C. Laustsen, V. Perot, F. Basseau, C. Moonen, and N. Grenier, "Renal hemodynamics and oxygenation in transient renal artery occluded rats evaluated with iron-oxide particles and oxygenation-sensitive imaging," *Zeitschrift für Medizinische Physik*, vol. 20, no. 2, pp. 134–142, 2010.

[19] S. Haneder, J. Augustin, G. Jost et al., "Impact of iso- and low-osmolar iodinated contrast agents on BOLD and diffusion MRI in swine kidneys," *Investigative Radiology*, vol. 47, no. 5, pp. 299–305, 2012.

[20] L.-P. Li, J. Lu, Y. Zhou et al., "Evaluation of intrarenal oxygenation in iodinated contrast-induced acute kidney injury-susceptible rats by blood oxygen level-dependent magnetic resonance imaging," *Investigative Radiology*, vol. 49, no. 6, pp. 403–410, 2014.

[21] K. Arakelyan, K. Cantow, J. Hentschel et al., "Early effects of an x-ray contrast medium on renal T_2^*/T_2 MRI as compared to short-term hyperoxia, hypoxia and aortic occlusion in rats," *Acta Physiologica*, vol. 208, no. 2, pp. 202–213, 2013.

[22] L.-P. Li, J. Thacker, J. Lu et al., "Efficacy of preventive interventions for iodinated contrast-induced acute kidney injury evaluated by intrarenal oxygenation as an early marker," *Investigative Radiology*, vol. 49, no. 10, pp. 647–652, 2014.

[23] F. Han, W. Xiao, Y. Xu et al., "The significance of BOLD MRI in differentiation between renal transplant rejection and acute tubular necrosis," *Nephrology Dialysis Transplantation*, vol. 23, no. 8, pp. 2666–2672, 2008.

[24] A. Djamali, E. A. Sadowski, M. Samaniego-Picota et al., "Non-invasive assessment of early kidney allograft dysfunction by blood oxygen level-dependent magnetic resonance imaging," *Transplantation*, vol. 82, no. 5, pp. 621–628, 2006.

[25] E. A. Sadowski, A. Djamali, A. L. Wentland et al., "Blood oxygen level-dependent and perfusion magnetic resonance imaging: detecting differences in oxygen bioavailability and blood flow in transplanted kidneys," *Magnetic Resonance Imaging*, vol. 28, no. 1, pp. 56–64, 2010.

[26] L. Hofmann, S. Simon-Zoula, A. Nowak et al., "BOLD-MRI for the assessment of renal oxygenation in humans: acute effect of nephrotoxic xenobiotics," *Kidney International*, vol. 70, no. 1, pp. 144–150, 2006.

[27] M. Tran, D. Tam, A. Bardia et al., "PGC-1α promotes recovery after acute kidney injury during systemic inflammation in mice," *Journal of Clinical Investigation*, vol. 121, no. 10, pp. 4003–4014, 2011.

[28] D. S. Williams, J. A. Detre, J. S. Leigh, and A. P. Koretsky, "Magnetic resonance imaging of perfusion using spin inversion of arterial water," *Proceedings of the National Academy of Sciences of the United States of America*, vol. 89, no. 1, pp. 212–216, 1992.

[29] J. A. Detre, H. Rao, D. J. J. Wang, Y. F. Chen, and Z. Wang, "Applications of arterial spin labeled MRI in the brain," *Journal of Magnetic Resonance Imaging*, vol. 35, no. 5, pp. 1026–1037, 2012.

[30] C. Kiefer, G. Schroth, J. Gralla, N. Diehm, I. Baumgartner, and M. Husmann, "A feasibility study on model-based evaluation

of kidney perfusion measured by means of FAIR prepared true-FISP arterial spin labeling (ASL) on a 3-T MR scanner," *Academic Radiology*, vol. 16, no. 1, pp. 79–87, 2009.

[31] J. Dong, L. Yang, T. Su et al., "Quantitative assessment of acute kidney injury by noninvasive arterial spin labeling perfusion MRI: a pilot study," *Science China Life Sciences*, vol. 56, no. 8, pp. 745–750, 2013.

[32] K. Hueper, M. Gutberlet, S. Rong et al., "Acute kidney injury: arterial spin labeling to monitor renal perfusion impairment in mice-comparison with histopathologic results and renal function," *Radiology*, vol. 270, no. 1, pp. 117–124, 2014.

[33] F. Zimmer, F. G. Zöllner, S. Hoeger et al., "Quantitative renal perfusion measurements in a rat model of acute kidney injury at 3T: testing inter- and intramethodical significance of ASL and DCE-MRI," *PLoS ONE*, vol. 8, no. 1, Article ID e53849, 2013.

[34] W. B. Chen, L. Liang, B. Zhang et al., "To evaluate the damage of renal function in CIAKI rats at 3T: using ASL and BOLD MRI," *BioMed Research International*, vol. 2015, Article ID 593060, 8 pages, 2015.

[35] J. Wang, D. C. Alsop, L. Li et al., "Comparison of quantitative perfusion imaging using arterial spin labeling at 1.5 and 4.0 Tesla," *Magnetic Resonance in Medicine*, vol. 48, no. 2, pp. 242–254, 2002.

[36] D. Le Bihan, R. Turner, P. Douek, and N. Patronas, "Diffusion MR imaging: clinical applications," *American Journal of Roentgenology*, vol. 159, no. 3, pp. 591–599, 1992.

[37] K. Hueper, S. Rong, M. Gutberlet et al., "T2 relaxation time and apparent diffusion coefficient for noninvasive assessment of renal pathology after acute kidney injury in mice: comparison with histopathology," *Investigative Radiology*, vol. 48, no. 12, pp. 834–842, 2013.

[38] D. Le Bihan, E. Breton, D. Lallemand, M.-L. Aubin, J. Vignaud, and M. Laval-Jeantet, "Separation of diffusion and perfusion in intravoxel incoherent motion MR imaging," *Radiology*, vol. 168, no. 2, pp. 497–505, 1988.

[39] H. Chandarana, V. S. Lee, E. Hecht, B. Taouli, and E. E. Sigmund, "Comparison of biexponential and monoexponential model of diffusion weighted imaging in evaluation of renal lesions: preliminary experience," *Investigative Radiology*, vol. 46, no. 5, pp. 285–291, 2011.

[40] E. E. Sigmund, P.-H. Vivier, D. Sui et al., "Intravoxel incoherent motion and diffusion-tensor imaging in renal tissue under hydration and furosemide flow challenges," *Radiology*, vol. 263, no. 3, pp. 758–769, 2012.

[41] S. Ichikawa, U. Motosugi, T. Ichikawa, K. Sano, H. Morisaka, and T. Araki, "Intravoxel incoherent motion imaging of the kidney: alterations in diffusion and perfusion in patients with renal dysfunction," *Magnetic Resonance Imaging*, vol. 31, no. 3, pp. 414–417, 2013.

[42] L. Liang, W. B. Chen, K. W. Chan et al., "Using intravoxel incoherent motion MR imaging to study the renal pathophysiological process of contrast-induced acute kidney injury in rats: comparison with conventional DWI and arterial spin labelling," *European Radiology*, 2015.

[43] Y. Fukuda, I. Ohashi, K. Hanafusa et al., "Anisotropic diffusion in kidney: apparent diffusion coefficient measurements for clinical use," *Journal of Magnetic Resonance Imaging*, vol. 11, no. 2, pp. 156–160, 2000.

[44] M. Kataoka, A. Kido, A. Yamamoto et al., "Diffusion tensor imaging of kidneys with respiratory triggering: optimization of parameters to demonstrate anisotropic structures on fraction anisotropy maps," *Journal of Magnetic Resonance Imaging*, vol. 29, no. 3, pp. 736–744, 2009.

[45] M. Notohamiprodjo, O. Dietrich, W. Horger et al., "Diffusion Tensor Imaging (DTI) of the kidney at 3 tesla-feasibility, protocol evaluation and comparison to 1.5 Tesla," *Investigative Radiology*, vol. 45, no. 5, pp. 245–254, 2010.

[46] J. S. Cheung, S. J. Fan, A. M. Chow, J. Zhang, K. Man, and E. X. Wu, "Diffusion tensor imaging of renal ischemia reperfusion injury in an experimental model," *NMR in Biomedicine*, vol. 23, no. 5, pp. 496–502, 2010.

[47] J. H. Jensen and J. A. Helpern, "MRI quantification of non-Gaussian water diffusion by kurtosis analysis," *NMR in Biomedicine*, vol. 23, no. 7, pp. 698–710, 2010.

[48] P. Raab, E. Hattingen, K. Franz, F. E. Zanella, and H. Lanfermann, "Cerebral gliomas: diffusional kurtosis imaging analysis of microstructural differences," *Radiology*, vol. 254, no. 3, pp. 876–881, 2010.

[49] M. F. Falangola, J. H. Jensen, J. S. Babb et al., "Age-related non-Gaussian diffusion patterns in the prefrontal brain," *Journal of Magnetic Resonance Imaging*, vol. 28, no. 6, pp. 1345–1350, 2008.

[50] G. Pentang, R. S. Lanzman, P. Heusch et al., "Diffusion kurtosis imaging of the human kidney: a feasibility study," *Magnetic Resonance Imaging*, vol. 32, no. 5, pp. 413–420, 2014.

[51] Y. Huang, X. Chen, Z. Zhang et al., "MRI quantification of non-Gaussian water diffusion in normal human kidney: a diffusional kurtosis imaging study," *NMR in Biomedicine*, vol. 28, no. 2, pp. 154–161, 2015.

Hindawi Publishing Corporation
BioMed Research International
Volume 2016, Article ID 4048390, 12 pages
http://dx.doi.org/10.1155/2016/4048390

Review Article

New Therapeutic Concept of NAD Redox Balance for Cisplatin Nephrotoxicity

Gi-Su Oh,[1] Hyung-Jin Kim,[1] AiHua Shen,[1] Su-Bin Lee,[1] Sei-Hoon Yang,[2] Hyeok Shim,[2] Eun-Young Cho,[2] Kang-Beom Kwon,[3] Tae Hwan Kwak,[4] and Hong-Seob So[1]

[1]*Center for Metabolic Function Regulation, Department of Microbiology, School of Medicine, Wonkwang University, Iksan, Jeonbuk 570-749, Republic of Korea*
[2]*Department of Internal Medicine, School of Medicine, Wonkwang University, Iksan, Jeonbuk 570-749, Republic of Korea*
[3]*Department of Oriental Medical Physiology, College of Korean Medicine, Wonkwang University, Iksan, Jeonbuk 570-749, Republic of Korea*
[4]*PAEAN Biotechnology, 160 Tachno-2 Street, Yuseong-gu, Daejeon 305-500, Republic of Korea*

Correspondence should be addressed to Hong-Seob So; jeanso@wku.ac.kr

Received 22 October 2015; Accepted 9 December 2015

Academic Editor: Jeremiah R. Brown

Cisplatin is a widely used chemotherapeutic agent for the treatment of various tumors. In addition to its antitumor activity, cisplatin affects normal cells and may induce adverse effects such as ototoxicity, nephrotoxicity, and peripheral neuropathy. Various mechanisms such as DNA adduct formation, mitochondrial dysfunction, oxidative stress, and inflammatory responses are closely associated with cisplatin-induced nephrotoxicity; however, the precise mechanism remains unclear. The cofactor nicotinamide adenine dinucleotide (NAD^+) has emerged as a key regulator of cellular energy metabolism and homeostasis. Recent studies have demonstrated associations between disturbance in intracellular NAD^+ levels and clinical progression of various diseases through the production of reactive oxygen species and inflammation. Furthermore, we demonstrated that reduction of the intracellular NAD^+/NADH ratio is critically involved in cisplatin-induced kidney damage through inflammation and oxidative stress and that increase of the cellular NAD^+/NADH ratio suppresses cisplatin-induced kidney damage by modulation of potential damage mediators such as oxidative stress and inflammatory responses. In this review, we describe the role of NAD^+ metabolism in cisplatin-induced nephrotoxicity and discuss a potential strategy for the prevention or treatment of cisplatin-induced adverse effects with a particular focus on NAD^+-dependent cellular pathways.

1. Introduction

cis-Diamminedichloroplatinum II (CDDP, cisplatin) is a widely used chemotherapeutic drug for the treatment of various solid tumors in the head and neck, bladder, lung, ovaries, testicles, and uterus [1–6]. The various adverse effects of cisplatin during the course of chemotherapy include ototoxicity, nephrotoxicity, myelosuppression, and peripheral neuropathy. Cisplatin accumulates in renal tissues and cells, which are primary sites for drug filtration, concentration, and excretion. Even if blood concentrations are held at nontoxic levels during chemotherapy, concentrations may reach toxic levels in the kidneys [4]. In general, cisplatin concentrations in tubular epithelial cells of kidney tissues are five times higher than those in blood, and the elevated concentration of cisplatin therein causes nephrotoxicity. Clinical signs of kidney damage are a decrease in renal plasma flow and glomerular filtration rate, an increase of serum creatinine and blood urea nitrogen, and a reduction of serum magnesium and potassium levels [7]. Cisplatin-induced nephrotoxicity is dose-dependent and therefore limits the potential to increase dosage for optimal cancer therapy [8]. Even though the establishment of cisplatin-induced nephrotoxicity can be alleviated by diuretics and prehydration of patients, the prevalence of cisplatin nephrotoxicity is still high, occurring in approximately one-third of patients who have undergone

cisplatin therapy [6]. Cisplatin nephrotoxicity can present in a number of ways, including acute kidney injury, hypomagnesemia, hypocalcemia, hyperuricemia, distal renal tubular acidosis, proximal tubular dysfunction, and chronic renal failure [7]. However, the most serious and one of the more common clinical features of cisplatin nephrotoxicity is acute kidney injury which occurs in 20–30% of patients. Recent studies have demonstrated that the cellular process of nephrotoxicity can be attributed to local accumulation of cisplatin inside the proximal tubule by membrane transportation, and intracellular conversion of the drug into toxic metabolites. Furthermore, various mechanisms such as DNA adduct formation, mitochondrial dysfunction, oxidative stress, inflammatory responses, and activation of apoptotic pathways are closely associated with cisplatin-induced nephrotoxicity [7].

The cofactor nicotinamide adenine dinucleotide (NAD^+) has emerged as a key regulator of cellular energy metabolism and homeostasis. Recently, it has been reported that intracellular NAD^+/NADH ratios are decreased in various pathological conditions such as diabetes [9], cisplatin-induced cochlear and kidney damage [10, 11], and in many tissues of aged animals and humans [12, 13]. Recent studies have demonstrated that a disturbance in intracellular NAD^+ levels is linked to the progression of various diseases through the production of reactive oxygen species (ROS) and inflammation [10, 11, 14]. Furthermore, reduction of the intracellular NAD^+/NADH ratio is critically involved in cisplatin-induced acute kidney damage; increasing the cellular NAD^+/NADH ratio by pharmacological agents suppresses cisplatin-induced acute kidney damage by downregulation of potential damage mediators such as oxidative stress and inflammatory responses [11]. The decrease in the NAD^+/NADH ratio has been attributed to hyperactivation of the NAD^+-consuming poly(ADP-ribose) polymerase 1 (PARP-1) induced by oxidative damage due to altered redox mechanisms and consequent DNA damage [10, 11]. Since silent mating type information regulation 2 homolog 1 (sirtuin 1, SIRT1) deacetylase activity is influenced by the NAD^+/NADH ratio [15], a significant reduction in the NAD^+/NADH ratio causes a concomitant decrease in SIRT1 deacetylase activity, which is critically involved in diverse biological functions. In addition, the α-ketoglutarate dehydrogenase (α-KGDH) complex, an enzyme complex of the Krebs cycle in mitochondria, facilitates the generation of ROS after NAD^+/NADH reduction [16]. Decreased NAD^+/NADH also favors ROS generation in the respiratory chain complex I [17]. Therefore, maintenance of adequate NAD^+ levels may be a critical factor for normal cellular function and could emerge as a useful strategy for treating many diseases.

Although there are review articles each focusing on cisplatin-mediated nephrotoxicity or beneficial role of NAD^+, there is lack of effort illustrating a potential therapeutic or preventive strategy of modulatory NAD^+ levels for treating cisplatin-associated nephrotoxicity. Therefore, we aimed to review a critical issue related to cisplatin-induced nephrotoxicity which can potentially be overcome by modulation of cellular NAD^+ levels. We searched PubMed for published articles using separate search terms "cisplatin-mediated nephrotoxicity" and "NAD^+-modulation and disease" and included only most recent and relevant publication including original research articles and reviews but excluded repetitive illustrations. In this review, we describe the mechanisms of cisplatin-mediated nephrotoxicity and the role of NAD^+ metabolism therein and discuss a potential strategy for prevention of the adverse effects of cisplatin through targeting of NAD^+-dependent cellular pathways.

2. Kidney-Specific Toxicity of Cisplatin: Cisplatin Transport and Biotransformation

Cisplatin is primarily cleared by the kidneys through both glomerular filtration and tubular secretion, whereas the biliary and intestinal excretions of this drug are negligible. During the excretion process, cisplatin is highly concentrated in the kidneys, which suggests an active accumulation of this drug by renal parenchymal cells, thereby explaining the particular damage caused by this drug to the kidneys compared to other organs. The toxic effects of cisplatin occur primarily in the renal proximal tubules, predominantly in the epithelial tubular cells of the S-3 segment [18]. Though the high concentrations of cisplatin in the kidneys favor its cellular uptake by passive diffusion, recent studies have demonstrated two different membrane transporters capable of facilitating the transport of cisplatin into cells. Copper transporter 1 (Ctr1) is highly expressed and localized in the basolateral membrane of the proximal tubule in the adult kidney [19]. Even though the role of Ctr1 in cisplatin nephrotoxicity *in vivo* has not been examined, cisplatin uptake and cytotoxicity were decreased by downregulation of Ctr1 expression in kidney cells *in vitro*, suggesting that Ctr1 is required for cisplatin uptake in these cells. In addition, the organic cation transporter 2 (OCT2) is specifically expressed in the basolateral membranes of the kidney renal proximal tubule cells, contributing to the etiology of the organ-specific toxicity of cisplatin. OCT2 expression is critical for the development of cisplatin-induced nephrotoxicity, and introduction of the OCT2 substrate cimetidine, a competing factor for transport, reduces nephrotoxicity [20], suggesting that OCT2 is critically involved in cisplatin uptake and its toxicity in these cells. In addition to specific expression of cisplatin transporter proteins in the kidney, many studies have demonstrated that cisplatin undergoes metabolic activation in the kidney to a more potent nephrotoxin. This process is initiated with the biotransformation of cisplatin-glutathione (GSH) conjugates by glutathione-S-transferase in the circulation [21]. When the cisplatin-GSH conjugate reaches and passes through the kidney, it is cleaved to a nephrotoxic metabolite primarily by the action of gamma-glutamyl transpeptidase, an enzyme principally located on the surface of the kidney proximal tubule cells. This metabolite is a highly reactive thiol/platinum compound that interacts with macromolecules, eventually leading to renal damage [22].

3. Mechanisms of Cisplatin Nephrotoxicity

3.1. Oxidative Stress in Cisplatin Nephrotoxicity. Oxidative stresses, including superoxide anions, hydrogen peroxide, and hydroxyl radicals, are unavoidable by-products of cellular respiration. Oxidative stress is also closely involved

in renal injury after cisplatin administration. In particular, production of ROS and antioxidant system dysfunction are associated with cisplatin-induced nephrotoxicity [23]. Due to their unstable and highly reactive nature, ROS may attack and modify multiple target molecules such as lipids, proteins, and DNA, producing cellular stress. ROS also activate important signaling pathways, including an apoptotic pathway, which leads to cell death in the event of cisplatin-induced nephrotoxicity [24]. Although the role of oxidative stress in renal damage is well established, its source is poorly understood. Potential sources of ROS include the mitochondrial electron transport chain system [25], xanthine oxidase [26], cytochrome P450 enzymes [27], and NADPH oxidase [28]. Cisplatin may produce ROS in microsomes via the cytochrome P450 system (CYP). *In vitro* and *in vivo* tests have demonstrated that CYP is an important source of catalytic iron for the generation of ROS during cisplatin treatment. Furthermore, the cisplatin-induced increase of ROS and kidney damage were attenuated in CYP2E1$^{-/-}$ mice [29]. Mitochondria have also been reported to be a major source of ROS. Disturbance of the mitochondrial electron transport chain system, which was accompanied by loss of mitochondrial membrane potential, an indicator of mitochondrial dysfunction, is a well-recognized mechanism responsible for the generation of ROS [25]. Interestingly, mitochondria themselves are particularly vulnerable to oxidative stress. Oxidative damage to mitochondria causes the impairment of mitochondrial function and subsequent cell death via apoptosis and necrosis [30]. Thus, ROS-mediated oxidative damage to mitochondria favors the generation of additional ROS, resulting in a vicious cycle. Many studies have demonstrated a clear association between mitochondrial ROS generation and cisplatin nephrotoxicity [6]. Membrane NAD(P)H oxidases (NOXs) are also one of the major sources for ROS generation. Especially in phagocytic cells such as neutrophils, superoxide is generated by NOX enzyme complexes [31]. However, many studies have recently found that superoxide-generating NOX expression is not restricted to phagocytic cells but is present in a wide variety of nonphagocytic cells and tissues [32]. In particular, it has been reported that superoxide-generating NOXs are expressed in the inner ear and in kidney tissues and that their expression is increased by exposure to cisplatin, thereby causing oxidative stress that leads to cisplatin-mediated ototoxicity and nephrotoxicity [11, 33, 34].

3.2. Inflammation in Cisplatin Nephrotoxicity. In addition to direct cellular toxicity, inflammation is closely associated with the pathogenesis of cisplatin nephrotoxicity. Over the last decade, it has been found that a number of mediators of inflammation, including TNF-α, IL-1β, TGF-β, RANTES, MIP2, and MCP1, are increased in cisplatin-induced renal injury. Inflammation contributes to the development of renal tissue damage and renal failure under pathological conditions. However, evidence for a functional role in renal damage for many of these cytokines still remains to be identified, with the exception of TNF-α [35, 36]. The proinflammatory cytokine TNF-α plays a central role in many infectious and inflammatory diseases. Relevantly, the functional involvement of TNF-α in the pathogenesis of cisplatin-induced acute renal failure was determined in mice treated with cisplatin in the presence or absence of TNF-α production inhibitors, as well as in TNF-α knockout mice. Treatment with TNF-α production inhibitors reduced cisplatin-induced renal damage and also reduced histologic evidence of injury. TNF-deficient mice were also resistant to cisplatin nephrotoxicity. These results indicated an important role for TNF-α in the pathogenesis of cisplatin nephrotoxicity [37]. Furthermore, this study showed that pharmacological inhibitors and antibodies against TNF-α markedly suppressed the induction of other cytokines during cisplatin nephrotoxicity, suggesting that TNF-α might be a key upstream regulator of the inflammatory response triggered by cisplatin. These observations have been confirmed and extended by other studies [38–40]. TNF-α can be produced by a variety of both immune and non-immune cells. However, Zhang et al. were able to determine the source of the TNF-α that was responsible for cisplatin-induced renal damage [39]. They created chimeric mice in which TNF-α could be produced by resident kidney cells or by circulating immune cells and evaluated kidney function, histology, and cytokine expression in these chimeric mice following cisplatin administration. In this study, they demonstrated that the local production of TNF-α by resident kidney cells, probably the renal epithelial cells themselves, was crucial to cisplatin-induced nephrotoxicity [39].

The next question, then, became: how does TNF-α stimulate the inflammatory response and contribute to cisplatin nephrotoxicity? The biological activities of TNF-α are primarily mediated by two functionally distinct receptors, TNFR1 and TNFR2, to induce a variety of cellular responses ranging from inflammation to cell death. TNFR1 and TNFR2 are also upregulated by cisplatin. While TNFR1 directly induces the extrinsic apoptotic pathway, TNFR2 is primarily associated with the inflammatory response, which amplifies the TNFR1 effects. Furthermore, as the TNFR2 protein does not contain the death domain necessary to trigger apoptosis, TNFR2, unlike TNFR1, would appear to indirectly induce apoptosis and necrosis in renal tubular epithelial cells [41, 42]. Conflictingly, Tsuruya et al. showed that TNFR1-deficient mice and renal tubular cells were more resistant to cisplatin-induced renal injury and apoptosis compared with wild type mice [43], whereas Ramesh and Reeves recently showed that cisplatin-induced tubular cell death and renal injury were clearly attenuated in TNFR2-deficient, but not in TNFR1-deficient, mice [41]. Although the cause of the inconsistency between these two studies has not been elucidated, together they suggest that TNF-α signaling plays a critical role for cisplatin nephrotoxicity. The production of TNF-α after cisplatin administration is highly dependent upon ROS, NF-κB activation, and activation of p38 MAPK. In fact, TNF-α both is an inducer of ROS and is induced by ROS generated by cisplatin [37]. ROS activates the transcription factor NF-κB, which in turn induces the production of proinflammatory cytokines such as TNF-α [42]. NF-κB activation is pivotal in the expression of proinflammatory cytokines and other mediators involved in acute inflammatory responses and other conditions associated with increased ROS generation [44]. In addition to direct oxidative damage to lipids, DNA, and proteins [23], ROS generated

by cisplatin activates p38 MAPK through the induction of p38 MAPK phosphorylation, which mediates the synthesis of TNF-α. Ramesh and Reeves demonstrated that inhibition of p38 MAPK reduced TNF-α production and protected against cisplatin-induced renal damage *in vivo* [45]. Activation of p38 MAPK led to the degradation of IκB (an inhibitor of NF-κB), thereby promoting translocation of NF-κB to the nucleus and the consequent stimulation of proinflammatory cytokine production, including TNF-α [46].

Toll-like receptors (TLRs) are a family of pattern recognition receptors that detect pathogenic elements such as viral RNA, bacterial DNA, lipopolysaccharides, or proteins, called pathogen-associated molecular patterns (PAMPs). TLRs play a pivotal role in host defense against infection by sensing the invasion of organisms and initiating both innate and adaptive immune responses [47]. TLRs also detect and respond to certain endogenous molecules such as high-mobility group box protein 1 (HMGB1), heat shock proteins (HSPs), and extracellular matrix components, termed damage-associated molecular pattern molecules (DAMPs). DAMPs are generally released by damaged or stressed tissues to "alert" the immune system to tissue injury or impending danger [48]. Cisplatin increases the expression of TLRs, including TLR4 in murine peritoneal macrophages *in vitro*, and subsequent stimulation by individual TLR-related ligands induces the production of proinflammatory cytokines such as TNF-α, IFN-γ, IL-1β, and IL-12 [49]. In addition, Zhang et al. have demonstrated that TLR4 is essential to the initiation of intrarenal inflammatory cytokine production associated with cisplatin-induced nephrotoxicity [50]. Ramesh et al. also have demonstrated that the combination of cisplatin and lipopolysaccharides, which are specific ligands for TLR4, acts synergistically to produce inflammatory cytokines such as TNF-α, IL-6, MCP-1, KC, and GM-CSF, thereby inducing nephrotoxicity in an acute renal failure model [51].

NF-κB activation is a critical bridge to the expression of inflammatory cytokines and other mediators involved in inflammatory responses through TLR signaling. After dimerization of TLR4 through engagement with its ligand, adapter molecules such as TIRAP and TRAM are recruited on the cytoplasmic domain of TLR4, which further interacts with MyD88 and TRIF, respectively, and then transduces a signal to the nucleus. MyD88 is critical for signaling by all TLRs except TLR3. After stimulation, MyD88 associates with the cytoplasmic portion of the TLR and recruits IL-1R-associated kinase- (IRAK-) 4 and -1 through a homophilic interaction of the death domains. Subsequently, TRAF6, TAK1, and NF-κB are activated, and then NF-κB is translocated into the nucleus where it regulates the genes for proinflammatory cytokines among others [52]. In contrast, in TLR4 knockout mice, the activation of p38, which is critical for cisplatin-induced TNF-α production, was significantly blunted [45]. Finally, the released nuclear protein HMGB1 has been shown to activate TLR4 in various pathologic conditions [48, 53]; however, the role of HMGB1 and other DAMPs in TLR4 activation associated with cisplatin nephrotoxicity remains to be elucidated.

3.3. Role of NAD Redox Balance in Cisplatin Nephrotoxicity. NAD is a metabolic cofactor that is present in cells either in its oxidized (NAD^+) or in its reduced (NADH) form. NAD^+ or NADH functions as a cofactor for a multitude of enzymatic reactions and therefore critically regulates cellular energy metabolism and homeostasis. As NAD^+ is critical for a variety of enzymatic reactions, including glycolysis, the NAD redox balance, represented as the NAD^+/NADH ratio, is tightly regulated [54], and its disruption has been associated with multiple clinical disorders and pathologies. For example, pellagra is caused by NAD^+ deficiency subsequent to poor dietary intake of NAD^+ biosynthesis precursors and can be easily cured by providing dietary nicotinic acid [55]. Pathological conditions such as diabetes and oxidative stress are also well correlated with decreased cellular NAD^+ levels [9, 56]. It has also been recently reported that the cellular NAD^+ level in many tissues declines with age [12, 13], implying the importance of maintaining optimal intracellular NAD^+ levels to prevent age-associated cellular dysfunction. Furthermore, cisplatin-induced cochlear and kidney damage are highly associated with the decreases of NAD^+/NADH ratios that accompany inflammation and oxidative stress [10, 11]. Cisplatin treatment resulted in a decrease of NAD^+/NADH ratio in renal tissue without significant changes of NADH level [11]. This suggests that the decrease of NAD^+/NADH ratio by cisplatin is mainly caused by reduction of NAD^+ level. Of note, β-lapachone coadministration with cisplatin also restored NAD^+/NADH ratio to control level through elevation of NAD^+ level, but not by decrease of NADH level. Together, these findings suggest that maintenance of the NAD redox balance is very important for general health.

3.4. Role of NAD^+-Dependent Enzymes in Cisplatin Nephrotoxicity. NAD^+ acts as a cofactor for numerous enzymes including SIRTs, PARPs, and cyclic ADP- (cADP-) ribose synthases [57]; therefore, NAD^+ might exert its biological effect through these enzymes. The mammalian sirtuin family consists of seven enzymes, SIRT1–7 [58], that are ubiquitously expressed yet show specific cellular localizations and functions. SIRT1, SIRT6, and SIRT7 are generally localized in the nuclei of cells, whereas SIRT3, SIRT4, and SIRT5 are localized in the mitochondria [59]. SIRT1 and SIRT5 act exclusively as deacetylases [60, 61], whereas SIRT2, SIRT3, SIRT4, and SIRT6 might also have a mono-ADP-ribosyl transferase activity [60, 62–64]. SIRT1 is the most widely studied sirtuin and has a *Km* for NAD^+ that lies within the range of the physiological changes in intracellular NAD^+ content. This suggests that sirtuin activity could be modulated by the physiological changes in intracellular NAD^+ levels [64]. Considering that the intracellular NAD^+/NADH ratios are decreased in various pathological conditions, including cisplatin-induced nephrotoxicity and ototoxicity [9–11, 56], SIRT1 activity might be reduced in the damaged tissues as well. In particular, Hasegawa et al. demonstrated that SIRT1 protects against oxidative stress-induced apoptosis in the kidney by inducing catalase, which catalyzes the decomposition of the ROS hydrogen peroxide, via deacetylation of FOXO3 in cultured proximal tubular cells [65]. Furthermore, Hasegawa et al. also reported that renal proximal tubular cell-specific *SIRT1* transgenic mice showed resistance to cisplatin-induced renal tubular cell injuries such as apoptosis by maintaining

peroxisome number and function, concomitant with upregulation of catalase and elimination of renal ROS [66]. In addition, it has been demonstrated that SIRT1 activation by resveratrol reduced cisplatin-induced proximal tubular cell apoptosis through deacetylation of p53 [67]. In contrast, Kim et al. and Oh et al. demonstrated that the reduction of intracellular NAD^+/NADH ratio in cisplatin-injected kidney and cochlear tissues was critically associated with the decline of SIRT1 activity, which thereby caused cisplatin-induced nephrotoxicity and ototoxicity through inflammation and oxidative stress [10, 11]. However, SIRT1 activation through the increase of the cellular NAD^+/NADH ratio suppressed the adverse effects of cisplatin by downregulation of potential damage mediators such as oxidative stress factors and inflammatory responses.

SIRT1 regulates diverse biological functions through direct interaction with and subsequent deacetylation of its targets, including p53 and NF-κB, which are closely related to its function in cisplatin-induced nephrotoxicity [7]. As described previously, the transcription factor NF-κB is one of the key regulators of inflammation. NF-κB activation is attained by either IκB phosphorylation and subsequent degradation or an IκB-independent pathway through post-translational modifications of the NF-κB Rel proteins, including acetylation of the NF-κB p65 subunit. NF-κB p65 can be acetylated at five specific lysine residues (Lys-122, Lys-123, Lys-218, Lys-221, and Lys-310). In particular, acetylation of the Lys-310 residue is required for the transcriptional activity of NF-κB, whereas the other acetylation sites are involved in DNA binding [68]. SIRT1 physically interacts with the nuclear translocated NF-κB p65 subunit and deacetylates it at Lys-310, thereby inhibiting the transcriptional activity of NF-κB [69]. An assortment of recent evidence indicates that SIRT1 regulates inflammatory response through NF-κB p65 deacetylation. In cisplatin-induced nephrotoxicity and ototoxicity, Kim et al. demonstrated that SIRT1 activation was critically associated with the deacetylation status of the NF-κB p65 subunit [10, 11]. In addition, it has been demonstrated that SIRT1 knockdown leads to inflammatory pathway activation with increased inflammatory gene expression, whereas SIRT1 activation produces anti-inflammatory effects [70].

The tumor suppressor p53 is another crucial transcription factor in the cellular stress response [71]. A number of post-translational modifications can occur in p53 that have critical effects on its stability and function, including phosphorylation, acetylation, sumoylation, neddylation, and methylation [72]. Cytosolic p53 is bound to Mdm2, a RING finger E3 ubiquitin ligase that facilitates protein degradation under normal conditions. Cellular stress, including DNA damage, hypoxia, or oxidative stress, induces rapid mitochondrial translocation of p53 and its posttranslational modification such as acetylation by p300/CBP or PCAF acetyltransferase [73]. The p53 is acetylated at lysine residues, including Lys-370, Lys-372, Lys-382, and Lys-386 in the carboxy-terminal region. Because acetylated p53 cannot bind to Mdm2, increased p53 acetylation levels strongly correlate with protein stabilization and activation in response to cellular stress [74]. Both nuclear SIRT1 and mitochondrial SIRT3 regulate p53 function through direct interaction and subsequent deacetylation of p53 [75]. In the nucleus, acetylation of p53 stimulates its sequence-specific DNA binding and subsequent recruitment of other transcription cofactors to promoter regions and thereby enhances transcription of target genes [76–78] such as the p53-upregulated modulator of apoptosis (PUMA), NADPH activator A (NOXA), and p53-induced gene 3 (PIG3), all of which are involved in the production of ROS through mitochondrial dysfunction or apoptosis. Deacetylation of p53 by nuclear-localized SIRT1 inactivates its sequence-specific transcriptional activity and represses p53-mediated cell growth arrest and apoptosis in response to DNA damage and oxidative stress [74]. Mitochondrial-localized SIRT3 deacetylates and activates several enzymes that are critical in maintaining cellular ROS levels and for apoptosis. Though it is not well understood whether acetylated p53 in mitochondria might have other functions, mitochondrial p53 interacts with anti- and proapoptotic Bcl-2 family members to either inhibit or activate them, thereby promoting apoptosis through robust mitochondrial outer membrane permeabilization and subsequent cytochrome c release [79, 80]. Deacetylation of p53 by mitochondrial-localized SIRT3 also represses p53-mediated cell growth arrest and apoptosis in response to DNA damage and oxidative stress [75]. On the other hand, Kim et al. demonstrated that cisplatin treatment led to substantial elevation of acetylated p53 levels in the kidney and cochlear tissues compared to those of untreated normal control mice [10, 11].

NAD^+ is consumed not only by sirtuins, but also by PARPs [81]. Cisplatin accumulation in target tissues produces ROS that deplete the cellular antioxidant defense factors necessary to reduce oxidative stress and DNA damage. Cisplatin also directly binds to DNA, resulting in the disruption of the synthesis of key proteins and leading to cell injury and cell death. Furthermore, accumulation of DNA damage can lead to cell cycle arrest or genomic instability. The removal of DNA damaged by oxidative stress is mediated by single-strand DNA break repair, which is facilitated by PARPs. PARP-1 is the most critical protein-modifying nuclear enzyme involved in DNA repair. PARP-1 is a major NAD^+ consumer, wherein the ADP-ribose moiety is transferred to PARP-1 itself or to other acceptor proteins in order to build the poly(ADP-ribose) polymer (PAR) [82]. PARP-1 is strongly activated by DNA damage and oxidative stress. Under physiological conditions, mild activation of PARP-1 can regulate several cellular processes, including DNA repair, cell cycle progression, cell survival, chromatin remodeling, and genomic stability [83]. However, hyperactivation of PARP-1 upon severe oxidative damage causes rapid depletion of intracellular NAD^+ and ATP levels and eventually leads to cell death and related pathological conditions [84, 85]. Kim et al. have demonstrated that hyperactivation of PARP-1 in cisplatin-treated cochlea led to a decline in intracellular NAD^+ levels and SIRT1 activity, thereby causing cochlear damage [10]. It is well established that PARP-1 and SIRT1 activity are interdependent as they compete for a limited pool of cellular NAD^+. However, the *Km* of PARP-1 for NAD^+ is two to ten times lower than that of SIRT1, which falls within the physiological range of cellular NAD^+ concentrations [86]. Thus, PAPR-1 activation might critically influence SIRT1

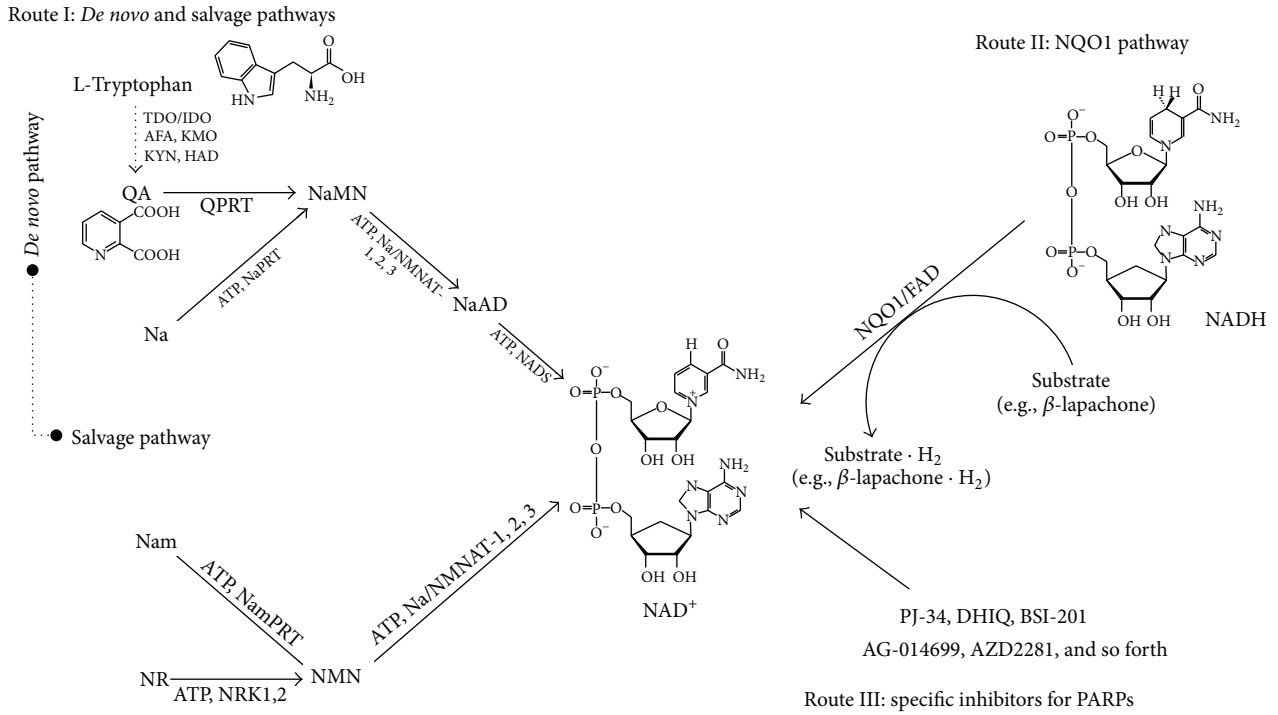

Figure 1: Possible pathways for mammalian NAD^+ biosynthesis. The biosynthesis of NAD^+ through *de novo*, salvage, NQO1 pathways, and specific inhibition for PARPs. ATP: adenosine triphosphate, FAD: flavin adenine dinucleotide, IDO: indoleamine 2,3-dioxygenase, Na: nicotinic acid, NaAD: nicotinic acid adenine dinucleotide, NAD: nicotinamide adenine dinucleotide, NADS: NAD synthetase, Nam: nicotinamide, NaMN: nicotinic acid mononucleotide, NaPRT: nicotinic acid phosphoribosyl transferase, NMN: nicotinamide mononucleotide, NMNAT: nicotinamide mononucleotide adenylyltransferase, NQO1: NAD(P)H:quinone oxidoreductase 1, NR: nicotinamide riboside, NRK1,2: nicotinamide riboside kinase 1, 2, NamPRT: nicotinamide phosphoribosyltransferase, NMNAT: nicotinamide mononucleotide adenyltransferase, QA: quinolinic acid, QPRT: quinolinate phosphoribosyltransferase, TDO: tryptophan 2,3-dioxygenase, AFA: arylformamidase, KMO: kynurenine 3-monooxygenase, KYN: kynureninase, HAD: 3-hydroxy-anthranilate 3,4-dioxygenase, and PARPs: poly(ADP-ribose) polymerases.

activity by reducing NAD^+ bioavailability. This model was further supported by recent studies wherein genetic depletion of PARP-1 or pharmacological inhibition of PARP-1 activity increased intracellular NAD^+ level and subsequent SIRT1 activity [10].

4. Therapeutic Considerations of Cisplatin Nephrotoxicity

The main protective actions currently employed in clinical practice to reduce nephrotoxicity during cisplatin chemotherapy are based on avoiding the extreme exposure of the kidneys to the drug. This is managed primarily by hydration/diuretics, monitoring of renal function by serum creatinine clearance, and decreasing cisplatin doses upon manifestation of renal dysfunction [87, 88]. However, even with aggressive hydration, renal toxicity occurs. Therefore, more effective preventative strategies without attenuation of tumoricidal activity need to be developed, taking into consideration the mechanisms underlying the adverse effects of cisplatin exposure. Although the exact mechanism responsible for cisplatin-associated cellular damage is still to be elucidated, numerous studies have indicated that ROS and increased inflammation are important factors. The roles of these two factors seem to be closely related, and thus their abnormal regulation impacts overlapping cellular processes. Accordingly, pharmacological interventions that reduce systemic inflammation and/or oxidative stress might prevent or alleviate the development and progression of cisplatin-induced nephrotoxicity. However, these effects need to be explored *in vivo* [7]. A better option might be to focus on maintaining a proper level of intracellular NAD^+. The decrease of cellular NAD^+ level in the kidney and cochlear tissues after cisplatin exposure [10, 11] implies the therapeutic potential of intracellular NAD^+ level modulation for cisplatin-associated adverse effects. The role of NAD^+ in the prevention and cure of diseases was first recognized in the 1930s by Conrad Elvehjem, who demonstrated the therapeutic effect of the vitamin nicotinic acid on pellagra in dogs [55]. Since then, the therapeutic potential of NAD^+ has been further evidenced by several studies. Araki et al. showed that addition of exogenous NAD^+ to neurons delayed axonal degeneration in response to mechanical or chemical damage [89]. Ying et al. also demonstrated that intranasal administration of NAD^+ profoundly decreased brain injury in a rat model of transient focal ischemia [90]. Pillai et al. showed that exogenous NAD^+ blocked cardiac hypertrophic response [91].

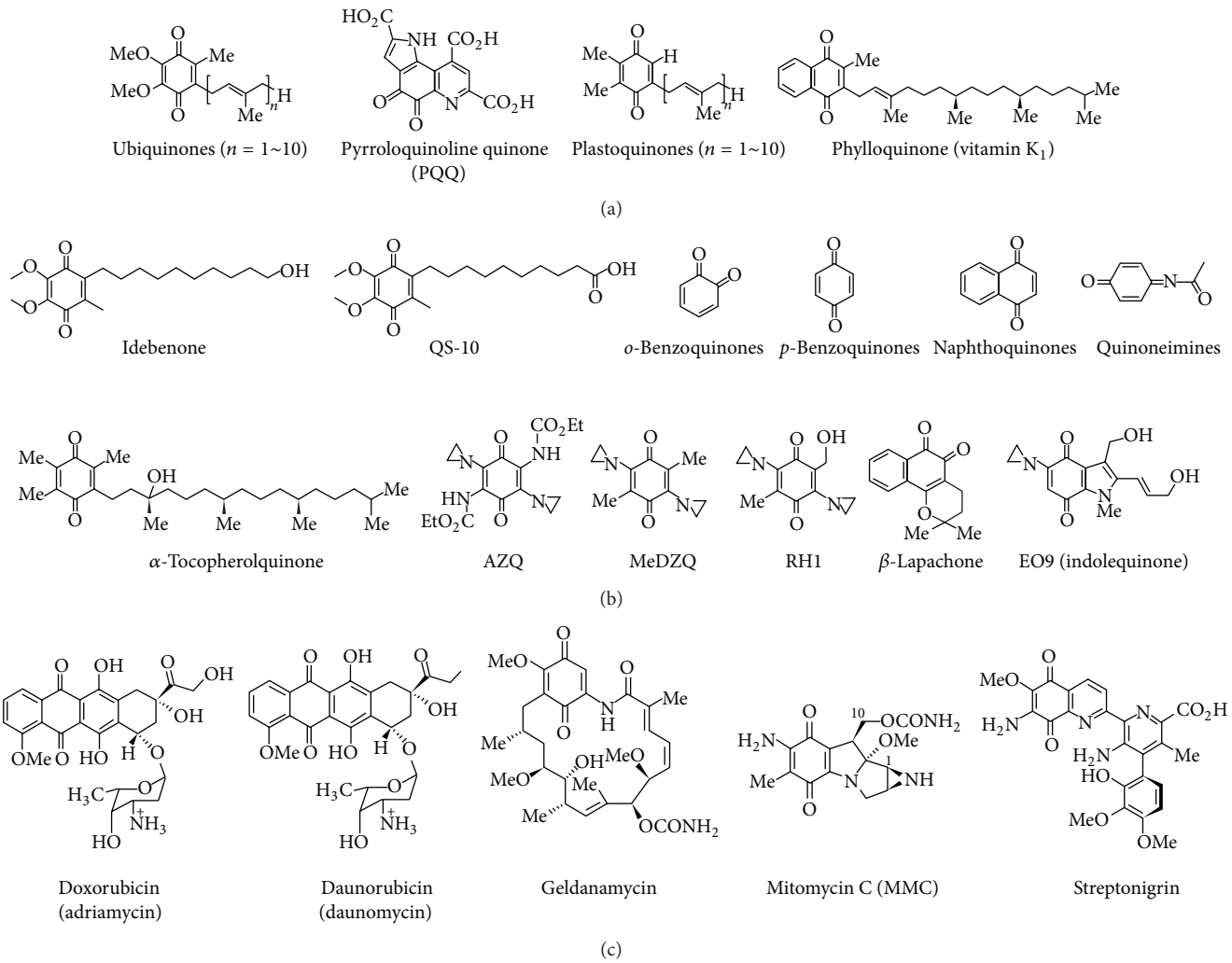

Figure 2: Substrates for NQO1. (a) Naturally occurring quinones as antioxidants. (b) Substrates for reduction by NQO1 and reactive quinone metabolites (benzoquinone, naphthoquinone, and quinoneimine). (c) Naturally occurring quinones with anticancer properties. QS-10: 6-(9-carboxynonyl)-2,3-dimethoxy-5-methyl-1,4-benzoquinone, AZQ: Diaziquine, MeDZQ: 2,5-diaziridinyl-3,6-dimethyl-1,4-benzoquinone, and RH1: 2,5-diaziridinyl-3-hydroxymethyl-6-methyl-1,4-benzoquinone.

As NAD^+ regulates SIRTs that are involved in various cellular processes, the beneficial effects observed following enhanced SIRT activity might be attributed to increased intracellular NAD^+ levels. Since both PARPs and SIRTs are NAD^+-consuming enzymes and thus compete for NAD^+, selective blockage of NAD^+-consuming PARPs might also potentially be a good strategy to increase NAD^+ levels. Consistent with this notion, targeted PARP inactivation has been shown to increase NAD^+ levels and increase SIRT1 activity [92], suggesting that the modulation of PARP activity could be a therapeutic strategy for the treatment of cisplatin-associated adverse effects. In addition, approaches aimed at increasing NAD^+ levels by supplementing NAD^+ precursors through the activation of *de novo* and salvage pathways (Figure 1) for NAD^+ biosynthesis have demonstrated cytoprotective effects against cellular damage. In fact, this specific strategy has been shown to increase NAD^+ levels both *in vitro* and *in vivo*. For example, the administration of nicotinamide, a NAD^+ precursor, showed a protective effect against oxidative stress and glucose deprivation *in vitro* and also alleviated tissue damage in animal models of ischemia [93, 94], spinal cord injury [95], and multiple sclerosis [96]. Similarly, nicotinic acid, another NAD^+ precursor, has also been used to treat hyperlipidemia [97], indicating the therapeutic potential of NAD^+ precursors. Although NAD^+ treatment has not been tested extensively for its cytoprotective effects, a recent report suggested that it might reduce brain damage by protecting against PARP-1-induced cell death [98, 99].

As shown in Figure 1, another strategy in addition to *de novo* and salvage NAD^+ biosynthesis pathways for regulating cellular NAD^+ levels might be to utilize the cytosolic flavoprotein NADH : quinone oxidoreductase 1 (NQO1) that normally participates in reduction of quinone compounds in exchange for NADH oxidation [100, 101]. NQO1 catalyzes the reduction of quinones to hydroquinones by utilizing NADH as an electron donor, which consequently increases intracellular NAD^+ levels. Therefore, it is plausible that endogenous factors or chemical agents that potentially activate NQO1

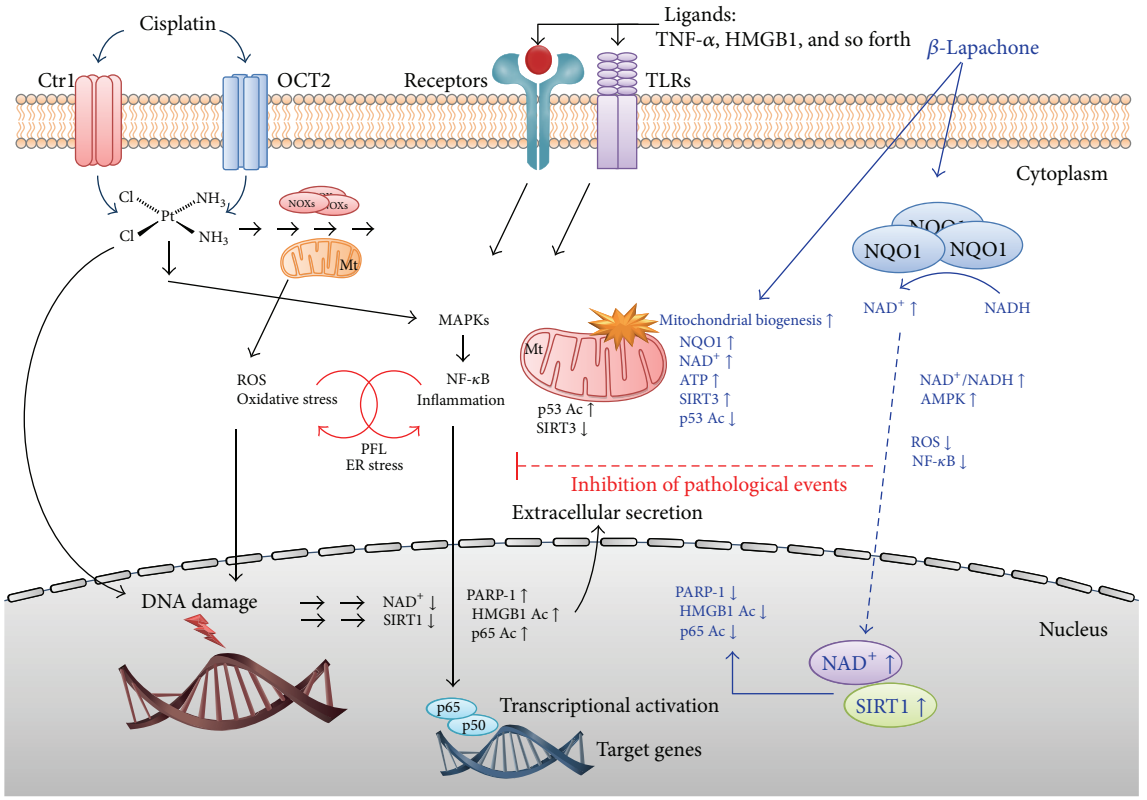

Figure 3: Role of NAD^+ and NAD^+-dependent enzymes in cisplatin-induced nephrotoxic mechanisms. Ctr1: copper transporter 1, OCT2: organic cation transporter 2, NOXs: NADPH oxidoreductases, Mt: mitochondria, ROS: reactive oxygen species, PFL: positive feedback loop, ER: endoplasmic reticulum, TLRs: toll-like receptors, HMGB1: high-mobility group box protein 1, TNF-α: tumor necrosis factor-α, NF-κB: nuclear factor-κB, NQO1: NAD(P)H:quinone oxidoreductase 1, and PARPs: poly(ADP-ribose) polymerases.

enzymatic activity or act as strong substrates of NQO1 might be beneficial for protection against cisplatin-induced toxicity by increasing intracellular NAD^+ levels. In addition, there is evidence that NQO1 also plays a role in other biological activities, including anti-inflammatory processes, the scavenging of superoxide anion radicals, and the stabilization of p53 and other tumor suppressor proteins [102–106]. As shown in Figure 2, several substrates of NQO1 enzyme, including mitomycin C, RH1, AZQ, Coenzyme Q10, and idebenone, have been identified [107, 108], of which β-lapachone (3,4-dihydro-2,2-dimethyl-2H-naphtho[1,2-b]pyran-5,6-dione) is recently well studied as a strong substrate of NQO1 [109, 110]. β-Lapachone was first isolated from the bark of the Lapacho tree and was reported to inhibit tumor growth [111]. Several reports have indicated that pharmacological substrates of NQO1 ameliorate phenotypic manifestations associated with pathological conditions in rodent models. In particular, metabolic diseases such as obesity and spontaneous hypertension were shown to be reversed upon NQO1 enzymatic action using β-lapachone [112, 113], and pathological conditions such as arterial restenosis due to tissue injury and cisplatin-associated nephrotoxicity were also ameliorated by NQO1 enzymatic action using this substrate [11, 114]. As summarized in Figure 3, the increase of the cellular NAD^+/NADH ratio by β-lapachone prevents cisplatin-induced kidney damage by modulation of potential damage mediators such as oxidative stress and inflammatory responses. Furthermore, β-lapachone did not interfere with the tumoricidal effect of cisplatin *in vivo* [11].

5. Conclusion

In conclusion, a NAD redox balance is critically important for sustaining a healthy condition, and maintenance of adequate NAD redox balance may show therapeutic benefits in various diseases through the regulation of NAD^+-dependent enzymes and their downstream targets including SIRTs, PARPs, NF-κB, and p53. In this review we strongly suggest for the first time that direct modulation of a cellular NAD redox balance by pharmacological agents could be a promising therapeutic approach for the treatment of various diseases, including cisplatin nephrotoxicity.

Conflict of Interests

All authors declare no competing interests.

Acknowledgment

This work was supported by National Research Foundation of Korea (NRF) grants funded by the Korean government (MSIP): no. 2011-0028866 and no. 2011-0030130.

References

[1] B. Rosenberg, L. Van Camp, and T. Krigas, "Inhibition of cell division in *Escherichia coli* by electrolysis products from a platinum electrode," *Nature*, vol. 205, no. 4972, pp. 698–699, 1965.

[2] D. Wang and S. J. Lippard, "Cellular processing of platinum anticancer drugs," *Nature Reviews Drug Discovery*, vol. 4, no. 4, pp. 307–320, 2005.

[3] S. M. Cohen and S. J. Lippard, "Cisplatin: from DNA damage to cancer chemotherapy," *Progress in Nucleic Acid Research and Molecular Biology*, vol. 67, pp. 93–130, 2001.

[4] I. Arany and R. L. Safirstein, "Cisplatin nephrotoxicity," *Seminars in Nephrology*, vol. 23, no. 5, pp. 460–464, 2003.

[5] Z. H. Siddik, "Cisplatin: mode of cytotoxic action and molecular basis of resistance," *Oncogene*, vol. 22, no. 47, pp. 7265–7279, 2003.

[6] N. Pabla and Z. Dong, "Cisplatin nephrotoxicity: mechanisms and renoprotective strategies," *Kidney International*, vol. 73, no. 9, pp. 994–1007, 2008.

[7] R. P. Miller, R. K. Tadagavadi, G. Ramesh, and W. B. Reeves, "Mechanisms of cisplatin nephrotoxicity," *Toxins*, vol. 2, no. 11, pp. 2490–2518, 2010.

[8] M. H. Hanigan and P. Devarajan, "Cisplatin nephrotoxicity: molecular mechanisms," *Cancer Therapy*, vol. 1, pp. 47–61, 2003.

[9] Y. Ido, "Pyridine nucleotide redox abnormalities in diabetes," *Antioxidants & Redox Signaling*, vol. 9, no. 7, pp. 931–942, 2007.

[10] H.-J. Kim, G.-S. Oh, A. Shen et al., "Augmentation of NAD^+ by NQO1 attenuates cisplatin-mediated hearing impairment," *Cell Death and Disease*, vol. 5, no. 6, Article ID e1292, 2014.

[11] G.-S. Oh, H.-J. Kim, J.-H. Choi et al., "Pharmacological activation of NQO1 increases NAD^+ levels and attenuates cisplatin-mediated acute kidney injury in mice," *Kidney International*, vol. 85, no. 3, pp. 547–560, 2014.

[12] N. Braidy, G. J. Guillemin, H. Mansour, T. Chan-Ling, A. Poljak, and R. Grant, "Age related changes in NAD+ metabolism oxidative stress and Sirt1 activity in wistar rats," *PLoS ONE*, vol. 6, no. 4, Article ID e19194, 2011.

[13] H. Massudi, R. Grant, N. Braidy, J. Guest, B. Farnsworth, and G. J. Guillemin, "Age-associated changes in oxidative stress and NAD+ metabolism in human tissue," *PLoS ONE*, vol. 7, no. 7, Article ID e42357, 2012.

[14] H.-J. Kim, G.-S. Oh, S.-K. Choe, T. H. Kwak, R. Park, and H.-S. So, "NAD^+ metabolism in age-related hearing loss," *Aging and Disease*, vol. 5, no. 2, pp. 150–159, 2014.

[15] D. Chen, J. Bruno, E. Easlon et al., "Tissue-specific regulation of SIRT1 by calorie restriction," *Genes and Development*, vol. 22, no. 13, pp. 1753–1757, 2008.

[16] V. Adam-Vizi and L. Tretter, "The role of mitochondrial dehydrogenases in the generation of oxidative stress," *Neurochemistry International*, vol. 62, no. 5, pp. 757–763, 2013.

[17] M. P. Murphy, "How mitochondria produce reactive oxygen species," *The Biochemical Journal*, vol. 417, no. 1, pp. 1–13, 2009.

[18] M. Werner, M. J. Costa, L. G. Mitchell, and R. Nayar, "Nephrotoxicity of xenobiotics," *Clinica Chimica Acta*, vol. 237, no. 1-2, pp. 107–154, 1995.

[19] N. Pabla, R. F. Murphy, K. Liu, and Z. Dong, "The copper transporter Ctr1 contributes to cisplatin uptake by renal tubular cells during cisplatin nephrotoxicity," *American Journal of Physiology—Renal Physiology*, vol. 296, no. 3, pp. F505–F511, 2009.

[20] G. Ciarimboli, "Membrane transporters as mediators of cisplatin side-effects," *Anticancer Research*, vol. 34, no. 1, pp. 547–550, 2014.

[21] D. M. Townsend, K. D. Tew, L. He, J. B. King, and M. H. Hanigan, "Role of glutathione S-transferase Pi in cisplatin-induced nephrotoxicity," *Biomedicine and Pharmacotherapy*, vol. 63, no. 2, pp. 79–85, 2009.

[22] R. D. Wainford, R. J. Weaver, K. N. Stewart, P. Brown, and G. M. Hawksworth, "Cisplatin nephrotoxicity is mediated by gamma glutamyltranspeptidase, not via a C-S lyase governed biotransformation pathway," *Toxicology*, vol. 249, no. 2-3, pp. 184–193, 2008.

[23] N. A. G. Santos, C. S. Catão, N. M. Martins, C. Curti, M. L. P. Bianchi, and A. C. Santos, "Cisplatin-induced nephrotoxicity is associated with oxidative stress, redox state unbalance, impairment of energetic metabolism and apoptosis in rat kidney mitochondria," *Archives of Toxicology*, vol. 81, no. 7, pp. 495–504, 2007.

[24] R. Çetin, E. Devrim, B. Kilicoglu, A. Avci, Ö. Çandir, and I. Durak, "Cisplatin impairs antioxidant system and causes oxidation in rat kidney tissues: possible protective roles of natural antioxidant foods," *Journal of Applied Toxicology*, vol. 26, no. 1, pp. 42–46, 2006.

[25] H. H. Szeto, "Mitochondria-targeted peptide antioxidants: novel neuroprotective agents," *The AAPS Journal*, vol. 8, no. 3, pp. E521–E531, 2006.

[26] C. E. Berry and J. M. Hare, "Xanthine oxidoreductase and cardiovascular disease: molecular mechanisms and pathophysiological implications," *Journal of Physiology*, vol. 555, no. 3, pp. 589–606, 2004.

[27] R. A. Gottlieb, "Cytochrome P450: major player in reperfusion injury," *Archives of Biochemistry and Biophysics*, vol. 420, no. 2, pp. 262–267, 2003.

[28] A. A. Miller, G. J. Dusting, C. L. Roulston, and C. G. Sobey, "NADPH-oxidase activity is elevated in penumbral and non-ischemic cerebral arteries following stroke," *Brain Research*, vol. 1111, no. 1, pp. 111–116, 2006.

[29] H. Liu and R. Baliga, "Cytochrome P450 2E1 null mice provide novel protection against cisplatin-induced nephrotoxicity and apoptosis," *Kidney International*, vol. 63, no. 5, pp. 1687–1696, 2003.

[30] J. Bai and A. I. Cederbaum, "Mitochondrial catalase and oxidative injury," *Biological Signals and Receptors*, vol. 10, no. 3-4, pp. 189–199, 2001.

[31] M. Geiszt, "NADPH oxidases: new kids on the block," *Cardiovascular Research*, vol. 71, no. 2, pp. 289–299, 2006.

[32] M. T. Quinn, M. C. B. Ammons, and F. R. DeLeo, "The expanding role of NADPH oxidases in health and disease: no longer just agents of death and destruction," *Clinical Science*, vol. 111, no. 1, pp. 1–20, 2006.

[33] B. Bánfi, B. Malgrange, J. Knisz, K. Steger, M. Dubois-Dauphin, and K.-H. Krause, "NOX3, a superoxide-generating NADPH oxidase of the inner ear," *The Journal of Biological Chemistry*, vol. 279, no. 44, pp. 46065–46072, 2004.

[34] H.-J. Kim, J.-H. Lee, S.-J. Kim et al., "Roles of NADPH oxidases in cisplatin-induced reactive oxygen species generation and ototoxicity," *Journal of Neuroscience*, vol. 30, no. 11, pp. 3933–3946, 2010.

[35] G. Ramesh and W. B. Reeves, "Inflammatory cytokines in acute renal failure," *Kidney International Supplement*, vol. 66, no. 91, pp. S56–S61, 2004.

[36] C. Y. Lu, J. Hartono, M. Senitko, and J. Chen, "The inflammatory response to ischemic acute kidney injury: a result of the 'right stuff' in the 'wrong place'?" *Current Opinion in Nephrology and Hypertension*, vol. 16, no. 2, pp. 83–89, 2007.

[37] G. Ramesh and W. Brian Reeves, "TNF-α mediates chemokine and cytokine expression and renal injury in cisplatin nephrotoxicity," *The Journal of Clinical Investigation*, vol. 110, no. 6, pp. 835–842, 2002.

[38] G. Ramesh, B. Zhang, S. Uematsu, S. Akira, and W. B. Reeves, "Endotoxin and cisplatin synergistically induce renal dysfunction and cytokine production in mice," *American Journal of Physiology—Renal Physiology*, vol. 293, no. 1, pp. F325–F332, 2007.

[39] B. Zhang, G. Ramesh, C. C. Norbury, and W. B. Reeves, "Cisplatin-induced nephrotoxicity is mediated by tumor necrosis factor-α produced by renal parenchymal cells," *Kidney International*, vol. 72, no. 1, pp. 37–44, 2007.

[40] Z. Dong and S. S. Atherton, "Tumor necrosis factor-α in cisplatin nephrotoxicity: a homebred foe?" *Kidney International*, vol. 72, no. 1, pp. 5–7, 2007.

[41] G. Ramesh and W. B. Reeves, "TNFR2-mediated apoptosis and necrosis in cisplatin-induced acute renal failure," *American Journal of Physiology—Renal Physiology*, vol. 285, no. 4, pp. F610–F618, 2003.

[42] P. D. Sánchez-González, F. J. López-Hernández, J. M. López-Novoa, and A. I. Morales, "An integrative view of the pathophysiological events leading to cisplatin nephrotoxicity," *Critical Reviews in Toxicology*, vol. 41, no. 10, pp. 803–821, 2011.

[43] K. Tsuruya, T. Ninomiya, M. Tokumoto et al., "Direct involvement of the receptor-mediated apoptotic pathways in cisplatin-induced renal tubular cell death," *Kidney International*, vol. 63, no. 1, pp. 72–82, 2003.

[44] E. Abraham, "Nuclear factor-κB and its role in sepsis-associated organ failure," *Journal of Infectious Diseases*, vol. 187, supplement 2, pp. S364–S369, 2003.

[45] G. Ramesh and W. B. Reeves, "p38 MAP kinase inhibition ameliorates cisplatin nephrotoxicity in mice," *American Journal of Physiology—Renal Physiology*, vol. 289, no. 1, pp. F166–F174, 2005.

[46] T. Yamakawa, S. Eguchi, T. Matsumoto et al., "Intracellular signaling in rat cultured vascular smooth muscle cells: roles of nuclear factor-κB and p38 mitogen-activated protein kinase on tumor necrosis factor-α production," *Endocrinology*, vol. 140, no. 8, pp. 3562–3572, 1999.

[47] R. Medzhitov and C. A. Janeway Jr., "Decoding the patterns of self and nonself by the innate immune system," *Science*, vol. 296, no. 5566, pp. 298–300, 2002.

[48] H. Kono and K. L. Rock, "How dying cells alert the immune system to danger," *Nature Reviews Immunology*, vol. 8, no. 4, pp. 279–289, 2008.

[49] D. U. Ferreiro and E. A. Komives, "Molecular mechanisms of system control of NF-κB signaling by IκBα," *Biochemistry*, vol. 49, no. 8, pp. 1560–1567, 2010.

[50] B. Zhang, G. Ramesh, S. Uematsu, S. Akira, and W. B. Reeves, "TLR4 signaling mediates inflammation and tissue injury in nephrotoxicity," *Journal of the American Society of Nephrology*, vol. 19, no. 5, pp. 923–932, 2008.

[51] G. Ramesh, S. R. Kimball, L. S. Jefferson, and W. B. Reeves, "Endotoxin and cisplatin synergistically stimulate TNF-α production by renal epithelial cells," *American Journal of Physiology—Renal Physiology*, vol. 292, no. 2, pp. F812–F819, 2007.

[52] A. F. McGettrick and L. A. J. O'Neill, "The expanding family of MyD88-like adaptors in Toll-like receptor signal transduction," *Molecular Immunology*, vol. 41, no. 6-7, pp. 577–582, 2004.

[53] A. Tsung, J. R. Klune, X. Zhang et al., "HMGB1 release induced by liver ischemia involves Toll-like receptor 4–dependent reactive oxygen species production and calcium-mediated signaling," *Journal of Experimental Medicine*, vol. 204, no. 12, pp. 2913–2923, 2007.

[54] R. H. Houtkooper, C. Cantó, R. J. Wanders, and J. Auwerx, "The secret life of NAD^+: an old metabolite controlling new metabolic signaling pathways," *Endocrine Reviews*, vol. 31, no. 2, pp. 194–223, 2010.

[55] C. A. Elvehjem, R. J. Madden, F. M. Strong, and D. W. Wolley, "The isolation and identification of the anti-black tongue factor. 1937," *The Journal of Biological Chemistry*, vol. 277, no. 34, article e22, 2002.

[56] W. Ying, "NAD+/NADH and NADP+/NADPH in cellular functions and cell death: regulation and biological consequences," *Antioxidants & Redox Signaling*, vol. 10, no. 2, pp. 179–206, 2008.

[57] P. Belenky, K. L. Bogan, and C. Brenner, "NAD^+ metabolism in health and disease," *Trends in Biochemical Sciences*, vol. 32, no. 1, pp. 12–19, 2007.

[58] N. Dali-Youcef, M. Lagouge, S. Froelich, C. Koehl, K. Schoonjans, and J. Auwerx, "Sirtuins: the 'magnificent seven', function, metabolism and longevity," *Annals of Medicine*, vol. 39, no. 5, pp. 335–345, 2007.

[59] E. Michishita, J. Y. Park, J. M. Burneskis, J. C. Barrett, and I. Horikawa, "Evolutionarily conserved and nonconserved cellular localizations and functions of human SIRT proteins," *Molecular Biology of the Cell*, vol. 16, no. 10, pp. 4623–4635, 2005.

[60] B. J. North, B. L. Marshall, M. T. Borra, J. M. Denu, and E. Verdin, "The human Sir2 ortholog, SIRT2, is an NAD^+-dependent tubulin deacetylase," *Molecular Cell*, vol. 11, no. 2, pp. 437–444, 2003.

[61] H. Vaziri, S. K. Dessain, E. Ng Eaton et al., "hSIR2(SIRT1) functions as an NAD-dependent p53 deacetylase," *Cell*, vol. 107, pp. 149–159, 2001.

[62] M. C. Haigis, R. Mostoslavsky, K. M. Haigis et al., "SIRT4 inhibits glutamate dehydrogenase and opposes the effects of calorie restriction in pancreatic β cells," *Cell*, vol. 126, no. 5, pp. 941–954, 2006.

[63] G. Liszt, E. Ford, M. Kurtev, and L. Guarente, "Mouse Sir2 homolog SIRT6 is a nuclear ADP-ribosyltransferase," *The Journal of Biological Chemistry*, vol. 280, no. 22, pp. 21313–21320, 2005.

[64] S. Imai, F. B. Johnson, R. A. Marciniak, M. McVey, P. U. Park, and L. Guarante, "Sir2: an NAD-dependent histone deacetylase that connects chromatin silencing, metabolism, and aging," *Cold Spring Harbor Symposia on Quantitative Biology*, vol. 65, pp. 297–302, 2000.

[65] K. Hasegawa, S. Wakino, K. Yoshioka et al., "Sirt1 protects against oxidative stress-induced renal tubular cell apoptosis by the bidirectional regulation of catalase expression," *Biochemical and Biophysical Research Communications*, vol. 372, no. 1, pp. 51–56, 2008.

[66] K. Hasegawa, S. Wakino, K. Yoshioka et al., "Kidney-specific overexpression of Sirt1 protects against acute kidney injury by retaining peroxisome function," *The Journal of Biological Chemistry*, vol. 285, no. 17, pp. 13045–13056, 2010.

[67] D. H. Kim, Y. J. Jung, J. E. Lee et al., "Sirt1 activation by resveratrol ameliorates cisplatin-induced renal injury through

deacetylation of p53," *American Journal of Physiology—Renal Physiology*, vol. 301, no. 2, pp. F427–F435, 2011.

[68] M. Neumann and M. Naumann, "Beyond IκBs: alternative regulation of NF-κB activity," *The FASEB Journal*, vol. 21, no. 11, pp. 2642–2654, 2007.

[69] F. Yeung, J. E. Hoberg, C. S. Ramsey et al., "Modulation of NF-κB-dependent transcription and cell survival by the SIRT1 deacetylase," *The EMBO Journal*, vol. 23, no. 12, pp. 2369–2380, 2004.

[70] T. Yoshizaki, J. C. Milne, T. Imamura et al., "SIRT1 exerts anti-inflammatory effects and improves insulin sensitivity in adipocytes," *Molecular and Cellular Biology*, vol. 29, no. 5, pp. 1363–1374, 2009.

[71] A. J. Levine and M. Oren, "The first 30 years of p53: growing ever more complex," *Nature Reviews Cancer*, vol. 9, no. 10, pp. 749–758, 2009.

[72] J.-P. Kruse and W. Gu, "Modes of p53 regulation," *Cell*, vol. 137, no. 4, pp. 609–622, 2009.

[73] Y. Tang, W. Zhao, Y. Chen, Y. Zhao, and W. Gu, "Acetylation is indispensable for p53 activation," *Cell*, vol. 133, no. 4, pp. 612–626, 2008.

[74] C. L. Brooks and W. Gu, "The impact of acetylation and deacetylation on the p53 pathway," *Protein and Cell*, vol. 2, no. 6, pp. 456–462, 2011.

[75] S. Li, M. Banck, S. Mujtaba, M.-M. Zhou, M. M. Sugrue, and M. J. Walsh, "p53-Induced growth arrest is regulated by the mitochondrial SirT3 deacetylase," *PLoS ONE*, vol. 5, no. 5, Article ID e10486, 2010.

[76] W. Gu and R. G. Roeder, "Activation of p53 sequence-specific DNA binding by acetylation of the p53 C-terminal domain," *Cell*, vol. 90, no. 4, pp. 595–606, 1997.

[77] Y. Zhao, S. Lu, L. Wu et al., "Acetylation of p53 at lysine 373/382 by the histone deacetylase inhibitor depsipeptide induces expression of $p21^{Waf1/Cip1}$," *Molecular and Cellular Biology*, vol. 26, no. 7, pp. 2782–2790, 2006.

[78] A. Kotsinas, V. Aggarwal, E.-J. Tan, B. Levy, and V. G. Gorgoulis, "PIG3: a novel link between oxidative stress and DNA damage response in cancer," *Cancer Letters*, vol. 327, no. 1-2, pp. 97–102, 2012.

[79] J. D. Amaral, J. M. Xavier, C. J. Steer, and C. M. P. Rodrigues, "Targeting the p53 pathway of apoptosis," *Current Pharmaceutical Design*, vol. 16, no. 22, pp. 2493–2503, 2010.

[80] A. V. Vaseva and U. M. Moll, "The mitochondrial p53 pathway," *Biochimica et Biophysica Acta (BBA)—Bioenergetics*, vol. 1787, no. 5, pp. 414–420, 2009.

[81] L. Mouchiroud, R. H. Houtkooper, and J. Auwerx, "NAD^+ metabolism: a therapeutic target for age-related metabolic disease," *Critical Reviews in Biochemistry and Molecular Biology*, vol. 48, no. 4, pp. 397–408, 2013.

[82] R. Krishnakumar and W. L. Kraus, "The PARP side of the nucleus: molecular actions, physiological outcomes, and clinical targets," *Molecular Cell*, vol. 39, no. 1, pp. 8–24, 2010.

[83] C. Thomas and A. V. Tulin, "Poly-ADP-ribose polymerase: machinery for nuclear processes," *Molecular Aspects of Medicine*, vol. 34, no. 6, pp. 1124–1137, 2013.

[84] P. M. Goodwin, P. J. Lewis, M. I. Davies, C. J. Skidmore, and S. Shall, "The effect of gamma radiation and neocarzinostatin of NAD and ATP levels in mouse leukaemia cells," *Biochimica et Biophysica Acta (BBA)—General Subjects*, vol. 543, no. 4, pp. 576–582, 1978.

[85] C. J. Skidmore, M. I. Davies, P. M. Goodwin et al., "The involvement of poly(ADP-ribose) polymerase in the degradation of NAD caused by gamma-radiation and N-methyl-N-nitrosourea," *European Journal of Biochemistry*, vol. 101, no. 1, pp. 135–142, 1979.

[86] C. Cantó and J. Auwerx, "NAD^+ as a signaling molecule modulating metabolism," *Cold Spring Harbor Symposia on Quantitative Biology*, vol. 76, pp. 291–298, 2011.

[87] V. Launay-Vacher, J.-B. Rey, C. Isnard-Bagnis, G. Deray, and M. Daouphars, "Prevention of cisplatin nephrotoxicity: state of the art and recommendations from the European Society of Clinical Pharmacy Special Interest Group on Cancer Care," *Cancer Chemotherapy and Pharmacology*, vol. 61, no. 6, pp. 903–909, 2008.

[88] G. Losonczy, C. Máthé, V. Müller, K. Szondy, and J. Moldvay, "Incidence, risk factors and prevention of cisplatin-induced nephrotoxicity in patients with lung cancer," *Magyar Onkologia*, vol. 54, no. 4, pp. 289–296, 2010.

[89] T. Araki, Y. Sasaki, and J. Milbrandt, "Increased nuclear NAD biosynthesis and SIRT1 activation prevent axonal degeneration," *Science*, vol. 305, no. 5686, pp. 1010–1013, 2004.

[90] W. Ying, G. Wei, D. Wang et al., "Intranasal administration with NAD^+ profoundly decreases brain injury in a rat model of transient focal ischemia," *Frontiers in Bioscience*, vol. 12, no. 7, pp. 2728–2734, 2007.

[91] V. B. Pillai, N. R. Sundaresan, G. Kim et al., "Exogenous NAD blocks cardiac hypertrophic response via activation of the SIRT3-LKB1-AMP-activated kinase pathway," *The Journal of Biological Chemistry*, vol. 285, no. 5, pp. 3133–3144, 2010.

[92] P. Bai, C. Cantó, H. Oudart et al., "PARP-1 inhibition increases mitochondrial metabolism through SIRT1 activation," *Cell Metabolism*, vol. 13, no. 4, pp. 461–468, 2011.

[93] I. A. Ayoub, E. Jian Lee, C. S. Ogilvy, M. F. Beal, and K. I. Maynard, "Nicotinamide reduces infarction up to two hours after the onset of permanent focal cerebral ischemia in Wistar rats," *Neuroscience Letters*, vol. 259, no. 1, pp. 21–24, 1999.

[94] I. A. Ayoub and K. I. Maynard, "Therapeutic window for nicotinamide following transient focal cerebral ischemia," *NeuroReport*, vol. 13, no. 2, pp. 213–216, 2002.

[95] K. L. Brewer and J. S. Hardin, "Neuroprotective effects of nicotinamide after experimental spinal cord injury," *Academic Emergency Medicine*, vol. 11, no. 2, pp. 125–130, 2004.

[96] S. Kaneko, J. Wang, M. Kaneko et al., "Protecting axonal degeneration by increasing nicotinamide adenine dinucleotide levels in experimental autoimmune encephalomyelitis models," *Journal of Neuroscience*, vol. 26, no. 38, pp. 9794–9804, 2006.

[97] A. A. Sauve, "NAD^+ and vitamin B_3: from metabolism to therapies," *The Journal of Pharmacology and Experimental Therapeutics*, vol. 324, no. 3, pp. 883–893, 2008.

[98] W. Ying, P. Garnier, and R. A. Swanson, "NAD^+ repletion prevents PARP-1-induced glycolytic blockade and cell death in cultured mouse astrocytes," *Biochemical and Biophysical Research Communications*, vol. 308, no. 4, pp. 809–813, 2003.

[99] W. Ying, C. C. Alano, P. Garnier, and R. A. Swanson, "NAD+ as a metabolic link between DNA damage and cell death," *Journal of Neuroscience Research*, vol. 79, no. 1-2, pp. 216–223, 2005.

[100] A. Gaikwad, D. J. Long II, J. L. Stringer, and A. K. Jaiswal, "*In vivo* role of NAD(P)H:Quinone Oxidoreductase 1 (NQO1) in the regulation of intracellular redox state and accumulation of abdominal adipose tissue," *The Journal of Biological Chemistry*, vol. 276, pp. 22559–22564, 2001.

[101] D. Ross, J. K. Kepa, S. L. Winski, H. D. Beall, A. Anwar, and D. Siegel, "NAD(P)H:quinone oxidoreductase 1 (NQO1): chemoprotection, bioactivation, gene regulation and genetic polymorphisms," *Chemico-Biological Interactions*, vol. 129, no. 1-2, pp. 77–97, 2000.

[102] M. Gao, A. Singh, K. Macri et al., "Antioxidant components of naturally-occurring oils exhibit marked anti-inflammatory activity in epithelial cells of the human upper respiratory system," *Respiratory Research*, vol. 12, article 92, 2011.

[103] D. K. Gessner, R. Ringseis, M. Siebers et al., "Inhibition of the pro-inflammatory NF-κB pathway by a grape seed and grape marc meal extract in intestinal epithelial cells," *Journal of Animal Physiology and Animal Nutrition*, vol. 96, no. 6, pp. 1074–1083, 2012.

[104] R. Pazdro and J. R. Burgess, "The antioxidant 3H-1,2-dithiole-3-thione potentiates advanced glycation end-product-induced oxidative stress in SH-SY5Y cells," *Experimental Diabetes Research*, vol. 2012, Article ID 137607, 8 pages, 2012.

[105] C. I. Jones III, H. Zhu, S. F. Martin, Z. Han, Y. Li, and B. R. Alevriadou, "Regulation of antioxidants and phase 2 enzymes by shear-induced reactive oxygen species in endothelial cells," *Annals of Biomedical Engineering*, vol. 35, no. 5, pp. 683–693, 2007.

[106] O. Moscovitz, P. Tsvetkov, N. Hazan et al., "A mutually inhibitory feedback loop between the 20S proteasome and its regulator, NQO1," *Molecular Cell*, vol. 47, no. 1, pp. 76–86, 2012.

[107] R. H. Haefeli, M. Erb, A. C. Gemperli et al., "NQo1-dependent redox cycling of idebenone: effects on cellular redox potential and energy levels," *PLoS ONE*, vol. 6, no. 3, Article ID e17963, 2011.

[108] X. Huang, Y. Dong, E. A. Bey et al., "An NQO1 substrate with potent antitumor activity that selectively kills by PARP1-induced programmed necrosis," *Cancer Research*, vol. 72, no. 12, pp. 3038–3047, 2012.

[109] A. B. Pardee, Y. Z. Li, and C. J. Li, "Cancer therapy with β-lapachone," *Current Cancer Drug Targets*, vol. 2, no. 3, pp. 227–242, 2002.

[110] L. S. Li, E. A. Bey, Y. Dong et al., "Modulating endogenous NQO1 levels identifies key regulatory mechanisms of action of β-lapachone for pancreatic cancer therapy," *Clinical Cancer Research*, vol. 17, no. 2, pp. 275–285, 2011.

[111] S. M. Planchon, S. Wuerzberger, B. Frydman et al., "β-Lapachone-mediated apoptosis in human promyelocytic leukemia (HL-60) and human prostate cancer cells: a p53-independent response," *Cancer Research*, vol. 55, no. 17, pp. 3706–3711, 1995.

[112] J. H. Hwang, D. W. Kim, E. J. Jo et al., "Pharmacological stimulation of NADH oxidation ameliorates obesity and related phenotypes in mice," *Diabetes*, vol. 58, no. 4, pp. 965–974, 2009.

[113] Y.-H. Kim, J. H. Hwang, J.-R. Noh et al., "Activation of NAD(P)H:quinone oxidoreductase ameliorates spontaneous hypertension in an animal model via modulation of eNOS activity," *Cardiovascular Research*, vol. 91, no. 3, pp. 519–527, 2011.

[114] S.-Y. Kim, N. H. Jeoung, C. J. Oh et al., "Activation of NAD(P)H:quinone oxidoreductase 1 prevents arterial restenosis by suppressing vascular smooth muscle cell proliferation," *Circulation Research*, vol. 104, no. 7, pp. 842–850, 2009.

Hindawi Publishing Corporation
BioMed Research International
Volume 2015, Article ID 867140, 10 pages
http://dx.doi.org/10.1155/2015/867140

Research Article

Tanshinone IIA Attenuates Renal Fibrosis after Acute Kidney Injury in a Mouse Model through Inhibition of Fibrocytes Recruitment

Chunming Jiang,[1] Qiuyuan Shao,[1] Bo Jin,[1] Rujun Gong,[2] Miao Zhang,[1] and Biao Xu[3]

[1]*Department of Nephrology, Affiliated Nanjing Drum Tower Hospital, Medical School of Nanjing University, Nanjing 21008, China*
[2]*Department of Medicine, Rhode Island Hospital, Brown University School of Medicine, Providence, RI 02903, USA*
[3]*Department of Cardiology, Affiliated Nanjing Drum Tower Hospital, Medical School of Nanjing University, Nanjing 21008, China*

Correspondence should be addressed to Biao Xu; xubiao@medmail.com.cn

Received 9 October 2015; Accepted 1 December 2015

Academic Editor: Jeremiah R. Brown

Acute kidney injury (AKI) is associated with an increased risk of developing advanced chronic kidney disease (CKD). Yet, effective interventions to prevent this conversion are unavailable for clinical practice. In this study, we examined the beneficial effects of Tanshinone IIA on renal fibrosis in a mouse model of folic acid induced AKI. We found that Tanshinone IIA treatment significantly attenuated the folic acid elicited kidney dysfunction on days 3, 14, and 28. This effect was concomitant with a much lessened accumulation of fibronectin and collagen in tubulointerstitium 28 days after folic acid injury, denoting an ameliorated renal fibrosis. The kidney protective and antifibrotic effect of Tanshinone IIA was likely attributable to an early inhibition of renal recruitment of fibrocytes positive for both CD45 and collagen I. Mechanistically, Tanshinone IIA treatment not only markedly diminished renal expression of chemoattractants for fibrocytes such as TGFβ1 and MCP-1, but also significantly reduced circulating fibrocytes at the acute phase of kidney injury. These data suggested that Tanshinone IIA might be a novel therapy for preventing progression of CKD after AKI.

1. Introduction

Acute kidney injury (AKI) is a severe and common disease found in clinical practice. Recent data demonstrated that AKI occurs in about 3.2–9.6% of hospital admissions with overall mortality around 20% [1, 2]. Notably, AKI has been projected to be more prevalent around the world in the future due to the increasing incidence of hypertension, diabetes mellitus, caloric nutritional overload, and aging [3]. By far, a growing body of evidence has shown a close connection between AKI and subsequent chronic kidney disease (CKD), which substantially increases the long-term morbidity and mortality of AKI [4, 5]. Because effective treatments for AKI are unavailable to date except for supportive measures, it is imperative to develop a new therapeutic strategy to prevent AKI to CKD transition [6].

Enormous efforts have been dedicated to the understanding of the underlying pathophysiology of AKI; nevertheless, the exact mechanism contributing to AKI to CKD transition has not been fully elucidated. Collagen-producing hematopoietic cells (fibrocytes), first reported in 1994 by Bucala et al., possess both characteristics of fibroblasts (expression of collagen type I) and hematopoietic cells (expression of CD45) [7]. Recent evidence indicates that fibrocytes play an important role in promoting tissue fibrosis in various diseases including CKD [8–11]. During the process of tissue injury, fibrocytes have been found to undergo a rapid proliferation in the bone marrow and then were released into the peripheral circulation and finally recruited into the injury sites. It is well recognized that the migration of fibrocytes is mainly determined by chemoattractants due to their high expression of chemokine receptors and quick presentation

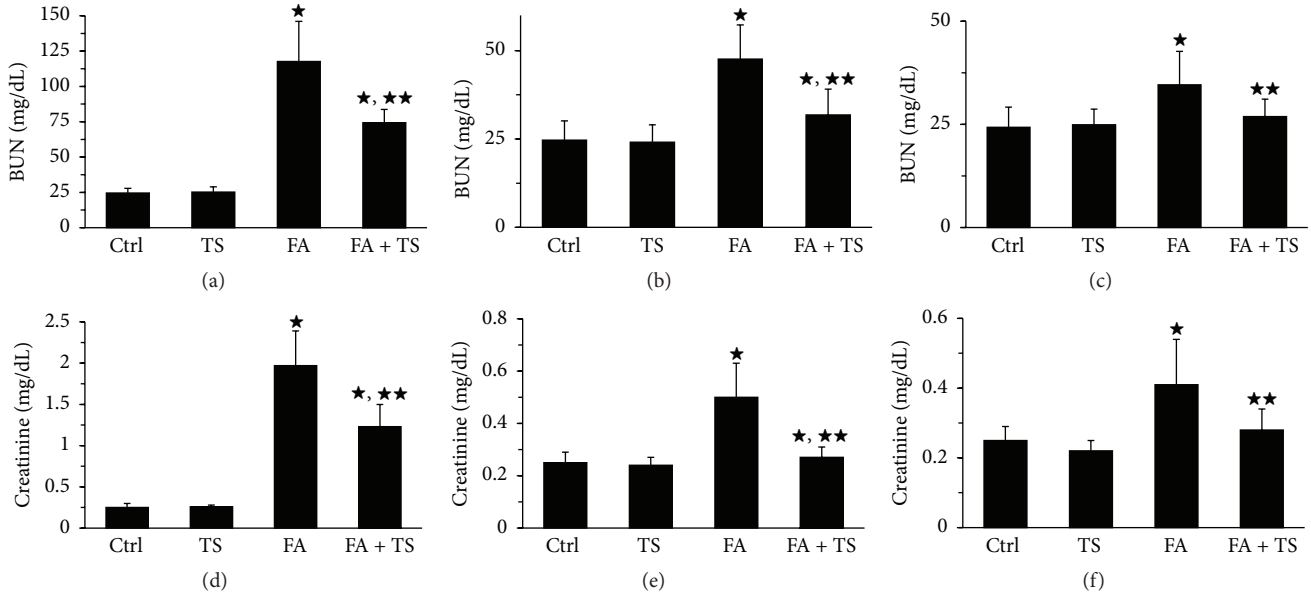

Figure 1: Tanshinone IIA ameliorates renal dysfunction in mice with folic acid induced acute kidney injury. Graphs show the time course of BUN and serum creatinine levels at day 3 (a, d), day 14 (b, e), and day 28 (c, f) among different groups ($n = 9$). Data are expressed as the mean ± SEM. $^{\star}P < 0.01$ versus group TS; $^{\star\star}P < 0.01$ versus group FA. Notes: blood urea nitrogen (BUN). Ctrl: mice treated with vehicle alone; TS: mice treated with Tanshinone IIA alone; FA: folic acid-treated mice followed by vehicle treatment; FA + TS: folic acid-treated mice subjected to Tanshinone IIA injection for 3 consecutive days.

in the inflammatory areas after injury. Up to now, several chemoattractants, such as transforming growth factor-beta (TGF-β), chemokines including monocyte chemotactic protein 1 (MCP-1), and lipopolysaccharide, which mediate the recruitment of fibrocytes have been identified [12–15].

Tanshinone IIA is a diterpene extracted from *Salvia miltiorrhiza*, a popular herb that has been safely and widely used in China and other Asian countries. Previous studies have demonstrated that Tanshinone IIA exerts prominent antifibrotic effect through modulating TGF-β signaling pathway and anti-inflammatory effect through inhibiting MCP-1 expression [16–24]. Thus, we hypothesized that Tanshinone IIA might attenuate renal fibrosis after AKI via regulating recruitment of fibrocytes into the kidney through its inhibition on TGF-β and MCP-1 in a mouse model of folic acid induced kidney injury.

2. Materials and Methods

2.1. Chemicals and Reagents. Tanshinone IIA was purchased from Jiangsu Carefree Group Co. (Nanjing, China). The structure of Tanshinone IIA is shown in Figure 1. Antibodies against fibronectin (ab2413), collagen I (ab34710), CD45 (ab25386), TGF-β1 (ab66043), and MCP-1 (ab25124) were obtained from Abcam, USA. Antibody against GAPDH (sc-48166) was obtained from Santa Cruz Biotechnology, USA. Both FITC- and HRP-conjugated secondary antibodies were purchased from Invitrogen, USA. ImmPRESS peroxidase polymer detection kits, DAB substrate (SK-4100), and Vectashield mounting medium with DAPI (H-1200) were obtained from Vector Laboratories, USA. BUN and creatinine assay kits were obtained from BioVision, USA. Hydroxyproline Assay Kit (MAK008), collagenase IV, and DNase I were purchased from Sigma, USA.

2.2. Animals. C57BL/6 mice weighing 180–220 g were obtained from Nanjing University Model Animal Research Center (Nanjing, China). The animals were housed in the animal facility of Nanjing University Model Animal Research Center with free access to food and water. The Institutional Animal Care and Use Committee at Drum Tower Hospital, the Affiliated Hospital of Nanjing University Medical School, approved all the animal protocols. The experiments were performed in accordance with the National Institutes of Health Guidelines on the Use of Laboratory Animals.

2.3. Experimental Procedures. C57BL/6 mice were randomly assigned to one of the four groups. In group Ctrl ($n = 18$), mice received 150 μL saline with 0.02% DMSO by tail vein injection; in group TS ($n = 18$), mice received Tanshinone IIA (15 mg/kg, dissolved in 150 μL saline with 0.02% DMSO) by tail vein injection; in group FA ($n = 18$), mice were injured with a single dose of folic acid (250 mg/kg, dissolved in 150 μL sodium bicarbonate) by intraperitoneal injection and treated with 150 μL saline with 0.02% DMSO by tail vein injection immediately after and on 2 other consecutive days following folic acid injection; in group FA + TS ($n = 18$), mice were injured with a single dose of folic acid (250 mg/kg) by intraperitoneal injection and treated with Tanshinone IIA (15 mg/kg) by tail vein injection immediately after and on

2 other consecutive days following folic acid injection. Mice were sacrificed at day 3 ($n = 9$ per group) or 28 ($n = 9$ per group) and kidney specimens were collected for further examinations. Blood samples were collected at days 3, 14, and 28 for detection of BUN and creatinine levels.

2.4. Renal Histopathology. Formalin-fixed kidneys were embedded in paraffin and prepared in 3 μm thick sections. Sections were stained with Masson's trichrome to evaluate collagen deposition in the kidney. One observer performed semiquantitative morphometric analysis in a blinded manner. Fibrosis score was accessed using semiquantitative measurements according to the proportion relative to the total section area and classified as follows: 0 (nil), 1 (<25%), 2 (25–50%), 3 (50–75%), and 4 (>75% of interstitium).

For immunostaining formalin-fixed sections, 3 μm thick kidney sections were deparaffinized and rehydrated. After microwave antigen retrieval, sections were H_2O_2 quenched and blocked in 3% BSA at room temperature. Tissues were incubated overnight with antibodies against TGF-β1 at 1 : 400, MCP-1 at 1 : 200 dilution at 4°C. ImmPRESS peroxidase polymer detection kits were used to conjugate secondary antibody for 60 minutes at room temperature. Slides were finally developed with DAB substrate. Negative controls were obtained by replacing the primary antibody with normal rabbit serum. The positive signal of TGF-β1 and MCP-1 staining was calculated with Image-Pro Plus 6.0 software (Media Cybernetics, Bethesda, MD). Each score was determined by five random fields per section and five sections per kidney.

Frozen tissue samples were cut into 3 μm thick sections. After fixation with 3.2% paraformaldehyde in PBS, sections were blocked for 30 minutes with 3% BSA and permeabilized with Triton X-100 for 15 minutes. Then, sections were incubated overnight at 4°C with antibodies against fibronectin at 1 : 150, CD45 at 1 : 200, or collagen I at 1 : 300 dilution; FITC-conjugated secondary antibody against various species was incubated for 60 minutes at room temperature appropriately. Finally, sections were mounted with Vectashield mounting medium with DAPI and visualized using a fluorescence microscope. The positive signal was calculated with Image-Pro Plus 6.0 software or by counting positive staining cells. Each score was determined by five random fields per section and five sections per kidney.

2.5. Measurement of Total Collagen Content in the Kidney. Hydroxyproline concentration was measured to determine the total collagen content in the kidney using the Hydroxyproline Assay Kit according to the manufacturer's instruction. In brief, half of the right kidney was homogenized using 100 μL H_2O for every 10 mg of tissue. Then, 100 μL of tissue homogenate was transferred to a pressure-tight vial; 100 μL concentrated hydrochloric acid (12 M) was added and hydrolyzed at 120°C for 3 h. Fifty μL of supernatant was transferred to a 96-well plate. Evaporate all wells to dryness under vacuum. Add 100 μL of the chloramine T/oxidation buffer mixture to each sample and standard well, incubated at room temperature for 5 minutes. Add 100 μL of the diluted DMAB reagent to each sample and standard well, incubated for 90 minutes at 60°C. Absorbance was measured at 560 nm in a microplate reader.

2.6. Western Blot Analysis. Mice cortical kidney specimens were homogenized in radioimmunoprecipitation assay buffer supplemented with protease inhibitors. Protein concentration was determined by using a bicinchoninic acid protein assay kit. Samples with equal amounts of total protein (50 μg/mL) were fractionated by 7.5–15% SDS-polyacrylamide gels under reduction. The antibodies against fibronectin, TGF-β1, MCP-1, and GAPDH were used as primary antibodies.

2.7. Measurement of Blood Urea Nitrogen (BUN) and Serum Creatinine. BUN and serum creatinine levels were measured using commercial assay kits according to the manufacturer's instruction.

2.8. Statistical Analysis. Normally distributed continuous variables are expressed as mean ± standard error. One-way analysis of variance was applied to compare the means of normally distributed continuous variables followed by multiple comparison tests as post hoc comparison. Mann-Whitney test or Kruskal-Wallis test was applied to compare the abnormally distributed continuous variables as appropriate. A value of $p < 0.05$ was considered statistically significant, and all tests were two-tailed. All statistical analyses were performed with the SPSS software application (version 17.0 for Windows: SPSS Institute, Chicago, IL, USA).

3. Result

3.1. Tanshinone IIA Treatment Improves Renal Function following Folic Acid Injury. The time-course change of renal function among different animal groups was shown in Figure 1. BUN and serum creatinine levels were markedly elevated on day 3 after folic acid injection and this was significantly lowered by concomitant Tanshinone IIA treatment (Figures 1(a) and 1(d)). Three days after folic acid injury, mice in group FA exhibited spontaneous recovery of kidney function, as shown by the decreased levels of BUN and serum creatinine on days 7 and 28. However, this recovery of kidney function was apparently incomplete, as evidenced by higher-than-normal levels of BUN and serum creatinine on day 28 in group FA (Figures 1(b), 1(c), 1(e), and 1(f)). In contrast, in mice treated with Tanshinone IIA, BUN and serum creatinine levels were almost fully restored at day 28 after folic acid exposure. These data indicate that Tanshinone IIA can effectively protect from kidney dysfunction elicited by folic acid injury.

3.2. Tanshinone IIA Ameliorates the Folic Acid Induced Kidney Fibrosis. Folic acid induced kidney injury can lead to progressive kidney fibrosis. In the present study, collagen deposition in the kidneys was assessed by Masson's trichrome staining. Folic acid insult resulted in a massive collagen deposition in renal tubulointerstitium on day 28 (Figures 2(a) and 2(b)). This was further confirmed by the detection

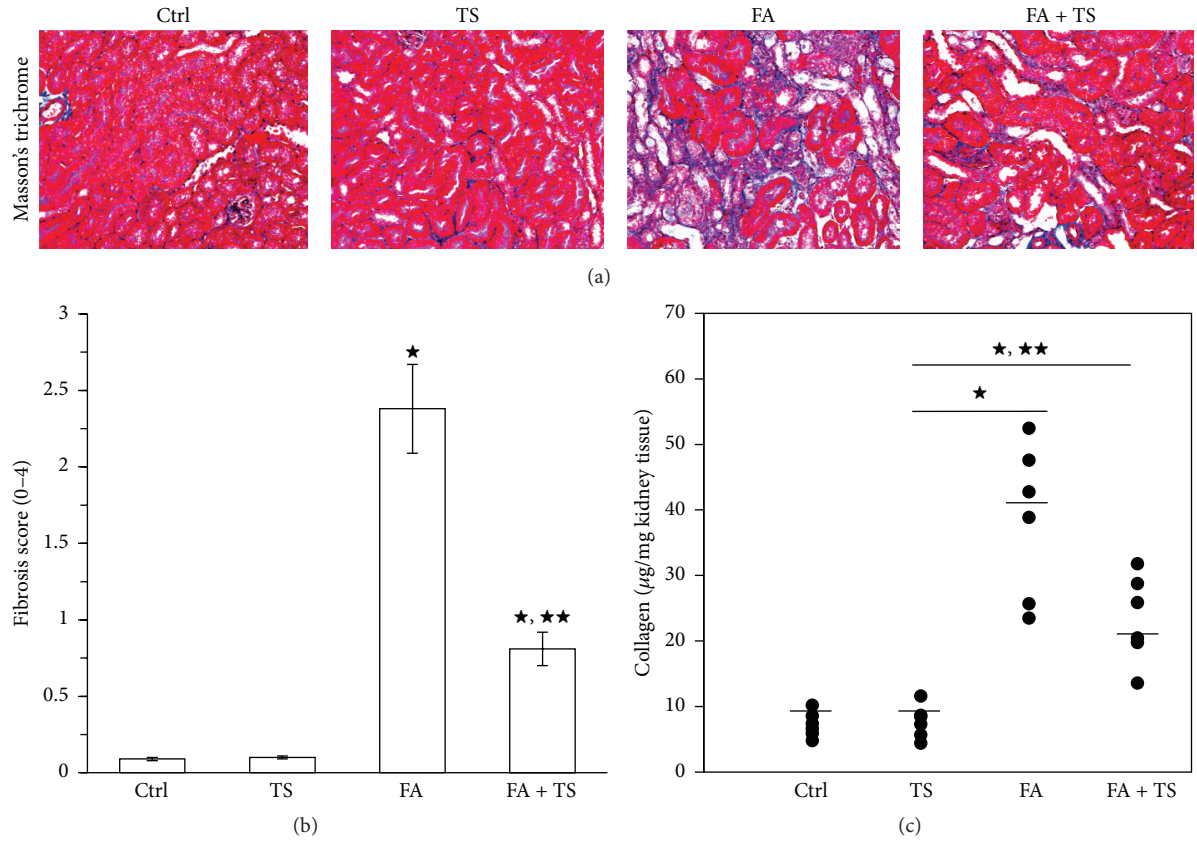

FIGURE 2: Tanshinone IIA reduces collagen deposition in the kidney 28 days after folic acid injury. (a) Representative Masson-stained sections of renal cortices at day 28 (original magnification ×200). (b) Semiquantification of kidney fibrosis score from Masson-stained sections. (c) Total kidney collagen content determined by hydroxyproline detection among different groups ($n = 6$). Data are expressed as the mean ± SEM ($n = 6$ or 9). $^{\star}P < 0.01$ versus group TS; $^{\star\star}P < 0.01$ versus group FA. Notes: Ctrl: mice treated with vehicle alone; TS: mice treated with Tanshinone IIA alone; FA: folic acid-treated mice followed by vehicle treatment; FA + TS: folic acid-treated mice subjected to Tanshinone IIA injection for 3 consecutive days.

of total collagen contents in the kidneys (Figure 2(c)). In accordance, increased accumulation of fibronectin in renal tubulointerstitium was also observed in group FA mice on day 28 (Figure 3). These fibrotic changes in the folic acid-injured kidneys were remarkably abrogated by Tanshinone IIA treatment, as shown by less collagen and fibronectin deposition in kidney sections. Collectively, these data suggest that Tanshinone IIA treatment at the early stage of AKI can improve the long-term outcome of the injured kidney by ameliorating kidney fibrosis.

3.3. Tanshinone IIA Reduces Renal Accumulation of Fibrocytes Early after Folic Acid Injury. Previously, fibrocytes have been demonstrated to contribute to kidney fibrosis after various chronic injuries. In the present study, we examined the influence of Tanshinone IIA on the accumulation of fibrocytes in folic acid-injured kidney on day 3. As shown in Figure 4, very few fibrocytes, determined by dual positive staining of CD45 and collagen I, were observed in the kidney sections from control or TS group mice. Administration of folic acid resulted in a significant increase in fibrocytes accumulation in the kidney on day 3. In contrast, treatment with Tanshinone IIA significantly decreased the numbers of fibrocytes presented in the sections. These data suggest that Tanshinone IIA attenuates folic acid induced kidney fibrosis at least partially by inhibiting accumulation of fibrocytes in the injured kidney.

3.4. Tanshinone IIA Decreases Renal Expression of TGF-β1 and MCP-1 Expression 3 Days after Folic Acid Injury. Both TGF-β1 and MCP-1 are important chemoattractants for fibrocytes and play critical roles in recruitment of fibrocytes into the injured tissues. In present study, we measured their expression by peroxidase immunohistochemistry staining and immunoblot analysis in the kidney 3 days after folic acid exposure. As shown in Figures 5(a), 5(b), 6(a), and 6(b), administration of folic acid resulted in a significant increase of TGF-β1 and MCP-1 expression in the kidney. In contrast, Tanshinone IIA treatment largely suppressed their expression. This was further confirmed by immunoblot analysis of kidney cortical lysates for TGF-β1 and MCP-1 (Figures 5(c), 5(d), 6(c), and 6(d)). These data suggest that

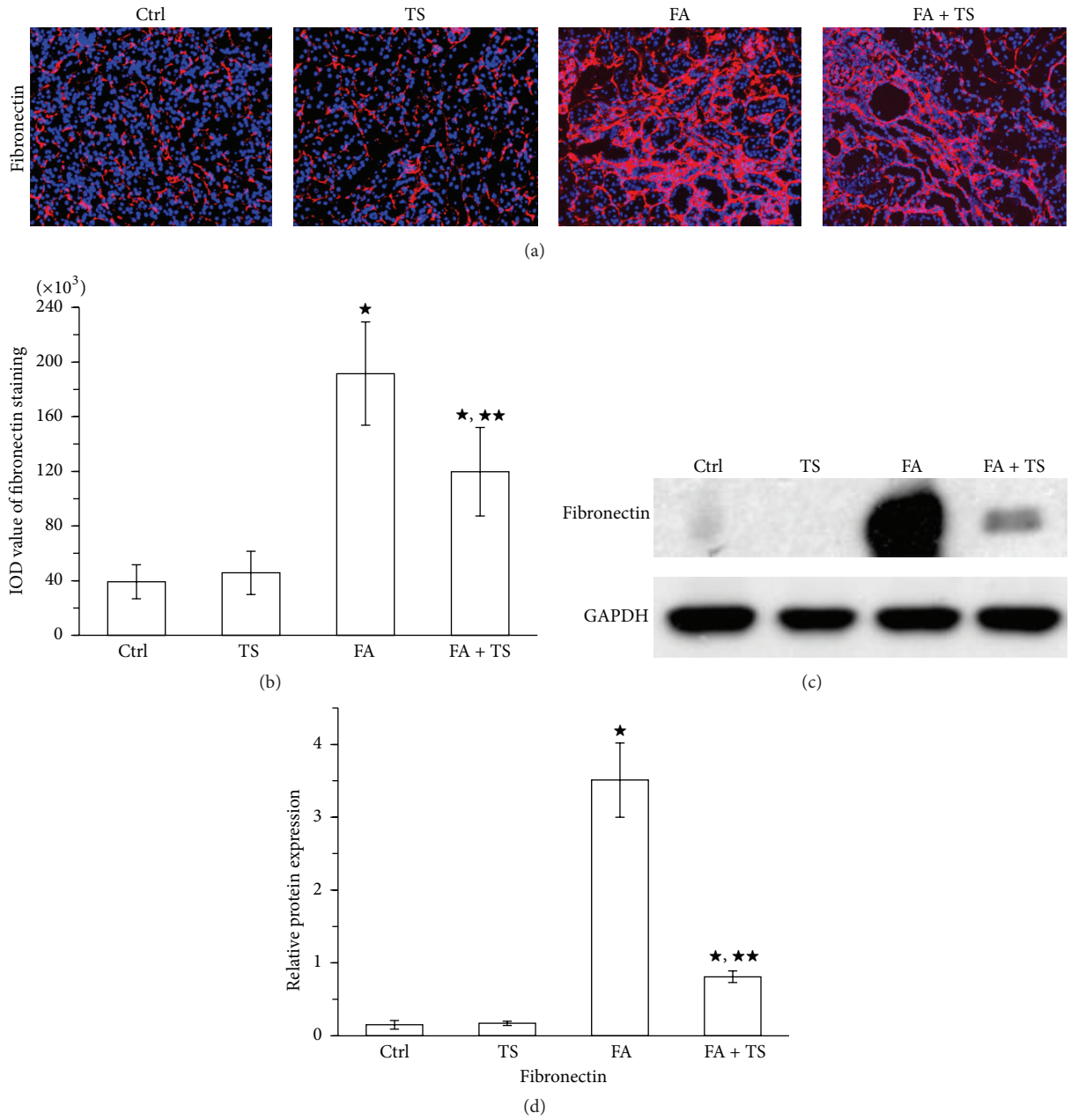

FIGURE 3: Tanshinone IIA inhibits fibronectin expression in the kidney 28 days after folic acid injury. (a) Representative images of fibronectin expression at day 28 stained by immunofluorescence (original magnification ×100). (b) Semiquantification of kidney fibronectin deposition from (a). (c) Representative immunoblots and semiquantification (d) of fibronectin in kidney cortical tissue lysates at day 28. Data are expressed as the mean ± SEM ($n = 9$). $^{\star}P < 0.01$ versus group TS; $^{\star\star}P < 0.01$ versus group FA. Notes: Ctrl: mice treated with vehicle alone; TS: mice treated with Tanshinone IIA alone; FA: folic acid-treated mice followed by vehicle treatment; FA + TS: folic acid-treated mice subjected to Tanshinone IIA injection for 3 consecutive days.

Tanshinone IIA may also reduce recruitment of fibrocytes into the kidney by inhibiting TGF-β1 and MCP-1 expression in the injured kidney.

4. Discussion

In this study, we demonstrate that Tanshinone IIA treatment exerts beneficial effects on renal fibrosis of a mouse model of folic acid induced AKI. Our results showed that the accumulation of fibrocytes in the kidney was evidently suppressed by Tanshinone IIA treatment at the early stage of AKI. The possible underlying mechanisms might be its inhibition of renal expression of TGF-β1 and MCP-1, key chemoattractants contributing to the fibrocytes recruitment into the injured kidney. These findings indicate that Tanshinone IIA is a potential agent to prevent progression of CKD after AKI.

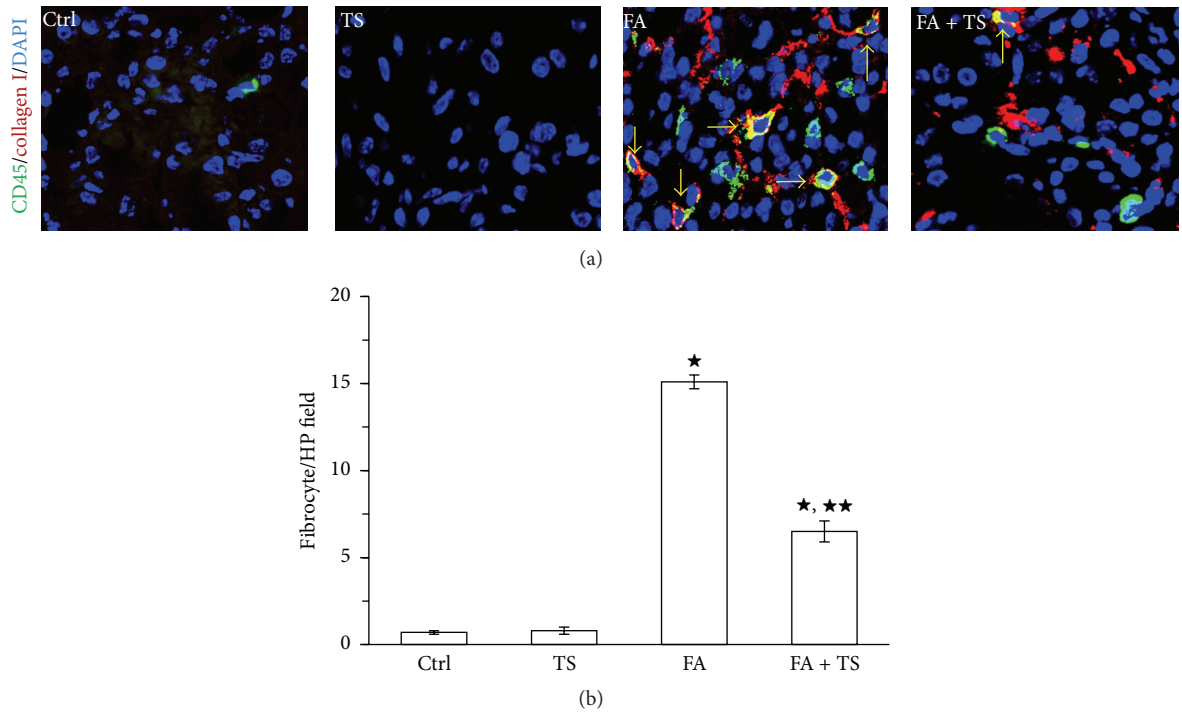

Figure 4: Tanshinone IIA inhibits recruitment of fibrocytes into the folic acid-injured kidney. (a) Representative images of fibrocytes in the kidney (yellow arrows), determined by dual staining of CD45 (green color) and collagen I (red color) in the kidney. (b) Quantification of fibrocytes in kidney sections evaluated in five random fields per section and five sections per kidney. Data are expressed as the mean ± SEM ($n = 9$). $^{\star}P < 0.01$ versus group TS; $^{\star\star}P < 0.01$ versus group FA. Notes: Ctrl: mice treated with vehicle alone; TS: mice treated with Tanshinone IIA alone; FA: folic acid-treated mice followed by vehicle treatment; FA + TS: folic acid-treated mice subjected to Tanshinone IIA injection for 3 consecutive days.

AKI is a severe disease which is increasingly prevalent around the world. Despite the fact that most AKI exhibit clinically spontaneous recovery, recent studies demonstrate that they are responsible for the development of subsequent CKD. However, effective therapies for preventing CKD after AKI are still scarce. Tanshinone IIA has been demonstrated to possess remarkable antifibrosis properties on various tissues or organs including peritoneum, heart, lung, and liver [16, 19–22, 25–27]. Notably, the effect of Tanshinone IIA on preventing renal fibrosis has also been proved. For example, Tanshinone IIA can attenuate renal fibrosis in a rat model of 5/6 nephrectomy [28]. Tanshinone IIA has also been shown to inhibit collagen deposition on a rat model of diabetic nephropathy [29]. In the present study, we explored the effect of Tanshinone IIA on preventing renal fibrosis after AKI and found that it can effectively improve kidney function and attenuate histological fibrosis 28 days after folic acid exposure. This result indicates that Tanshinone IIA is a potent agent for preventing renal fibrosis after AKI.

Despite the fact that the precise mechanisms by which renal fibrosis occurred after AKI are not clear yet, fibrocytes have attracted much attention for their role in tissue repair and fibrosis via various mechanisms. A recent study showed that the depletion of fibrocytes by diphtheria toxin resulted in a significant reduction of collagen deposition in the obstructed mice kidney [11]. In the present study, we found that Tanshinone IIA significantly reduced the accumulation of fibrocytes in the kidney 3 days after folic acid insult. This finding suggests that interception of the recruitment of fibrocytes into the injured kidney might be an important mechanism underlying the antifibrotic effects of Tanshinone IIA. To our knowledge, this is the first study to show the beneficial effects of Tanshinone IIA on preventing renal fibrosis via inhibiting accumulation of fibrocytes in the kidney.

How Tanshinone IIA intercepts renal recruitment of fibrocytes, however, is still unknown. TGF-β1 is a well-recognized growth factor that causes fibrosis. TGF-β1 can promote fibrosis by enhancing the synthesis and by suppressing the degradation of extracellular matrix. Moreover, recent studies have also demonstrated a role of TGF-β1 in chemoattracting fibrocytes into various injured organs [12, 14, 15, 30]. For example, infection of mice with TGF-β1 expressing adenoviral vector resulted in a rapid recruitment of fibrocytes to the liver [31]. Similarly, TGF-β1 also evidently triggered fibrocyte mobilization into fibrotic lungs and kidneys [12, 13]. Previous studies have clearly demonstrated that Tanshinone IIA can inhibit TGF-β1 expression in many organs including the heart, kidney, and lung [18, 32, 33]. In agreement, our recent data also revealed that Tanshinone IIA could attenuate peritoneal fibrosis by suppressing TGFβ1 expression [22]. Again, in the present study, we confirmed the effect of Tanshinone IIA on inhibiting TGF-β1 in folic acid induced kidney injury. Our data indicated the role of

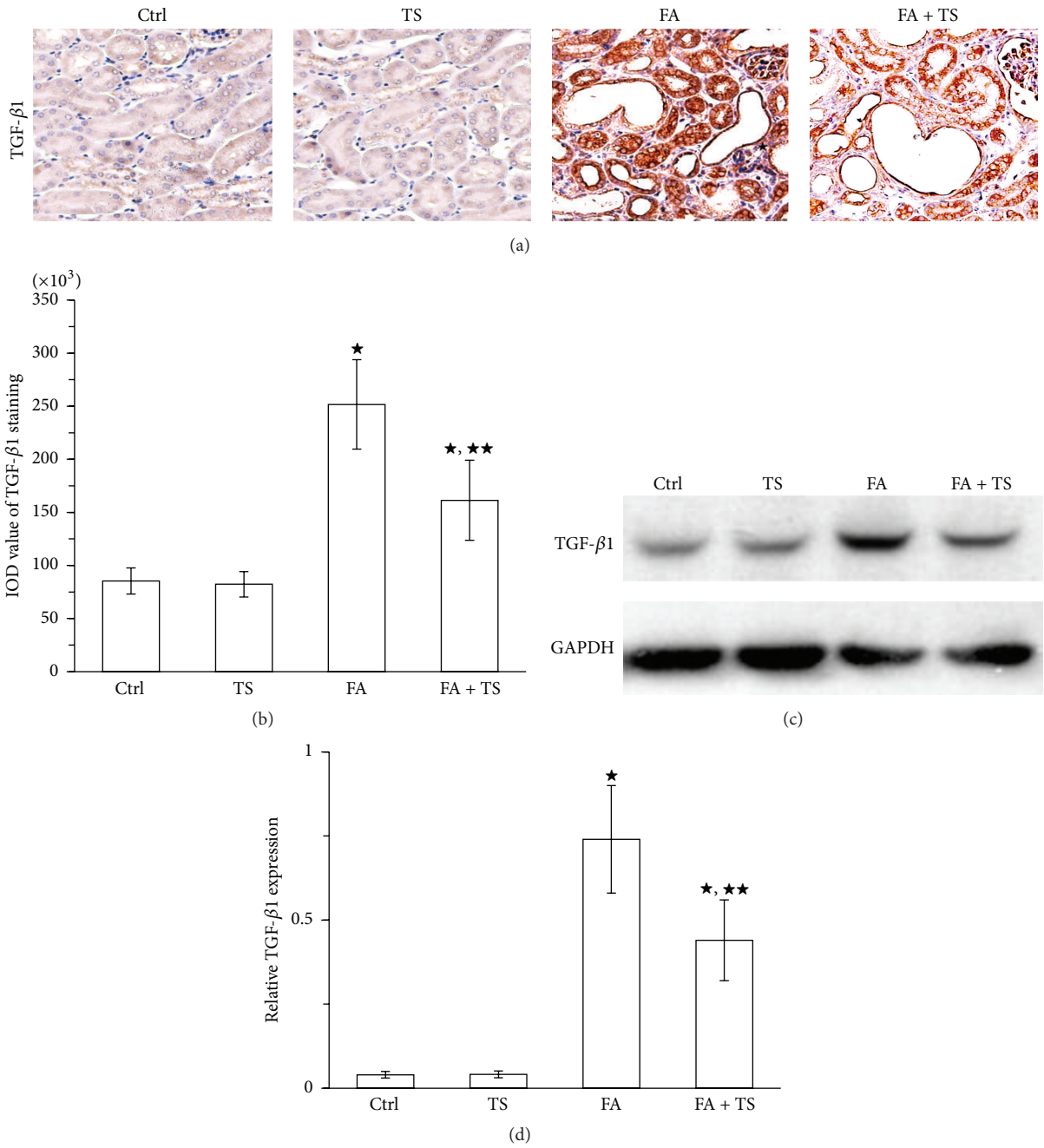

FIGURE 5: Tanshinone IIA inhibits TGF-β1 expression in folic acid-injured kidney at day 3. (a) Representative images and semiquantification (b) of TGF-β1 (original magnification ×400) stained by immunohistochemistry in the kidney sections at day 3. (c) Representative immunoblot and quantification (d) of TGF-β1 in kidney cortical tissue lysates at day 3. Data are expressed as the mean ± SEM ($n = 9$). $^{\star}P < 0.01$ versus group TS; $^{\star\star}P < 0.01$ versus group FA. Notes: transforming growth factor-beta 1 (TGF-β1); Ctrl: mice treated with vehicle alone; TS: mice treated with Tanshinone IIA alone; FA: folic acid-treated mice followed by vehicle treatment; FA + TS: folic acid-treated mice subjected to Tanshinone IIA injection for 3 consecutive days.

Tanshinone IIA in preventing recruitment of fibrocytes into the kidney by reducing TGF-β1 expression.

In addition to TGF-β1, chemokines also play important roles in mediating the homing of fibrocytes to fibrotic lesions [8, 34]. Previous studies demonstrated that MCP-1 signaling pathway regulates fibrocytes migration into the kidney and evidently contributed to the renal fibrosis [35, 36]. Recently, Tanshinone IIA has been found to reduce MCP-1 expression in various organs, including cardiac tissues subjected to myocardial infarction and kidneys after 5/6 nephrectomy or subjected to uric acid injury [24, 37]. Consistently, we demonstrated in this study that Tanshinone IIA treatment significantly attenuated MCP-1 expression in the folic acid induced kidney injury, suggesting that Tanshinone IIA may

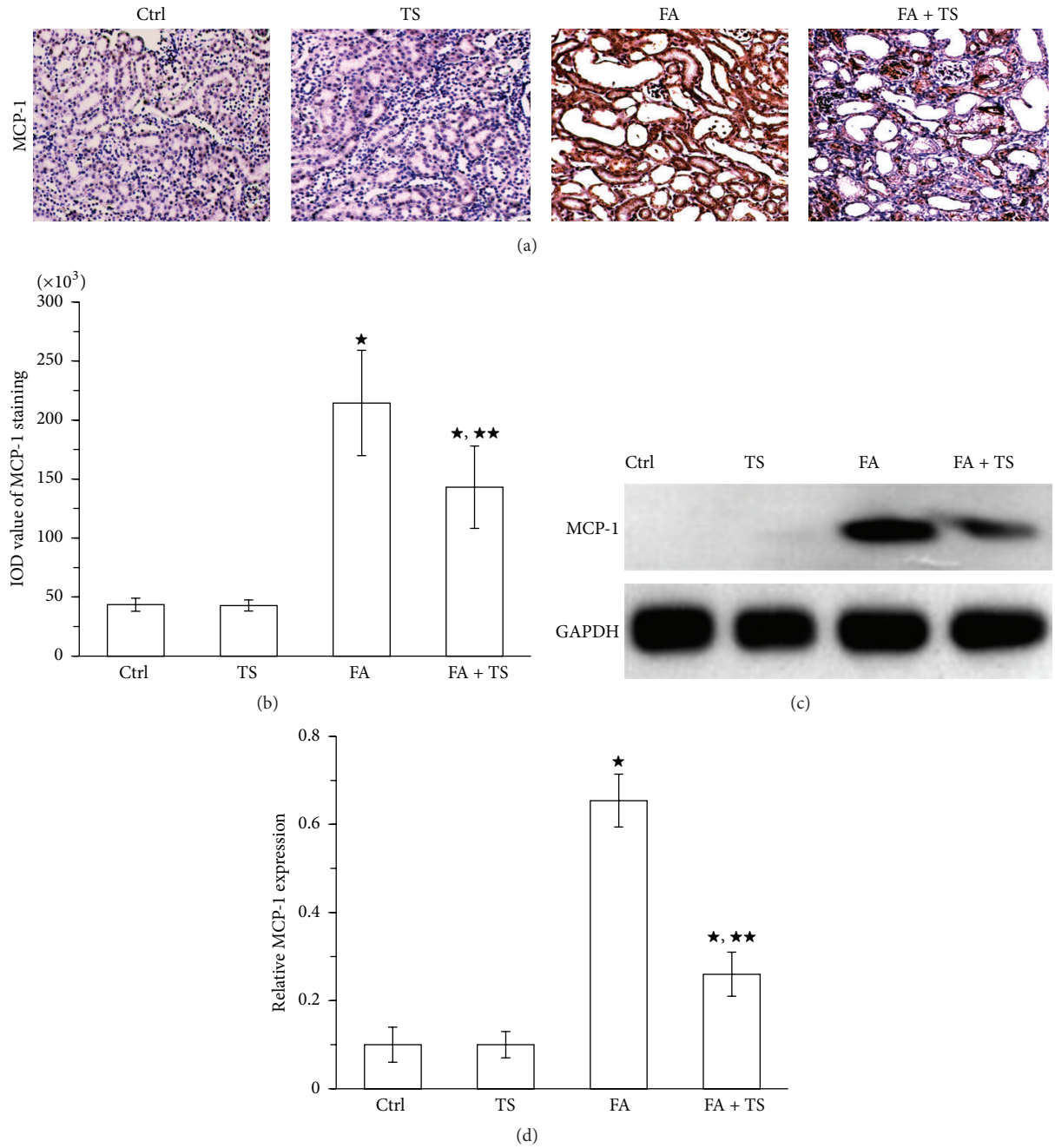

Figure 6: Tanshinone IIA inhibits MCP-1 expression in the folic acid-injured kidney at day 3. (a) Representative images and semiquantification (b) of MCP-1 (original magnification ×100) stained by immunohistochemistry in the kidney sections at day 3. (c) Representative immunoblot and quantification (d) of MCP-1 in kidney cortical tissue lysates at day 3. Data are expressed as the mean ± SEM ($n = 9$). $^{\star}P < 0.01$ versus group TS; $^{\star\star}P < 0.01$ versus group FA. Notes: monocyte chemotactic protein 1 (MCP-1); Ctrl: mice treated with vehicle alone; TS: mice treated with Tanshinone IIA alone; FA: folic acid-treated mice followed by vehicle treatment; FA + TS: folic acid-treated mice subjected to Tanshinone IIA injection for 3 consecutive days.

inhibit the migration of fibrocytes into the injured kidney by downregulating MCP-1 expression. Moreover, Tanshinone IIA was likely effective in reducing the amount of fibrocytes after kidney injury.

In addition to the above-mentioned mechanism, other potential possibilities contributing to the decrease of fibrocytes in the injured kidney by Tanshinone IIA need further study. For example, in vitro experiments are helpful to address whether Tanshinone IIA could directly modulate fibrocytes differentiation for we found that Tanshinone IIA significantly reduced circulating fibrocytes on day 3 after folic acid administration (data shown in Supplementary Material available online at http://dx.doi.org/10.1155/2015/867140). Moreover, the mechanism responsible for AKI to CKD transition is

complicated and far from being elucidated. By far, several factors including the severity of AKI, maladaptive repair of injured renal cells, and unresolved inflammation are the main suspected culprits for CKD development after AKI. As implied by other studies, Tanshinone IIA might possess activities on reducing tissue damage, promoting cell recovery, and inhibiting inflammation response during the acute phase of organ injury. Therefore, our study does not exclude other potential possibilities that could contribute to antifibrotic effect of Tanshinone IIA.

5. Conclusion

Tanshinone IIA significantly attenuated the folic acid induced kidney fibrosis by inhibiting the recruitment of fibrocytes into the kidney. This action of Tanshinone IIA is at least partially associated with its inhibitory effect on TGF-β1 and MCP-1 expression, important chemoattractants for fibrocytes recruitment into the kidney. Our findings suggest that Tanshinone IIA might be a potential agent to be applied in clinic for preventing progression of CKD after AKI. Further studies are needed to investigate its role in other models of kidney injury such as unilateral ureteral occlusion and ischemia-reperfusion injury.

Conflict of Interests

The authors declare that there is no conflict of interests regarding the publication of this paper.

Authors' Contribution

Chunming Jiang was involved in immunoblots, statistical analysis, and paper writing. Qiuyuan Shao and Bo Jin were responsible for histopathological examinations. Miao Zhang was responsible for acquisition of data and helped with the technical procedures. Rujun Gong was responsible for language editing and supplemental experiment. Biao Xu was responsible for acquisition and interpretation of data and was involved in paper revising.

Acknowledgment

This study was supported by the Key Science and Technology Development Program of Nanjing City (YKK11093).

References

[1] Y. Fang, X. Ding, Y. Zhong et al., "Acute kidney injury in a Chinese hospitalized population," *Blood Purification*, vol. 30, no. 2, pp. 120–126, 2010.

[2] J.-P. Lafrance and D. R. Miller, "Acute kidney injury associates with increased long-term mortality," *Journal of the American Society of Nephrology*, vol. 21, no. 2, pp. 345–352, 2010.

[3] P. K. T. Li, E. A. Burdmann, R. L. Mehta, and World Kidney Day Steering Committee, "Acute kidney injury: global health alert," *Kidney International*, vol. 83, no. 3, pp. 372–376, 2013.

[4] L. S. Chawla and P. L. Kimmel, "Acute kidney injury and chronic kidney disease: an integrated clinical syndrome," *Kidney International*, vol. 82, no. 5, pp. 516–524, 2012.

[5] M. A. Venkatachalam, K. A. Griffin, R. Lan, H. Geng, P. Saikumar, and A. K. Bidani, "Acute kidney injury: a springboard for progression in chronic kidney disease," *American Journal of Physiology—Renal Physiology*, vol. 298, no. 5, pp. F1078–F1094, 2010.

[6] R. Murugan and J. A. Kellum, "Acute kidney injury: what's the prognosis?" *Nature Reviews Nephrology*, vol. 7, no. 4, pp. 209–217, 2011.

[7] R. Bucala, L. A. Spiegel, J. Chesney, M. Hogan, and A. Cerami, "Circulating fibrocytes define a new leukocyte subpopulation that mediates tissue repair," *Molecular Medicine*, vol. 1, no. 1, pp. 71–81, 1994.

[8] D. Scholten, D. Reichart, Y. H. Paik et al., "Migration of fibrocytes in fibrogenic liver injury," *American Journal of Pathology*, vol. 179, no. 1, pp. 189–198, 2011.

[9] A. Mackinnon and S. Forbes, "Bone marrow contributions to fibrosis," *Biochimica et Biophysica Acta (BBA)—Molecular Basis of Disease*, vol. 1832, no. 7, pp. 955–961, 2013.

[10] T. Wada, N. Sakai, Y. Sakai, K. Matsushima, S. Kaneko, and K. Furuichi, "Involvement of bone-marrow-derived cells in kidney fibrosis," *Clinical and Experimental Nephrology*, vol. 15, no. 1, pp. 8–13, 2011.

[11] B. Reich, K. Schmidbauer, M. Rodriguez Gomez et al., "Fibrocytes develop outside the kidney but contribute to renal fibrosis in a mouse model," *Kidney International*, vol. 84, no. 1, pp. 78–89, 2013.

[12] T. Wada, N. Sakai, K. Matsushima, and S. Kaneko, "Fibrocytes: a new insight into kidney fibrosis," *Kidney International*, vol. 72, no. 3, pp. 269–273, 2007.

[13] S. K. Mathai, M. Gulati, X. Peng et al., "Circulating monocytes from systemic sclerosis patients with interstitial lung disease show an enhanced profibrotic phenotype," *Laboratory Investigation*, vol. 90, no. 6, pp. 812–823, 2010.

[14] T. Kisseleva, M. von Köckritz-Blickwede, D. Reichart et al., "Fibrocyte-like cells recruited to the spleen support innate and adaptive immune responses to acute injury or infection," *Journal of Molecular Medicine*, vol. 89, no. 10, pp. 997–1013, 2011.

[15] R. A. Reilkoff, R. Bucala, and E. L. Herzog, "Fibrocytes: emerging effector cells in chronic inflammation," *Nature Reviews Immunology*, vol. 11, no. 6, pp. 427–435, 2011.

[16] J. P. Dai, D. X. Zhu, J. T. Sheng et al., "Inhibition of tanshinone IIA, salvianolic acid A and salvianolic acid B on areca nut extract-induced oral submucous fibrosis in vitro," *Molecules*, vol. 20, no. 4, pp. 6794–6807, 2015.

[17] C.-Y. Zhan, J.-H. Tang, D.-X. Zhou, and Z.-H. Li, "Effects of tanshinone IIA on the transforming growth factor β1/Smad signaling pathway in rat cardiac fibroblasts," *Indian Journal of Pharmacology*, vol. 46, no. 6, pp. 633–638, 2014.

[18] J. Tang, C. Zhan, and J. Zhou, "Effects of tanshinone IIA on transforming growth factor β1-Smads signal pathway in renal interstitial fibroblasts of rats," *Journal of Huazhong University of Science and Technology—Medical Science*, vol. 28, no. 5, pp. 539–542, 2008.

[19] X. Jiang, Y. Chen, H. Zhu et al., "Sodium tanshinone IIA sulfonate ameliorates bladder fibrosis in a rat model of partial bladder outlet obstruction by inhibiting the TGF-β/Smad pathway activation," *PLoS ONE*, vol. 10, no. 6, Article ID e0129655, 2015.

[20] L. Yang, X.-J. Zou, X. Gao et al., "Sodium tanshinone IIA sulfonate attenuates angiotensin II-induced collagen type I expression in cardiac fibroblasts *in vitro*," *Experimental and Molecular Medicine*, vol. 41, no. 7, pp. 508–516, 2009.

[21] J. Gu, H.-L. Li, H.-Y. Wu et al., "Sodium tanshinone IIA sulfonate attenuates radiation-induced fibrosis damage in cardiac fibroblasts," *Journal of Asian Natural Products Research*, vol. 16, no. 9, pp. 941–952, 2014.

[22] J. Chunming, Z. Miao, S. Cheng et al., "Tanshinone IIA attenuates peritoneal fibrosis through inhibition of fibrogenic growth factors expression in peritoneum in a peritoneal dialysis rat model," *Renal Failure*, vol. 33, no. 3, pp. 355–362, 2011.

[23] Q. Shang, H. Wang, S. Li, and H. Xu, "The effect of sodium tanshinone IIA sulfate and simvastatin on elevated serum levels of inflammatory markers in patients with coronary heart disease: a study protocol for a randomized controlled trial," *Evidence-Based Complementary and Alternative Medicine*, vol. 2013, Article ID 756519, 8 pages, 2013.

[24] Z. H. Ren, Y. H. Tong, W. Xu, J. Ma, and Y. Chen, "Tanshinone II A attenuates inflammatory responses of rats with myocardial infarction by reducing MCP-1 expression," *Phytomedicine*, vol. 17, no. 3-4, pp. 212–218, 2010.

[25] J. Fang, S.-W. Xu, P. Wang et al., "Tanshinone II-A attenuates cardiac fibrosis and modulates collagen metabolism in rats with renovascular hypertension," *Phytomedicine*, vol. 18, no. 1, pp. 58–64, 2010.

[26] H. Wu, Y. Li, Y. Wang et al., "Tanshinone IIA attenuates bleomycin-induced pulmonary fibrosis via modulating angiotensin-converting enzyme 2/angiotensin-(1–7) axis in rats," *International Journal of Medical Sciences*, vol. 11, no. 6, pp. 578–586, 2014.

[27] Y.-W. Liu and Y.-T. Huang, "Inhibitory effect of tanshinone IIA on rat hepatic stellate cells," *PLoS ONE*, vol. 9, no. 7, Article ID e103229, 2014.

[28] D. T. Wang, R. H. Huang, X. Cheng, Z. H. Zhang, Y. J. Yang, and X. Lin, "Tanshinone IIA attenuates renal fibrosis and inflammation via altering expression of TGF-beta/Smad and NF-kappaB signaling pathway in 5/6 nephrectomized rats," *International Immunopharmacology*, vol. 26, no. 1, pp. 4–12, 2015.

[29] S. K. Kim, K.-H. Jung, and B.-C. Lee, "Protective effect of tanshinone IIA on the early stage of experimental diabetic nephropathy," *Biological and Pharmaceutical Bulletin*, vol. 32, no. 2, pp. 220–224, 2009.

[30] R. M. Strieter, E. C. Keeley, M. D. Burdick, and B. Mehrad, "The role of circulating mesenchymal progenitor cells, fibrocytes, in promoting pulmonary fibrosis," *Transactions of the American Clinical and Climatological Association*, vol. 120, pp. 49–59, 2009.

[31] J. Xu, M. Cong, T. J. Park, D. Scholten, D. A. Brenner, and T. Kisseleva, "Contribution of bone marrow-derived fibrocytes to liver fibrosis," *Hepatobiliary Surgery and Nutrition*, vol. 4, no. 1, pp. 34–47, 2015.

[32] Y. Li, Y. Yang, D. Yu, and Q. Liang, "The Effect of Tanshinone IIA upon the TGF-beta1/Smads signaling pathway in hypertrophic myocardium of hypertensive rats," *Journal of Huazhong University of Science and Technology—Medical Science*, vol. 29, no. 4, pp. 476–480, 2009.

[33] H. Tang, H. He, H. Ji et al., "Tanshinone IIA ameliorates bleomycin-induced pulmonary fibrosis and inhibits transforming growth factor-β-β-dependent epithelial to mesenchymal transition," *Journal of Surgical Research*, vol. 197, no. 1, pp. 167–175, 2015.

[34] R. Abe, S. C. Donnelly, T. Peng, R. Bucala, and C. N. Metz, "Peripheral blood fibrocytes: differentiation pathway and migration to wound sites," *The Journal of Immunology*, vol. 166, no. 12, pp. 7556–7562, 2001.

[35] N. Sakai, T. Wada, H. Yokoyama et al., "Secondary lymphoid tissue chemokine (SLC/CCL21)/CCR7 signaling regulates fibrocytes in renal fibrosis," *Proceedings of the National Academy of Sciences*, vol. 103, no. 38, pp. 14098–14103, 2006.

[36] N. Sakai, K. Furuichi, Y. Shinozaki et al., "Fibrocytes are involved in the pathogenesis of human chronic kidney disease," *Human Pathology*, vol. 41, no. 5, pp. 672–678, 2010.

[37] X. Wu, L. Liu, H. Xie et al., "Tanshinone IIA prevents uric acid nephropathy in rats through NF-κB inhibition," *Planta Medica*, vol. 78, no. 9, pp. 866–873, 2012.